MOLECULAR AND CELLULAR STUDIES OF THE ROLE OF UROKINASE PLASMINOGEN ACTIVATOR IN CUTANEOUS WOUND HEALING

by

Richard James Daniel

A thesis submitted for the degree of Doctor of Philosophy

Centre for Dermatology
Department of Medicine
University College London

October 2003

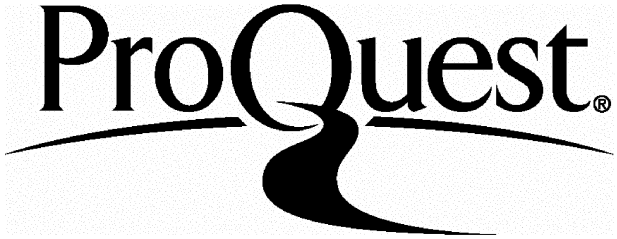

ABSTRACT

Re-epithelialization is a pivotal process in normal skin repair. Studies from knockout mice demonstrate that an intact plasminogen activator system is an essential requirement for this process and thus for wound healing. In this study, transgenic mice were generated overexpressing urokinase plasminogen activator (uPA) to assess the effect on cutaneous wound healing. Constitutive epidermal overexpression resulted in embryonic toxicity. However, mice generated with uPA under the inducible control of the Cre/LoxP system or K6 promoter (K6-uPAtg) facilitated effective uPA induction. Importantly, analysis of K6-uPAtg mice demonstrated a marked induction of functional uPA upon cutaneous wounding. Subsequent wounding analyses, however, showed no gross differences from wild-type wounds, suggesting that complex regulation of uPA occurs within cutaneous wounds.

A key consequence of cutaneous wounding is the development of tissue hypoxia, a potent stimulus for increased keratinocyte migration and hence re-epithelialization. As the mechanisms responsible for this remain unclear, the relationship between hypoxia, plasminogen activation and *in vitro* wound healing was assessed. Exposure of keratinocytes to hypoxia resulted in upregulation of uPA and uPAR mRNA and an increase in functional uPA. Addition of a serine protease inhibitor or selective uPA inhibitors, significantly reduced keratinocyte motility in hypoxic cultures and abrogated the hypoxic enhancement of *in vitro* wound closure. These data indicate a central role for uPA in hypoxic keratinocyte migration and suggest a mechanism for enhanced re-epithelialization of wounds under low oxygen tensions.

An important inhibitor of uPA, PAI-1, is also implicated in wound-related cellular migration. The effect of hypoxia on keratinocyte PAI-1 expression was therefore evaluated. Exposure to hypoxia resulted in upregulation of PAI-1 mRNA and protein. Antibody-mediated neutralisation of VEGF partially inhibited this hypoxic induction, suggesting that VEGF stimulates PAI-1 in hypoxic keratinocytes. The subsequent detection of VEGF receptor mRNA in keratinocytes indicated a potential signalling pathway for this VEGF-mediated stimulation.

TABLE OF CONTENTS

PUBLICATIONS ARISING FROM THIS WORK

At the time of submission, 4 abstracts based on the work in this thesis had been published and 1 manuscript was in press, as detailed below.

Abstracts:

Daniel RJ and Groves RW

Hypoxic induction of plasminogen activator inhibitor 1 in murine keratinocytes is partially regulated by vascular endothelial growth factor

BJD, **142**: 621 (2000)

Daniel RJ and Groves RW

Effects of hypoxia on the murine keratinocyte plasminogen activation system

J Invest Dermatol, **113**: 156 (1999)

Daniel RJ and Groves RW

Cre-recombinase mediated induction of urokinase plasminogen activator: a novel genetic switch

J Invest Dermatol, **113**: 383 (1999)

Daniel RJ and Groves RW

Induction of plasminogen activator inhibitor-1 by hypoxia in murine keratinocytes

J Invest Dermatol, **112**: 615 (1999)

Manuscript in press:

Daniel RJ and Groves RW

Increased migration of murine keratinocytes under hypoxia is mediated by induction of urokinase plasminogen activator

J Invest Dermatol, In Press (2002)

ABBREVIATIONS

ATF	Amino-terminal fragment
cDNA	Complementary deoxyribonucleic acid
CHO	Chinese hamster ovary
CTGF	Connective tissue growth factor
DDCs	Dermal dendritic cells
ddH_2O	Double-distilled water
DEPC	Diethyl pyrocarbonate
DETC	Dendritic epidermal T cell
DMSO	Dimethyl sulphoxide
DNA	Deoxyribonucleic acid
dNTP	Deoxynucleotide triphosphate
ECM	Extracellular matrix
EGF	Epidermal growth factor
EGFR	Epidermal growth factor receptor
ELISA	Enzyme-linked immunosorbent assay
FGF	Fibroblast growth factor
GFD	Growth factor-like domain
GPI	Glycosyl-phosphatidyl-inositol
gro	Growth related protein
HB-EGF	Heparin-binding epidermal growth factor
H&E	Haematoxylin and eosin
HGF	Hepatocyte growth factor
HGH	Human growth hormone
HGX	Mutated human growth hormone
ICAM	Intercellular adhesion molecule
IgG	Immunoglobulin G
IGF	Insulin-like growth factor
IL	Interleukin
K	Keratin
KGF	Keratinocyte growth factor
LBD	Ligand-binding domain
LDH	Lactate dehydrogenase
LFA	Lymphocyte function-associated antigen
MCP	Monocyte chemotactic protein
MMP	Matrix metalloproteinase
mRNA	Messenger ribonucleic acid
OHT	4-Hydroxytamoxifen
PAF	Platelet activating factor
PAI	Plasminogen activator inhibitor
PCR	Polymerase chain reaction
PDGF	Platelet-derived growth factor
PECAM	Platelet-endothelial cell adhesion molecule
PMA	Phorbol 12-myristate 13-acetate
PMNs	Polymorphonuclear cells
pro-uPA	Single-chain urokinase plasminogen activator
RA	Retinoic acid
RNA	Ribonucleic acid
RPMI	Roswell Park Memorial Institute
RT	Reverse transcription/transcriptase
RT-PCR	Reverse transcription polymerase chain reaction
SCID	Severe combined immunodeficient
sc-tPA	Single-chain tissue plasminogen activator
SDS	Sodium dodecyl sulphate
tc-tPA	Two-chain tissue plasminogen activator
TGF	Transforming growth factor
TIMP	Tissue inhibitor of metalloproteinases
TNF	Tumour necrosis factor
tPA	Tissue plasminogen activator
TSS	Transcriptional stop signal
uPA	Urokinase plasminogen activator
uPAR	Urokinase plasminogen activator receptor
UV	Ultraviolet
VEGF	Vascular endothelial growth factor
VPF	Vascular permeability factor

ACKNOWLEDGEMENTS

I am indebted to Professor Richard Groves for the opportunity to work in such a stimulating academic environment and for his support, guidance and boundless enthusiasm. Special thanks are also due to my secondary supervisor, Dr Jill Norman, who has been an excellent mentor and supplied expert and frank advice throughout. The contributions of the following present and former colleagues are also very gratefully acknowledged: Katie Gardiner (Institute of Child Health, London) and Dr Colin Hetherington (University of Oxford), for their transgenic expertise; David Williams, for the wound histology work; Dr Ian Zachary, for guidance on the VEGF aspects of the project, and Jeff Packman, for his exemplary management of the Biological Services Unit.

The work presented in this thesis was generously funded by Pfizer Global Research and Development. Although many of my collaborators at Pfizer have come and gone over the course of this project, I am particularly grateful to Dr Frank Burslem and Dr Mike Collis for all their help and enthusiasm.

Finally, I would like to express my sincere gratitude to the following people who have, in one way or another, contributed to the successful completion of this work: Ms Annette Argent and Dr Gordon Stewart, for their guidance during the early years; Drs John Mee, Yasmin Alam and Christos Antonopoulos, for unconditional support and friendship throughout; Paul Stockall, Sam Scutt and Grace Beesley, for keeping me sane at home; my parents and Claire and Alaric, for family support most would only dream of; and last, but by no means least, Colonel Sanders, for providing sustenance and finger-lickin' good nutrition when it was most needed.

CHAPTER 1

INTRODUCTION

1.1 THE SKIN

As the largest organ in the human body, skin performs numerous vital functions, the most important of which is its protective role. Indeed, as the external barrier, skin is constantly traumatised and has therefore developed a sophisticated way of restoring and maintaining cutaneous integrity. Although this specialised wound-activated response is reliant on the actions of a variety of infiltrating cell types, cells permanent to the skin also play a pivotal role, and are crucial to the process of skin repair and regeneration.

1.1.1 Skin structure and composition

The skin is composed of two distinct yet interacting cell layers, the epidermis and the dermis, situated above a varying depth of subcutaneous fat. The structure and composition of the skin is reasonably uniform, however variation with body site is observed, suggesting an innate evolutionary ability to adapt to environmental forces.

1.1.1.1 The epidermis

The epidermis is a highly keratinised stratified squamous epithelial layer predominantly populated by keratinocytes. Inter-dispersed amongst this keratinocyte population are small numbers of antigen-presenting Langerhans cells, melanocytes, neuronal cells and, in certain species, dendritic epidermal T cells (DETC). The epidermis is a dynamic tissue, constantly renewed in a homeostatic balance between cellular proliferation and cell loss, and is highly responsive to external stimuli and mechanical damage. In healthy epidermis, keratinocytes differentiate from the basal layer (stratum basale) through the spinous (stratum spinosum), granular (stratum granulosum) and cornified (stratum corneum) layers (figure 1.1), prior to desquamation at the skin surface. This process of terminal differentiation takes approximately 4 weeks (Haake *et al,* 2001), and is characterised by modification of both morphological and biochemical properties.

Keratinocytes of the basal layer, or stratum basale, are attached to a carpet of specialised matrix known as basement membrane. Association of basal keratinocytes with the basement membrane is critical to epidermal structural integrity and involves keratinocyte attachment to hemidesmosomes. These multiprotein complexes facilitate linkage of the keratinocyte cytoskeleton with laminin components of the basement

membrane via bullous pemphigoid antigens 1 and 2, plectin and α6β4 integrin, the latter of which is suggested to be a route of signalling pathways that determine cell phenotype (Borradori and Sonnenberg, 1999). The importance of interactions between basal keratinocytes and the basement membrane has been demonstrated in transgenic models in which altered expression of various hemidesmosome components results in several cutaneous blistering disorders (van der Neut *et al,* 1996; Georges-Labouesse *et al,* 1996; Andra *et al,* 1997).

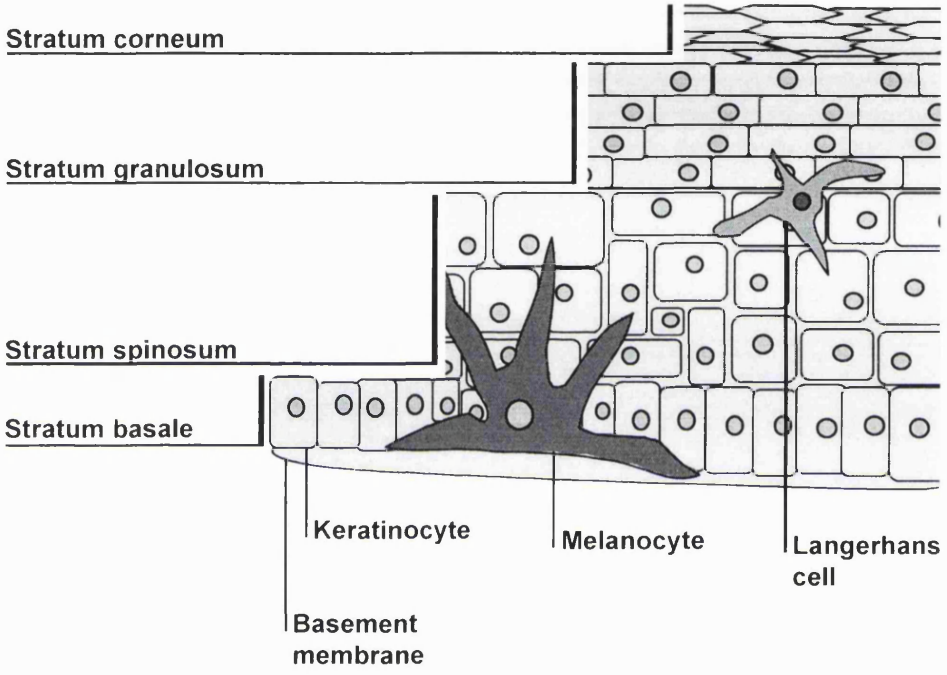

Figure 1.1 Schematic representation of epidermal layers of the skin (adapted from Brocard *et al,* 1997)

The stratum basale is one of the putative locations of keratinocyte stem cells (Haake *et al,* 2001). Although not all keratinocytes in the basal layer have the potential to divide, stem cell mitotic division constitutes the initial step in the transit of keratinocytes from the basal layer to suprabasal layers, a process that is characterised by altered keratin expression. Keratins are a large group of intermediate filament proteins, specifically expressed in epithelia, that contribute significantly to the structure and function of the epithelial cytoskeleton (reviewed in Steinert and Roop, 1988 and Fuchs and Weber, 1994). Mutations in keratin proteins, as observed in patients with diseases such as epidermolysis bullosa simplex and epidermolytic hyperkeratosis, results in disruption of intracellular scaffolding, and subsequent pathologic changes, such as skin

fragility and blister formation (Coulombe *et al,* 1991; Ishida-Yamamoto *et al,* 1992). Keratin proteins are classified as either acidic (type I) or basic (type II), and are usually co-expressed in defined pairs. Modified keratin expression is one of the earliest markers of terminal differentiation, with basal undifferentiated keratinocytes expressing keratins 5, 14 (Nelson and Sun, 1983) and low amounts of keratin 15 (Lloyd *et al,* 1995); and suprabasal cells, of the spinous and granular layers, typically expressing keratins 1 and 10 (Fuchs and Green, 1980), and at a later stage of differentiation keratin 2e (Collin *et al,* 1992). Furthermore, in pathological conditions characterised by hyperproliferation, such as psoriasis and epidermal malignancies, as well as in cutaneous wound healing, the normal process of terminal differentiation is disrupted and this is characterised by altered keratin expression, predominantly of keratins 6, 16 and 17 (Weiss *et al,* 1984; Mansbridge and Knapp, 1987; Stoler *et al,* 1988; Paladini *et al,* 1996).

As the cuboidal basal keratinocytes progress into the stratum spinosum, they lose their association with the basement membrane and develop prominent cell-to-cell attachments. Further progress into the granular layer is characterised by expression of precursors of the cornified envelope, such as filaggrin, involucrin and loricrin, and subsequent accumulation of dense keratohyaline granules (Rice and Green, 1979; Lynley and Dale, 1983; Steven *et al,* 1990; Magnaldo *et al,* 1992). The final stage of differentiation occurs after dissolution of the nuclei and organelles and results in formation of cornified envelopes that are organised into the metabolically quiescent stratum corneum.

1.1.1.2 The dermis

The dermis consists of a complex connective tissue matrix that makes up about 90% of the skin's thickness. Although primarily comprised of collagen (~70%), which imparts strength and toughness to the dermis, the matrix also contains a network of loosely arranged elastin fibres that provide elasticity to the skin. These fibrillary components are anchored to a semi-solid layer of glycosaminoglycan ground substance, consisting of various polysaccharide-protein macromolecules such as heparan sulphate, chondroitin-4-sulphate and hyaluronic acid (Stadelmann *et al,* 1998a). The dense matrix of collagen and elastin provides support for many components of the dermis, including lymph vessels, nerves, muscle cells, sweat and sebaceous glands, and hair follicles. In addition, the dermis also provides important structural support for the cutaneous

vasculature, comprised of two main horizontal layers with vertical connections that terminate in a fine network of capillaries just beneath the epidermis. These blood vessels play a critical role in the maintenance of skin integrity by supplying important nutrients and oxygen to resident dermal and epidermal cells.

The dermis is populated by many cell types, including fibroblasts, macrophages, mast cells, basophils and dermal dendritic cells (DDCs). Dermal tissue is dynamic and shares an intimate relationship, at both the structural and biochemical level, with the overlying epidermis. As the predominant cell type within the dermis, the principal function of the dermal fibroblast is the synthesis of the collagenous and non-collagenous proteins that constitute the connective tissue matrix and ground substance. Fibroblasts have also been shown to enjoy a direct regulatory relationship with epidermal keratinocytes (reviewed in Werner and Smola, 2001) although this paracrine regulation is more relevant to patho-physiological processes which require cellular activation and proliferation, such as cutaneous wound healing and psoriasis. Other cell types present in the dermis include macrophages, derived from circulating monocytes, which are involved in both immune and inflammatory responses; mast cells, involved in the release of inflammatory mediators, a process triggered by other inflammatory stimuli such as neuropeptides and complement components (Marshall and Bienenstock, 1994) and DDCs, which may provide a similar antigen-presenting function to their epidermal counterparts, Langerhans cells.

1.2 CUTANEOUS WOUND HEALING

The disruption of normal cutaneous structure and function by wounding, initiates a number of co-ordinated regulatory mechanisms and pathways that ultimately result in restoration of cutaneous integrity. These complex wound-related responses are reliant on cells of varying lineage acting in concert to regulate proliferation, migration, matrix reconstruction and wound closure. The function of these cells is therefore pivotal to successful wound repair. The wound healing response was historically defined as consisting of three classic phases – inflammation, fibroplasia, and maturation (Howes *et al*, referenced in Stadelmann *et al,* 1998a). In recent years, however, this scheme has been broadened to include several overlapping and interactive phases, involving fibrin clot formation, recruitment of inflammatory cells, wound re-epithelialization and matrix degradation, development of granulation tissue, re-vascularisation, and scar-tissue formation.

1.2.1 Formation of the fibrin clot

Skin injuries usually result in the disruption of vasculature and extravasation of blood constituents. Subsequent formation of a fibrin-rich clot, by blood coagulation and platelet aggregation, initially serves to restore haemostasis, temporarily protects denuded tissues, and provides a provisional matrix to facilitate cell migration during the early wound healing process (Martin, 1997). The clot itself consists of a mass of aggregated blood platelets embedded within a network of cross-linked fibrin fibres, derived by thrombin cleavage of fibrinogen, as well as smaller amounts of plasma fibronectin, vitronectin, thrombospondin and tenascin. Wound-induced fibrin clots act as reservoirs for growth factors and cytokines released by degranulating platelets, for example, platelet-derived growth factor (PDGF) and transforming growth factor β (TGF-β) both of which attract and activate fibroblasts and macrophages (table 1.1 and figure 1.2). In the absence of haemorrhage, platelets are not required, and the wound healing response is driven by chemoattractants and vasoactive mediators provided by the activated complement pathway and damaged or activated native skin cells (Clark, 1996a). This early expression/release of potent soluble mediators in response to cutaneous wounding, subsequently acts to regulate chemotaxis, migration, proliferation and differentiation of various cell types involved in the ensuing wound response.

1.2.2 Wound inflammation

Following cutaneous tissue damage a period of pronounced vasodilation and increased capillary permeability is observed, accompanied by an influx of a variety of inflammatory cell populations. Cellular infiltration is an orderly sequential process in which initially large numbers of polymorphonuclear cells (PMNs) are attracted to the wound site. Shortly after this initial neutrophil accumulation, monocytes, and later lymphocytes, are recruited. The potential biochemical mediators of inflammatory recruitment are diverse and can include certain platelet degranulation-derived growth factors and cytokines, complement cascade products, C3a and C5a; formyl methionyl peptides cleaved from bacterial proteins and various products of fibrin degradation (reviewed in Clark, 1996a). Furthermore, activated cells native to the skin, such as keratinocytes, as well as members of the inflammatory infiltrate, are capable of expressing specific chemotactic factors, or chemokines, that facilitate leukocyte recruitment.

Wound-induced expression of chemokines follows an orderly pathway that directly correlates with the sequential recruitment of inflammatory cells. For example, interleukin-8 (IL-8) and growth related oncogene-α (gro-α), which selectively recruit neutrophils and possibly lymphocytes (Baggiolini *et al,* 1994; Devalaraja and Richmond, 1999), are highly expressed for the initial 24 hours post wounding, a period during which neutrophils are the predominant infiltrating cell type, yet rapidly decline by day 4 in line with a reduction in neutrophil accumulation. Moreover, increased expression of monocyte chemoattractant protein-1 (MCP-1) also peaks at 24 hours, yet the decline is more gradual facilitating MCP-1 mediated recruitment of monocytes and later lymphocytes (Engelhardt *et al,* 1998). The various chemokines released by wound-activated cells play an important role in inflammatory recruitment, as in addition to providing a chemotactic gradient to guide infiltrating leukocytes to the wound area, they are responsible for activation of tethered leukocytes prior to extravasation from blood capillaries. Recent transgenic studies have begun to demonstrate exactly how important these chemokine functions really are, as reduced neutrophil recruitment and severely impaired wound closure was recently observed in knockout mice lacking the IL-8 and gro-α receptor, CXCR2 (Devalaraja *et al,* 2000).

GROWTH FACTORS IN WOUND HEALING		
Growth Factor	**Source**	**Target Cells and Effects**
EGF	platelets	keratinocyte motogen and mitogen
TGF-α	macrophages; keratinocytes	keratinocyte motogen and mitogen
HB-EGF	macrophages	keratinocyte motogen and mitogen
FGF-1	macrophages; endothelial cells	angiogenesis and fibroblast mitogen
FGF-2	macrophages; endothelial cells	angiogenesis and fibroblast mitogen
KGF	dermal fibroblasts	keratinocyte motogen and mitogen
TGF-β(1 / 2)	platelets; macrophages	keratinocyte motogen; chemotactic for macrophages and fibroblasts; fibroblast matrix synthesis
TGF-β3	macrophages	antiscarring
PDGF	platelets; macrophages; keratinocytes	chemotactic for macrophages and fibroblasts; macrophage activation; fibroblast mitogen and matrix synthesis
VEGF	keratinocytes; macrophages	angiogenesis
TNF-α	neutrophils	pleiotropic growth factor expression
IL-1α & -β	neutrophils	pleiotropic growth factor expression
IGF-1	plasma; platelets; fibroblasts; keratinocytes	endothelial cell and fibroblast mitogen
Activin	fibroblasts; keratinocytes	fibroblast activation/regulation

Table 1.1 The major growth factors and cytokines involved in cutaneous tissue repair (adapted from Martin, 1997 and Singer and Clark, 1999)

Inflammatory cell recruitment also depends on modification of adhesion molecule expression by microvascular endothelial cells present in capillaries lining the wound site. Upregulation of members of the selectin family of adhesion molecules facilitates weak binding of specific constitutively expressed counter-ligands on neutrophils, monocytes and at later stages of the wound healing process, lymphocytes. Tethered leukocytes are then activated by chemokines, and stronger adhesions are facilitated by interaction of β_2 integrins, such as lymphocyte function-associated antigen-1 (LFA-1) with intracellular adhesion molecule-1 (ICAM-1) (Springer, 1994).

This cell arrest allows inflammatory leukocytes to position themselves between endothelial cells and cross the endothelial basement membrane to emerge in the wound area, prior to migration along the chemotactic gradient. The importance of these adhesion molecules in the wound healing response has recently been demonstrated in studies showing reduced inflammatory cell recruitment and impaired wound healing in P-selectin/E-selectin (Subramaniam *et al,* 1997), and ICAM-1/L-selectin double knockout mice (Nagaoka *et al,* 2000).

The primary function of wound-induced inflammatory cells is clearance of bacteria and assistance in removal of devitalised tissue fragments and debris. Activated neutrophils release oxygen free-radicals and lysosomal enzymes, such as collagenases and elastases which help fight infection and clean the wound (reviewed in Clark, 1996a). In addition, neutrophils have been shown to be a primary source of pro-inflammatory cytokines, such as interleukin-1α and β (IL-1α and β) and tumour necrosis factor-α (TNF-α), that potentially act as primary signals for local keratinocyte and fibroblast activation (Feiken *et al,* 1995; Hubner *et al,* 1996). In normal wounds, neutrophil accumulation will cease after approximately 4 days at which point the predominant cell type in the leukocyte population is the macrophage (Engelhardt *et al,* 1998).

Wound-induced infiltrating macrophages are derived from circulating blood monocytes and promote wound repair by migrating through fibrin-rich provisional matrix clearing apoptosed neutrophils by phagocytosis. This neutrophil apoptosis is either spontaneous or influenced by monocyte secretory products. However, a recent study demonstrates that macrophages are capable of inducing PMN apoptosis directly, via cell-to-cell contact and constitutive macrophage expression of β_3 integrin subunits, CD36, and membrane bound TNF-α (Meszaros *et al,* 2000). Moreover, neutrophil clearance may provide a mechanism allowing regulation of the inflammatory phase of wound healing, as ingestion of apoptotic PMNs triggers macrophage production of anti-inflammatory mediators, such as TGF-β and platelet-activating factor (PAF) (Fadok *et al,* 1998). As well as clearing neutrophil derived debris from the wound area, infiltrating macrophages release numerous growth factors and cytokines (table 1.1 and figure 1.2) that maintain and modify the wound repair signals initiated by degranulating platelets and infiltrating neutrophils.

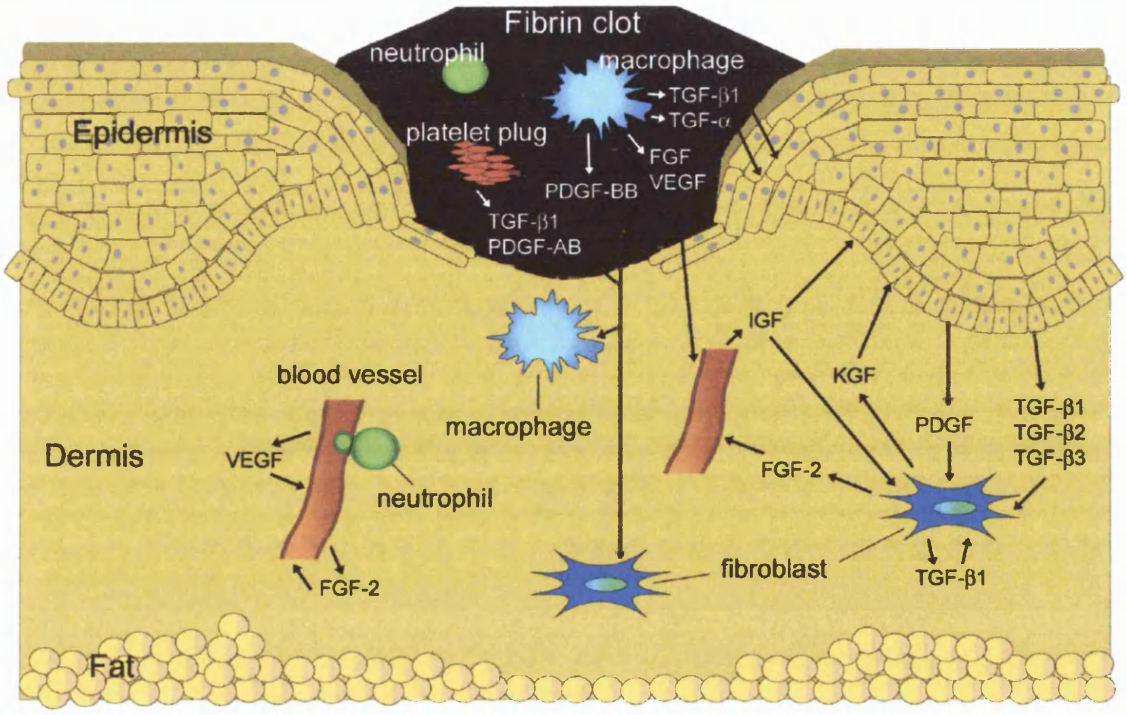

Figure 1.2 Schematic representation of a cutaneous wound three days after injury. Abbreviations: TGF-β1, TGF-β2 and TGF-β3 denote transforming growth factor-β1, -β2, and -β3, respectively; TGF-α = transforming growth factor-α; FGF = fibroblast growth factor, VEGF = vascular endothelial growth factor; PDGF = platelet-derived growth factor; IGF = insulin-like growth factor; KGF = keratinocyte growth factor (adapted from Singer and Clark, 1999).

1.2.3 Wound re-epithelialization

As in the dermis, cutaneous wounding is characterised by a dramatic sequence of cellular alterations in the epidermis that result in the transformation of stationary keratinocytes to motile cells. This transformation subsequently facilitates the migration of keratinocytes from the wound edges to a point where denuded tissues are resurfaced with neoepidermis, a process termed re-epithelialization. Candidate initiators and mediators of the epidermal cell proliferation and migration required for re-epithelialization include wound-induced release of cytokines and growth factors from platelets, leukocytes, and native skin cells; as well as the loss of contact inhibition caused by tissue damage. Early keratinocyte responses to this wound-induced activation include secretion of growth factors and cytokines, altered or modified keratin and integrin expression, and regulation of proteolytic enzymes, such as plasminogen activators and matrix metalloproteinases (MMPs). Co-ordination of these diverse responses is critical to re-epithelialization, and thus to wound healing overall.

1.2.3.1 Keratin reorganisation

Wound re-epithelialization is associated with several keratinocyte morphological changes that include retraction of tonofilaments, dissolution of intercellular desmosomes, and formation of peripheral cytoplasmic actin filaments (Falabella and Falanga, 2001). These morphological changes ultimately aim to facilitate modification of sessile cells to motile cells and are accompanied by, and most likely related to, altered keratin expression. Cutaneous wounding has been demonstrated to be a stimulus for both increased and decreased expression of keratins (Mansbridge and Knapp, 1987; Paladini *et al,* 1996; Werner and Munz, 2000), although the specific responses are generally dependent on the epidermal position and differentiation status of the keratinocytes.

One of the most striking responses to cutaneous tissue damage is the rapid upregulation of keratins 6, 16 and 17. Although normally undetectable in interfollicular epidermis, all are rapidly induced post-wounding, as keratin 6 (K6) and keratin 16 (K16) are detectable in injured epidermis after 6 hours, and K17 after 12 hours (Paladini *et al,* 1996). The subsequent early accumulation of K6 and K16 in activated keratinocytes correlates directly with a general reorganisation of keratin filaments from a pan-cytoplasmic conformation to one in which keratin filaments are retracted into juxtanuclear aggregates, a process that is suggested to prepare keratinocytes for a migratory lifestyle. Moreover, forced expression of K16 has revealed that this filament retraction is mediated by K16 alone (Paladini *et al,* 1996). Interestingly, despite this potential role for K16 in preparing keratinocytes for migration, keratinocytes cultured from mice overexpressing K16 showed a reduction in *in vitro* migration (Wawersik and Coulombe, 2000). Although it is highly likely that altered keratin expression and subsequent reorganisation of the cytoskeleton is involved in priming keratinocytes for migration, the importance of keratins in maintaining normal epidermal integrity can impede conventional transgenic analyses, and thus, to date the exact relationship between keratins and wound-activated keratinocyte migration remains to be defined.

1.2.3.2 Integrin modification

Following cutaneous wounding, basal keratinocytes proximal to damaged tissues dissolve hemidesmosomal attachments to the basement membrane and modify expression of integrins to facilitate migration across the provisional clot matrix.

Integrins are a family of heterodimeric cell membrane receptors, each consisting of two transmembrane glycoprotein subunits (α and β subunit), that mediate cell-to-cell and cell-matrix adhesions. Integrin mediated attachments have been implicated in regulation of cell differentiation, proliferation and migration (Hynes, 1992), and these functions are modulated significantly by extracellular matrix (ECM) derived signalling pathways (Damsky and Werb, 1992).

In normal skin and stratified keratinocyte cultures, integrin expression is normally restricted to the basal layer, facilitating attachment of keratinocytes to the basement membrane and adjacent cells (Peltonen *et al,* 1989; De Luca *et al,* 1990; Larjava *et al,* 1990; Marchisio *et al,* 1991). Upon tissue disruption, and subsequent exposure to matrix proteins, migrating keratinocytes alter their integrin expression to include receptors specific for components of the provisional matrix; for example, human wounding studies have demonstrated increased keratinocyte expression of the α5β1 fibronectin receptor, the αvβ6 fibronectin/tenascin receptor, and the αvβ5 vitronectin receptor, at different stages of re-epithelialization (Cavani *et al,* 1993; Clark *et al,* 1996b; Haapasalmi *et al,* 1996). Moreover, in wounded epidermis, constitutively expressed α2β1 integrin is redistributed and polarized at the frontobasal end of migrating keratinocytes (Guo *et al,* 1991). Wound-induced modification of integrin expression seems to vary depending on type of wound (incisional, excisional or suction blister) (Hertle *et al,* 1992; Cavani *et al,* 1993; Haapasalmi *et al,* 1996; Clark *et al,* 1996b), and source of tissue (upper arm, buttock or foreskin transplants on severe combined immunodeficient (SCID) mice) (Cavani *et al,* 1993; Juhasz *et al,* 1993; Clark *et al,* 1996b), suggesting that keratinocyte integrin-related responses are specific to a particular wound environment. Interestingly, during wound healing, altered integrin expression is observed in both basal and suprabasal keratinocytes and clearly extends more than ten cells back from the leading edge (Hertle *et al,* 1992); an observation that lends weight to the "leap-frog hypothesis" of re-epithelialization, established in keratinocyte organotypic cultures, wherein suprabasal keratinocytes roll over adjacent cells to reach the wound area (Garlick and Taichman, 1994).

There is now much evidence suggesting a direct role for integrins in keratinocyte migration. *In vitro* studies have indicated that several wound-induced and constitutive integrins (α5β1, αvβ5, αvβ6, and α2β1) play a functional role in keratinocyte migration on their respective matrix components (Kim *et al,* 1992 and

1994; Huang *et al,* 1998 and 2000). Furthermore, although analysis of excisional wounds in β5 integrin knockout mice showed normal wound closure, β5 deficient keratinocytes showed impaired migration in culture (Huang *et al,* 2000), suggesting that a high level of biochemical redundancy exists *in vivo*. Interestingly, recent data has suggested a novel mechanism for integrin regulation of keratinocyte migration involving a direct relationship between integrin receptors and the activity of MMPs (Pilcher *et al,* 1997; Thomas *et al,* 2001).

1.2.3.3 Protease expression

Activated keratinocytes involved in re-epithelialization of cutaneous wounds express numerous proteases, including MMPs and plasminogen activators (reviewed in Mignatti *et al,* 1996 and Parks, 1999). The primary function of these proteases is to regulate dissolution of matrix components facilitating migration of keratinocytes, and other cell types, through the wound site. Although MMPs and plasminogen activators have distinct substrate specificity, there is significant functional overlap between the MMP and plasminogen activator systems (Lund *et al,* 1999), and much data suggests that the co-ordinated action of these proteases is crucial to normal wound re-epithelialization.

1.2.3.3.1 Plasminogen activators

The primary plasminogen activator expressed by keratinocytes during re-epithelialization is urokinase plasminogen activator (uPA). Upon cutaneous wounding, expression of uPA, and its specific receptor uPAR, is upregulated in leading edge keratinocytes (Grondahl-Hansen *et al,* 1988), thus facilitating the proteolytic conversion of ubiquitous plasminogen to the broad range protease plasmin, which in turn degrades components of the ECM (Mignatti *et al,* 1996). This localised ECM degradation subsequently facilitates keratinocyte migration across and through the provisional matrix and is fundamental to re-epithelialization. The specific roles of uPA and uPA-derived plasmin in re-epithelialization are discussed in detail in section 1.4.2.2

1.2.3.3.2 MMPs

In addition to uPA, wound-activated leading-edge keratinocytes express numerous MMPs, such as MMP-1 (collagenase-1), MMP-9 (gelatinase-B), and MMP-10 (stromelysin-2) (Salo *et al,* 1994; Inoue *et al,* 1995; Madlener *et al,* 1996; Okada *et*

al, 1997). MMP-3 (stromelysin-1) is also produced upon cutaneous wounding, although expression is restricted to a distinct hyperproliferative subpopulation of keratinocytes positioned behind the leading-edge cells (Saarialho-Kere *et al,* 1994). Although the specific signals regulating wound-induced keratinocyte expression of MMP-3 and -10 have yet to be defined, expression of MMP-1 is induced, both *in vitro* and *in vivo*, by keratinocyte contact with type I collagen (Saarialho-Kere *et al,* 1993; Pilcher *et al,* 1997). Interestingly, addition of antibodies against the α2 integrin subunit blocks collagen-mediated induction of MMP-1 (Pilcher *et al,* 1997). Furthermore, blockade of epidermal growth factor receptor (EGFR) binding and signal transduction functions inhibits MMP-1 expression in migrating keratinocytes, leading to the hypothesis that MMP-1 expression is initiated by collagen binding via α2β1, but is sustained by autocrine or paracrine stimulation of the EGFR (Pilcher *et al,* 1999). Similarly, expression of MMP-9 in keratinocytes cultured on fibronectin is inhibited by addition of antibodies against αvβ6, suggesting that MMP-9 expression is mediated by this integrin (Thomas *et al,* 2001). Moreover, since αvβ6 expression is markedly induced during cutaneous remodelling and repair (Breuss *et al,* 1995; Clark *et al,* 1996b; Haapasalmi *et al,* 1996), this may constitute a specialised mechanism whereby MMP-9 is upregulated in wound-activated keratinocytes (Thomas *et al,* 2001).

Many studies have identified potential roles for MMPs in keratinocyte motility *in vitro*. For example, whereas MMP-1 expression is not required for keratinocyte migration on gelatin, it is essential for migration on type I collagen (Pilcher *et al,* 1997). Moreover, MMP-1 has been shown to co-localise at sites of α2β1 integrin binding to collagen, and this complex of protease, integrin and substrate is suggested to drive and regulate keratinocyte migration on collagen substrates (Dumin *et al,* 2001). Furthermore, epidermal growth factor (EGF)- and hepatocyte growth factor (HGF)-induced migration on type I and type IV collagen is inhibited by MMP-9 neutralising antibodies, suggesting MMPs may be critical to growth factor-induced keratinocyte migration (McCawley *et al,* 1998). *In vivo* analyses have also indicated a role for MMPs in keratinocyte motility, as wound closure in wild-type mice treated with the broad spectrum MMP inhibitor, galardin was significantly impaired, and microscopic analysis revealed this was due to reduced keratinocyte migration in galardin-treated wounds (Lund *et al,* 1999). Although these *in vivo* data demonstrate that MMP activity is crucial during wound-induced keratinocyte migration, the shared substrate specificity among

MMPs results in a significant level of biochemical redundancy and hinders transgenic or knockout analysis of their individual roles in re-epithelialization.

1.2.3.4 Cytokines and growth factors

Keratinocyte responses to cutaneous tissue damage primarily involve activation of proliferative and/or migratory pathways. This wound-induced activation is mediated by a cocktail of cytokines and growth factors released by various activated cell types functioning in the wound site. Many cytokines and growth factors are involved in the regulation of re-epithelialization (table 1.1, page 18). Members of the epidermal growth factor family (EGFs), such as epidermal growth factor (EGF) itself, and transforming growth factor α (TGF-α), are considered to be key regulators of epidermal proliferation at the wound edge (Nanney and King Jr, 1996). EGFs are released in abundance upon tissue damage, and have been shown to stimulate keratinocyte proliferation and migration *in vitro* (Barrandon and Green, 1987; Ando and Jensen, 1993; Hashimoto *et al,* 1994), via their shared receptor, EGFR. Furthermore, application of EGF and TGF-α to burn wounds was shown to enhance keratinocyte re-epithelialization in animal models (Brown *et al,* 1986; Schultz *et al,* 1987). Interestingly, several reports have identified a link between EGF family molecules and keratinocyte expression of MMPs (McCawley *et al,* 1998; Pilcher *et al,* 1999), urokinase plasminogen activator (Jensen and Rodeck, 1993), the α2 integrin subunit (Chen *et al,* 1993) and K6 and K16 (Jiang *et al,* 1993), suggesting multiple roles for these growth factors in keratinocyte re-epithelialization.

Keratinocyte growth factor (KGF or FGF-7), a member of the fibroblast growth factor family, has also been implicated in the regulation of wound re-epithelialization. Upon cutaneous wounding, high levels of KGF are released by dermal fibroblasts (Werner *et al,* 1992; Marchese *et al,* 1995). However, the receptor for KGF, KGFR, is expressed predominantly on epithelial cells, suggesting a paracrine mechanism of keratinocyte activation (reviewed in Werner and Smola, 2001). The role of KGF in epidermal repair is likely to involve its observed mitogenic and motogenic effects on keratinocytes both *in vitro* and *in vivo* (reviewed in Werner, 1998), however, data from KGF knockout mice, demonstrating that KGF is not required for normal wound healing (Guo *et al,* 1996) suggest the presence of growth factor compensatory mechanisms *in vivo*. A candidate for this compensation, fibroblast growth factor 10 (FGF-10 or KGF-

2), is expressed in the dermal compartment of the skin (Beer *et al,* 1997) and is an alternative ligand for KGFR (Igarashi *et al,* 1998). Moreover, FGF-10 has recently been shown to promote keratinocyte proliferation *in vitro* (Marchese *et al,* 2001); and application of FGF-10 enhances re-epithelialization and wound breaking strength in ischemic and normal animal wounds, respectively (Xia *et al,* 1999; Jimenez and Rampy, 1999). Interestingly, transgenic mice expressing a dominant-negative mutant of KGFR showed impaired wound re-epithelialization (Werner *et al,* 1994), suggesting that activation of keratinocyte KGFR, by KGF or FGF-10, is a critical stimulus for normal keratinocyte re-epithelialization.

In addition to members of the epidermal and fibroblast growth factor families, other growth factors and cytokines can influence keratinocyte expression and thus could mediate wound re-epithelialization. TGF-β is released in abundance in the wound environment (reviewed in Roberts and Sporn, 1996) and is capable of inducing keratinocyte expression of MMPs (Han *et al,* 2001), components of the plasminogen activation system (Wikner *et al,* 1990; Keski-Oja and Koli, 1992) and integrin receptors (Gailit *et al,* 1994). Moreover, TNF-α, a pleiotropic cytokine present in wounded tissues (Hubner *et al,* 1996), also stimulates keratinocyte expression of MMPs (Han *et al,* 2001) and upregulates plasminogen activating activity (Bechtel *et al,* 1996). Furthermore, novel factors may play important roles in re-epithelialization, as demonstrated recently with leptin, a cytokine implicated in mediating epidermal repair since it has been demonstrated as mitogenic for keratinocytes *in vitro* (Stallmeyer *et al,* 2001) and enhances wound re-epithelialization in leptin deficient *ob/ob* mice (Frank *et al,* 2000).

1.2.3.5 Completion of re-epithelialization

Throughout the process of re-epithelialization, migrating keratinocytes express basement membrane proteins in an ordered sequence from the wound margins inwards (Clark, 1996c). Once re-epithelialization is complete and keratinocyte migration has ceased, the gradual restoration of the basement membrane facilitates the re-establishment of a stratified epidermis. This is accompanied by reversion of keratinocytes to their normal phenotype, i.e. normal integrin and keratin expression (Hertle *et al,* 1992; Garlick and Taichman, 1994) and resumption of the differentiation pathway observed in normal epidermis. The exact 'stop' signals involved have yet to be

defined, but are likely to include stimulation of contact inhibition-specific pathways as keratinocytes re-establish interactions with components of the basement membrane, such as laminin, a known inhibitor of keratinocyte migration (Woodley *et al,* 1988; O'Toole *et al,* 1997a), and adjacent cells.

1.2.4 Wound-induced granulation tissue formation

Approximately 3 or 4 days after cutaneous tissue damage, a large number of fibroblasts, macrophages and endothelial cells migrate into the wound area to facilitate formation of granulation tissue (Eckes *et al,* 1996). As the predominant cell type present in the infiltrating population, fibroblasts primarily function to replace the fibrin-rich clot matrix with a collagen-rich ECM, an initial step in restoring normal dermal structure. For the first 2-3 days post-wounding, fibroblast ECM production is limited and consequently this period was formerly referred to as the "lag" phase. This term has since been abandoned as it has become clear that there is a vast amount of fibroblast proliferation, modification and migration prior to collagen synthesis.

Upon cutaneous wounding, fibroblasts, present in dermal regions adjacent to the wound, are activated by platelet and inflammatory cell derived growth factors and cytokines, such as PDGF and TGF-β (Heldin and Westermark, 1996; Roberts and Sporn, 1996), as well as by components of the provisional matrix (Gray *et al,* 1993; Xu and Clark, 1996). Fibroblasts initially respond to these stimuli by proliferating, modifying their integrin receptor expression and migrating into the wound space. These fibroblast responses are highly specific and seem to be mediated by several distinct signals. This specificity was demonstrated in a recent study in which fibroblasts, cultured in fibrin-fibronectin gels, responded to PDGF stimulation by upregulating the provisional-matrix integrin subunits, α3 and α5, whereas fibroblasts cultured in collagen gels responded to PDGF by upregulating collagen specific α2 subunits (Xu and Clark, 1996). Fibroblasts stimulated by TGF-β, but not by PDGF, have also been shown to upregulate expression of connective tissue growth factor (CTGF) (Igarashi *et al,* 1993). CTGF is a potent fibroblast mitogen and chemoattractant that influences fibroblast expression of integrin subunits and ECM components *in vitro* (Bradham *et al,* 1991; Frazier *et al,* 1996). Moreover, *in vivo* injections of CTGF caused an increase in connective tissue cells and ECM material in neonatal mouse skin (Frazier *et al,* 1996). In respect of current data concerning CTGF, a hypothetical pathway has been proposed

whereby fibroblasts, initially activated by TGF-β, upregulate CTGF expression, which in turn maintains fibroblast activation by both autocrine and paracrine mechanisms. Interestingly, very recent data demonstrate that keratinocytes express CTGF mRNA in normal human skin (Quan *et al,* 2002), suggesting that, during cutaneous wound repair, keratinocyte-derived CTGF may contribute to fibroblast activation and function.

As fibroblasts migrate into the wound site, clearance of the provisional matrix is facilitated by an active proteolytic system, involving fibroblast-derived MMPs and plasminogen activators (Mignatti *et al,* 1996). Once within the wound site, fibroblasts initially synthesize ECM components such as fibronectin and hyaluronic acid, however, as the granulation tissue matures, fibroblasts increasingly deposit type I and type III collagen. Interestingly, although type III collagen is found only in small amounts in normal dermis, it is the predominant collagen synthesized in early wound healing (Falabella and Falanga, 2001). A major stimulus for fibroblast expression of ECM seems to come from TGF-β. *In vitro,* TGF-β stimulates expression of matrix components, such as fibronectin and type I collagen (Ignotz and Massague, 1986; Roberts *et al,* 1986; Raghow *et al,* 1987) and recent data suggest TGF-β stimulation of CTGF may be required for collagen synthesis in cultured fibroblasts (Duncan *et al,* 1999). Moreover, although analysis of wound repair is hindered by multifocal inflammation and early death in TGF-β1 deficient mice (Shull *et al,* 1992), recent analysis of healing wounds in immunodeficient TGF-β1 knockout mice, which have essentially normal longevity, revealed both reduced collagen deposition and diminished and irregularly shaped granulation tissue (Crowe *et al,* 2000). As the new ECM is formed, a subset of fibroblasts is phenotypically altered to display features characteristic of both fibroblasts and smooth muscle cells, such as expression of α-smooth muscle actin (Desmouliere and Gabbiani, 1996). The appearance of these myofibroblasts coincides with contraction of the wound.

1.2.5 Wound contraction and tissue remodeling

As provisional matrix components are replaced by newly formed granulation tissue, myofibroblasts appear and wound contraction is initiated. Suggested mediators of wound contraction have included TGF-β and PDGF stimulation, fibroblast interactions with the collagen matrix via integrins, and cross-links between individual bundles of collagen (Singer and Clark, 1999). Furthermore, exposure of myofibroblasts

to several factors, including angiotensin, prostaglandins and bradykinins leads to muscle-like contraction (Falabella and Falanga, 2001).

Following wound contraction, the ECM is slowly remodelled, a process that culminates in the replacement of collagen III with collagen I. Collagen replacement during the tissue remodelling phase has been suggested to result in increased strength in the resulting scar tissue, although the final tensile strength is only ever 70-80% of undamaged skin (Levenson *et al,* 1965). This remodelling phase is reliant on the actions of several MMPs, and subsequently on their activation by other proteases (Mignatti *et al,* 1996). Exquisite control of the activity of these MMPs thus allows degradation of components of the granulation tissue matrix and replacement with components of the normal dermal matrix.

1.2.6 Wound angiogenesis

As indicated above, formation of wound-induced granulation tissue is facilitated by an influx of fibroblasts, macrophages and endothelial cells. In response to a variety of stimuli, discussed below, endothelial cells, in the form of developing capillary sprouts, utilise MMP- and plasminogen activator-mediated proteolysis to digest and penetrate the underlying vascular basement membrane, and subsequently to invade the ECM (Conway *et al,* 2001). Modification of matrix receptor expression in response to soluble factors and ECM interactions further enhances extension and branching of blood vessels, facilitating re-vascularization of the wounded tissue, a process known as angiogenesis (Tonnesen *et al,* 2000). These newly formed blood vessels carry oxygen and nutrients necessary for the prolific cellular activity occurring in the wound site, and consequently, co-ordination of endothelial cell angiogenic responses plays an important role in wound healing overall.

1.2.6.1 Soluble factors affecting wound angiogenesis

Throughout the process of wound angiogenesis, endothelial cells proliferate and migrate in response to soluble growth factors released by activated macrophages, parenchymal cells and injured endothelial cells. Early studies suggested fibroblast growth factors 1 and 2 were primarily responsible for these angiogenic responses (Folkman and Klagsbrun, 1987), and impaired wound angiogenesis was observed after antibody mediated blockade of FGF-2 (Broadley *et al,* 1989). However, various *in vivo*

and *in vitro* models of wound repair and neovascularization have identified numerous other soluble factors as either pro-angiogenic or anti-angiogenic, including TGF-β, PDGF-BB, and members of the angiopoietin family (see table 1.2), indicating that angiogenesis is a complex process regulated by numerous factors.

ACTIVATORS AND INHIBITORS OF ANGIOGENESIS			
Activators	**Function**	**Inhibitors**	**Function**
VEGF family members	Stimulate angiogenesis and permeability	VEGFR-1, soluble VEGFR-1 and NRP-1	Sink for VEGF, VEGF-B and PIGF
VEGFR-2 and NRP-1	Integrate angiogenic and survival signals	Angiopoietin-2*	Antagonist of angiopoietin-1
Angiopoietin-1 and Tie2 receptor	Stabilise vessels and inhibit permeability	Thrombospondin –1 and -2	Inhibit endothelial cell growth, migration and adhesion
PDGF-BB and receptors	Recruit smooth muscle cells	Angiostatin and related plasminogen kringles	Suppress tumour angiogenesis
TGF-β*, endoglin and TGF-β receptors	Stimulate ECM production	Endostatin	Inhibits endothelial survival and migration
FGF, HGF and MCP-1	Stimulate angiogenesis	Vasostatin, calreticulin	Inhibit endothelial growth
Integrins αvβ3, α5β1 and αvβ5	Receptors for matrix macromolecules and proteases	Platelet factor-4	Inhibits binding of FGF-2 and VEGF
VE-cadherin and PECAM	Endothelial junction molecules	Tissue-inhibitors of MMPs and PEX	Suppress pathological angiogenesis
Proteases and MMPs	Remodel matrix and activate growth factors	Interferon α, β, γ; IP-10, IL-4, IL-12 and IL-18	Inhibit endothelial migration; down regulate FGF-2
PAI-1	Stabilises nascent vessels	Prothrombin kringle-2 and antithrombin III fragment	Suppress endothelial growth
NOS and COX-2	Stimulate angiogenesis and vasodilation	16 kDa-prolactin	Inhibits FGF-2 and VEGF
AC133	Regulates angioblast differentiation	Osteopontin fragment	Interferes with integrin signalling
Chemokines*	Pleiotropic role in angiogenesis	Maspin	Protease inhibitor
Inhibitors of differentiation-1 and -3	Determine endothelial plasticity	VEGI	Modulates cell growth

Table 1.2 Angiogenic activators and inhibitors (adapted from Carmeliet and Jain, 2000). Abbreviations: VEGFR, VEGF receptor; NRP-1, neuropilin-1; PEX, proteolytic fragment of MMP-2; NOS, nitric oxide synthase; COX-2, cyclooxygenase-2; VEGI, vascular endothelial growth inhibitor. * = opposite effects in some contexts.

Vascular endothelial growth factor (VEGF), which was originally known as vascular permeability factor (VPF) due to its ability to induce ascites fluid accumulation, has also been identified as a key factor regulating angiogenesis in the skin. *In vitro*, VEGF is mitogenic for human dermal microvascular endothelial cells (Detmar *et al,* 1995) and enhances endothelial cell migration, partly through stimulation of αv and β1 integrin expression (Senger *et al,* 1996 and 1997). Moreover, in combination with FGF-2 and TNF-α, VEGF stimulates formation of tubular structures by human microvascular endothelial cells cultured in a fibrin matrix (Koolwijk *et al,* 1996). *In vivo*, VEGF mediates increased vascular permeability and angiogenesis (Senger *et al,* 1983; Connolly *et al,* 1989), and upregulation of VEGF, and its receptors Flt-1 and KDR, has been demonstrated in both acute and chronic cutaneous wounds (Brown *et al,* 1992; Frank *et al,* 1995; Lauer *et al,* 2000). Furthermore, recent data has suggested that, whereas FGF-2 may drive the angiogenic response in the initial 3 days of wound healing, VEGF is critical for angiogenic responses during the formation of granulation tissue on days 4 through 7 (Nissen *et al,* 1998). Although the majority of data regarding VEGF and its receptors has been concerned with general angiogenic functions, the observed importance of VEGF in angiogenesis indicates a primary role for this factor in wound-related neovascularization.

1.2.6.2 Wound angiogenesis and matrix components

Approximately 3 days after cutaneous wounding, blood vessels adjacent to the wound site transiently deposit increased amounts of fibronectin within their vascular walls (Clark *et al,* 1982a and b). In addition, fibrin and fibronectin leak from the intravascular space into the perivascular stroma (Tonnesen *et al,* 2000), most likely as a result of increased vascular permeability stimulated by VEGF. At approximately 4 days post-wounding, capillary sprouts branch off from main blood vessels and invade the wound site (McClain *et al,* 1996), presumably using the deposited fibronectin and fibrin as a stepping stone to the provisional matrix. Wound-induced invasion of new blood vessels actually precedes the vast influx of fibroblasts associated with granulation tissue formation (Clark *et al,* 1996d), and subsequently endothelial cells at the capillary tips migrate through a fibrin/fibronectin-rich provisional clot matrix. The matrix composition seems to be fundamental to the process of angiogenesis, and several *in vitro* studies have recently investigated potential relationships between the composition

of the matrix and efficiency of blood vessel formation (reviewed in Tonnesen *et al,* 2000).

One particular study utilised a novel *in vitro* system of human microvascular sprout angiogenesis designed to closely mimic capillary invasion of wound tissue. Endothelial cells, cultured on microcarrier beads, were embedded in 3-dimensional ECM and stimulated with angiogenic factors, such as VEGF and FGF-2. Preliminary unpublished results (reviewed in Tonnesen *et al,* 2000) suggest that when the ECM is composed of fibrin, angiogenic stimulation facilitates initial development of capillary sprouts, followed later by full development of capillary networks; an observation supported by earlier related studies (Koolwijk *et al,* 1996). However, when stimulated with identical angiogenic factors in a collagen ECM, matrix invasion involved individual endothelial cell migration, without capillary formation. Furthermore, when fibrin was added to the collagen ECM, capillary formation was restored. These observations, albeit unpublished at present, suggest that the composition of the wound matrix may determine the efficiency of wound angiogenesis, most likely via ECM regulation of endothelial cell integrin expression.

1.2.6.3 Wound angiogenesis and integrins

Upon angiogenic stimulation, endothelial cells, in a similar manner to wound-activated keratinocytes and fibroblasts, modify their integrin receptor expression patterns to facilitate migration into the wound site. Expression of integrin receptors by endothelial cells is a necessary component of angiogenesis (Brooks *et al,* 1994; Bloch *et al,* 1997; Senger *et al,* 1997), and is mediated by soluble factors such as FGF-2 and VEGF (Enenstein *et al,* 1992; Swerlick *et al,* 1993; Senger *et al,* 1997), as well as components of the ECM, including fibronectin and collagen (Davis and Camarillo, 1995; Feng *et al,* 1999). Regulation of these endothelial cell responses is highly specific as cells cultured on different matrix components upregulate different integrin subunits; for example, dermal microvascular endothelial cells cultured on fibronectin showed higher levels of αv and β3 mRNA compared with cells cultured on collagen type I. Moreover, endothelial cells cultured on collagen type I showed higher levels of β1 mRNA, compared with cells cultured on fibronectin (Feng *et al,* 1999).

Recently, *in vivo* models of cutaneous tissue repair have begun to suggest that endothelial cell integrins have important roles in wound angiogenesis. Analysis of full thickness wounds in pigs showed endothelial cell expression of αvβ3 and the β1 integrin subunit. Moreover, whereas β1 expression was detected throughout the newly forming capillary network, αvβ3 expression was most prominent at the tips of invading capillaries. Interestingly, in this model, blockage of αvβ3 interactions, by monoclonal antibodies and cyclic peptides, transiently inhibited granulation tissue formation and disrupted αvβ3 distribution on invading capillary endothelial cells (Clark *et al,* 1996d). Models of human wound healing, using human skin transplants on SCID mice, have also demonstrated differential transient upregulation of αvβ3, αvβ5 and αvβ6 integrins during wound angiogenesis. Furthermore, in this model, inhibition of αvβ3 completely blocked formation of new capillaries (Christofidou-Solomidou *et al,* 1997), suggesting endothelial cell expression of specific integrins may be critical to wound angiogenesis.

1.3 HYPOXIA AND CUTANEOUS WOUND HEALING

A major physiological consequence of cutaneous wounding is reduced tissue oxygen tension, or hypoxia. Decreasing oxygen tensions were first identified in pioneering animal and human wound studies, conducted nearly 30 years ago by Niinikoski and Hunt (Niinikoski *et al,* 1971; Niinikoski *et al,* 1972a). In the interim, prolonged wound-induced tissue hypoxia has been found to expose wounds to bacterial infection, protracted inflammatory responses and tissue necrosis (Niinikoski *et al,* 1972b; Franklin and Poyton, 1996); and extended tissue hypoxia is now clinically associated with impaired healing in chronic wounds such as venous and arterial ulcers, and diabetic ulcers (reviewed in Stadelmann *et al,* 1998b). In contrast, transient hypoxia is recognised as a stimulatory factor for numerous cell types, and conventional wisdom suggests that throughout normal wound healing, cells present in the wound site will experience hypoxia and therefore will adapt and respond to low oxygen environments (Niinikoski *et al,* 1991).

The precise spatial and temporal distribution of hypoxia throughout wound healing remains to be defined. Early studies detected reductions in oxygen tension of ~30 mmHg over the first 3-4 days post-wounding, however, these analyses were generally performed using Silastic tubes embedded under the skin, and therefore measured average oxygen tensions in the damaged cutaneous region (Niinikoski *et al,* 1972a; Chang *et al,* 1983). Modern techniques such as polarographic analysis are perhaps more accurate, and have provided much useful data regarding tumour oxygenation (Hockel *et al,* 1991; Brizel *et al,* 1996), yet no significant analysis of wound healing has been attempted using this technology. A recent study, using 2-nitroimidazole hypoxia markers, has provided intriguing new data regarding the wound-induced distribution of hypoxia (Haroon *et al,* 2000), however, further analysis is required before the specific oxygen tensions encountered by cells within the wound site can be elucidated. Despite this lack of clear *in vivo* data, numerous *in vitro* studies have begun to identify the specific effects of altered oxygen tensions on various cell types, and the collective data suggest that hypoxia may be a regulatory factor in several phases of cutaneous tissue repair.

1.3.1 Hypoxia and keratinocyte re-epithelialization

The re-epithelialization of denuded tissue by migrating keratinocytes constitutes an essential phase of wound repair (see section 1.2.3). The exact role of hypoxia in wound re-epithelialization is presently unknown, however early *in vivo* studies identified a potential link between the rapid application of occlusive dressings, subsequent enhancement of re-epithelialization (Winter *et al*, 1962; Alvarez *et al,* 1983; Woodley and Kim, 1992), and the acutely hypoxic wound environment created by these dressings (Varghese *et al,* 1986). Recently, hypoxia has been shown to be a potent stimulus for keratinocyte migration *in vitro*, as keratinocytes cultured under hypoxic conditions showed enhanced migration and *in vitro* wound closure compared to normoxic cells (O'Toole *et al,* 1997b; Xia *et al,* 2001). Moreover, these hypoxic keratinocytes upregulated several MMPs and the TGF-β receptor type I; as well as co-ordinately reducing laminin-5 secretion (O'Toole *et al,* 1997b; Xia *et al,* 2001), presumably to facilitate migration. Interestingly, addition of a TGF-β neutralizing polypeptide completely inhibited both the hypoxic induction of MMP-1 and –9, and the enhanced keratinocyte migration under hypoxic conditions (Xia *et al,* 2001). These observations strongly suggest that hypoxia enhanced keratinocyte migration may be regulated by TGF-β.

In contrast to the potentially beneficial effects of transient hypoxia, prolonged periods of low oxygen tension are frequently associated with chronic wounds. Recently, the relationship between hypoxic keratinocyte responses and age were investigated in a direct comparison of normal human keratinocytes from young donors (20-39y old) and from old donors (≥60y old) (Xia *et al,* 2001). In contrast to young keratinocytes, aged keratinocytes, cultured under hypoxic conditions, showed no difference in MMP-1 expression, a reduction in MMP-9 expression, negligible induction of TGF-β receptor type I expression, and most significantly a reduced migration index. These findings indicate that whereas wound-induced hypoxia may be a positive mediator of migration in young keratinocytes, old keratinocytes seem to loose their tolerance for hypoxic stress, suggesting a potential cause of the increased incidence of chronic wounds in elderly patients (Xia *et al,* 2001).

1.3.2 Hypoxia and fibroblast function

Upon cutaneous wounding, activated fibroblasts invade the provisional matrix, mediate the formation of granulation tissue and modify the ECM to facilitate wound contraction and closure (see sections 1.2.4 and 1.2.5). These wound-induced fibroblast responses are regulated by many factors, including growth factors, cytokines and ECM components. In addition, *in vitro* evidence suggests that hypoxia may also play a role in modulating fibroblast function during wound repair. Early studies identified hypoxia as a positive regulator of fibroblast proliferation and longevity (Falanga and Kirsner, 1993) and culture under conditions of low oxygen tension upregulated dermal fibroblast synthesis of TGF-β (Falanga *et al,* 1991), a known inducer of fibroblast-mediated ECM modification (Roberts and Sporn, 1996). Moreover, several studies have demonstrated that hypoxia regulates fibroblast expression of collagens I and III *in vitro* (Falanga *et al,* 1993; Herrick *et al,* 1996; Yamanaka and Ishikawa, 2000). Furthermore, elevated levels of MMP-1 mRNA can be detected in hypoxic dermal fibroblast cultures (Yamanaka and Ishikawa, 2000), suggesting that hypoxia may mediate fibroblast migration during granulation tissue formation.

In addition to potentially modulating fibroblast function, hypoxia may also influence fibroblast regulation of wound responses. Human dermal fibroblasts exposed to hypoxia increase secretion of the chemokines MCP-1 and IL-8, and conditioned medium from hypoxic fibroblasts is chemotactic for monocytes (Galindo *et al,* 2001) suggesting that fibroblast responses to low oxygen tensions may influence the inflammatory phase of wound healing. Furthermore, VEGF mRNA expression was upregulated in fibroblasts cultured under hypoxic conditions (Detmar *et al,* 1997), indicating that hypoxic fibroblasts may also contribute to angiogenic responses in the wound environment. Although clear *in vivo* data are lacking, these *in vitro* observations indicate that hypoxia may play a part in regulating fibroblast function throughout several phases of wound repair.

1.3.3 Hypoxia and wound angiogenesis

Wound-activated angiogenesis primarily involves migration of endothelial cells into the wound site and subsequent formation of new capillary networks (see section 1.2.6). Endothelial cell angiogenic responses are mediated by an assortment of factors, including cytokines, growth factors, cell-surface receptors and proteolytic enzymes

(reviewed in Carmeliet and Jain, 2000). In addition, environmental alterations, such as a reduction in oxygen tension, can induce the formation of neovasculature (Knighton *et al,* 1981; Adair *et al,* 1990). Under hypoxic conditions *in vitro*, endothelial cells, derived from various tissues, increase expression of IL-1α (Shreeniwas *et al,* 1992), IL-8 (Karakurum *et al,* 1994), the urokinase plasminogen activator receptor (Graham *et al,* 1998; Kroon *et al,* 2000a), and several integrin receptor subunits (Suzuma *et al,* 1998; Kroon *et al,* 2000a); these *in vitro* hypoxic responses may well relate to functions in wound angiogenesis *in vivo*. Hypoxic endothelial cells have also been shown to upregulate VEGF mRNA and protein (Namiki *et al,* 1995; Detmar *et al,* 1997). This is, however, a contentious issue, as other studies failed to detect VEGF in hypoxic endothelial cell cultures, using Northern blot, RT-PCR and ELISA methods of analysis (Marti and Risau, 1998; Kroon *et al,* 2000a). Although it is probable that hypoxic modulation of endothelial cell expression patterns contributes to angiogenesis, the formation of capillary-like tubes, by endothelial cells in a 3-dimensional fibrin matrix, was not enhanced by culture under hypoxic conditions (Kroon *et al,* 2000a). This observation suggests that hypoxia alone is not sufficient to stimulate angiogenesis.

Upon cutaneous wounding, a myriad of cell types become activated and migrate into the wound space. As increased cellular metabolism depletes available oxygen, these cells presumably secrete soluble factors that induce an angiogenic response. Clearly, this makes perfect biological sense; cells are starved of oxygen, cells release pro-angiogenic factors, new capillary networks are formed, and finally, increased vascularization provides the cells with much needed oxygen. In support of this hypothesis, macrophages cultured under hypoxic conditions have been shown to secrete angiogenic factors such as FGF-2 (Kuwabara *et al,* 1995) and VEGF (Knighton *et al,* 1983; Xiong *et al,* 1998). Moreover, conditioned medium from hypoxic macrophages increases endothelial cell growth *in vitro* (Kuwabara *et al,* 1995) and angiogenesis *in vivo* (Xiong *et al,* 1998). In addition, under conditions of low oxygen tension keratinocytes and dermal fibroblasts upregulate VEGF mRNA (Detmar *et al,* 1997; Steinbrech *et al,* 1999).

The exact role of hypoxia in wound angiogenesis *in vivo* requires clarification. Wound-activated keratinocytes express VEGF *in vivo* (Brown *et al,* 1992), and macrophages infiltrating the wound site have been shown to express both FGF-2 and VEGF (Brown *et al,* 1992; Nissen *et al,* 1998; Kibe *et al,* 2000). However, whether this

is due to wound-induced hypoxia, alternative effector molecules, such as growth factors and cytokines, or co-stimulation by multiple factors, is at present unclear. Despite this lack of clear *in vivo* data, recent *in vitro* studies have suggested that angiogenesis is initiated and maintained by numerous distinct, yet interacting, signals. For example, human microvascular endothelial cells, cultured in a fibrin matrix, formed capillary-like tubular structures only when stimulated with both FGF-2 and TNF-α. When stimulated with FGF-2 alone no capillary formation was observed (Koolwijk *et al,* 1996). However, using an identical model of angiogenesis, the same authors were able to induce capillary formation with FGF-2 alone if the cells were cultured under hypoxic conditions (Kroon *et al,* 2000b).

1.4 PLASMINOGEN ACTIVATORS AND CUTANEOUS WOUND HEALING

Throughout cutaneous wound healing, many different proteolytic enzymes, or proteases, are produced. These enzymes are supplied by cells permanent to the skin, such as keratinocytes and fibroblasts, as well as cells that migrate to the skin and are active during wound repair, such as neutrophils and macrophages. Although wound-associated proteases are related by their proteolytic activity, their functions are diverse. One group of enzymes that are of particular interest in the study of cutaneous wound healing are the plasminogen activators, which belong to a tightly regulated proteolytic system known as the plasminogen activator system. Components of this system regulate plasmin-mediated cleavage of ECM components, facilitating cell migration and tissue remodelling (Mignatti *et al,* 1996). Moreover, several non-proteolytic functions that modulate cell adhesion and migration have been attributed to plasminogen activator system components, and these combined functions are believed to be critical in normal cutaneous wound healing.

1.4.1 The plasminogen activator system

The plasminogen activator system has two key components, tissue plasminogen activator (tPA) and urokinase plasminogen activator (uPA). tPA and uPA are serine proteases, and thus belong to the same proteolytic family as leukocyte elastase and cathepsin B. Although evolved from a common ancestral gene (Patthy, 1985), tPA and uPA differ in the domain organisation and function of their noncatalytic regions, as well as having distinct roles in physiological processes that require plasminogen activation. The primary function of plasminogen activators is conversion of the ubiquitous zymogen plasminogen, to active plasmin, a broad spectrum proteolytic enzyme. Control of tPA and uPA functions is mediated by a tightly regulated system involving a specific urokinase receptor, uPAR, and two plasminogen activator inhibitors, PAI-1 and PAI-2. The structure and function of these molecules is discussed below.

1.4.1.1 tPA

tPA was first identified over 35 years ago and has since been demonstrated as a ubiquitous molecule predominantly produced in vascular endothelium (Bell, 1996). The gene for human tPA is located on chromosome 8 (Rajput *et al,* 1985), contains 14

exons, and is ~30 kb in length (Saksela and Rifkin, 1988). tPA is synthesised as a highly glycosylated single-chain polypeptide (sc-tPA) containing 530 amino acid residues (Jornvall *et al,* 1983; Pennica *et al,* 1983), and has a molecular weight of ~70 kDa. Limited proteolysis of the Arg275-Ile276 bond, by plasmin, kallikrein or factor Xa, can convert sc-tPA to two-chain tPA (tc-tPA), although both tPA forms are capable of plasminogen activation (Hoylaerts *et al,* 1982; Petersen *et al,* 1988a). tPA protein is comprised of four domains; an amino-terminal domain, highly homologous to fibrin-binding fingers found in fibronectin (F-domain); a growth factor domain, homologous to EGF (E-domain); two adjacent kringle regions (k1/k2-domain); and a serine protease active site formed of residues His322, Asp371, and Ser478 (P-domain) (figure 1.3).

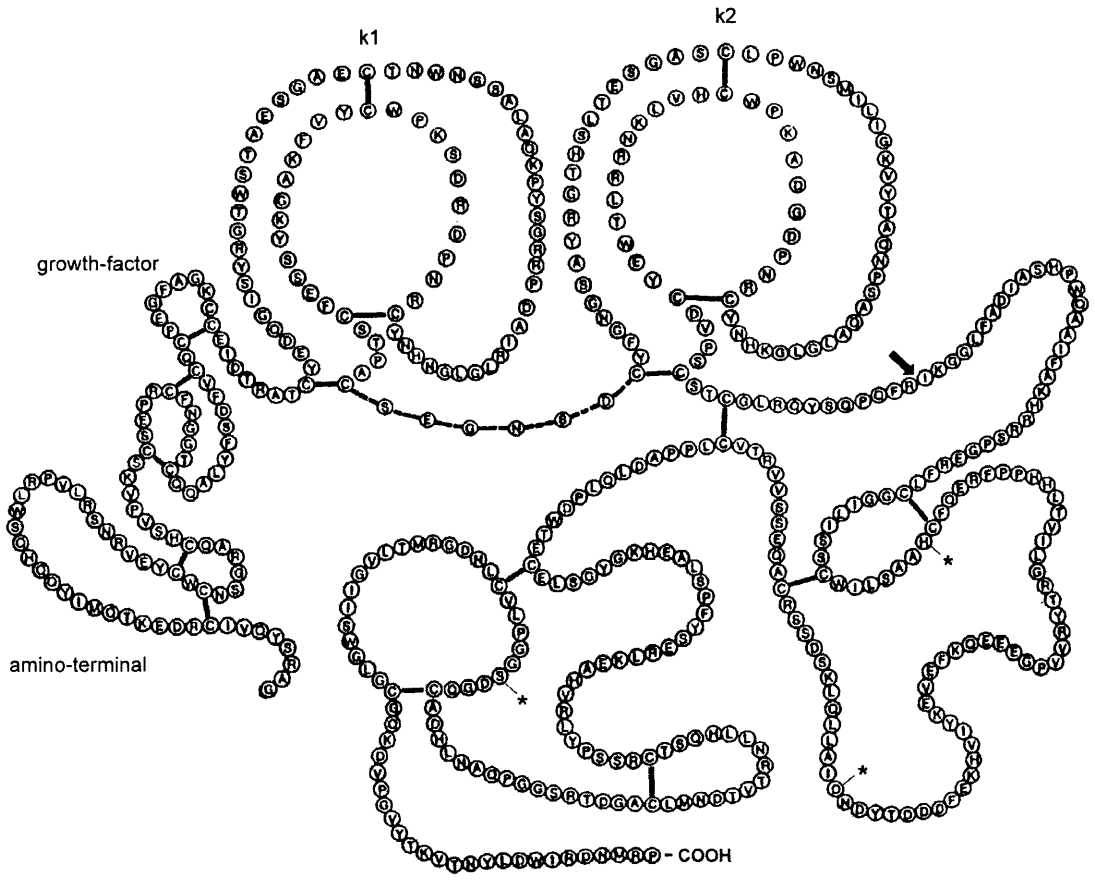

Figure 1.3 Amino acid structure of tPA. Arrow indicates site of proteolytic cleavage converting single-chain tPA to two-chain tPA (Arg275-Ile276). * = amino acid residues comprising the proteolytic site of two-chain tPA (His322, Asp371, and Ser478) (adapted from Pennica *et al,* 1983).

The primary function of tPA is conversion of plasminogen to plasmin, however, tPA alone is a relatively ineffective plasminogen activator. In contrast, in the presence of fibrin, the affinity of tPA for plasminogen is increased and subsequently tPA-

mediated plasminogen activation is markedly enhanced (Hoylaerts *et al,* 1982). Early studies demonstrated that the association of tPA with fibrin was mediated by specific binding via the F-domain and k2 kringle region (van Zonneveld *et al,* 1986). Moreover, as plasmin accumulates and fibrin is partially degraded, newly exposed residues further enhance binding of both tPA and plasminogen, facilitating increased plasminogen activation (reviewed in Collen and Lijnen, 1991). The affinity of tPA for fibrin and the subsequent feedback mechanism whereby plasmin degradation of fibrin enhances tPA:plasminogen interactions, indicate that tPA has an important role in processes that require dissolution of fibrin clots, such as wound healing.

1.4.1.2 uPA

Urokinase was originally isolated from urine, in which it occurs at relatively high concentrations (reviewed in Dano *et al,* 1985). In 1985, the full cDNA for human uPA was cloned (Holmes *et al,* 1985), and demonstrated extensive homology with both mouse (Belin *et al,* 1985) and porcine (Nagamine *et al,* 1984) cDNA sequences. The gene for human uPA is located on chromosome 10 (Rajput *et al,* 1985), contains 11 exons, and has a length of 6.4 kb (Riccio *et al,* 1985). uPA is synthesised as a single chain precursor (pro-uPA) and in humans consists of 411 amino acid residues and has a molecular weight of ~50 kDa (Gunzler *et al,* 1982). In contrast, mouse pro-uPA lacks an N-glycosylation site (Asn-x-Ser/Thr) and consequently has a molecular weight of ~45 kDa (Belin *et al,* 1985). In its single chain form, uPA has minimal intrinsic plasminogen activating activity (Ellis *et al,* 1987; Petersen *et al,* 1988b; Lijnen *et al,* 1990). However, cleavage of the Lys158-Ile159 bond facilitates conversion of the single chain precursor to an active two chain enzyme with enhanced plasminogen activating activity (reviewed in Dano *et al,* 1985). Although this cleavage is predominantly mediated by plasmin, other proteases including cathepsins B and L (Kobayashi *et al,* 1991; Goretzki *et al,* 1992), human mast cell tryptase (Stack and Johnson, 1994), human T cell-associated serine proteinase-1 (Brunner *et al,* 1992), and kallikrein (Ichinose *et al,* 1986; List *et al,* 2000) are capable of activating pro-uPA. Interestingly, pro-uPA can also be cleaved between Glu143 and Leu144. This cleavage, possibly mediated by MMP-3 (Ugwu *et al,* 1998), creates a 32 kDa single chain derivative that can be activated by plasmin, but cannot bind uPAR (Stump *et al,* 1986). In contrast, cleavage by thrombin, between Arg156 and Phe157, produces a relatively inactive single-chain form of pro-uPA that cannot be activated (Ichinose *et al,* 1986).

Active two-chain uPA is comprised of an A-chain and B-chain linked by a single disulphide bond. The amino-terminal A-chain consists of 159 amino acid residues and contains a growth factor-like domain (GFD, aa 4-43) that shares homology with EGF, and mediates binding to the specific urokinase receptor (uPAR) (Appella *et al,* 1987). Moreover, the A-chain also contains a structurally independent kringle domain (aa 45-134, see figure 1.4) that was recently implicated in the induction of cellular chemotaxis by uPA (Mukhina *et al,* 2000). The B chain, consisting of 252 amino acid residues, contains a serine protease active site formed from residues His204, Asp255 and Ser356 (Saksela and Rifkin, 1988). Further plasmin mediated proteolysis, between Lys135 and Lys136, can process two-chain uPA to a 33 kDa molecule containing an intact B chain and 24 residues of the A-chain (Collen and Lijnen, 1991). This 33 kDa uPA is unable to bind uPAR, yet retains its proteolytic activity. Interestingly, a recent study has demonstrated plasmin-mediated cleavage of uPA between Lys46 and Ser47, resulting in the loss of the GFD. The remaining GFD-deficient uPA is unable to bind uPAR, and is rapidly internalised and degraded, possibly via association with a member of the low-density lipoprotein receptor family (Poliakov *et al,* 2001).

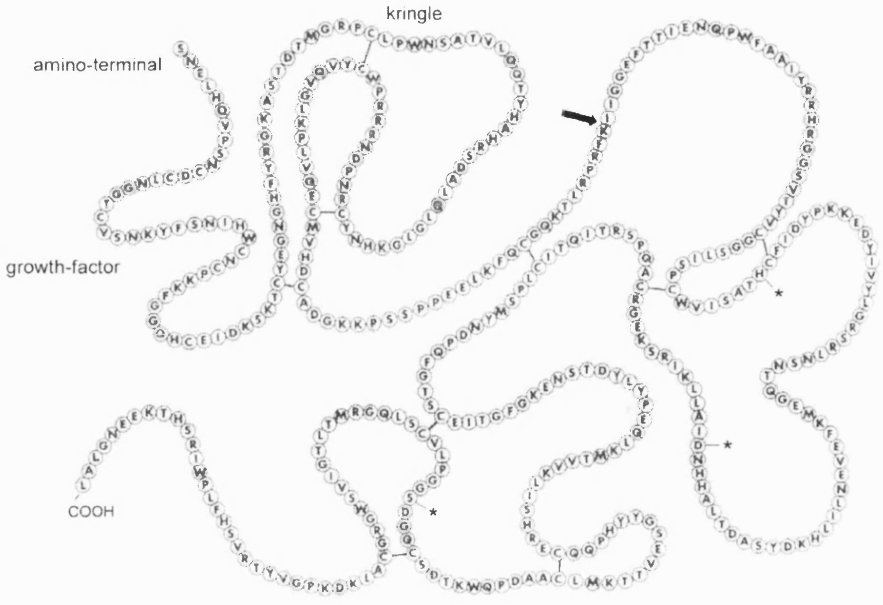

Figure 1.4 Amino acid structure of uPA. Arrow indicates site of proteolytic cleavage converting single-chain uPA to active two-chain uPA (Lys158-Ile159). * = amino acid residues comprising the proteolytic site of two-chain tPA (His204, Asp255 and Ser356) (adapted from Heyneker *et al,* 1983).

uPA is expressed in a variety of cell types from which it is secreted in a single chain form. Secreted pro-uPA can bind uPAR with high affinity, and is converted to active uPA by primarily plasmin-mediated limited proteolysis. Active uPA subsequently converts cell-bound plasminogen to plasmin, a process that can trigger the proteolytic cascade (figure 1.5). Although uPA binding by uPAR increases the efficiency of plasminogen activation (Ellis *et al,* 1991), recent *in vitro* (Longstaff *et al,* 1999), and *in vivo* studies (Bugge *et al,* 1996a; Carmeliet *et al,* 1998) have shown unimpaired uPA-mediated plasminogen activation in uPAR deficient cells and tissues. These observations have indicated that uPA is capable of plasminogen activation in the absence of uPAR, possibly by associating with cell-surface or ECM components (Carmeliet *et al,* 1998; Longstaff *et al,* 1999). An important feature of the proteolytic cascade is the positive feedback loop created by plasmin-mediated activation of pro-uPA and uPA-mediated activation of plasminogen. Due to the ubiquitous nature of plasminogen expression, small amounts of uPA can, via the proteolytic cascade, result in high levels of plasmin, indicating an important role for uPA in processes that require plasmin mediated proteolysis, such as wound healing.

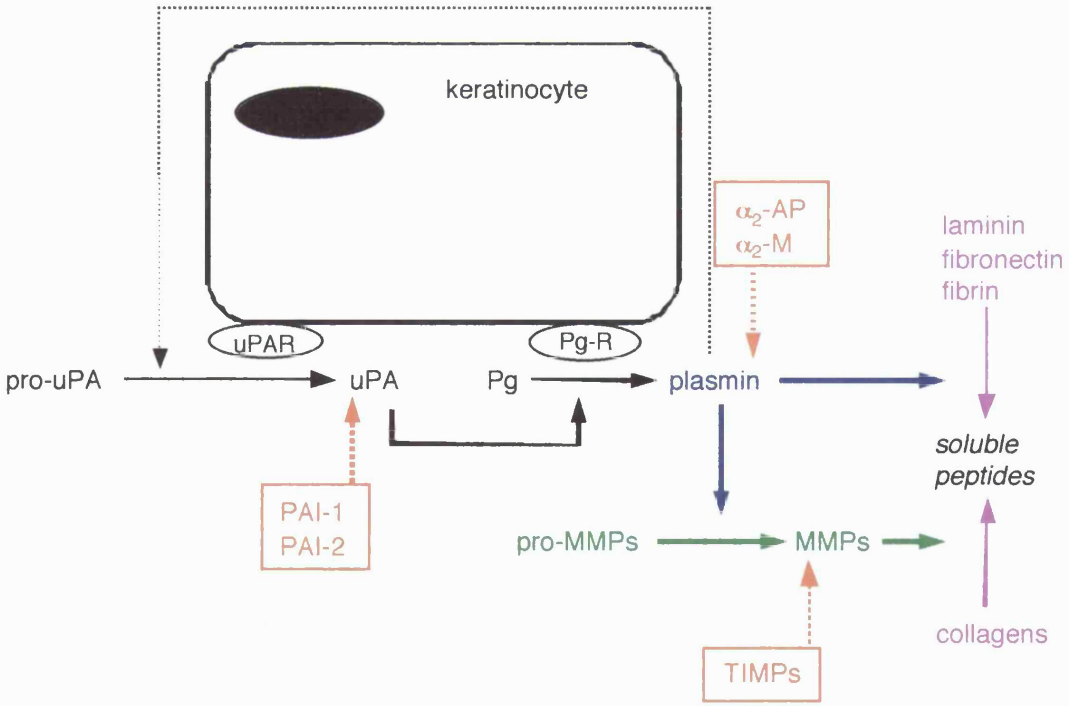

Figure 1.5 Schematic representation of the proteolytic cascade. Red dashed lines indicate inhibition. Abbreviations: Pg = plasminogen; Pg-R = plasminogen receptor; TIMPs = tissue inhibitors of metalloproteinases; α_2-AP = α_2-antiplasmin; α_2-M = α_2-macroglobulin.

1.4.1.3 Conversion of plasminogen to plasmin

The primary function of tPA and uPA is the selective conversion of plasminogen to plasmin. Plasminogen is a 92 kDa glycoprotein that consists of 790 amino acid residues and is present in plasma at high concentrations. Upon cleavage of plasminogen between Arg560 and Val561, the two chain protease plasmin is formed with an active site comprised of His602, Asp645 and Ser740 (reviewed in Collen and Lijnen, 1991). Plasmin, like tPA and uPA, is a member of the serine protease family. However, unlike these relatively selective proteases, plasmin has a broad trypsin-like substrate specificity and can degrade several ECM components, including laminin, fibronectins and fibrin (Mignatti *et al,* 1996) (figure 1.5). Moreover, plasmin can activate certain MMPs (He *et al,* 1989; Mazzieri *et al,* 1997; Ramos-DeSimone *et al,* 1999), as well as several growth factors, such as FGF-2 and TGF-β (Lyons *et al,* 1988; Saksela and Rifkin, 1990). The conversion of plasminogen to plasmin is not exclusively mediated by uPA and tPA. A number of proteases including kallikrein, factors XI and XII and the bacterial protein, streptokinase are capable of plasminogen activation (reviewed in Dano *et al,* 1985), though both uPA and tPA are kinetically more efficient.

1.4.1.4 uPAR

The receptor for human uPA was originally cloned as a 1.4 kb cDNA from an SV40-transformed fibroblast library (Roldan *et al,* 1990). Subsequent studies identified uPAR as a 55-65 kDa single-chain glycoprotein that is folded, through disulphide bonding, into three homologous domains (domains 1-3). Domain 1, consisting of the amino-terminal 87 residues, contains the classical uPA binding site (Behrendt *et al,* 1991). However, recent evidence indicates that distinct regions of domain 3 may also participate in assembly of the ligand-binding site, and domains 2 and 3 increase the affinity of uPA binding to uPAR (Behrendt *et al,* 1996; Ploug, 1998; Gardsvoll *et al,* 1999). Post-translational processing of uPAR at the carboxy-terminal (domain 3) forms a glycosyl-phosphatidyl-inositol (GPI) anchor (Ploug *et al,* 1991), which targets the receptor to the cell surface. Interestingly, specific phospholipase cleavage of the GPI anchor results in a soluble form of uPAR (s-uPAR), detectable in cell supernatants *in vitro* (Mustjoki *et al,* 2000; Sidenius *et al,* 2000), and in various cell types and tissues *in vivo* (Pedersen *et al,* 1993; Ronne *et al,* 1995; Wahlberg *et al,* 1998). On the surface of cells, uPAR exists in either its native three-domain form, or as a two-domain form, lacking domain 1. Two-domain uPAR does not bind uPA, and is created by uPAR

cleavage by uPA or plasmin. This cleavage is thought to be a self-regulating mechanism whereby uPA and plasmin modulate their own activity (Hoyer-Hansen *et al,* 1992).

Upon secretion, pro-uPA can be bound by uPAR and is activated by plasmin-mediated limited proteolysis. uPAR bound uPA subsequently activates cell-bound plasminogen and facilitates localised cell-surface enzyme activity. This feature of the plasminogen activator system has been shown to be highly specialised as several cell types polarise expression of uPAR to the leading edge during migration (Estreicher *et al,* 1990; Romer *et al,* 1994; Okada *et al,* 1995). Moreover, kinetic studies indicate that uPA binding to uPAR actually increases the efficiency of activation of both pro-uPA and plasminogen (Ellis *et al,* 1991). Although localisation of uPA activity is considered to be a primary function of uPAR, recent studies have identified alternative roles for the receptor that are distinct from the proteolytic activity of uPA. uPAR has been implicated in the regulation of cellular adhesion and migration via its interactions with matrix-associated vitronectin (Wei *et al,* 1994; Kanse *et al,* 1996) and integrin receptors (reviewed in Chapman, 1997). Moreover, many of these interactions are enhanced by receptor occupancy by uPA (Waltz and Chapman, 1994; Yebra *et al,* 1999). In addition, interaction of uPA with uPAR has recently been suggested to expose a chemotactic epitope on uPAR that triggers chemotaxis via an as yet unidentified transmembrane protein (Fazioli *et al,* 1997). As uPAR lacks a cytoplasmic signalling domain, the association of uPAR with these transmembrane proteins has been shown to facilitate uPAR-mediated transmission of intracellular signals. Moreover, this signal transduction is suggested to play a part in cell growth and migration (reviewed in Ossowski and Aguirre-Ghiso, 2000) and, thus, uPAR functions are likely to be important in physiological and patho-physiological processes that rely on cell motility.

1.4.1.5 PAI-1

PAI-1 was originally identified in cultured bovine endothelial cells, and known as endothelial plasminogen activator inhibitor (Loskutoff and Edgington, 1977). Further detection of PAI-1 in various cell types and tissues, however, led to its reclassification as plasminogen activator inhibitor type 1 or PAI-1 (Loskutoff *et al,* 1989). The gene for human PAI-1 is located on chromosome 7, consists of 9 exons and has a length of 12.2 kb (Saksela and Rifkin, 1988). Transcription of the PAI-1 gene results in two mRNAs, 2.2 and 3.0 kb in size, that differ in the 3' untranslated region (Ginsburg *et al,* 1986; Ny

et al, 1986). Both mRNAs subsequently translate to a single chain glycoprotein, consisting of 379 amino acid residues, and having a molecular weight of ~52 kDa. PAI-1 is a member of the serine protease inhibitor (serpin) family and inhibits sc-tPA, tc-tPA, active uPA, but not pro-uPA (Andreasen *et al,* 1986). Inhibition of plasminogen activators by PAI-1 is facilitated by high-affinity reversible binding, followed by covalent formation of an irreversible complex via proteolytic cleavage of the Arg346-Met347 bond within the inhibitor (Bell, 1996).

PAI-1 is initially secreted in a conformation possessing full inhibitory activity. However, in contrast to other serpins, inhibitory PAI-1 is an unstable molecule and rapidly converts to an inactive latent form unless stabilised by binding to soluble or matrix-associated vitronectin (Salonen *et al,* 1989; Mimuro and Loskutoff, 1989). Moreover, as plasma concentrations of PAI-1 are in the nanomolar range and concentrations of vitronectin are in the micromolar range, almost all inhibitory PAI-1 in plasma is likely to be in complex with vitronectin (Podor *et al,* 2000). Interestingly, matrix-associated PAI-1 has prolonged inhibitory activity compared to PAI-1 in the fluid phase (Knudsen *et al,* 1987; Levin and Santell, 1987), suggesting that additional matrix-derived stabilising factors may exist. In fact, binding of inhibitory PAI-1 to fibrin enables complex formation with plasminogen activators and facilitates inhibition of fibrinolysis (Wagner *et al,* 1989; Braaten *et al,* 1993). Furthermore, a recent study showed that high affinity binding of PAI-1 to fibrin was only observed in the presence of vitronectin, suggesting that vitronectin and fibrin can co-operate in the binding and stabilisation of inhibitory PAI-1 (Podor *et al,* 2000). In addition to the inhibitory and latent forms, PAI-1 can also exist in a non-inhibitory substrate conformation which is readily cleaved by tPA, uPA and thrombin (Declerck *et al,* 1992). This conversion of substrate PAI-1 to an inactive degradation product is believed to constitute a mechanism whereby the plasminogen activator system regulates its own activity.

As its name suggests, the primary function of PAI-1 is inhibition of plasminogen activation. In fact, of all the serpins, PAI-1 is the most efficient inhibitor of tPA and uPA. Interestingly, several recent studies have identified PAI-1 functions that are independent of its inhibitory actions. For example, PAI-1 binding of vitronectin actually blocks vitronectin binding to uPAR (Deng *et al,* 1996; Kanse *et al,* 1996; Waltz *et al,* 1997) and αv integrins (Stefansson and Lawrence, 1996; Kjoller *et al,* 1997) and, thus, is suggested to constitute a mechanism whereby PAI-1 regulates cell adhesion and

migration (reviewed in Chapman, 1997). Moreover, PAI-1 may regulate vitronectin interactions with uPAR indirectly, as PAI-1:uPA complexes bound to uPAR are internalised resulting in clearance of the receptor from the cell surface (Cubellis *et al,* 1990; Olson *et al,* 1992; Conese *et al,* 1995). In addition, uPA may actually act as an inhibitor of these PAI-1 functions, as the clearance of uPA:PAI-1 complexes would allow vitronectin to associate with specific integrin receptors (Stefansson and Lawrence, 1996). Although the exact mechanisms involved remain to be elucidated, the collective data suggest that the interaction of PAI-1 with vitronectin, integrin receptors and other components of the plasminogen activator system plays an important role in cellular adhesion and motility (reviewed in Chapman, 1997).

1.4.1.6 PAI-2

PAI-2, another serpin, was first described in human placenta and known as placental-type plasminogen activator inhibitor (Kawano *et al,* 1968). Subsequent detection in various cell types and tissues indicated that inhibitor expression was widely distributed *in vivo* and led to its reclassification as PAI-2 (reviewed in Kruithof *et al,* 1995). The gene for human PAI-2 is located on chromosome 18, consists of 8 exons and has a length of 16 kb. Synthesised PAI-2 contains 415 amino acid residues and exists in one of two molecular forms derived from a single mRNA (Belin *et al,* 1989). One form, a non glycosylated protein of ~45 kDa accumulates in the cytosol, whereas the other, a glycosylated protein of ~60 kDa is secreted. Surprisingly, both forms of PAI-2 are functionally and immunologically indistinguishable (Genton *et al,* 1987; Wohlwend *et al,* 1987) and recent studies have suggested that the variant distribution of PAI-2 is a result of both its relatively inefficient internal secretion sequence (von Heijne *et al,* 1991), and its affinity for spontaneous intracellular polymerisation (Mikus and Ny, 1996). The relative distribution of cytosolic PAI-2 and secreted PAI-2 varies widely depending on cell type, but the inhibitor is found mainly intracellularly. However, under certain conditions, the secreted form constitutes the major fraction, suggesting that the cellular distribution of newly synthesised PAI-2 can be modulated (Ye *et al,* 1988; Quax *et al,* 1990). The exact mechanism whereby PAI-2 is secreted remains unclear; however, a recent study identified an ER-Golgi independent secretion pathway in monocytes similar, though not identical, to IL-1β secretion (Ritchie and Booth, 1998).

Like PAI-1, the primary function of PAI-2 is inhibition of plasminogen activation. PAI-2 inhibits active uPA (rate constant: 10^6 M^{-1} s^{-1}) and tc-tPA (rate constant: 2.10^5 M^{-1} s^{-1}), albeit 10 and 50 times less efficiently than PAI-1, respectively. In contrast, PAI-2 is a poor inhibitor of sc-tPA and is unable to inhibit tPA associated with fibrin (Kruithof *et al,* 1995). Interestingly, although pro-uPA is unable to form stable complexes with PAI-2, the single-chain form of uPA can inhibit complex formation of active uPA with PAI-2, indicating a potential regulatory mechanism (Schwartz, 1994). Inhibition of plasminogen activators by PAI-2 is typical of serpin family members, with initial high affinity reversible binding of inhibitor and activator, followed by formation of covalent complexes via the cleavage of the Arg380-Thr381 bond within PAI-2 (Kiso *et al,* 1988). As tPA and uPA are extracellular targets for inhibitors, and a significant proportion of PAI-2 is located intracellularly, alternative functions for cytosolic PAI-2 have been suggested that are distinct from its inhibitory activity. For example, PAI-2 may protect cells from TNF-α-mediated apoptosis (Kumar and Baglioni, 1991; Dickinson *et al,* 1995) and from the cytocidal effects of intracellular mycobacterial and viral infections (Gan *et al,* 1995; Antalis *et al,* 1998). Furthermore, as PAI-2 becomes incorporated into the cornified envelope during epidermal differentiation, it has been suggested that PAI-2 may have an intracellular role associated with the terminal stage of keratinocyte differentiation (Jensen *et al,* 1995).

1.4.2 The plasminogen activator system in cutaneous wound repair

As detailed in section 1.2, wound repair and regeneration is comprised of several overlapping phases. Involvement of the plasminogen activator system in each phase has been investigated and data suggest that components of the plasminogen activator system have important functions throughout wound healing. These functions vary and involve both regulation of plasminogen activation, as well as roles distinct from plasmin-mediated proteolysis. The involvement of plasminogen activator system components in different phases of wound repair and regeneration is discussed in the following sections.

1.4.2.1 The plasminogen activator system in wound clot formation and inflammation

Cutaneous tissue damage is generally characterised by an initial phase involving release of blood constituents from damaged vessels and subsequent formation of a

fibrin-rich clot (see section 1.2.1). As blood plasma is released into the wound area, plasma constituents such as kallikrein and factors XI and XII can directly activate plasminogen in surrounding tissues, albeit with low efficiency (Mignatti *et al,* 1996). Plasma release also provides trace amounts of uPA which can activate tissue plasminogen and initiate the positive feedback loop outlined in figure 1.5. Moreover, further modulation of uPA activity may be provided via cleavage of pro-uPA by plasma kallikrein and thrombin (Ichinose *et al,* 1986). The disruption of vasculature and extravasation of blood constituents can also release plasma tPA and PAI-1, both of which are likely to be associated with the forming fibrin-rich clot. Furthermore, PAI-2 was recently shown to bind to fibrin clots via tissue transglutaminase and factor XIII, facilitating localised inhibition of fibrin clot lysis (Ritchie *et al,* 1999). Interestingly, analysis of human wound sections by overlay zymography (up to 3 days post-wounding (p.w.)) suggested early proteolysis is predominantly plasminogen-independent (Schaefer *et al,* 1994). Moreover, examination of early stage wound fluid (days 1-3 p.w.) showed negligible levels of plasminogen activating activity, but high levels of a uPA stimulatory factor, most probably FGF-2 (Chen *et al,* 1992). In contrast, zymography analysis of animal wound homogenates demonstrated tPA and uPA activity just 8 hours p.w. (Arumugam *et al,* 1999). Taken together, these *in vivo* data suggest that, in the early stages of wound repair, tPA and uPA activity is primarily tissue associated, and subsequent plasmin-mediated proteolysis constitutes only a small portion of total proteolytic activity.

Upon formation of the fibrin clot, inflammatory cells such as PMNs and macrophages migrate into the wound site in response to numerous chemotactic and stimulatory factors (see section 1.2.2 and table 1.1). Interestingly, *in vitro* studies suggest that components of the plasminogen activator system could play a part in this inflammatory cell migration. PMNs are known to express both uPA (Granelli Piperno *et al,* 1977; Heipel and Ossowski, 1986) and uPAR (Miles and Plow, 1989); and uPA has been shown to stimulate chemotaxis in human neutrophils (Gudewicz and Bilboa, 1987). Moreover, uPA also stimulates chemotaxis in monocytes (Resnati *et al,* 1996) and uPAR expression was shown to be a requirement for monocyte chemotaxis towards the chemoattractants, FMLP and recombinant MCP-1 (Gyetko *et al,* 1994). In addition, monocyte differentiation towards a macrophage-like phenotype is accompanied by upregulation of both uPA and uPAR (Stoppelli *et al,* 1985; Picone *et al,* 1989). Despite these suggested *in vitro* functions, immunohistochemical analysis of inflammatory cells

in healing human wounds showed strong uPA and uPAR staining only after 6 days of healing, predominantly in monocytes/macrophages. Both molecules were barely detectable in infiltrating populations 3 days p.w. (Schaefer *et al,* 1994). As inflammatory infiltration begins within 24 hours of tissue injury, this observation suggests that whilst the plasminogen activator system may not play a significant role in the initial migration of inflammatory cells *in vivo*, it may be important for later phases of inflammatory cell recruitment. Interestingly, no difference in wound inflammatory cell recruitment was observed between wild-type and plasminogen knockout mice (Romer *et al,* 1996); suggesting that if plasminogen activation does have a role in wound-induced cellular infiltration, there is sufficient biochemical redundancy to facilitate compensatory mechanisms in its absence.

1.4.2.2 The plasminogen activator system in wound re-epithelialization

Re-epithelialization primarily involves the migration of wound-edge keratinocytes across and through provisional matrix. This keratinocyte migration is facilitated by the actions of various proteolytic enzymes, and there is much evidence suggesting a pivotal role for the plasminogen activator system in this process. In wounding experiments *in vitro*, increased keratinocyte expression of uPA, uPAR and PAI-1 is observed, specifically localised to keratinocytes proximal to the wound edge (Morioka *et al,* 1987a; McNeill and Jensen, 1990; Staiano Coico *et al,* 1996). In addition, analysis of keratinocyte tunnel formation in fibrin matrices showed that upon removal of plasminogen or addition of PAI-1, tunnel formation was severely reduced (Ronfard and Barrandon, 2001). Interestingly, inhibition of uPA was found to have no effect on *in vitro* migration of wounded keratinocyte monolayers (Ando and Jensen, 1996), suggesting that uPA-mediated proteolysis may be essential for migration through a matrix, but not across a substratum. *In vitro* studies have also suggested alternative non-proteolytic roles for the plasminogen activator system. Studies utilising the uPA A-chain or an amino-terminal fragment of the A-chain (uPA-ATF) (i.e. devoid of proteolytic activity) showed that binding of the A-chain/uPA-ATF to uPAR stimulated chemotaxis in a keratinocyte cell line (Del Rosso *et al,* 1990 and 1993). Moreover A-chain binding to uPAR also stimulated keratinocyte expression of endogenous uPA (Fibbi *et al,* 1990); suggesting an autocrine/paracrine mechanism may exist whereby uPA binding to uPAR at the leading edge, stimulates increased uPA expression and subsequently creates a chemotactic gradient. Interestingly, a recent study demonstrated

significant inhibition of migration in wounded keratinocyte monolayers upon transfection of an antisense PAI-1 expression vector. However, the exact mechanism whereby PAI-1 regulates keratinocyte migration has yet to be defined (Li *et al,* 2000a).

One result of the mass influx of cells into a wound site is the secretion of various cytokines and growth factors (see table 1.1). Several of these factors including TGF-α (Schultz *et al,* 1987), TGF-β (Mustoe *et al,* 1987) and EGF (Brown *et al,* 1986 and 1989) have been shown to promote re-epithelialization in animal wound models and it is possible that this enhanced wound closure may be due to effects of these growth factors on components of the plasminogen activator system. Various growth factors and cytokines have been shown to regulate plasminogen activator system components in keratinocytes *in vitro.* TGF-α and EGF increase cell-surface and secreted uPA levels in cultured keratinocytes, via their shared receptor (Jensen and Rodeck, 1993). Moreover, KGF stimulates both keratinocyte migration and uPA-mediated plasminogen activation (Tsuboi *et al,* 1993). In addition, TNF-α and IL-1β increase uPA and uPAR levels in keratinocytes (Bechtel *et al,* 1996), and IL-1β also stimulates tPA secretion (Rox *et al,* 1996). Interestingly, TGF-β stimulation of keratinocytes *in vitro* upregulates expression of both uPA and its primary inhibitor, PAI-1 (Keski-Oja and Koli, 1992). As many of these growth factors and cytokines are produced by keratinocytes, as well as other cell types present in wounded tissue, it is possible that autocrine/paracrine mechanisms regulate components of the plasminogen activator system during wound re-epithelialization.

In addition to the *in vitro* data discussed above, much *in vivo* data exists indicating a central role for the plasminogen activator system in re-epithelialization. In both animal and human studies, uPA and PAI-1 expression is increased significantly in wounded epidermis, with the former detected in both basal and suprabasal keratinocytes and the latter in basal keratinocytes and the basement membrane (Grondahl-Hansen *et al,* 1988; Romer *et al,* 1991). uPAR synthesis is also increased in healing epidermis, with expression restricted to keratinocytes at the leading edge, suggesting a potential role in localised proteolysis (Romer *et al,* 1994). Moreover, examination of healing human burn wounds, indicated that increased expression of PAI-2 occurred throughout the advancing epithelial sheets (Bechtel *et al,* 1998). Immunohistochemical analysis of wounded epidermis showed little or no significant staining for tPA, suggesting uPA is

the primary mediator of keratinocyte-derived proteolysis during re-epithelialization (Grondahl-Hansen *et al,* 1988).

The specific importance of the plasminogen activator system in wound re-epithelialization has been conclusively demonstrated in a variety of *in vivo* transgenic studies. Full thickness incisional wounds in plasminogen knockout mice showed impaired healing that was characterised by severely reduced re-epithelialization (Romer *et al,* 1996). Moreover, uPA/tPA double knockout mice showed almost identical healing impairments (Bugge *et al,* 1996a), indicating an absolute requirement for plasminogen activation during wound re-epithelialization. Interestingly, wounded uPAR/tPA double knockout mice showed normal wound healing (Bugge *et al,* 1996a), suggesting that uPA is capable of mediating re-epithelialization in the absence of its receptor. Further transgenic studies have suggested that defective fibrin lysis is the cause of impaired re-epithelialization in plasminogen knockout mice, as wound closure in mice deficient for both plasminogen and fibrinogen was normal (Bugge *et al,* 1996b). Taken together these observations suggest that plasminogen activation is essential for keratinocyte migration through the fibrin/fibrinogen-rich provisional matrix and, consequently, is critical to wound healing overall.

1.4.2.3 The plasminogen activator system in granulation tissue formation

Wound-induced formation of granulation tissue is facilitated by a mass influx of fibroblasts, endothelial cells and macrophages. Subsequently, new matrix components are produced and the provisional fibrin matrix is replaced with a collagen-rich ECM (see section 1.2.4 and 1.2.5). This tissue remodelling is dependent on a balance between matrix degradation and synthesis and is mediated largely by macrophages (degradation) and fibroblasts (synthesis). The plasminogen activator system may play a role in this phase of wound healing as numerous studies have demonstrated expression of plasminogen activator system components in fibroblasts and macrophages *in vitro*, and many correlate expression of these components with cell growth and migration. In cell proliferation experiments, both uPA and tPA are mitogenic for human skin fibroblasts (De Petro *et al,* 1994). Moreover, interaction of the uPA-ATF with uPAR was able to induce chemotaxis in these cells, suggesting fibroblast migration may be regulated by uPA and uPAR in a non-proteolytic fashion (Anichini *et al,* 1994). In addition, invasion of plasma clots and fibrin matrices by dermal fibroblasts was dependent on plasminogen

activation (Knox *et al,* 1987; Greiling and Clark, 1997) although, as with keratinocytes, fibroblast migration across a substratum was not reliant on plasmin activity (Greiling and Clark, 1997). Macrophage migration is also regulated by components of the plasminogen activator system *in vitro*. In chemotactic studies, monocyte/macrophage migration is dependant on uPAR expression (Gyetko *et al,* 1994), and these migrating cells polarise expression of the receptor to the leading edge (Estreicher *et al,* 1990). Moreover, macrophage migration may be further regulated by PAI-1 inhibition of uPAR interactions with vitronectin (Waltz *et al,* 1997). Interestingly, a recent study demonstrated that PAI-1 expression in a mouse macrophage cell line was upregulated by hypoxia (Pinsky *et al,* 1998), suggesting a mechanism whereby reduced oxygen tensions may modulate macrophage migration.

Considering this wealth of *in vitro* data, it is reasonable to speculate that the plasminogen activator system has a role in granulation tissue formation *in vivo*. Indeed, studies of healing human and animal wounds have shown increased staining for uPA and PAI-1 in fibroblasts and macrophages associated with newly forming granulation tissue. Moreover, staining for uPAR was also increased, specifically in granulation tissue-associated macrophages (Romer *et al,* 1991; Schaefer *et al,* 1994). Interestingly, however, analysis of wound healing in plasminogen knockout mice shows normal infiltration of macrophages and fibroblasts, and normal formation of granulation tissue (Romer *et al,* 1996). Furthermore, although specific analysis of this phase of wound healing was not performed, no gross abnormalities in granulation tissue formation were reported for uPA/tPA, uPAR/tPA, or PAI-1/PAI-2 knockout mice (Bugge *et al,* 1996a; Dougherty *et al,* 1999). Although these results seem to contradict much of the *in vitro* and *in vivo* data, it is possible that, in these knockout mice, alternative proteolytic mechanisms compensate for the loss of plasminogen activator system components during wound-induced granulation tissue formation.

1.4.2.4 The plasminogen activator system in wound angiogenesis

Just prior to the initiation of granulation tissue formation, endothelial cells invade the provisional matrix and mediate the development of new capillary networks. This process of angiogenesis is regulated by various pro-and anti-angiogenic factors that modulate endothelial cell function (see section 1.2.6), and interestingly, the plasminogen activator system may play a part in this phase of wound repair. *In vitro,*

migrating endothelial cells produce elevated levels of uPA, uPAR, and PAI-1 (Pepper *et al,* 1987, 1992 and 1993); and tPA was also detected in supernatants of these cells, although primarily in complex with PAI-1 (Pepper *et al,* 1993). Wound-induced angiogenic factors have also been shown to regulate the plasminogen activator system. uPA, tPA, uPAR, and PAI-1 expression is increased by VEGF in microvascular endothelial cells (Pepper *et al,* 1991). Moreover, FGF-2 stimulation of endothelial cells increased expression of uPA and uPAR *in vitro* (Saksela *et al,* 1987; Mignatti *et al,* 1991). In addition, a recent study showed that the significant increase in endothelial cell uPAR expression upon culture under hypoxic conditions, was increased further following FGF-2 stimulation of the endothelial cells (Kroon *et al,* 2000b), suggesting a potential dual mechanism of uPAR regulation.

Many *in vitro* studies suggest that plasminogen activator system components may be essential for endothelial cell migration and angiogenesis. Blockade of uPAR, using uPA-ATF linked to human serum albumin, significantly reduced endothelial cell migration (Lu *et al,* 1996). Moreover, both FGF-2/TNF-α and FGF-2/hypoxia-stimulated formation of capillary tubes in fibrin matrices was severely impaired by addition of blocking antibodies to uPA and uPAR (Kroon *et al,* 1999 and 2000b). In addition, a recent study demonstrated enhanced migration of microvascular endothelial cells across fibronectin and increased capillary tube formation in fibronectin gels in response to PAI-1 (Isogai *et al,* 2001). These observations thus indicate that multiple components of the plasminogen activator system mediate *in vitro* endothelial cell migration, presumably via the co-ordinated regulation of ECM proteolysis, uPAR-mediated cell adhesion and intracellular signalling.

In addition to the *in vitro* data, many *in vivo* studies have identified a potential requirement for the plasminogen activator system in angiogenesis. This requirement appears, however, to be dependent on the particular circumstances in which angiogenesis occurs. In vascular wounding experiments, reduced angiogenesis in uPA knockout mice was observed after acute myocardial infarction (Heymans *et al,* 1999). Moreover, angiogenesis was significantly reduced in tumours arising from injection of malignant cells engineered to express only A-chain uPA (Evans *et al,* 1997). Furthermore, after implantation of malignant keratinocytes in PAI-1 knockout mice, angiogenesis of the subsequent tumours was impaired (Bajou *et al,* 1998). In contrast, normal endothelial cell migration and subsequent neovascularization was observed in

healing skin wounds from plasminogen knockout mice (Romer *et al,* 1996). Moreover, no gross angiogenic abnormalities were reported in skin wounds from uPA/tPA, uPAR/tPA, or PAI-1/PAI-2 knockout mice (Bugge *et al,* 1996a; Dougherty *et al,* 1999), suggesting that in the cutaneous microenvironment compensatory mechanisms may exist that counteract the loss of plasminogen activator system components.

1.4.2.5 Plasminogen activators and MMPs

Although the plasminogen activator system has many important proteolytic functions throughout the wound healing process, it does not work alone. For many years, studies have investigated the wound-associated activities of MMPs, a group of related proteases that can collectively degrade most, if not all, components of the ECM. At present more than 20 MMPs have been identified, and they are characterised by several common features, including secretion as an inactive proenzyme, an ability to degrade several ECM components, and inhibition by tissue inhibitors of metalloproteinases (TIMPs). Like components of the plasminogen activator system, most MMPs are not expressed at significant levels in resting skin. The one exception to this, MMP-2, is believed to be sequestered in its pro form in the dermal matrix awaiting activation by migrating cells (Murphy and Gavrilovic, 1999). Upon cutaneous wounding, MMP expression and activation is upregulated by various cell types including neutrophils, macrophages, fibroblasts and keratinocytes. These wound-induced MMPs have been suggested to mediate numerous healing functions, including regulation of cellular migration and collagen remodelling, and collectively these functions are likely to be critical for wound healing (reviewed in Parks, 1999).

Many recent *in vitro* studies have begun to identify functional interactions between the plasminogen activator and MMP systems. Plasmin activates several pro-MMPs (He *et al,* 1989; Okumura *et al,* 1997; Murphy and Gavrilovic, 1999), and this feature of MMP activation has been suggested to be a mechanism whereby uPA or tPA-derived plasmin regulates MMP functions. For example, analysis of migration in wounded bronchial epithelial monolayers indicated a potential activation pathway involving uPA-mediated activation of plasmin, plasmin-mediated activation of MMP-9, and MMP-9-mediated initiation of cell migration (Legrand *et al,* 2001). Moreover, a human carcinoma line engineered to express pro-MMP-9 showed enhanced ECM degradation upon addition of plasminogen and pro-MMP-3, suggesting another

potential activation pathway involving uPA, plasmin, MMP-3, and MMP-9 (Ramos-DeSimone *et al,* 1999). In addition, although uPA-derived plasmin activates proMMP-2 and proMMP-9 when all factors are cell-associated, it readily degrades both MMPs in solution (Mazzieri *et al,* 1997), indicating a regulatory mechanism that may prevent excessive MMP-mediated proteolysis. Interestingly, it seems that the interactions are not all one-way. Recent studies have demonstrated that MMP-12 can cleave uPAR on endothelial cells, releasing the uPA binding domain (domain 1) (Koolwijk *et al,* 2001). Moreover, MMP-3 can cleave both pro-uPA and active uPA resulting in the release of a 32 kDa form of uPA that retains its proteolytic activity, but cannot bind uPAR (Ugwu *et al,* 1998). Furthermore, MMP-3 can also cleave the inhibitory form of PAI-1, efficiently inactivating the inhibitor (Lijnen *et al,* 2000). These observations indicate that the plasminogen activator and MMP systems interact with one another and each has the potential to regulate the activity of the other, a feature that may be important during cutaneous wound repair.

1.5 AIMS OF THE STUDY

At the onset of this study, it was becoming increasingly clear that components of the plasminogen activator system were pivotal in many physiological and patho-physiological processes characterised by cellular migration and tissue remodelling, including cutaneous wound repair. In particular, the activity of the predominant cutaneous serine protease, uPA, was strongly implicated in wound-induced cellular migration both *in vitro* and *in vivo*, and knock-out mouse studies had indicated that serine protease-mediated plasminogen activation was required for normal wound re-epithelialization. Although several such knock-out mouse lines had been generated to assess the role of various plasminogen activator system components in cutaneous wound repair, no data were available concerning the effect of elevated uPA levels on wound-induced keratinocyte migration *in vivo*, and moreover, on the overall wound healing process. Thus, the initial aim of the present study was to generate a transgenic system of cutaneous uPA overexpression, by specifically targeting uPA to basal keratinocytes using the keratin 14 promoter/enhancer sequence. The resulting transgenic mice could thus provide useful information regarding the histological and molecular consequences of epidermal uPA overexpression on murine development, physiology and wound repair.

In addition to identifying potential roles for the plasminogen activator system, early reports from cutaneous wound healing models had also indicated that, following skin injury, a significant reduction in tissue oxygen tension was apparent in the cutaneous wound site. Thus, a second aim of this study was to use the current *in vitro* methods of hypoxic culture to analyse the effect of reduced oxygen tension on expression of plasminogen activator system components in a murine keratinocyte cell line, PAM 212. The subsequent data could then be used to speculate on the potential effects of wound-induced hypoxia on keratinocyte regulation of the plasminogen activator system during cutaneous tissue repair *in vivo*.

CHAPTER 2

MATERIALS AND METHODS

2.1 MOLECULAR BIOLOGY METHODS

2.1.1 DNA preparation

Preparation of DNA from various sources was performed as described below.

2.1.1.1 Small-scale plasmid preparation

Ampicillin resistant DH5α colonies (American Type Culture Collection) were picked individually using autoclaved toothpicks, transferred to 5 ml aliquots of LB medium (0.5% yeast extract, 1% bacto-tryptone, 0.5% sodium chloride, 1 mM NaCl) and agitated at 37°C for 8 hours. 1.5 ml aliquots of the subsequent starter cultures were centrifuged at 16,000x g for 1 minute and the cell pellet resuspended in 100 μl of GET solution (50 mM glucose, 10 mM EDTA, 25 mM Tris-HCl, pH 8.0) containing 100 μg/ml lysozyme (Sigma). 200 μl of lysis buffer (0.2 M NaOH, 1% SDS) was added, and the solution gently mixed by inversion, prior to incubation on ice for 5 minutes. 150 μl of neutralization buffer (3 M KOAc) was then added and following vigorous mixing, the solution was centrifuged at 16,000x g for 10 minutes. 400 μl of clarified supernatant was subsequently retained, mixed with 400 μl of PCI (phenol:chlorofom:isoamyl alcohol (24:24:1), Sigma), and centrifuged at 16,000x g for 3 minutes. Finally, 400 μl of the upper aqueous phase was removed to a fresh tube, mixed thoroughly with 1 ml of ethanol, and centrifuged at 16,000x g for 10 minutes. The resulting plasmid DNA pellet was washed once with 500 μl of 70% ethanol, air dried for 5 minutes and resuspended in 40 μl of TE (10 mM Tris pH 8.0, 1 mM EDTA) containing 20 μg/ml RNase A (Sigma). Plasmid DNA samples were stored at –20°C.

2.1.1.2 Large-scale plasmid preparation

Large-scale plasmid preparation was performed using the Qiagen Plasmid Maxi Kit (Qiagen), according to the manufacturer's instructions. Briefly, 200 ml of LB medium was inoculated with 2 ml of starter culture (see section 2.1.1.1) and agitated (200 rpm) at 37°C for 16 hours. The subsequent culture was centrifuged at 6000x g for 15 minutes at 4°C, and the cell pellet resuspended in 10 ml of Buffer P1 (50 mM Tris-HCl, pH 8.0, 10 mM EDTA, 100 μg/ml RNase A). 10 ml of Buffer P2 (0.2 M NaOH, 1% SDS) was added and the solution mixed gently, prior to incubation at room temperature for 5 minutes. 10 ml of Buffer P3 (3 M KOAc) was then added and

following immediate mixing, the solution was incubated on ice for 20 minutes. The subsequent lysed cultures were centrifuged at 20,000x g for 30 minutes at 4°C, and the supernatant was removed to an equilibrated QIAGEN-tip 500 column (Qiagen). After the supernatant was allowed to enter the QIAGEN-tip 500 resin bed by gravity flow, the column was subjected to two washes with 30 ml of Buffer QC (1 M NaCl, 50 mM MOPS, pH 7.0, 15% isopropanol). The flow-through was discarded and 15 ml of Buffer QF (1.25 M NaCl, 50 mM Tris-HCl, pH 8.5, 15% isopropanol) was added to the column to facilitate plasmid DNA elution. The eluate was collected and 10.5 ml of isopropanol was added, prior to thorough mixing and immediate centrifugation at 15,000x g for 30 minutes at 4°C. The resulting plasmid DNA pellet was washed once with 5 ml of 70% ethanol, air dried for 5 minutes and resuspended in 50-100 μl of ddH_20 (dependent on pellet size). Plasmid DNA samples were stored at –20°C.

2.1.1.3 Crude genomic DNA preparation

Tissue samples (approximately 2 mm^2) were incubated in 20 μl of crude DNA extraction buffer (50 mM Tris-HCl, pH 8.0; 20 mM NaCl; 1 mM EDTA; 1% SDS) containing 0.5 mg/ml proteinase K (Roche) at 55°C for 1 hour. 180 μl of ddH_20 was added and solutions were heated at 99°C for 5 minutes, prior to cooling on ice. Crude genomic DNA samples were stored at –20°C.

2.1.1.4 High quality genomic DNA preparation

Tissue samples (approximately 6 mm^2) were incubated in 700 μl of genomic DNA extraction buffer (50 mM Tris-HCl, pH 7.5; 100 mM NaCl, 10 mM EDTA, 1% SDS) containing 0.5 mg/ml proteinase K (Roche) at 55°C for 16 hours. 500 μl of 6 M NaCl was added and the samples agitated for 5 minutes. After centrifugation at 10,000x g for 7 minutes, 750 μl of supernatant was removed to a fresh tube. 500 μl isopropanol was added and the mixture was agitated for 2 minutes, prior to centrifugation at 10,000x g for 5 minutes. The resulting DNA pellet was washed once with 500 μl of 70% ethanol and resuspended in 200 μl of ddH_20.

To facilitate removal of any contaminating protein, resuspended DNA samples were mixed with 200 μl of PCI (phenol:chlorofom:isoamyl alcohol (24:24:1), Sigma) and centrifuged at 16,000x g for 3 minutes. 200 μl of the upper aqueous phase was retained, mixed with 200 μl of chloroform (Sigma), and centrifuged at 16,000x g for 3

minutes. The upper aqueous phase was again retained, and mixed with 20 μl of 7.5 M ammonium acetate and 600 μl of ethanol. DNA precipitation was encouraged by incubation on ice for 10 minutes, followed by 10 minutes centrifugaton at 16,000x g. The resulting pellet was washed once in 1 ml cold (-20°C) 70% ethanol, resuspended in 50-200 μl of ddH_20 (dependent on pellet size) and stored at 4°C.

2.1.1.5 DNA preparation from adherent cells

Cultured cell monolayers were split as described (section 2.2.1) and the cell number determined using a standard haemocytometer (Weber Scientific Int.). Approximately 10,000 cells were transferred to a fresh tube and centrifuged at 15,000x g for 2 minutes. The cell pellet was resuspended in 200 μl of 1x PBS and centrifuged again at 15,000x g for 2 minutes. The resulting cell pellet was resuspended in 20 μl of 1x PCR buffer (50 mM KCl, 20 mM Tris-HCl pH 8.4; Gibco) and subjected to two 10 minute freeze-thaw cycles. 1 μl of proteinase K (20 mg/ml, Roche) was then added and the reaction incubated at 55°C for 30 minutes, followed by heating at 94°C for 10 minutes, cooling on ice, and subsequent storage at –20°C.

2.1.2 Restriction enzyme digestion

Restriction enzyme reactions were prepared by mixing DNA samples with 2μl of the appropriate buffer (buffers used : NEB Buffer 1 (10 mM bis Tris propane-HCl, 10 mM $MgCl_2$, 1 mM dithiothreitol; pH 7.0), NEB Buffer 2 (50 mM NaCl, 10 mM Tris-HCl, 10 mM $MgCl_2$, 1 mM dithiothreitol; pH 7.9), NEB Buffer 3 (100 mM NaCl, 50 mM Tris-HCl, 10 mM $MgCl_2$, 1 mM dithiothreitol; pH 7.9), NEB Buffer 4 (50 mM potassium acetate, 20 mM Tris-acetate, 10 mM magnesium acetate, 1 mM dithiothreitol; pH 7.9), NEB *Bam* HI Buffer (150 mM NaCl, 10 mM Tris-HCl, 10 mM $MgCl_2$, 1 mM dithiothreitol; pH 7.9), NEB *Eco* RI Buffer (50 mM NaCl, 100 mM Tris-HCl, 10 mM $MgCl_2$, 0.025% (v/v) Triton X-100; pH 7.5); New England BioLabs), 0.2 μl 100x BSA (optional), 1 unit/μg of the appropriate restriction enzyme(s) and ddH_20 to give a total volume of 20 μl (see table 2.1 for specific conditions). Reactions were mixed thoroughly and pulse-centrifuged, prior to incubation at 37°C for 4 hours unless otherwise stated (see table 2.1).

Restriction enzyme(s)	NEB Buffer	BSA	Recognition site (5' – 3')	Non-standard Conditions
***Bam* HI**	*Bam* HI	Yes	G▼GATCC	-
***Bgl* I**	3	No	GCCNNNN▼NGGC	-
***Eco* R1**	*Eco* R1	No	G▼AATTC	-
***Eco* RV**	3	Yes	GAT▼ATC	-
***Sma* I**	4	No	CCC▼GGG	25°C-4 hours
***Xba* I**	2	Yes	T▼CTAGA	-
Double digests				
***Xba* I / *Bgl* II**	2	Yes	T▼CTAGA / A▼GATCT	-
***Bam* HI / *Bgl* II**	*Bam* HI	No	G▼GATCC / A▼GATCT	-
***Kpn* I / *Sph* I**	1	Yes	GGTAC▼C / GCATG▼C	-
***Kpn* I / *Xba* I**	2	Yes	GGTAC▼C / T▼CTAGA	-
***Dra* I / *Sma* I**	4	No	TTT▼AAA / CCC▼GGG	25°C-2 hours/37°C-2 hours
***Avr* II / *Sma* I**	4	No	C▼CTAGG / CCC▼GGG	25°C-2 hours/37°C-2 hours
***Hinc* II / *Sma* I**	4	Yes	GTPy▼PuAC/ CCC▼GGG	25°C-2 hours/37°C-2 hours

Table 2.1 Details of specific conditions for restriction enzyme digestions performed.

2.1.3 Ligation and transformation

Agarose-gel purified (see section 2.1.5) insert and vector DNA fragments were mixed at a 3:1 molar ratio (insert:vector) and diluted to a total volume of 8 μl with ddH_20. 1 μl of 10x ligation buffer (500 mM Tris-HCl pH 7.5, 100 mM $MgCl_2$, 100 mM dithiothreitol, 10 mM ATP, 250 μg/ml bovine serum albumin; New England BioLabs) and 1 μl of T4 DNA ligase (30 Weiss units/μl; New England BioLabs) were added, prior to incubation at room temperature for 16 hours. Control reactions were also prepared with insert or vector DNA omitted. 5 μl aliquots of each reaction were added

to 50 μl aliquots of competent DH5α cells on ice, and the transformation reaction mixed gently, prior to incubation on ice for 30 minutes. Cells were then heat-shocked at 42°C for 90 seconds and 500 μl of pre-warmed (37°C) LB medium added. Cultures were agitated (200 rpm) at 37°C for 30 minutes, then 200 μl spread evenly over the surface of LB agar plates (LB medium with 1.5% (w/v) bacteriological agar) containing 100 μg/ml ampicillin (Sigma). Inoculated LB agar plates were incubated at 37°C for 16 hours.

2.1.4 Agarose-gel electrophoresis

A 1% (w/v) agarose (molecular biology grade, Roche) solution in 1x TBE (0.9 M Tris base, 0.9 M boric acid, 20 mM EDTA (pH 8.0)) was heated for 4 minutes in a 500W microwave oven. 2.5 μl of a 10 mg/ml ethidium bromide solution was added to 200 ml of agarose solution which was left to cool at room temperature for 30 minutes. A gel tray was prepared by sealing both ends with autoclave tape and positioning a comb approximately 1 cm from the end of the tray. The agarose solution was then poured into the prepared tray and left to set at room temperature for a further 30 minutes.

Loading samples were prepared by addition of 15% (v/v) of appropriate loading dye (either bromophenol blue (40% (w/v) sucrose solution in 1x TBE with 0.16% (w/v) bromophenol blue crystals) for products >1200 bp, or xylene cyanol (as bromophenol blue, but with 0.16% (w/v) xylene cyanol crystals) for products < 1200 bp). DNA ladders (either the 500 bp DNA ladder (0.25 μg/μl; Roche), comprising fragments between 500 and 5000 bp in 500 bp increments; or the 100 bp DNA ladder (0.25 μg/μl; Roche), comprising fragments between 100 and 1500 bp in 100 bp increments and an additional band of 2642 bp) were also prepared by mixing the stock DNA ladder solution with both bromophenol blue and xylene cyanol loading dyes in a 2:1:1 ratio. The set gel was transferred to an electrophoresis tank (DNA Mini or Midi Sub Electrophoresis Tanks, BioRad) which was filled with 1x TBE to a level approximately 5 mm above the gel surface. 20 μl of each sample and 5 μl of DNA ladder were then loaded into the appropriate wells and the gel run at 95V for 90 minutes. DNA was visualised under ultra-violet (UV) transillumination and the results photographed (Polaroid 677 print film).

2.1.5 Agarose-gel purification of DNA

DNA samples were prepared and separated on a 1% (w/v) agarose gel as described (section 2.1.4). Under long wavelength UV transillumination (302 nm), a slit was made in the gel approximately 3 mm in front of the band of interest into which an appropriately sized piece of DEAE NA 45 charged cellulose membrane (Schleicher & Schuell) was carefully positioned. After 15 minutes of further electrophoresis, DNA bound to the membrane was visualised under long wavelength UV transillumination (302 nm). The membrane was then removed from the gel, cut into 5 mm^2 pieces, and incubated in 300 μl of gel extraction solution (50 mM arginine, 1 M NaCl) at 55°C for 30 minutes. After centrifugation at 16,000x g for 2 minutes, the supernatant was removed to a fresh tube and 900 μl of ethanol added. DNA precipitation was encouraged by incubation at –70°C for 15 minutes, followed by 10 minutes centrifugation at 16,000x g. The resulting DNA pellet was washed once in 500 μl of ice-cold (4°C) 70% ethanol and resuspended in 50 μl of ddH_20.

2.1.6 Spectrophotometry

DNA and RNA yield and purity were assessed by spectrophotometry at 260 and 280 nm, using 100x dilutions of samples in ddH_20. The formulae used were (OD_{260} x 100) x 0.05 = DS DNA yield ($\mu g/\mu l$), and (OD_{260} x 100) x 0.04 = total RNA yield ($\mu g/\mu l$), where 0.05 to 1.2 was the accurate, linear range of absorbance at 260 nm. OD_{260}:OD_{280} ratios of between 1.6 and 2.0 represented high purity genetic material with low protein contamination.

2.1.7 RNA preparation

Homogenisation of tissues

Freshly dissected samples from wild-type or transgenic mice were rapidly transferred to 1.8 ml cryovials and snap frozen in liquid nitrogen for long term storage. Upon removal from liquid nitrogen, tissue samples were transferred to 15 ml Falcon tubes containing 2 ml of Trizol® Reagent (Gibco) and immediately homogenised for 15 seconds using a Polytron (Polytron® PT 1200; Kinematica AG). 1.7 ml of homogenised sample was transferred to a 2 ml microcentrifuge tube and left for 5 minutes at room temperature to allow complete dissociation of nucleoprotein complexes.

Homogenisation of adherent cells

For RNA preparation from adherent cells, PAM 212 keratinocyte monolayers were lysed *in situ* by addition of 1.7 ml of Trizol® Reagent (Gibco) per 60 mm diameter tissue culture dish. The cell lysate was passed through a pipette several times, transferred to a 2 ml microcentrifuge tube and left for 5 minutes at room temperature to allow complete dissociation of nucleoprotein complexes.

RNA extraction

Phase separation of homogenised samples was initiated by addition of 340 μl of chloroform, followed by vigorous mixing for 15 seconds and incubation at room temperature for 3 minutes. After centrifugation at 12,000x g for 15 minutes at 4°C, 1 ml of the colourless upper aqueous phase was carefully transferred to a fresh tube. 850 μl of isopropanol was added and the solution incubated at room temperature for 10 minutes, prior to centrifugation at 12,000x g for 10 minutes at 4°C. The subsequent RNA precipitate was washed once with 2 ml of 75% ethanol and re-centrifuged at 7,500x g for 5 minutes at 4°C. The RNA pellet was then air dried for 7 minutes and resuspended in 30-100 μl of DEPC-treated ddH_20 (autoclaved ddH_20 containing 0.1% (v/v) diethyl pyrocarbonate), depending on the pellet size. RNA samples were incubated at 57°C for 10 minutes to facilitate complete dissolution of RNA, and stored at –80°C.

2.1.8 Primer design and preparation

DNA or mRNA sequences were initially downloaded from the Entrez database (www.ncbi.nlm.nih.gov/Entrez/nucleotide.html) and vector sequences obtained from specific supplier websites. Predicted cloning construct sequences were assembled using EditSeq (v3.82) and MapDraw (v3.03) software (DNASTAR Inc) and primers were designed to span the region of interest using Primer software (v0.5, Whitehead Institute), adapted for Apple Macintosh. Parameters used for selection of individual primers included optimal lengths between 23 and 28 bases, melting temperatures between 57 and 63°C, GC content between 40 and 65%, and self-complementarity of less than 6 bases overall and less than 2 bases at the 3' end. Selected primers were then paired and tested using Amplify software (v1.2, University of Wisconsin) to determine the avidity of primer binding to template, product sizes and the potential for significant dimerisation between paired primers. Finally the specificity of primers was assessed by running a BLAST search (www.ncbi.nlm.nih.gov/BLAST/) to examine the possibility

of amplifying other known sequences. Customised synthesis and purification of all oligonucleotide primers was performed by Sigma Genosys Ltd.

2.1.9 PCR amplification

Target Sequence	Primer Sequences	Program	Size (bp)
Human keratin 14 promoter (K14)	K14-for : 5' CACGATACACCTGACTAGCTGGGTG 3' K14-rev : 5' CATCACCCACAGGCTAGCGCCAACT 3'	94°C 5' (x1) 94°C 30" 60°C 30" (x35) 72°C 30" 72°C 5' (x1)	514
Mutated Human Growth Hormone (HGX)	HGX-for : 5' CTCACCTAGCTGCAATGG 3' HGX-rev : 5' AAGGCACTGCCCTCTTGAAGC 3'	94°C 5' (x1) 94°C 30" 60°C 30" (x35) 72°C 30" 72°C 5' (x1)	352
Cre recombinase	CRE-for : 5' ATCCGAAAAGAAAACGTTGA 3' CRE-rev : 5' ATCCAGGTTACGGATATAGT 3'	94°C 5' (x1) 94°C 1' 60°C 1' (x35) 72°C 1' 72°C 5' (x1)	632
SV40 intron	SV40for : 5' GGACAAACCACAACTAG 3' SV40rev : 5' GTAGAGGTTTTACTTGC 3'	94°C 2' (x1) 94°C 30" 53°C 30" (x30) 72°C 20" 72°C 2' (x1)	183
***In vitro* recombination**	Rec1 : 5' ACTAGTAACGGCCGCCAGTGT 3' Rec2 : 5' ATGGCTGCGAACCAGGGCTGG 3'	94°C 5' (x1) 94°C 1' 60°C 1' (x35) 72°C 1' 72°C 5' (x1)	wt: 1068 rec: 694
***In vivo* recombination**	Rec3 : 5' AGAAAGCCCAAAACACTCCAAAC 3' Rec4 : 5' CCACCTTCAGAGTTTTTCACCAC 3'	94°C 5' (x1) 94°C 1' 60°C 1' (x35) 72°C 1' 72°C 5' (x1)	wt: 739 rec: 365
cDNA probe preparation	cProbe1 : 5' AATGTGCACAGCCATCCAGGT 3' cProbe2 : 5' CCTCAGCTACCTGAGGGCCAT 3'	94°C 5' (x1) 94°C 1' 60°C 1' (x30) 72°C 1' 72°C 5' (x1)	437

Table 2.2 Details of specific conditions for PCR amplifications performed. Primer sequences are shown as forward (sense) primer above reverse (antisense) primer. Size = PCR product size (bp); wt = wild-type unrecombined sequence; rec = recombined sequence; ' = minutes; " = seconds; (xN) = number of cycles.

PCR amplification reactions were prepared as mastermixes and consisted of the following reagents per reaction: 35.5 µl of ddH_20, 5 µl of 10x PCR buffer (500 mM KCl, 200 mM Tris-HCl pH 8.4; Gibco), 2 µl of $MgCl_2$ (50 mM; Gibco), 4 µl of dNTP mix (dATP, dCTP, dGTP and dTTP at 2.5 mM each; Promega) and 1 µl of each primer (diluted to 100 pmole/µl in ddH_20). 0.5 µl of *Taq* DNA polymerase (5 U/µl; Gibco) and 1 µl of DNA template (approximately 150 pg of plasmid DNA or 500 ng of genomic DNA) were then added to each reaction prior to thermocycling using specific PCR conditions as outlined above (table 2.2). Separation and analysis of PCR products was performed as described (section 2.1.4).

2.1.10 RT-PCR

Reverse transcription

Prior to cDNA synthesis, aliquots of total RNA samples were diluted to 0.3 µg/µl in DEPC-treated ddH_20. Reverse transcription reactions were prepared as mastermixes and consisted of the following reagents per reaction: 5 µl of 10x PCR buffer (500 mM KCl, 200 mM Tris-HCl pH 8.4; Gibco), 10 µl of $MgCl_2$ (50 mM; Gibco), 20 µl of dNTP mix (dATP, dCTP, dGTP and dTTP at 2.5 mM each; Promega), 1.5 µl of RNase inhibitor (33 U/µl RNAsin; Promega), 1.5 µl of oligo d(T) primer (0.5 µg/µl; Promega), 1.5 µl of AMV reverse transcriptase (25 U/µl; Promega) and 10.5 µl of diluted RNA sample. Reactions were mixed thoroughly and transferred to an automated thermocycler and heated thus: 42°C for 2 hours, 99°C for 5 minutes and 4°C hold. RT products were stored at –20°C.

RT-PCR amplification

RT-PCR amplification reactions were prepared as mastermixes and consisted of the following reagents per reaction: 14.1 µl of ddH_20, 2.5 µl of 10x PCR buffer (500 mM KCl, 200 mM Tris-HCl pH 8.4; Gibco), 0.5 µl of $MgCl_2$ (50 mM; Gibco), 2 µl of dNTP mix (dATP, dCTP, dGTP and dTTP at 2.5 mM each; Promega), 0.3 µl of each primer (diluted to 100 pmole/µl in ddH_20), 0.3 µl of *Taq* DNA polymerase (5 U/µl; Gibco) and 5 µl of RT product. Reactions were mixed thoroughly and thermocycled thus: 95°C for 5 minutes (1 cycle), 95°C for 1 minute > 60°C for 1 minute > 72°C for 1 minute 20 seconds (25 to 40 cycles), 72°C for 5 minutes (1 cycle) and 4°C hold. RT-PCR amplification products were stored at 4°C. Separation and analysis of RT-PCR amplification products was performed as described (section 2.1.4).

2.1.11 Northern blotting

Formaldehyde-gel electrophoresis and RNA transfer

Formaldehyde gels were prepared thus: 2 g of agarose (molecular biology grade; Roche) was mixed with 146 ml of DEPC treated ddH_20 and 10 ml of 10x MOPS buffer (0.2 M MOPS, 0.3 M NaAc, 10 mM EDTA (pH 8.0) 0.1% DEPC). The agarose solution was heated for 4 minutes in a 500W microwave oven and left to cool at room temperature for 15 minutes. 34 ml of formaldehyde (37% (v/v); Sigma) was then added and the gel solution poured into a prepared gel tray (section 2.1.4) and left to set at room temperature for 15 minutes.

Northern loading buffer was prepared as a mastermix and consisted of the following reagents per sample: 12.5 μl of deionized formamide (Sigma), 2.5 μl of 10x MOPS, 4 μl of formaldehyde (37% (v/v); Sigma) and 1 μl of a 10 mg/ml ethidium bromide solution. Loading samples were prepared by mixing 10 μl of total RNA sample (diluted to 1 $\mu g/\mu l$ in DEPC treated ddH_20) with 20 μl of Northern loading buffer and heating at 65°C for 10 minutes. Samples were chilled on ice and 2 μl of Northern loading dye (50% (v/v) glycerol solution in DEPC treated ddH_20 with 1 mM EDTA, 0.25% (w/v) bromophenol blue crystals and 0.25% (w/v) xylene cyanol crystals) added. The set formaldehyde gel was transferred to an electrophoresis tank (DNA Mini or Midi Sub Electrophoresis Tanks, BioRad) which was filled with 1x MOPS to a level approximately 5 mm above the gel surface. 32 μl of each sample was then loaded into the appropriate wells and the gel run at 100V for 2.5 hours. RNA was visualised under long wavelength UV transillumination (302 nm) and the gel photographed (Polaroid 677 print film) in the presence of a fluorescent ruler (BioRad).

For transfer of formaldehyde-gel separated RNA samples, a transfer tank was filled with 20x SSC (3 M NaCl, 0.3 M sodium citrate; pH 7.0) and an upturned gel tray placed in the centre to act as a platform for the transfer stack. The transfer stack was assembled from the following: 3 sheets of Whatman 3MM paper (Whatman) (equal in length to the gel, but several cms wider at each side), soaked in 20x SSC and positioned on the platform such that the ends dipped into the SSC solution; the gel, positioned wells up; 1 sheet of Hybond N+ nylon membrane (Amersham Pharmacia) cut to the exact size of the gel, pre-wet in ddH_20 and soaked in 20x SSC; 2 sheets of Whatman 3MM paper, cut to the exact size of the gel and soaked in 20x SSC; and finally, a stack

of absorbent towels cut to the approximate size of the gel. Saran wrap was positioned around the gel edges and the stack was weighed down with a Sigma catalogue. RNA transfer was performed for 16 hours at room temperature, after which the transfer stack was dismantled and the membrane washed briefly with 2x SSC. After blotting dry on 3MM paper, RNA was fixed to the membrane by UV crosslinking at 120,000 microjoules.

cDNA probe preparation

The uPA cDNA probe was prepared using a 437 bp PCR product (pos: 865 – 1302) amplified from full length murine uPA cDNA (pDB1519; American Type Culture Collection); amplification was performed using the specific primers, cProbe1 and cProbe2, as described in section 2.1.9. Radioactive oligolabelling was performed using the Oligonucleotide Kit (Amersham Pharmacia). Initially, PCR products were denatured by heating at 99°C for 3 minutes followed by immediate transfer to ice for a further 2 minutes. 50 μl reactions were then prepared by mixing 34 μl of denatured PCR product (1.5 μg/ml in ddH_20), 10 μl of Reagent Mix (a buffered aqueous solution containing dATP, dGTP, dTTP and random hexadeoxyribonucleotides; Amersham Pharmacia), 5 μl of [α-^{32}P]dCTP (3000 Ci/mmol, Amersham Pharmacia) and 1.5 μl of Klenow Fragment (Amersham Pharmacia), prior to incubation at 37°C for 1 hour.

Labelled cDNA probe was separated from unincorporated [α-^{32}P]dCTP using spun-column chromatography. Spun-columns were prepared by plugging the bottom of a 1 ml syringe with glass wool (BDH), and filling the syringe with Sephadex G-50 (Sigma) equilibrated in 1x TEN buffer (10 mM Tris-HCl, pH 8.0; 1 mM EDTA, pH 8.0; 100 mM NaCl). Columns were flushed with TEN buffer and centrifuged at 1600x g in a swing-bucket rotor. 50 μl oligolabelling reactions were mixed with 50 μl of ddH_20, and carefully applied to the spun-column. Columns were centrifuged again at 1600x g and the eluted probe retained and stored at –20°C.

RNA probe (riboprobe) preparation

Radioactive labelling of uPAR and PAI-1 riboprobes was performed using the MAXIscript™ SP6/T7 Kit (Ambion), according to the manufacturer's instructions. Briefly, 20 μl reactions were prepared by mixing 7 μl of nuclease-free ddH_20, 1 μl of linearized DNA template (*Xba* I digested pGEM-uPAR (1 μg/μl) and *Eco* RI digested

pGEM-PAI-1 (1 μg/μl); both kind gifts of Dr F Lupu, Thrombosis Research Institute, London), 2 μl of Transcription Buffer, 1 μl of ATP (10 mM), 1 μl of CTP (10 mM), 1 μl of GTP (10 mM), 5 μl of [α-^{32}P]UTP (800 Ci/mmol, Amersham Pharmacia) and 2 μl of SP6 or T7 polymerase (10 U/μl) containing RNase inhibitor (2 U/μl). Reactions were incubated at 37°C for 1 hour followed by removal of template DNA by addition of 1 μl of RNase-free DNase I (2 U/μl) and incubation at 37°C for 15 minutes. Labelled riboprobe was separated from unincorporated [α-^{32}P]UTP using Quick Spin™ Columns specific for radiolabeled RNA purification (Roche). 21 μl reactions were mixed with 29 μl of nuclease-free dd$H_2$0 (Ambion) and carefully applied to prepared Quick Spin™ Columns, prior to centrifugation at 1100x g for 4 minutes. Eluted riboprobes were transferred to –20°C for short term (up to 24 hours) storage.

Hybridisation

cDNA probed membranes were pre-hybridised in 30 cm hybridisation bottles (Hybaid), containing 15 ml of ExpressHyb™ Hybridization Solution (Clontech), at 68°C for 1 hour. 100 μl of [α-^{32}P]dCTP labelled cDNA probe was heated at 99°C for 5 minutes, mixed with 15 ml of ExpressHyb™ Hybridization Solution and added to the pre-hybridisation solution, prior to hybridisation at 68°C for 1 hour.

Riboprobed membranes were pre-hybridised in 30 cm hybridisation bottles, containing 15 ml of NorthernMax™ Prehybridisation/Hybridisation Buffer (Ambion), at 68°C for 1 hour. 50 μl of [α-^{32}P]UTP labelled riboprobe was mixed with 15 ml of NorthernMax™ Prehybridisation/Hybridisation Buffer and added to the pre-hybridisation solution, prior to hybridisation at 68°C for 16 hours.

Washing and visualisation of Northern blot

Following hybridisation, membranes were exposed to four 15 minute washes each comprising 100 ml of 1x SSC, 0.1% SDS; followed by two washes in 100 ml of 0.1x SSC, 0.1% SDS for 15 minutes each, with all washes performed at 68°C. The membrane was subsequently monitored to ensure specific signal with low background irradiation, sealed in Saran wrap, and exposed to radiographic film (X-OMAT AR scientific imaging film, Kodak) for 2-7 days at –80°C.

Densitometry of Northern blots

Northern blot radiographs and their corresponding RNA gel photographs were scanned using an Epson EP101 scanner attached to a standard IBM computer. Using dedicated Imagemaster software (v1.1), relative mRNA levels were determined for Northern blot bands following equalisation of the 18s and 28s RNA densitometry values between lanes. The control mRNA level was subsequently given an arbitrary value of 100%, and relative differences in mRNA levels expressed as percentage of control.

2.1.12 Southern blotting of PCR products

Agarose-gel electrophoresis and transfer of PCR product

20 μl aliquots of PCR product were prepared and separated on a 1% (w/v) agarose gel as described (section 2.1.4), and the gel photographed under UV transillumination in the presence of a fluorescent ruler (BioRad). A transfer tank was filled with 0.4 M NaOH and an upturned gel tray placed in the centre to act as a platform for the transfer stack. The transfer stack was assembled as described (section 2.1.11) with the following alterations. Sheets of Whatman 3MM paper were soaked in 0.4 M NaOH; the gel was washed in 0.4 M NaOH and positioned wells down, and the sheet of Hybond N+ nylon membrane (Amersham Pharmacia) was soaked in 0.4 M NaOH. PCR product transfer was performed for 4 hours at room temperature, after which the transfer stack was dismantled and the membrane washed briefly with 2x SSC.

Probe preparation and hybridisation

The cDNA probe was prepared using a 514 bp PCR product amplified from the human keratin 14 promoter (K14-for/K14-rev product; see table 2.2). Radioactive oligolabelling and separation of unincorporated [α-^{32}P]dCTP was performed as described (section 2.1.11).

Membranes were pre-hybridised and hybridised as described previously for cDNA membranes (section 2.1.11), with the exception that all steps were performed at 60°C.

Washing and visualisation of Southern blot

Washing and visualisation of the Southern blot was performed as described (section 2.1.11) with the exception that all washes were performed at 60°C, and exposure to radiographic film was limited to 90 seconds at room temperature.

2.1.13 Automated sequencing

DNA sequencing was performed using the ABI PRISM™ Dye Terminator Cycle Sequencing Ready Reaction Kit (ABI Perkin Elmer). 20 μl reaction mixtures, containing 0.5 μg of template DNA, 10 pmoles of specific primer, and 8 μl of ABI PRISM™ Reaction Mix (A-Dye Terminator, C-Dye Terminator, G-Dye Terminator, T-Dye Terminator, dITP, dATP, dCTP, dTTP, Tris-HCl pH 9.0, $MgCl_2$, thermal stable pyrophosphatase and AmpliTaq™ DNA Polymerase), were prepared and thermocycled thus: 96°C for 30 seconds > 50°C for 15 seconds > 60°C for 4 minutes (25 cycles), 4°C (hold). To each reaction, 2 μl of 3 M NaAc pH 4.6 and 50 μl of 95% ethanol were added and DNA precipitation promoted by incubation on ice for 10 minutes, followed by 30 minutes centrifugation at 16,000x g. The resulting DNA pellets were washed with 200 μl of 70% ethanol, dried at 80°C for 1 minute, and resuspended in 5 μl of sequencing loading dye (a formamide:25 mM EDTA (5:1) solution containing 50 mg/ml Blue dextran). Finally, reactions were heated to 95°C for 2 minutes, chilled on ice and 5 μl loaded onto the sequencing gel. Reaction product separation and analysis was performed using a 373 automated DNA sequencer (ABI Perkin Elmer) connected to an Apple Macintosh running EditView sequencing software (v1.0.1, ABI Perkin Elmer). Consensus sequences were assembled using SeqMan software (v3.03, DNASTAR Inc).

2.1.14 Microinjection

Purification of cloning construct

Cloning constructs were excised from K14-uPA-HGX (*Kpn* I/*Sph* I double digest, table 2.1) or K14-uPA$^{(loxTlox)}$-HGX plasmids (*Kpn* I/*Xba* I double digest, table 2.1) as described (section 2.1.2). After agarose gel purification (section 2.1.5), 150 μl of ethanol was added and the solution mixed, prior to incubation at –20°C for 30 minutes. The DNA was centrifuged at 16000x g for 10 minutes and the subsequent pellet exposed to four brief washes in 200 μl of 70% ethanol. The resulting DNA pellet was resuspended in 50 μl of embryo-pure TE (10 mM Tris pH 7.6, 1 mM EDTA, in embryo-

pure ddH_20; Sigma) and the concentration determined by spectrophotometry (section 2.1.6). The cloning constructs were then diluted to 4 ng/μl in embryo-pure TE, filtered in spin-tubes (0.2 μm MC Bucket Filter; Millipore), and aliquoted into pre-rinsed (embryo-pure TE) screw-capped microcentrifuge tubes, prior to storage at –20°C.

Cloning construct microinjection

Microinjection of the cloning constructs from K14-uPA-HGX and K14-uPA$^{(loxTlox)}$-HGX was performed by Ms K Gardiner (Institute of Child Health, UCL) and Dr C Hetherington (Biological Services Department, University of Oxford) respectively. Single-use aliquots were transported to both destinations at –20°C.

2.2 TISSUE CULTURE METHODS

2.2.1 PAM 212 keratinocyte cell culture

The mouse keratinocyte cell line PAM 212 was cultured in RPMI growth medium (RPMI 1640 medium (Gibco) containing 10% (v/v) complement-inactivated newborn calf serum (Gibco), 1% (v/v) L-glutamine (200 mM; Gibco), 1% (v/v) penicillin (10,000 IU/ml) + streptomycin (10,000 μg/ml; Gibco) and 1% HEPES buffer (1 M; Gibco)) and maintained at 37°C in a 20% O_2, 5% CO_2, 75% N_2 atmosphere in a humidified CO_2 incubator (LEEC). Once confluence was reached, cells were briefly washed with 10 ml of RPMI serum free medium to remove serum, and split by the addition of 3.5 ml of 1x Trypsin-EDTA (0.05% Trypsin, 0.53 mM EDTA; Gibco) and incubation at 37°C for 10 minutes. Cell monolayers were washed from the surface of tissue culture dishes by addition of 6.5 ml of RPMI growth medium and the resulting cell suspension centrifuged at 500x g for 5 minutes. Cell pellets were resuspended in 8 ml of RPMI growth medium and 0.5 ml of PAM 212 keratinocyte suspension re-seeded in 75 cm^2 flasks (Costar) after mixing with 9.5 ml of fresh RPMI growth medium.

2.2.2 Chinese hamster ovary (CHO) cell culture

Culture of the CHO cell line was performed as described (section 2.2.1) with the exception that culture was performed in DMEM growth medium (Dublecco's Modified Eagle Medium (Gibco) containing 10% (v/v) complement-inactivated newborn calf

serum (Gibco), 1% (v/v) L-glutamine (200 mM; Gibco), 1% (v/v) penicillin (10,000 IU/ml) + streptomycin (10,000 μg/ml; Gibco)).

2.2.3 Transient transfection

CHO cells were split as described (section 2.2.2) and seeded into 6-well tissue culture plates (Costar) at a density of 2 x 10^5 cells per well. Cells were cultured until approximately 60% confluent and transfected with the appropriate vector DNA using FuGENE™ 6 Transfection Reagent (Roche), according to the manufacturer's instructions. Briefly, 5 μl of FuGENE™ 6 Transfection Reagent was mixed with 95 μl of RPMI serum free medium (RPMI 1640 medium containing 1% (v/v) L-glutamine, 1% (v/v) penicillin + streptomycin and 1% HEPES buffer) in a 1.5 ml microcentrifuge tube and incubated at room temperature for 5 minutes. 100 μl of diluted FuGENE™ 6 Transfection Reagent was then added drop-wise into a second 1.5 ml microcentrifuge tube containing 2 μl of appropriate vector DNA (1 μg/μl) and the transfection solution gently mixed, prior to incubation at room temperature for 15 minutes. Control reactions were also prepared with vector DNA omitted. 400 μl of RPMI growth medium was then added and the diluted transfection solution mixed, prior to transfer to wells containing CHO cell monolayers in 2 ml of RPMI growth medium.

For DNA analysis, transfected cultures were incubated for 30 hours at 37°C in a CO_2 incubator and processed for DNA as described (section 2.1.1.5). For protein analysis, transfected cultures were incubated for 30 hours at 37°C in a CO_2 incubator and the medium refreshed with 2 ml of RPMI serum free medium, prior to a further 24 hours incubation. CHO conditioned medium was then retained, cleared by centrifugation at 1000x g, and stored at –80°C.

2.2.4 Stable transfection

PAM 212 keratinocytes were split as described (section 2.2.1) and seeded into 60 mm diameter tissue culture dishes (Costar) at a density of 2 x 10^5 cells per dish. Cells were cultured until approximately 40% confluent and transfected with the appropriate vector DNA using LIPOFECTIN® Reagent (Gibco), according to the manufacturer's instructions. Briefly, 30 μl of LIPOFECTIN® Reagent was mixed with 70 μl of RPMI serum free medium in a 1.5 ml microcentrifuge and incubated at room temperature for 45 minutes. In a second microcentrifuge, 2 μl of pcDNA.3 vector DNA (1 μg/μl;

containing neomycin resistance gene) and 10 μl of K14-uPA-HGX vector DNA (1 μg/μl) were mixed and RPMI serum free medium added to a total volume of 100 μl. The two solutions were then combined, mixed gently and incubated at room temperature for 15 minutes. Control reactions were also prepared with K14-uPA-HGX vector DNA omitted. 800 μl of RPMI serum free medium was added and the diluted transfection solution gently mixed. PAM 212 keratinocyte monolayers were washed, refreshed with 3 ml of RPMI serum free medium and 1 ml of diluted transfection solution added drop-wise, prior to incubation at 37°C in a CO_2 incubator. After 6 hours, the DNA-containing medium was replaced with 4 ml of RPMI growth medium (see section 2.2.1) and the transfected monolayers were incubated for a further 48 hours.

Transfected PAM 212 keratinocyte monolayers were split as described and resuspended in RPMI selection medium (RPMI growth medium (see section 2.2.1) containing 250 μg/ml geneticin (Roche)), prior to re-seeding in 100 mm diameter tissue culture dishes (Costar). Cultures were maintained in RPMI selection medium for 2 weeks and the resulting neomycin resistant monolayers split (section 2.2.1) into 150 mm diameter tissue culture dishes (Costar) at a density of 1 x 10^3 cells per dish. Following a further 3 weeks' culture in RPMI selection medium, discs of Whatman 3MM paper; cut to 5 mm diameter, autoclaved and soaked in 1x Trypsin-EDTA (Gibco); were placed over each individual neomycin resistant colony and the plate incubated at 37°C for 10 minutes. Each cloning disc was then carefully removed to individual wells of 48-well tissue culture plates (Costar) containing 500 μl of RPMI selection medium. After 1 week, the cloning discs were removed and the colonies allowed to grow to confluence. Viable colonies were split as described (section 2.2.1) and re-seeded in 12-well tissue culture plates (Costar) at a density of 1 x 10^5 cells per well. Cells were cultured until approximately 75% confluent and refreshed with 1 ml of RPMI serum free medium. After 48 hours incubation, conditioned medium was retained, cleared by centrifugation at 1000x g, and stored at –80°C.

2.2.5 Hypoxic conditions

PAM 212 keratinocyte cultures were transferred to dedicated apparatus (Billups Rothenberg Chamber™, ICN; see figure 2.1) and flushed with a 1% O_2, 5% CO_2, 94% N_2 gas mix for 25 minutes. Valves were rapidly closed and the sealed chambers transferred to a 37°C incubator.

Figure 2.1 The Billups Rothenburg Chamber™, used for the culture of cells under hypoxic conditions.

2.2.6 *In vitro* wounding of cell monolayers

PAM 212 keratinocytes were split as described (section 2.2.1) and seeded into 6-well tissue culture plates (Costar) at a density of 2.5 x 10^5 cells per well. Cells were cultured until confluent, when the medium was removed and the cells refreshed with 2 ml of RPMI serum free medium. Cell monolayers were scratched across the well diameter with a blue plastic 1 ml pipette tip, creating a cell-free area approximately 2 mm in width, and cell debris was removed by a brief wash in RPMI serum free medium. The underside of each well was marked across a perpendicular diameter with a scalpel blade to create a constant point of reference. The marked area of the wound was then photographed under phase-contrast microscopy (a Polaroid camera attached to a Labovert FS microscope (Leitz) set at x10 magnification). Wounded monolayers were refreshed with 2 ml of RPMI serum free medium and either cultured at 37°C in a CO_2 incubator (normoxia) or maintained under hypoxic conditions as described (section 2.2.5). Following 16 hours' incubation, the marked area of the wound was again photographed under phase-contrast microscopy.

2.2.6.1 *In vitro* wounding and uPA inhibition

The uPA inhibitor amiloride (Sigma) and the broad-spectrum protease inhibitor p-aminobenzamidine (Sigma) were dissolved in dimethyl sulphoxide (DMSO; Sigma) and ddH_20 respectively, to yield 1M stock solutions. The selective uPA inhibitor WX-293 (a kind gift of Dr K Wosikowski, Wilex Biotechnology GmbH, Munich, Germany) was dissolved in 5% (v/v) ethanol in ddH_20, to yield a 5 mM stock solution. Single-use aliquots of inhibitor stocks were stored at –20°C.

To determine the effects of uPA inhibition on *in vitro* wound healing, inhibitors were analysed in separate experiments, each using two 6-well tissue culture plates containing confluent PAM 212 keratinocyte monolayers. Following wounding and initial photographic analysis as described (section 2.2.6), the wounded monolayers were refreshed thus: for each plate, two wells were refreshed with 4 ml of RPMI serum free medium containing inhibitor (0.4 μl of amiloride stock (0.1 mM final concentration), 4 μl of p-aminobenzamidine stock (1 mM final concentration), 80 μl of WX-293 stock (0.1 mM final concentration) or 160 μl of WX-293 stock (0.2 mM final concentration)); two wells were refreshed with 4 ml of RPMI serum free medium containing controls (0.4 μl of DMSO (amiloride control), 4 μl of ddH_20 (p-aminobenzamidine control) or 160 μl of 5% (v/v) ethanol in ddH_20 (WX-293 control)); and two wells were refreshed with 4 ml of RPMI serum free medium alone (plate control). One plate was then cultured at 37°C in a CO_2 incubator (normoxia) and one maintained under hypoxic conditions as described (section 2.2.5). Following 16 hours' incubation, wounds were photographed again as described (section 2.2.6).

2.2.6.2 *In vitro* wounding and inhibition of migration and proliferation

The inhibitor of cell proliferation, mitomycin C (Sigma), was dissolved in sterile 1x PBS to yield a 0.5 mg/ml stock solution. The inhibitor of cell migration, cytochalasin B (Sigma), was dissolved in DMSO to yield a 10 mM stock solution. Inhibitor stocks were stored at 4°C.

To determine the effects of inhibition of migration and proliferation on *in vitro* wound healing, two 6-well tissue culture plates containing confluent PAM 212 keratinocyte monolayers were incubated thus: for each plate, two wells were refreshed with 4 ml of RPMI serum free medium containing 40 μl of mitomycin C stock (5 μg/ml

final concentration); two wells were refreshed with 4 ml of RPMI serum free medium containing 20 μl of cytochalasin B stock (50 μM final concentration); and two wells were refreshed with 4 ml of RPMI serum free medium containing 20 μl of DMSO (plate control). Cultures were then maintained at 37°C in a CO_2 incubator and after 4 hours, cell monolayers were scratched (vertically and horizontally) with a plastic pipette tip, creating a cell-free 'cross wound'. Following removal of cell debris and initial photographic analysis (section 2.2.6), the wounded monolayers were refreshed thus: mitomycin C pre-treated wells were refreshed with 4 ml of RPMI serum free medium; cytochalasin B pre-treated wells were refreshed with 4 ml of RPMI serum free medium containing 20 μl of cytochalasin B stock (50μM final concentration); and control wells were refreshed with 4 ml of RPMI serum free medium containing 20 μl of DMSO. One plate was then cultured at 37°C in a CO_2 incubator (normoxia) and one maintained under hypoxic conditions (section 2.2.5). Following a further 20 hours' incubation, wounds were photographed again as described (section 2.2.6)

2.2.7 *In vitro* wound analysis

Photographs of *in vitro* wounds, pre- and post-incubation under normoxic and hypoxic conditions, were scanned into an Apple Macintosh computer and the wound area recovered (mm^2) was determined using the public domain NIH Image software (v1.62; developed at the U.S. National Institutes of Health and available for download at www.rsb.info.nih.gov/nih-image/).

2.2.8 Neutralisation of TGF-β and VEGF

Antibody-mediated neutralisation of TGF-β and VEGF was performed as follows. PAM 212 keratinocytes were split as described (section 2.2.1), seeded into two 6-well tissue culture plates (Costar) and cultured until approximately 60% confluent. Cells were refreshed with RPMI serum free medium and maintained at 37°C in a CO_2 incubator for 24 hours. Following a brief wash with RPMI serum free medium, cultures were refreshed thus: for each plate, one well was refreshed with 2 ml of RPMI serum free medium containing 100 μl of rabbit anti-VEGF IgG (1 mg/ml, NeoMarkers); one well was refreshed with 2 ml of RPMI serum free medium containing 100 μl of rabbit anti-TGF-β IgG (1 mg/ml, R&D Systems); one well was refreshed with 2 ml of RPMI serum free medium containing 100 μl of both antibodies as above; one well was refreshed with 2 ml of RPMI serum free medium containing 13 μl of non-specific rabbit

IgGs (7.5 mg/ml, Vector Labs); one well was refreshed with 2 ml of RPMI serum free medium containing 26 μl of non-specific rabbit IgGs (7.5 mg/ml, Vector Labs); and one well was refreshed with 2 ml of RPMI serum free medium containing 200 μl of 1x PBS (plate control). One plate was then cultured at 37°C in a CO_2 incubator (normoxia) and one maintained under hypoxic conditions as described (section 2.2.5). Following 24 hours' incubation, protein lysates were prepared as described (section 2.3.1.1).

2.2.9 Normoxic and hypoxic conditioned medium transfer

Transfer of PAM 212 keratinocyte conditioned medium from normoxic and hypoxic cultures was performed as follows. Day 1: a confluent 75 cm^2 flask (Costar) of PAM 212 keratinocytes was split as described (section 2.2.1) and seeded into two 60 mm diameter tissue culture dishes at a density of 2.5 x 10^5 cells per dish (dishes 1&2). Day 2: a confluent 75 cm^2 flask of PAM 212 keratinocytes was split (section 2.2.1) and seeded into two 60 mm diameter tissue culture dishes at a density of 2.5 x 10^5 cells per dish (dishes 3&4). Day 3: dishes 1&2 were refreshed with 4 ml of RPMI serum free medium, prior to incubation at 37°C in a CO_2 incubator, to facilitate quiescence. Day 4: dishes 1&2 were refreshed with 3 ml of RPMI serum free medium and dish 1 cultured at 37°C in a CO_2 incubator (normoxia) and dish 2 maintained under hypoxic conditions (section 2.2.5). Also on day 4, dishes 3&4 were refreshed with 4 ml of RPMI serum free medium, prior to incubation at 37°C in a CO_2 incubator, to facilitate quiescence. Day 5: quiescent medium was removed from dishes 3&4 and replaced with conditioned medium from dishes 1&2, prior to culture at 37°C in a CO_2 incubator. Immediately after removal of conditioned medium from dishes 1&2, protein or RNA was prepared from the cell monolayers as described (sections 2.3.1.1 and 2.1.7 respectively). Day 6: conditioned medium was removed from dishes 3&4 and protein or RNA was prepared as on day 5.

2.2.10 Analysis of cell viability

Lactate dehydrogenase (LDH) release

LDH released from PAM 212 keratinocytes was determined using the LDH Assay Kit (Sigma) according to the manufacturer's instructions. Briefly, conditioned medium from PAM 212 keratinocyte cultures was retained, cleared by centrifugation at 1000x g for 5 minutes, and stored on ice. Cell monolayers were refreshed with RPMI serum free medium containing 1% (v/v) LDH Lysis Solution and incubated at 37°C.

After 45 minutes, the PAM 212 lysate (100% control) was harvested, cleared by centrifugation as above, and stored on ice. The LDH assay mixture was prepared in a 1.5 ml microcentrifuge tube as a master mix and consisted of the following reagents per reaction: 40 μl of LDH Substrate Solution, 40 μl of LDH Enzyme and 40 μl of LDH Dye Solution. 120 μl of LDH assay mixture was transferred to wells of a 96-well tissue culture plate (Costar) containing 60 μl of PAM 212 conditioned medium or 100% lysis control (each sample was analysed in triplicate wells). Reactions were mixed thoroughly and incubated in the dark at room temperature for 30 minutes. Reactions were terminated by the addition of 18 μl of 1 N HCl (4.3 ml of concentrated hydrochloric acid mixed with 45.7 ml of ddH_20) per well and solutions mixed thoroughly, prior to spectrophotometric analysis at 490 nm absorbance (SpectraCount™ plate reader, Packard BioScience). LDH levels in PAM 212 keratinocyte conditioned medium was determined as a percentage of total LDH (100% lysis control)

Trypan blue exclusion

PAM 212 keratinocyte cultures were split as described (section 2.2.1) and resuspended in RPMI growth medium. 100 μl of PAM 212 suspension was mixed with 100 μl of Trypan blue solution (0.4% (w/v) Trypan blue crystals in 1x PBS) and incubated at room temperature for 5 minutes. Cells were then counted using a standard haemocytometer (Weber Scientific Int.) and the number of stained cells (non viable) was calculated as a percentage of the total cell number (non viable + viable).

2.3 PROTEIN METHODS

2.3.1 Protein preparation

Protein preparation from various sources was performed as described below.

2.3.1.1 Protein preparation from adherent cells

PAM 212 keratinocyte monolayers were exposed to two washes with cold (4°C) 1x PBS and lysed directly in tissue culture dishes by addition of 600 μl of hot (95°C) 2x Gel Loading Buffer (100 mM Tris-HCl pH 6.8, 4% SDS, 20% (v/v) glycerol, 0.1% (w/v) bromophenol blue, 5% (v/v) β-mercaptoethanol) per 60 mm diameter dish. Cell

lysates were harvested using cell scrapers and transferred to pre-chilled (4°C) microcentrifuge tubes on ice. Lysates were then passed through a 26 gauge needle (attached to a 1 ml syringe) four times and centrifuged at 16,000x g for 10 minutes, prior to storage at –20°C.

Conditioned medium from PAM 212 keratinocyte monolayers was rapidly transferred from tissue culture dishes to pre-chilled (4°C) 12 ml centrifuge tubes (Greiner Labortechnik), and centrifuged at 1000x g for 10 minutes at 4°C. Concentration of samples was performed using Centricon® 30 concentrators (Amicon) and Microcon® 30 microconcentrators (Amicon) according to the manufacturer's instructions. Conditioned medium samples were stored at –80°C.

2.3.1.2 Protein preparation from tissues

Freshly dissected tissue from wild-type or transgenic mice was rapidly transferred to 1.8 ml cryovials and snap frozen in liquid nitrogen for long term storage. Upon removal from liquid nitrogen, samples were transferred to 15 ml centrifuge tubes (Falcon) containing 1 ml of Tissue lysis buffer (100 mM Tris-HCl, 2 mM EDTA; pH 7.6) and immediately homogenised for 20 seconds using a power polytron (Polytron® PT 1200; Kinematica AG). Homogenised samples were transferred to 2 ml microcentrifuge tubes and centrifuged at 14,000x g for 30 minutes at 4°C. 800 μl of supernatant was then removed to Spin-X® centrifuge tube filters (Costar), centrifuged at 14,000x g for 15 minutes at 4°C and the filtrate transferred to fresh microcentrifuge tubes on ice.

Tissue homogenate protein levels were determined using the Bradford Reagent (Sigma) protein assay. A 10 mg/ml bovine serum albumin (BSA; Sigma) solution in ddH_20 was prepared and diluted to obtain standards of 2, 1, 0.5, 0.25 and 0.125 mg/ml. 6 μl of sample or standard was mixed with 474 μl of ddH_20 in clean 1.5 ml microcentrifuge tubes, and 120 μl of Bradford Reagent (Sigma) added. Reactions were mixed thoroughly and 120 μl removed to 96-well plates (Costar), prior to spectrophotometry at 595 nm absorbance (SpectraCount™ plate reader, Packard BioScience). Protein levels were determined by reference to the BSA standard curve, and samples diluted to equal concentration, prior to storage at –80°C.

2.3.2 Western blotting

Polyacrylamide Gel Electrophoresis (PAGE) and transfer

Two glass plates (inner : 7.3 x 10.2 cm; outer : 8.3 x 10.2 cm) and 1 mm spacers were assembled in a dedicated apparatus (Mini-PROTEAN II, BioRad). A 10% separating gel solution was prepared by mixing 6 ml of ddH_20, 2.5 ml of 40% acrylamide solution (29:1 (w/v) acrylamide:bisacrylamide, National Diagnostics), 1.25 ml of buffer A (3 M Tris-HCl, pH 8.9) and 0.2 ml of 10% SDS. 100 μl of 10% (w/v) ammonium persulphate and 10 μl of TEMED (*N,N,N',N'*-tetramethylethylenediamine, Sigma) were subsequently added to initiate and accelerate (respectively) the polymerisation process. The gel solution was then carefully poured between the glass plates to a point 2 cm from the top of the inner plate, overlaid with 100 μl of ddH_20-saturated butanol, and left to set at room temperature for 1 hour.

A 4% stacking gel solution was prepared by mixing 5.76 ml of ddH_20, 0.75 ml of 40% acrylamide solution, 0.96 ml of buffer B (850 mM Tris-HCl, pH 6.9) and 0.15 ml of 10% SDS. 100 μl of 10% (w/v) ammonium persulphate and 10 μl of TEMED were added, and, after removal of the ddH_20-saturated butanol, the solution was carefully applied to the top of the separating gel. A 10 well comb (BioRad) was then placed between the glass plates and the gel was left to set at room temperature for 30 minutes.

30 μl loading samples (30 μl of neat cell lysate or 20 μl of concentrated conditioned medium mixed with 10 μl of 2x Gel Loading Buffer (see section 2.3.1.1) were prepared for gel separation by heating at 99°C for 5 minutes. Samples were subsequently chilled on ice and loaded onto the prepared polyacrylamide gel. 10 μl of Kaleidoscope Pre-Stained Standards (BioRad) was also loaded to facilitate accurate product sizing, and the gel run at 150V for 1.5 hours in 1x running buffer (25 mM Tris, 192 mM glycine, 0.2% SDS, pH 8.9).

For transfer of polyacrylamide gel separated samples, a transfer stack was assembled in a dedicated apparatus (Semi-Dry Transfer System, BioRad), from the following: 3 sheets of Whatman 3MM paper, cut to 10 x 12 cm and soaked in transfer buffer (25 mM Tris, 200 mM glycine, 20% (v/v) methanol, pH 8.4); 1 sheet of nitrocellulose membrane (Protran BA 85 Cellulosenitrate, Schleicher & Schuell), cut to

9 x 11 cm and soaked in transfer buffer; the polyacrylamide gel, rinsed in transfer buffer and 3 sheets of Whatman 3MM paper, cut to 10 x 12 cm and soaked in transfer buffer. Lysate and conditioned medium samples were then transferred at 15V for 45 minutes, and equality of loading/transfer was assessed by staining of the membrane in 100 ml of Ponceau S solution (0.5 g of Ponceau S (Sigma) in 1 ml of glacial acetic acid; dilute with 100 ml of ddH_20) for 5 minutes, followed by 5 minutes de-stain in ddH_20.

Immunoblotting and visualisation

Non-specific antibody binding to nitrocellulose membranes was prevented by incubation in 10 ml of Killer Blocking Buffer (KBB; 1 M glycine, 5% dry skimmed milk, 1% BSA, 5% newborn calf serum), at room temperature for 1 hour. Blocked membranes were transferred to 10 ml of KBB containing 40 μl of sheep anti-mouse PAI-1 IgG (1 mg/ml; American Diagnostica), and incubated at 4°C for 16 hours. After three 5 minute washes in 10 ml of TBS-Tween (150 mM NaCl, 25 mM Tris-HCl pH 7.5, 0.05% (v/v) Tween-20), one 10 minute wash in 10 ml of UTG buffer (2 M urea, 100 mM glycine, 1% (v/v) Triton X-100) and a final 5 minute wash in 10 ml of TBS-Tween, membranes were transferred to 10 ml of KBB containing 10 μl of peroxidase-conjugated rabbit anti-sheep immunoglobulins (1.3 mg/ml; Dako) and incubated at room temperature for 1 hour. Membranes were subsequently washed again as described above, incubated in 10 ml of ECL Mix (1:1, detection reagent 1: detection reagent 2; Amersham Pharmacia) for 1 minute, sealed in Saran wrap, and exposed to chemiluminescence sensitive film (Hyperfilm-ECL, Amersham Pharmacia) for 1-15 minutes at room temperature.

2.3.3 Plasminogen-linked zymography

Zymography gel electrophoresis and visualisation

Zymography gels were prepared and assembled as described (section 2.3.2) with the following alterations. The separating gel comprised a 13% solution prepared by mixing 4.3 ml of ddH_20, 5.3 ml of 40% acrylamide solution, 4 ml of gel buffer I (1.5 M Tris, pH 8.6; 0.4% SDS), 1.6 ml of β-casein (2% (w/v) β-casein (Sigma) in 0.375 M Tris, pH 8.6; 0.1% SDS) and 0.8 ml of plasminogen (0.3 mg/ml human plasminogen (Chromogenix) in 0.375 M Tris, pH 8.6; 0.1% SDS). The stacking gel was composed of a 6% solution prepared by mixing 2.7 ml ddH_20, 0.75 ml of 40% acrylamide solution,

1.25 ml of gel buffer II (0.5 M Tris, pH 7.4; 0.4% SDS) and 0.35 ml of 75% glycerine (1:3 (v/v) ddH_20:glycerol).

35 μl loading samples were prepared by mixing 20 μl of conditioned medium or tissue homogenate with 15μl of 2x Tris-Glycine SDS Sample Buffer (Novex). Positive control samples were also prepared by mixing 5 μl of mouse urine with 5 μl of 2x Tris-Glycine SDS Sample Buffer (Novex). Samples were chilled on ice and loaded onto the prepared zymography gel. 10 μl of Kaleidoscope Pre-Stained Standards (BioRad) was also loaded to facilitate accurate product sizing, and the gel run at 150V for 3.5 hours at 4°C in pre-chilled (4°C) 1x Tris-Glycine SDS Running Buffer (Novex).

Following electrophoresis, the gel was incubated in 200 ml of 1x Zymogram Renaturing Buffer (Novex) for 20 minutes, washed once with ddH_20, and incubated in 200 ml of fresh 1x Zymogram Renaturing Buffer (Novex) for a further 20 minutes. The gel was then incubated in 200 ml of 1x Zymogram Developing Buffer (Novex) for 16 hours and stained in 200 ml of Colloidal Blue Staining Kit Solution (Novex) for 6 hours. After 15 minutes de-stain in ddH_20, the gel was dried using the Gel Drying System (Promega) according to the manufacturer's instructions.

Densitometry of zymography gels

Densitometry analysis of uPA activity levels was performed as described in section 2.1.11, with the following changes. Zymography gels were scanned, and relative uPA activity levels determined following direct comparison with a control densitometry value (wild-type value – day 3). The control uPA activity level was subsequently given an arbitrary value of 1, and relative differences expressed as fold induction/reduction.

2.3.4 Indirect chromogenic peptide assay

Plasminogen activation in conditioned medium and tissue homogenates was measured using an indirect chromogenic peptide assay. In 96 well plates (Costar), 60 μl of sample was mixed with 20 μl of S-2251 chromogenic peptide substrate (Chromogenix) (diluted to 2 mg/ml in assay buffer: 30 mM Tris-HCl, pH 7.4; 60 mM NaCl; 0.05% NaN_3), prior to incubation at 37°C for 10 minutes. Control reactions were also prepared with 0.1 mM amiloride (Sigma). 20 μl of human plasminogen (Chromogenix) (diluted to 0.4 mg/ml in assay buffer) was then added and plates were

incubated at 37°C for 3 hours with spectrophotometric analysis at 405 nm absorbance (SpectraCount™ plate reader, Packard BioScience) performed at 20 minutes intervals. The rate of change of absorbance at 405 nm against time was calculated from sample readings, and uPA values (IU/ml or IU/mg) determined by reference to a human urokinase (Calbiochem) standard curve generated in parallel with samples.

2.3.5 VEGF ELISA

Conditioned medium from PAM 212 keratinocyte cultures was harvested as described (section 2.3.1.1) and VEGF levels determined using the Mouse VEGF Quantikine™ M kit (R&D Systems), according to the manufacturer's instructions. Briefly, 50 μl of Assay Diluent 'RD1N' was pipetted into wells of a 96 well microtitre plate coated with a primary polyclonal antibody against murine VEGF. 50 μl of neat or diluted conditioned medium was added to each well and the plate mixed for 1 minute, followed by incubation at room temperature for 2 hours. Wells were then washed 4 times with Kit Wash Buffer and 100 μl of secondary, peroxidase-conjugated, polyclonal anti-VEGF antibody added, prior to incubation at room temperature for a further 2 hours. Wells were washed as before and 100 μl of Kit Substrate Solution added, prior to incubation at room temperature for 30 minutes. 100 μl of Kit Stop Solution was then added and spectrophotometry at 450 nm and 590 nm absorbance (reference filter) was performed using a 96 well plate reader (SpectraCount™ plate reader, Packard BioScience). VEGF concentrations (pg/ml) were determined using dedicated software (iSmart v2.0; Packard BioScience) with reference to the assay standard curve.

2.4 *IN VIVO* METHODS

2.4.1 Mice

All mice used throughout the project were 8-12 weeks old and were housed in microisolator cages in an isolated animal care facility devoid of known mouse pathogens. Mice were maintained on a 12 hours light/12 hours dark cycle and given access to mouse chow and sterilised water. Experiments were performed in accordance with ethical guidelines and complied with Home Office personal and project license restrictions.

2.4.2 Anaesthesia for non-surgical procedures

Preparation of wild-type or transgenic mice for non-surgical procedures was performed by placing individual animals in a dedicated anaesthetic chamber supplied with inhalation anaesthetic (Halothane Ph. Eur.; Merial Animal Health Ltd) via a series 5 T.C. Vaporiser (IMS). Animals were closely observed until the desired level of anaesthesia was attained, as indicated by respiratory rate.

2.4.3 Anaesthesia for surgical procedures

Surgical anaesthetic was prepared by mixing 10 ml of sterile saline, 1.87 ml of xylazine (20 mg/ml; Rompun®, Bayer) and 2.5 ml of ketamine (100 mg/ml; Vetalar™ V, Pharmacia & Upjohn). Wild-type and transgenic animals were weighed individually and surgical anaesthetic administered by intra-peritoneal injection at a dosage of 0.12 ml per 20 g of body mass. Animals were closely observed for the initial 15 minutes to ensure the desired level of anaesthesia was achieved.

2.4.4 Non-reversible anaesthesia

Sacrifice of wild-type or transgenic mice to facilitate tissue collection was performed using a pentobarbitone sodium-based anaesthetic (Sagatal; Rhone Merieux) at lethal dosage. Animals were weighed individually and anaesthetic administered by intra-peritoneal injection at a dosage of 0.2 ml per 20 g of body mass. Animals were closely observed for 5 minutes to ensure absence of life signs.

2.4.5 Intra-dermal injections

pPGK-CRE plasmid DNA (a kind gift of Dr F Sablitzky, The Institute of Genetics, University of Nottingham) was prepared as described (section 2.1.1.2) and diluted to a concentration of 1 μg/μl in TE buffer. Intra-dermal injections were performed on K14-uPA$^{(loxTlox)}$-HGX transgenic mice as follows. Day 0: mice were anaesthetised as described (section 2.4.2) and 50 μl of pPGK-CRE (1 μg/μl) administered to the right ear by intra-dermal injection. As a control, 50 μl of TE was administered to the left ear of each mouse. Day 4: intra-dermal injections were performed as on day 0. Day 7: mice were sacrificed as described (section 2.4.4) and the ears harvested to individual 7 ml tubes, containing 5 ml of PBS-EDTA (1 x PBS, 0.02 M EDTA), prior to incubation at 37°C for 90 minutes. Ears were then split dorsally and

epidermal sheets removed using fine forceps. Genomic DNA was prepared from epidermal sheets as described (section 2.1.1.4).

2.4.6 Tamoxifen treatment

Stock solutions of tamoxifen (Tam) were prepared by dissolving 10 mg of Tam (free base, Sigma) in 100 μl of ethanol. 900 μl of autoclaved sunflower oil was added and the solution mixed by vigorous vortexing. Tam stock solutions were stored at –20°C.

Tamoxifen application was performed on K14-uPA$^{(loxTlox)}$-HGX single transgenic and K14-uPA$^{(loxTlox)}$-HGX/K14-Cre-ER^{T2} double transgenic animals as follows. Day 0: mice were anaesthetised as described (section 2.4.2) and samples of tail tissue removed for storage at –20°C. Days 1-5: a single 100 μl dose of Tam stock solution (10 mg/ml) was administered daily, by intra-peritoneal injection. Day 7 or 12: mice were sacrificed as described (section 2.4.4) and various tissue samples dissected, prior to storage at –20°C. Upon removal from storage, tissue samples were thawed at room temperature and genomic DNA or protein was prepared as described (sections 2.1.1.4 and 2.3.1.2).

2.4.7 Topical application of phorbol 12-myristate 13-acetate

Single application

Phorbol 12-myristate 13-acetate (PMA) stock solutions were prepared by dissolving 1 mg of PMA (Sigma) in 10 ml of ethanol, prior to storage at –20°C. 125 μl of PMA stock solution was then mixed with 875 μl of ethanol to obtain a 12.5 μg/ml working solution.

Wild-type and K6-uPA transgenic mice were anaesthetised as described (section 2.4.2) and 40 μl of PMA working solution topically applied to the right ear of each mouse (0.5 μg of PMA/ear). As a control, 40 μl of ethanol was applied to the left ear of each mouse. After 24 hours, ears were harvested, rapidly transferred to liquid nitrogen and RNA prepared as described (section 2.1.7).

Repeated application

Prolonged PMA treatment of wild-type and K6-uPA transgenic mice was performed as described for the single application, with the following alterations. 40 μl of PMA working solution was applied to both ears of the same mouse (0.5 μg of PMA/ear); control mice received 40 μl of ethanol to each ear; and topical application of PMA was repeated 2 days after the initial dose (day 0) and every 2 days thereafter. PMA treated mice were sacrificed (section 2.4.4) on day 1, day 7 and day 15, and dissected ears transferred to liquid nitrogen, prior to protein preparation as described (section 2.3.1.2). PMA treated mice were also sacrificed on day 15, and dissected ears transferred to individual tubes containing 5 ml of formal saline (Adams Healthcare), prior to processing for histology.

2.4.8 Topical application of retinoic acid

Single application

Retinoic acid (RA) stock solutions were prepared by dissolving 2.5 mg of all trans-RA (Sigma) in 1 ml of ethanol, prior to storage at –80°C. Upon removal from –80°C storage, RA solutions were vigorously mixed by vortexing, prior to application.

RA application was performed as described (section 2.4.7) with the following alteration. 20 μl of RA stock solution (50 μg of RA/ear) and 20 μl of ethanol were applied to the right and left ears, respectively. After 24 hours, ears were harvested, rapidly transferred to liquid nitrogen and RNA prepared as described (section 2.1.7).

Repeated application

Prolonged RA treatment of wild-type and K6-uPA transgenic mice was performed as described for the single dose, with the following alterations. 20 μl of RA stock solution was applied to both ears of the same mouse (50 μg of RA/ear); control mice received 20 μl of ethanol to each ear; and topical application of RA was repeated 24 hours after the initial dose (day 0) and every 24 hours thereafter. RA treated mice were sacrificed (section 2.4.4) on day 1, day 3 and day 7 and dissected ears transferred to liquid nitrogen, prior to protein preparation as described (section 2.3.1.2).

2.4.9 Intra-dermal injection of epidermal growth factor

Epidermal growth factor (EGF) stock solutions were prepared by reconstituting 100 μg of Murine Natural Epidermal Growth Factor (Gibco) in 150 μl of ddH_20.

Wild-type and K6-uPA transgenic mice were anaesthetised as described (section 2.4.2) and 50 μl of EGF (0.66 $\mu g/\mu l$) administered to the right ear by intra-dermal injection. As a control, 50 μl of ddH_20 was administered to the left ear of each mouse. After 24 hours, ears were harvested, rapidly transferred to liquid nitrogen and RNA prepared as described (section 2.1.7).

2.4.10 Tape-stripping

Wild-type and K6-uPA transgenic mice were anaesthetised as described (section 2.4.2) and the right ear of each mouse tape-stripped 8 times using standard Sellotape™. As a control, the left ear of each mouse remained untreated. After 24 hours, ears were harvested, rapidly transferred to liquid nitrogen and RNA prepared as described (section 2.1.7).

2.4.11 *In vivo* wounding

Wild-type and K6-uPA transgenic mice were anaesthetised as described (section 2.4.3). Once a suitable level of anaesthesia was attained, a 5 x 2.5 cm area of back skin was shaved and cleaned thoroughly using 100% ethanol. Two sections of back skin were removed from the shaved area using 4 mm punch biopsies (Stiefel), as shown in figure 2.2. After allowing the wounds to air-dry for 20 minutes, a 5 cm^2 sheet of RELEASE™ Non-adherent Absorbent Dressing (Johnson & Johnson Medical) was applied and secured using Transpore™ tape (3M). Wounded mice were then left on a heated bedding mat (39°C) to recover from surgery and subsequently housed individually in microisolator cages. 24 hours after recovery, dressings were carefully removed to allow full mobility of animals.

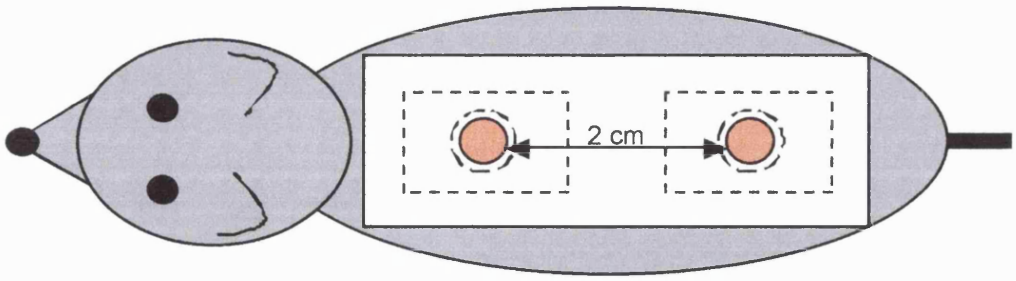

Figure 2.2 Schematic of *in vivo* wounding protocol. White box = shaved area; grey shaded circle = wound region; dashed box = area harvested for sectioning; dashed circle = area harvested for protein analysis.

2.4.11.1 Wound processing for protein analysis

Wounded wild-type and K6-uPA mice were sacrificed (section 2.4.4) 3, 5 or 7 days post-surgery. Viable wounds were carefully dissected within a 1.5 cm^2 section of back skin, immediately trimmed of all non-wound tissue (see figure 2.2) and rapidly transferred to liquid nitrogen. Upon removal from liquid nitrogen storage, wounds from two mice (4 wounds) were pooled and protein prepared as described (section 2.3.1.2).

2.4.11.2 Wound processing for histology

Preparation of wounds for histology was performed as described (section 2.4.11.1) with the following alterations. Dissected 1.5 cm^2 sections of back skin were carefully mounted on 2.5 cm^2 sheets of card, prior to transfer to individual tubes containing 5 ml of formal saline (Adams Healthcare) for no longer than 2 weeks.

Upon removal from formal saline, wounds were divided in half through the least healed portion and embedded in paraffin. Wound specimens were mounted so that the midportion of the wound was cut in 10 μm sections. All wound sections were stained with haematoxylin and eosin (H&E) stains.

2.4.12 *In vivo* wound analysis

H&E stained wound sections from wild-type and K6-uPA transgenic mice were examined under light microscopy (Axioskop 20; Carl Zeiss) and analysed as described below.

2.4.12.1 Wound diameter

Two H&E stained sections per wound were examined at x5 magnification and an Indexed Grid 1.0mm No. Squares graticule (26 mm diameter, Carl Zeiss) used to measure the distance between the leading edge of each migrating epithelial tongue (figure 2.3, panel A). The mean wound diameter for each wound (the average of the wound diameter measurements from two sections) was used for the subsequent statistical analyses.

2.4.12.2 Wound-edge epidermal thickness

Two H&E stained sections per wound were examined at x20 magnification and an Indexed Grid 1.0mm No. Squares graticule used to measure the thickness of epidermis at a point exactly 0.25 mm from the leading edge of each migrating epithelial tongue (figure 2.3, panel B). The mean wound-edge epidermal thickness for each wound (the average of four wound-edge epidermal thickness measurements from two sections) was used for the subsequent statistical analyses.

2.4.12.3 Number of infiltrating cells

One H&E stained section per wound was examined at x40 magnification and the number of infiltrating cells in a defined field 0.125 mm below the migrating epithelial tongue determined using an Indexed Grid 1.0mm No. Squares graticule (figure 2.3, panel C). The field of vision was then shifted towards the wound centre and infiltrating cell numbers determined once more. This procedure was repeated across the wound and the mean number of infiltrating cells (of six) was used for the subsequent statistical analyses.

2.4.13 Genotyping

All animals used in the project were analysed for the presence or absence of incorporated transgenes. Selected mice were scruffed and ear marked for identification, prior to dissection of approximately 0.2 cm of tail tip. Tail tips were transferred to individually labelled 0.5 ml microcentrifuge tubes and stored at –20°C. Upon removal from storage, genomic DNA was prepared as described (section 2.1.1.3) and incorporated transgene detected by specific PCR analysis (see section 2.1.9 and table 2.2).

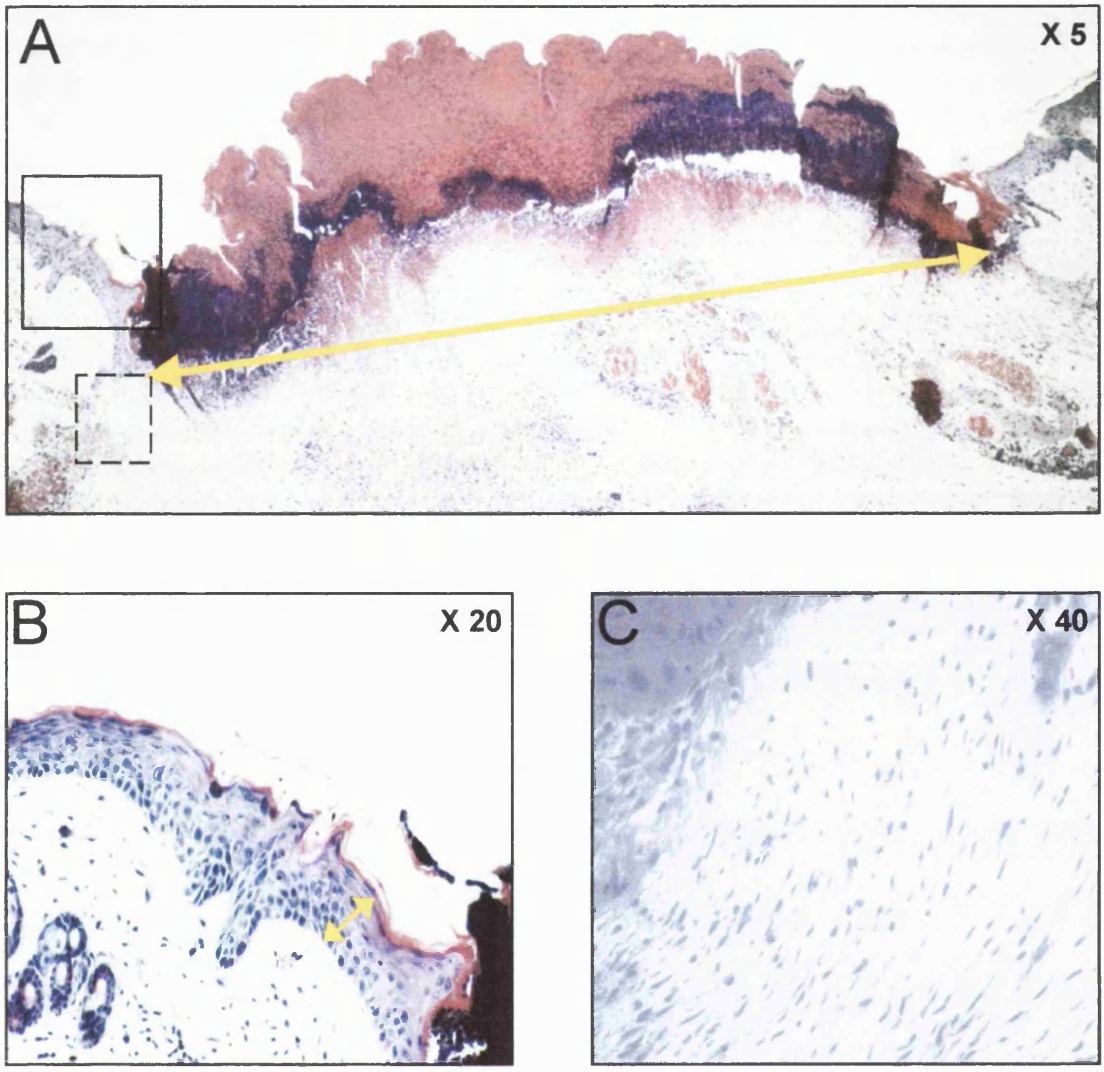

Figure 2.3 Wound analysis strategy. H&E stained sections were analysed at the indicated magnifications, for wound diameter (yellow arrow, panel A), wound-edge epidermal thickness (yellow arrow, panel B) and infiltrating cell number (panel C). Panel B corresponds to solid box in panel A. Panel C corresponds to dashed box in panel A.

CHAPTER 3

K14 PROMOTER DRIVEN CONSTITUTIVE uPA EXPRESSION: IN VITRO *ANALYSIS AND EMBRYONIC LETHALITY ?*

3.1 INTRODUCTION

Following cutaneous injury, cells of varying lineage migrate from adjacent undamaged tissue into the wound area, primarily to facilitate tissue regeneration (see sections 1.2). Wound-induced migration and tissue remodelling are essential for successful wound repair and both processes are highly dependent on the controlled proteolysis of ECM components. The specific proteases and protease systems regulating this cellular motility and matrix modification have been the subject of intense study for many years. However, it is only in the last decade, with the development of *in vitro* wound models and advances in *in vivo* genetic manipulation, that protease function during wound-induced migration and tissue regeneration has been efficiently analysed at the molecular level.

The first protease system associated with wound healing was the plasminogen activator system. This association was initially based on three lines of evidence; firstly, that fibrin and fibronectin are the major constituents of the provisional wound matrix (Clark *et al,* 1982a-c); secondly, that plasmin is a potent fibrinolytic enzyme (Astrup, 1978), and thirdly, that many cell types, including PMNs (Granelli Piperno *et al,* 1977), macrophages (Unkeless *et al,* 1974), endothelial cells (Pepper *et al,* 1987), and keratinocytes (Morioka *et al,* 1987a) produce plasminogen activators *in vitro.* Further evidence for a role in wound repair was subsequently provided by *in vivo* analyses showing that expression of plasminogen activator system components was abnormal in cutaneous wounds. For example, uPA, the predominant plasminogen activator in skin, was significantly upregulated in healing animal and human skin wounds, with increased expression detected in wound-activated keratinocytes, macrophages and fibroblasts (Grondahl-Hansen *et al,* 1988; Romer *et al,* 1991; Schaefer *et al,* 1994). In addition, co-ordinate upregulation of uPAR or PAI-1 was observed in these cell types (Romer *et al,* 1991 and 1994; Schaefer *et al,* 1994), suggesting that, during cutaneous wound healing, the plasminogen activator system is tightly regulated.

In parallel with these *in vivo* wound studies, *in vitro* and *ex vivo* analyses suggested potential roles for the observed wound-induced upregulation of uPA. Macrophage invasion of amnion tissue was inhibited by uPA neutralizing antibodies and PAI-2 (Kirchheimer and Remold, 1989), indicating that uPA activity may be important for macrophage migration during the inflammation and tissue remodelling

phases of wound repair. Moreover, uPA-derived plasmin activity was also required for fibroblast migration into plasma clots (Knox *et al,* 1987), and plasmin was shown to be capable of activating several MMPs (He *et al,* 1989; Okumura *et al,* 1997; Mazzieri *et al,* 1997), suggesting increased uPA activity could be critical during granulation tissue formation and matrix maturation. Furthermore, a role for uPA in endothelial cell migration and possibly wound-angiogenesis was demonstrated, as capillary tube-like formation in fibrin matrices was blocked by inhibitors of uPA proteolytic activity (Koolwijk *et al,* 1996). Interestingly, *in vitro* studies also identified potential non-proteolytic roles for uPA in wound repair, as interaction of the uPA A-chain or ATF with uPAR was shown to initiate signal transduction pathways and promote chemotaxis in several cell types, including monocytes/macrophages (Resnati *et al,* 1996), keratinocytes (Del Rosso *et al,* 1990) and fibroblasts (Anichini *et al,* 1994).

Further importance was attached to the role of the plasminogen activator system in cutaneous wound healing by the generation of knockout mice in which elements of this proteolytic system were deleted. Mice deficient in the plasminogen gene showed severely impaired wound healing that was primarily associated with delayed re-epithelialization (Romer *et al,* 1996). Moreover, analysis of uPA/tPA knockout mice showed identical wound impairments (Bugge *et al,* 1996a), indicating an absolute requirement for plasminogen activation in wound re-epithelialization. In addition, as wound repair in uPAR/tPA knockout mice was normal with no significant delay in re-epithelialization, it was also suggested that uPA is capable of mediating wound closure in the absence of its receptor (Bugge *et al,* 1996a). Interestingly, wound healing in homozygous diabetic mice, which is characterised by delayed cellular infiltration, granulation tissue formation and re-epithelialization; was significantly enhanced upon topical application of uPA, and this enhancement was associated with increased fibroblast and keratinocyte migration (Jimenez *et al,* 1997). Furthermore, in the same study, topical uPA treatment of cutaneous wounds in normal non-diabetic littermates increased wound closure, suggesting that exogenous uPA could potentially stimulate keratinocytes and subsequently promote re-epithelialization.

In addition to data indicating a role for uPA in cell migration and tissue regeneration during normal wound repair, detection of aberrant protease expression in chronic ulcers suggested a potential role for uPA in non-healing wound pathology. uPA activity at both the wound-edge and wound-base of chronic leg ulcers is significantly

increased compared to adjacent intact skin (Stacey *et al,* 1993; Palolahti *et al,* 1993; Lotti and Benci, 1995). Moreover, this uPA activity directly correlates with upregulation of uPA mRNA and protein expression, primarily detected in migrating keratinocytes and granulation tissue (Stacey *et al,* 1993; Vaalamo *et al,* 1996). At the onset of this project, the precise role of abnormal uPA expression in chronic wounds was open to speculation, however, the detection of aberrant levels of other proteases and protease inhibitors suggested that elevated uPA activity could potentially contribute to the pathology of chronic wounds. For example, analysis of wound fluid from chronic leg ulcers showed higher levels of plasmin (Palolahti *et al,* 1993), and lower levels of a plasmin inhibitor, α2-macroglobulin (Grinnell and Zhu, 1996); compared to acute wound fluid, suggesting that uPA-derived plasmin-mediated proteolysis may play a role in ulcer pathology through unregulated excessive degradation of components of the ECM and basement membrane. Moreover, as uPA-derived plasmin had been shown to activate several MMPs (He *et al,* 1989; Baramova *et al,* 1997; Mazzieri *et al,* 1997), and analysis of chronic wounds showed elevated levels of MMP activity (Wysocki *et al,* 1993; Yager *et al,* 1996; Weckroth *et al,* 1996) and reduced levels of TIMP-1 (Bullen *et al,* 1995; Vaalamo *et al,* 1996) compared to acute wounds, the increased uPA expression in non-healing ulcers could trigger a proteolytic cascade further promoting uncontrolled ECM proteolysis.

In view of the extensive data demonstrating that increased uPA expression and activity is a feature of both acute and chronic wounds, as well as data indicating that plasminogen activation is essential for keratinocyte re-epithelialization and subsequent wound closure *in vivo*, it was postulated that forced overexpression of uPA in epidermal tissue might have a significant effect on acute cutaneous wound healing. The aim of the present work was to generate transgenic mice with uPA expression targeted to epidermis by the keratin 14 (K14) promoter. Analysis of these mice would subsequently determine the effect of constitutive epidermal uPA expression on cutaneous physiology and wound repair.

3.2 RESULTS

3.2.1 Creation of constitutive uPA expression vector

To facilitate construction of the constitutive expression vector, uPA cDNA was originally obtained from the American Type Culture Collection (ATCC) in the pDB1519 vector (ATCC #: 63256). This vector consists of a 2.0 kb *Xba*I-*Sma*I fragment, containing the complete murine uPA coding sequence (position: 21–1322), cloned into the cognate sites of pUC19. Following large scale plasmid preparation, a 1670 bp *Xba*I-*Bgl*II restriction digest product, containing murine uPA, was isolated from pDB1519 and ligated into *Xba*I-*Bgl*II digested pET.5a (Promega). Sub-cloning of the uPA cDNA in pET.5a was necessary to ensure availability of the cohesive ends required for ligation with the selected transgene expression vector. pET.5a-uPA vector was subsequently digested with *Bam*HI and *Bgl*II, and a 1748 bp restriction digest fragment, containing 1670 bp of murine uPA and 78 bp of pET.5a polylinker sequence, was isolated.

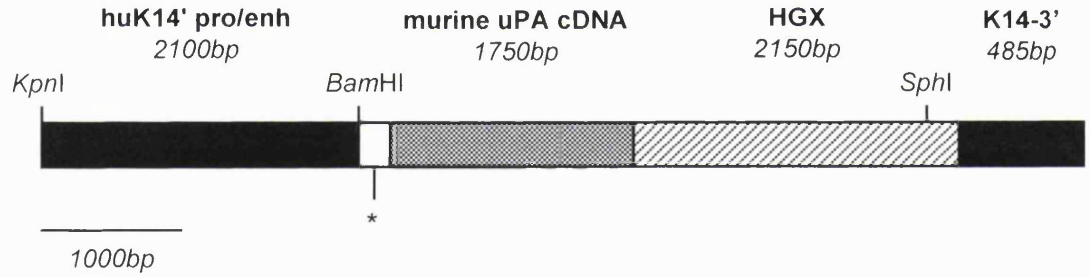

Figure 3.1 Schematic representation of the constitutive uPA expression vector, K14-uPA-HGX. huK14 pro/enh = human Keratin-14 promoter/enhancer sequence; HGX = mutated Human Growth Hormone/PolyA sequence; K14-3' = human Keratin-14 3' sequence; * = 78 bp sequence derived from pET.5a polylinker.

The vector selected for constitutive *in vivo* expression of murine uPA was K14-HGX (a kind gift of Prof. Ifor Williams, Harvard Medical School, Boston, MA, USA). The K14-HGX vector consists primarily of a 2.1 kb human keratin 14 promoter/enhancer sequence, upstream of a *Bam*HI cloning site; a 2.15 kb mutated Human Growth Hormone/Poly A sequence, previously modified so that it no longer supported transcription of active growth hormone (Williams *et al,* 1997); and a 485 bp sequence derived from the 3' end of keratin 14. Following large scale plasmid preparation, K14-HGX was digested with *Bam*HI and ligated with the 1748bp *Bam*HI-

*Bgl*II restriction digest product, isolated from pET.5a-uPA. The resulting constitutive uPA expression vector, K14-uPA-HGX (figure 3.1), was sequenced and the uPA coding region was found to be identical to the published sequence for murine uPA (GenBank Accession No. X-02389).

3.2.2 Analysis of functional uPA expression by K14-uPA-HGX

To determine the functionality of the K14-uPA-HGX construct, PAM 212 keratinocyte monolayers were co-transfected with K14-uPA-HGX and pcDNA.3 or transfected with pcDNA.3 alone. Co-transfection with pcDNA.3 was necessary as the K14-HGX expression vector does not contain a neomycin-resistance gene. Following culture in the presence of geneticin, neomycin-resistant colonies were selected and uPA activity in conditioned medium assessed by indirect chromogenic peptide assay. The level of functional uPA secreted was consistently increased in PAM 212 keratinocyte colonies co-transfected with K14-uPA-HGX and pcDNA.3, compared with control colonies transfected with pcDNA.3 alone. uPA levels detected in conditioned medium from representative neomycin-resistant colonies, 5.96 ± 1.25 IU/ml in co-transfected PAM 212 keratinocytes and 0.25 ± 0.0125 IU/ml in control colonies, are shown in figure 3.2.

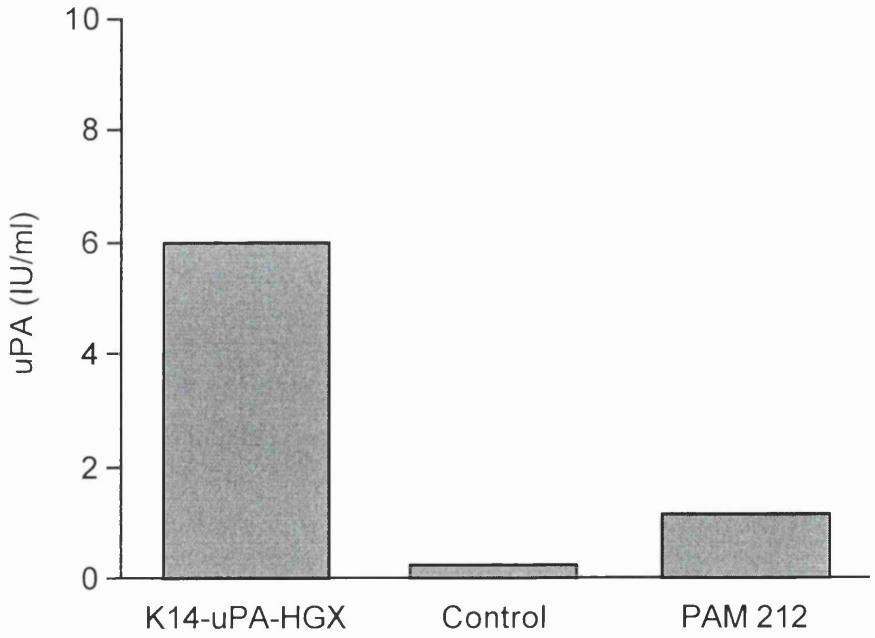

Figure 3.2 Detection of functional uPA expression by K14-uPA-HGX. Indirect chromogenic peptide assay analysis of uPA activity in conditioned medium from PAM 212 keratinocytes transfected with K14-uPA-HGX and pcDNA.3 (K14-uPA-HGX) or pcDNA.3 alone (Control). PAM 212 = untransfected control colonies cultured in absence of geneticin. Data presented (mean) are from 2 independent experiments.

3.2.3 K14-uPA-HGX microinjection and analysis of viable progeny

Having demonstrated functionality of the constitutive expression construct, a 5745 bp *Kpn*I-*Sph*I restriction digest product, containing the human K14 promoter/enhancer region, the full murine uPA coding sequence and the mutated Human Growth Hormone/Poly A region, was isolated from K14-uPA-HGX. Following purification, the isolated transgene was microinjected into fertilised mouse eggs, prior to transfer to recipient pseudo-pregnant females. Subsequent transgene incorporation was analysed in viable progeny by K14 and HGX specific PCR. The micro-injection schedule detailed in table 3.1 shows the successful detection of a single transgenic founder animal (#30) from a total of 37 progeny. This rate of transgenesis (1/37; 2.7%) was below that normally associated with the Institute of Child Health transgenic unit (1-2/20; 5-10%) and suggested that uPA expression might be toxic during mouse development. Interestingly, PCR analysis of tissue samples from the transgenic founder animal resulted in extremely low band intensities, suggesting the possibility of mosaic incorporation, and as a consequence, the K14 PCR product was analysed by Southern blotting to confirm that transgene incorporation had occurred.

Eggs injected and transferred	Recipient females	Viable progeny	uPA transgenics identified
435	13	37	1

Table 3.1 Summary of K14-uPA-HGX microinjection schedule and transgenic progeny detection.

Following positive identification of the K14 PCR product by Southern blotting, as shown in figure 3.3, the transgenic founder male was examined macroscopically and found to have a normal phenotype. Histochemical analysis of tissue samples from this animal also showed no gross skin abnormalities. The founder male was subsequently mated with wild-type females and the progeny analysed by K14 and HGX specific PCR. All offspring resulting from these breeding pairs were negative for the transgene, further suggesting that mosaic incorporation had occurred in the founder male (#30).

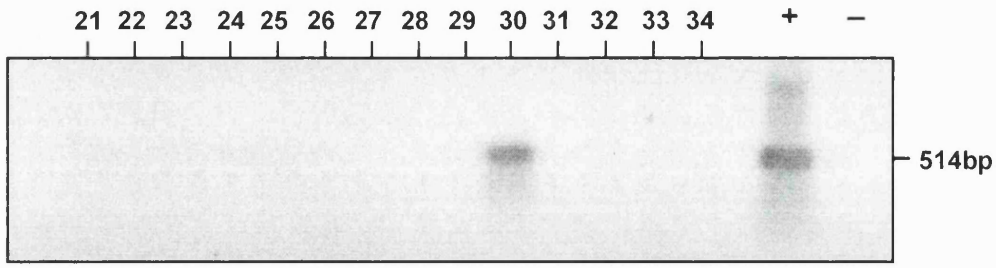

Figure 3.3 Southern blot analysis of K14 specific PCR product. Gel presented shows potential founder animals #21-34; + = K14-IL-1α-HGX transgenic positive control; – = no template control.

3.2.4 K14-uPA-HGX microinjection and analysis of E.10 embryos

To investigate whether the low number of K14-uPA-HGX positive mice was a result of low transgene incorporation efficiency or embryonic toxicity, recipient pseudo-pregnant females were sacrificed 10 days after transfer of microinjected eggs, and the E.10 embryos harvested. This time-point was selected as the promoter sequence from human keratin 5 (K5), the keratin partner of K14, shows initial activity on E.9.5 (Byrne *et al,* 1994). Thus, analysis of E.10 embryos would allow transgene detection prior to significant K14 promoter activity. Following harvesting of the E.10 embryos, DNA was prepared and transgene incorporation analysed by K14 and HGX specific PCR. As shown in figure 3.4, of 37 embryos analysed, 4 (#9, #14, #24 and #27) were identified as positive for transgene incorporation by K14 specific PCR. This improved rate of transgenesis (4/37; >10%) in E.10 embryos compared with viable progeny suggested that uPA overexpression might be causing embryonic lethality. A summary of the micro-injection schedule and transgenic embryos detected is detailed in table 3.2.

Eggs injected and transferred	Recipient females	E.10 embryos harvested	uPA transgenics identified
117	4	37	4

Table 3.2 Summary of K14-uPA-HGX microinjection schedule and transgenic embryo detection.

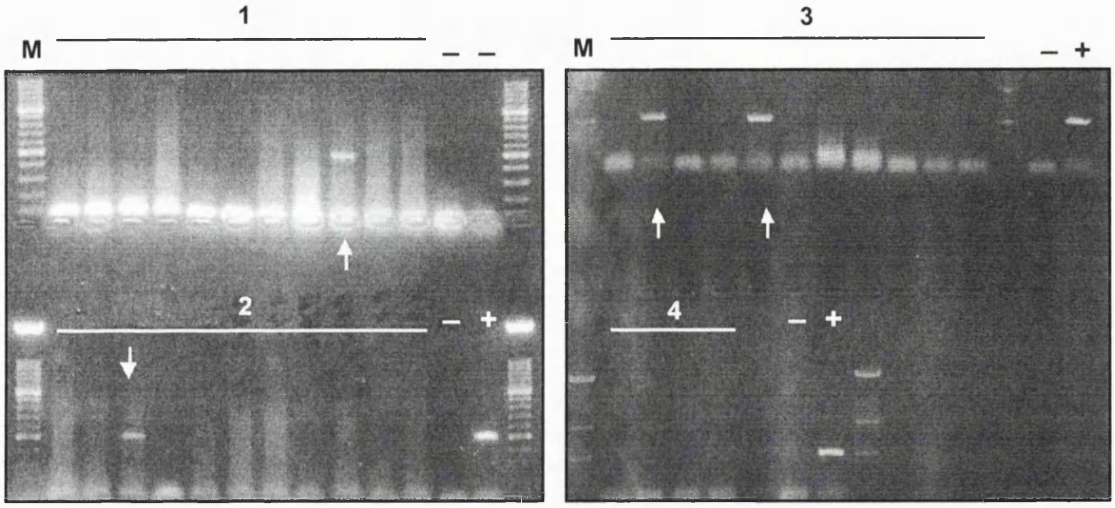

Figure 3.4 Detection of K14-uPA-HGX positive embryos using K14 specific PCR. Arrows indicate positive lanes. 1 = embryos (#1-11); 2 = embryos (#12-22); 3 = embryos (#23-33); 4 = embryos (#34-37) – = no template control; + = K14-IL-1α-HGX transgenic positive control. M = 100bp DNA ladder.

3.3 DISCUSSION

Despite the reported importance of uPA for normal wound closure, as well as suggestions of a potential role for uPA in non-healing chronic wounds, no analysis of the effects of elevated uPA expression on cutaneous physiology and wound repair had been undertaken at the onset of this project. This study therefore set out to examine these effects by generating transgenic mice designed to constitutively overexpress uPA in epidermal tissues. Using a 2.1 kb keratin 14 (K14) promoter/enhancer sequence, uPA would be targeted to basal keratinocytes of the skin, although variant expression in thymus, oral epithelia, oesophagus, and the outer root sheath of the hair follicle was also expected (Vassar *et al,* 1989; Cheng *et al,* 1992; Wang *et al,* 1997).

Following successful cloning of the murine uPA coding sequence into a K14-HGX transgene expression vector, as outlined in section 3.2.1, the functionality of the constitutive uPA construct was assessed. Consistently increased uPA levels in conditioned medium from K14-uPA-HGX transfected PAM 212 keratinocytes over control transfected and non-transfected cells confirmed that the K14 promoter was able to drive high level gene expression, in keeping with previous reports (e.g. Vassar and Fuchs, 1991; Wang *et al,* 1997). Furthermore, this observation also demonstrated that the cloned uPA sequence coded for a protein that was fully capable of converting plasminogen to proteolytic plasmin, also as previously demonstrated (Belin *et al,* 1985). Although uPA was uniformly increased in K14-uPA-HGX transfected cells, representative data was presented as the level of uPA activity (IU/ml) varied considerably between cultures derived from different geneticin-resistant colonies, and this was presumably due to differences in transfection efficiency.

As indicated in table 3.1, microinjection of the constitutive uPA construct resulted in a very low ratio of viable progeny to number of injected eggs transferred (37:435, i.e. < 10% success rate). Moreover, only one K14-uPA-HGX positive offspring was identified which was barely detectable by K14-specific PCR, and subsequently failed to produce any transgenic progeny, a characteristic highly suggestive of germline mosaicism (Wilkie *et al,* 1986). Such a result initially suggested either a lack of efficient K14-uPA-HGX transgene incorporation, or alternatively, embryonic lethality. Although the exact spatial and temporal activity of the 2.1 kb K14 promoter during mouse development remains to be defined, human keratin 5 (K5) promoter driven

expression of β-galactosidase (β-gal) can be detected as early as E.9.5 (Byrne *et al,* 1994). Moreover, since K5 and K14 are generally expressed concomitantly, Byrne *et al* suggested that K14 expression would also begin at this early stage of embryogenesis. As a consequence of this observation, E.10 embryos were harvested and analysed in order to detect transgene incorporation prior to significant K14 promoter-driven uPA expression. The subsequent detection of four K14-uPA-HGX positive embryos, from a total of 37 harvested, indicated a stark increase in the number of transgene positive E.10 embryos compared to transgene positive viable progeny, and suggested that the constitutive uPA construct was in some way toxic during mouse development.

Exactly how the K14-uPA-HGX transgene could be embryonic lethal remains unclear. The 2.1 kb K14 promoter/enhancer sequence used in this project has been demonstrated as non-toxic, as K14-targeted overexpression of many genes including TGF-α, TNF-α, and IL-1α, has resulted in viable transgenic progeny (Vassar and Fuchs, 1991; Cheng *et al,* 1992; Groves *et al,* 1995). Moreover, the mutated human growth hormone sequence (HGX) has also been used successfully in the generation of several transgenic mouse lines (Williams *et al,* 1997; Muller-Rover *et al,* 2000). These reports of viable progeny carrying K14-HGX DNA thus suggest that if the constitutive uPA construct is embryonic lethal, it is likely to be mediated by the cloned uPA sequence.

The primary function of uPA is the conversion of ubiquitous plasminogen to proteolytic plasmin. Plasmin is subsequently capable of degrading many matrix molecules, including laminin (Liotta *et al,* 1981a and b) and fibronectin (Liotta *et al,* 1981a), as well as activating several MMPs, including type IV collagenases (He *et al,* 1989; Okumura *et al,* 1997; Mazzieri *et al,* 1997). As laminin, fibronectin, and type IV collagen contribute to the structural integrity of most basement membranes (Mosher *et al,* 1992; Timpl, 1996; Timpl and Brown, 1996), and the basement membrane plays a potentially important role in embryo development, by mediating cell proliferation, migration, differentiation and attachment (Timpl, 1989; Yurchenco and O'Rear, 1994); it is possible that in K14-uPA-HGX transgenic mice, elevated levels of uPA during early embryogenesis facilitate excessive proteolysis of basement membranes leading to retardation of development and possibly death. Interestingly, uPA-mediated pathogenic proteolysis has been observed previously in mice expressing uPA under the control of an albumin promoter (Heckel *et al,* 1990). Although born viable, these Alb-uPA mice are characterised by fatal neonatal bleeding, which was directly related to

overexpression of the uPA transgene in the liver and the subsequent elevated levels of plasma uPA. In addition to their proteolytic function, uPA and plasmin have also been shown to activate certain growth factors, including TGF-β, FGF-2 and HGF-SF (Saksela and Rifkin, 1990; Lyons *et al,* 1988; Naldini *et al,* 1992), and therefore it is possible that elevated levels of cutaneous uPA during embryogenesis could lead to increased activation of these growth factors, and thus could have further negative effects on murine development.

During the course of this work a paper was published describing the generation of transgenic mice with uPA targeted to epidermal tissues using a bovine keratin 5 promoter (Zhou *et al,* 1999). K5-uPA mice were born viable and expressed transgene-specific uPA in the basal epidermal layer of the skin, the outer root sheath of hair follicles and the enamel organ. Soon after weaning, K5-uPA transgenic mice showed defects in tooth development characterised by fragile, chalky-white incisors. More specifically, these tooth defects were correlated with disruption of laminin-5 in the enamel basement membrane of transgenic mice, presumably due to uPA-mediated proteolysis. Interestingly, K5-uPA transgenic mice showed no defects in skin basement membrane or skin integrity overall, and this was suggested to be due to several features of enamel basement membrane that distinguishes it from skin basement membrane (Zhou *et al,* 1999).

There are several possible explanations for the discrepancy between our work and that of Zhou *et al.* Analysis of human K5 promoter-driven expression of β-gal during mouse embryogenesis revealed promoter activity as early as E.9.5 (Byrne *et al,* 1994). Since Byrne *et al* suggested that K14 would be concomitantly expressed with K5, it could be speculated that the human K14 promoter used in this project is also active at this early stage of development. In contrast, similar analysis of the bovine keratin 5 promoter used by Zhou *et al,* failed to detect promoter activity in mouse skin prior to E.13.5 (Ramirez *et al,* 1994), suggesting that species-specific differences in the temporal activity of the human K14 and bovine K5 promoters could differentially influence mouse development, and perhaps result in embryonic lethality in the K14-uPA-HGX transgenic mice. In addition, although direct comparison of the relative *in vivo* activity of the bovine K5 and human K14 constructs has not been performed, it is possible that differences in regulatory regions within the promoters, or alternatively differences in poly A sequences (Pfarr *et al,* 1986; Gottschling *et al,* 1993), could

influence the level of epidermal uPA expression during embryogenesis, and subsequently produce divergent phenotypic outcomes.

Speculation that the bovine K5 and human K14 promoters direct distinct *in vivo* uPA expression levels, and that this may differentially affect mouse development, is supported by several reports describing divergent phenotypic alterations in TGF-β1 transgenic mice. Mice overexpressing TGF-β1 under the control of a bovine cytokeratin IV promoter, the homologue of human keratin 10, were born viable, developed normally and showed only modest phenotypic changes (Cui *et al,* 1995). In contrast, mice overexpressing TGF-β1 under the control of a human keratin 1 promoter, showed different phenotypic alterations and died during neonatal development (Sellheyer *et al,* 1993). Higher levels of transgene expression by the keratin 1 promoter were subsequently postulated as an explanation for these opposing results (Cui *et al,* 1995). In addition, a recent study using a tetracycline-based inducible system, has shown that whereas high level expression of TGF-β1 during development results in embryonic lethality, antibiotic-mediated induction of lower TGF-β1 expression levels, results in the production of viable progeny (Liu *et al,* 2001), further suggesting that variant embryonic expression of the same gene can result in contrasting phenotypic consequences.

Thus, we hypothesise that early and/or high level expression of uPA is toxic during mouse development. As the primary aim of this project was to develop a model to permit the study of the effect of elevated uPA activity on cutaneous wound healing, and as alternative inducible systems of cutaneous uPA overexpression were already in development (see Chapters 4 and 5), no further analysis of K14-uPA-HGX transgene toxicity during embryogenesis was performed.

CHAPTER 4

CRE RECOMBINASE-MEDIATED EXPRESSION OF uPA: IN VITRO *ANALYSIS AND TAMOXIFEN-MEDIATED INDUCIBILITY* IN VIVO

4.1 INTRODUCTION

Genetic manipulation of the mouse genome to facilitate expression of exogenous genes has provided much useful data regarding the specific function of these genes in mammalian development and physiology (Jaenisch, 1988). Introduction of foreign DNA under the control of ubiquitous or tissue-specific promoters can, however, have its limitations. Constitutive overexpression of an exogenous transgene may result in embryonic or neonatal lethality (e.g. Sellheyer *et al,* 1993; Simonet *et al,* 1995), thus precluding analysis of gene function in viable adult mice. Furthermore, early constitutive expression of transgenes may result in compensatory changes that could prevent the appearance of an abnormal phenotype in adult animals, and mask the true function of the gene during subsequent patho-physiological analysis. As a consequence of these limitations, alternative molecular systems that facilitate controlled gene expression have been investigated, and although inducible gene expression has been possible since the very early days of transgenic technology (Brinster *et al,* 1982; Palmiter *et al,* 1982), it is only recently that mechanisms have been developed allowing efficient spatial and temporal control of gene expression *in vivo.*

Initial systems of inducible gene expression primarily used mammalian control elements, such as the metallothionein promoter, heat-shock promoters, or steroid response elements. Although functional *in vivo*, the usefulness of these systems was generally limited by high background expression levels and the toxic or physiologic effects of the inducer (reviewed in Yarranton, 1992). More recently, alternative inducible systems have been developed based on non-mammalian mechanisms of gene regulation, although these systems also possess practical limitations. For example, the insect moulting hormone ecdysone has been used to stimulate complex formation of exogenous retinoid X receptor (RXR) and the ecdysone receptor, and this complex subsequently induces target gene expression via stimulation of ecdysone response elements positioned upstream of the gene of interest (No *et al,* 1996). Although successfully utilised in transgenic mice (No *et al,* 1996), a major drawback of this system is the potential for endogenous gene activation by RXR. Other inducible systems have utilised modified regulatory elements from the Tn10-encoded tetracycline resistance operon of *E. coli*, to facilitate induction or repression of gene expression in the presence of tetracycline (Gossen and Bujard, 1992; Gossen *et al,* 1995). These antibiotic-based systems have also been used to successfully induce foreign gene

expression in both mammalian cells and transgenic mice (Furth *et al,* 1994; Gossen *et al,* 1995; Shockett *et al,* 1995; Schultze *et al,* 1996), although on several occasions high levels of basal-transcriptional activity were reported (Furth *et al,* 1994; Howe *et al,* 1995; Kistner *et al,* 1996).

In addition to inducible systems utilising non-mammalian regulatory elements, alternative mechanisms of genome manipulation have been developed based on the ability of Cre recombinase to mediate DNA recombination. Cre recombinase is a 38 kDa P1 bacteriophage-derived protein that catalyses the recombination of DNA between two specific recognition sites, known as loxP (Sternberg and Hamilton, 1981; Hoess *et al,* 1982). LoxP sites are 34 bp consensus sequences containing an 8 bp core that defines loxP orientation. Upon binding of a single Cre recombinase molecule to two orientated loxP sites, the DNA in between is excised leaving a single loxP site (Rajewsky *et al,* 1996). Although originally defined in bacteria, the Cre-loxP system is fully functional both in mammalian cells in culture (Sauer and Henderson, 1988 and 1989) and in transgenic mice (Orban *et al,* 1992). Moreover, subsequent modification of this system has been shown to facilitate Cre-mediated activation of exogenous gene expression (figure 4.1). In the first example of this, Lakso *et al* demonstrated that cloning of a loxP flanked transcriptional/translational stop signal (TSS) between the alpha A-crystallin promoter and the large T antigen gene prevented the development of lens tumours in subsequent transgenic mice. However, upon breeding of these transgenic mice with mice constitutively expressing Cre recombinase, all subsequent progeny developed lens tumours as a result of Cre-mediated excision of the TSS (Lakso *et al,* 1992).

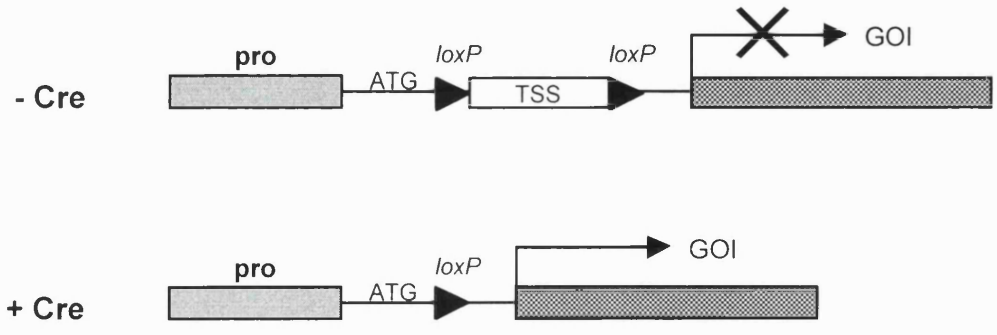

Figure 4.1 Schematic representation of Cre-mediated activation of exogenous gene expression. Pro = ubiquitous or tissue-specific promoter; ATG = translational start codon; TSS = transcriptional (AATAAA polyadenylation sequence)/translational (TGA) stop signal; GOI = gene of interest.

Despite its usefulness in 'proof of principle' experiments, the breeding of mice carrying a Cre-inducible transgene with mice constitutively expressing Cre recombinase results in activation of the exogenous transgene during development, and thus does not facilitate precise temporal control of gene expression. Moreover, if inducible expression is required due to transgene-mediated lethality or compensation, this activation of the exogenous gene during embryogenesis would be undesirable. As a consequence, various transgenic mouse lines have been generated in which expression of Cre recombinase is controlled by specific inducible elements. For example, inducible promoters, such as the interferon-sensitive Mx promoter (Kuhn *et al,* 1995) and the tetracycline-controlled CMV-tetO promoter (St Onge *et al,* 1996), have been shown to efficiently induce Cre-recombinase expression and activity *in vivo* (St Onge *et al,* 1996; Ayrall *et al,* 1998). Furthermore, alternative inducible elements have been developed by fusing Cre-recombinase to the mutated ligand-binding domain (LBD^{mut}) of several steroid receptors, and these Cre-LBD^{mut} fusion proteins have also been utilised in either *in vitro* or *in vivo* induction of Cre-recombinase activity (Zhang *et al,* 1996; Feil *et al,* 1996; Kellendonk *et al,* 1996; Schwenk *et al,* 1998; Brocard *et al,* 1998). Interestingly, under normal circumstances, Cre-LBD^{mut} fusion proteins are constitutively expressed and accumulate in the cytoplasm. However, in the presence of synthetic steroid ligands that bind the mutated LBD, the fusion protein is translocated into the cell nucleus thus facilitating Cre-mediated recombination (see Brocard *et al,* 1997 for immunohistochemical demonstration). Importantly, although these synthetic ligands can bind the mutated LBDs, natural ligands cannot, thus preventing endogenous stimulation of Cre-recombinase activity (Zhang *et al,* 1996; Feil *et al,* 1996; Kellendonk *et al,* 1996; Brocard *et al,* 1998).

Although several LBD^{mut}-based systems exist, those utilising the Cre-ER^T fusion protein, comprised of Cre-recombinase fused to a mutated human oestrogen receptor LBD (Feil *et al,* 1997), have been described in most detail. Nuclear translocation of the Cre-ER^T protein is stimulated in both mammalian cells and transgenic mice following application of synthetic oestrogen homologues, such as tamoxifen or 4-hydroxytamoxifen (OHT) (Feil *et al,* 1996; Brocard *et al,* 1997; Danielian *et al,* 1998). In contrast, Cre-mediated recombination is undetectable in Cre-ER^T positive cells following treatment with 17β-oestradiol, a natural ligand of the oestrogen receptor (Feil *et al,* 1996 and 1997). Moreover, nuclear translocation of the Cre-ER^T fusion protein is not observed in untreated transgenic mouse tissue (Brocard *et al,* 1997), further

indicating that Cre-ER^{T} activation is tamoxifen dependent. Interestingly, alternative mutations within the human oestrogen receptor LBD sequence resulted in the generation of a novel fusion protein (Cre-ER^{T2}) which is approximately 10-fold more sensitive to OHT-mediated induction (Feil *et al,* 1997; Indra *et al,* 1999), and thus could provide a more efficient system of Cre-recombinase activation.

Despite the availability of technology facilitating inducible gene activation *in vivo*, and the recognised advantages of spatial and temporal control of gene expression during the physiological and patho-physiological analysis of gene function, no skin-specific method of gene induction had been developed at the onset of this project. In addition, as one of the primary aims of the project was to determine the effects of elevated uPA levels on wound healing in the skin, and as these effects would be better dissected using a system that facilitated temporal control of cutaneous uPA expression, this study set out to generate transgenic mice in which K14 promoter-driven expression of uPA could be transiently induced by synthetic ligand application. Subsequent analyses could thus determine the effect of transient uPA overexpression on cutaneous wound repair, as well as providing information on the regulation and potential roles of the plasminogen activator system in skin development and physiology.

4.2 RESULTS

4.2.1 Creation of inducible uPA expression vector

A 676 bp sequence of 5' murine uPA was amplified by PCR using the pDB1519 vector (ATCC#:63256) as template DNA, and the following primers: 5'-AGCGGCACT ACCTTTAAAGTCTGGCTG-3' (CS1) for the sense strand and 5'-ACTCCCACCACA CCCGGGGGAGGGAGGACT-3' (CS2) for the antisense strand. The sense primer was designed to replace the uPA start codon (ATG) and the primary transcription codon (AAA) with a *Dra*I restriction enzyme recognition site (TTTAAA), thereby facilitating in-frame expression of uPA upon Cre-mediated recombination. Furthermore, the antisense primer was designed to replace a *Dra*I restriction enzyme recognition site with a *Sma*I restriction enzyme recognition site at the 3' end of the subsequent PCR product (figure 4.2).

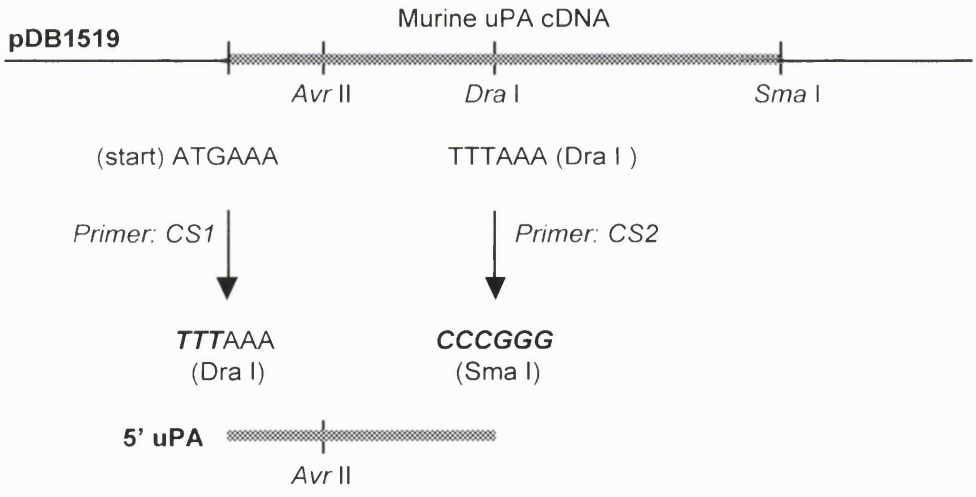

Figure 4.2 Schematic representation of PCR strategy designed to remove ATG start codon and provide specific restriction enzyme sites for subsequent cloning.

The 5' uPA PCR product was subsequently digested with *Dra*I and *Sma*I and blunt-end ligated with *Sma*I digested pGEM$^{(loxTlox)}$ (pGEM 5'loxP-TSS(Poly A)-3'loxP (-G) vector; a kind gift of Prof. Fred Sablitzky, The Institute of Genetics, University of Nottingham), as detailed in figure 4.3a. As the *Dra*I-*Sma*I digested 5' uPA PCR product was blunt-ended it could ligate into pGEM$^{(loxTlox)}$ in either a forward or reverse orientation. Therefore, 15 colonies were selected and pGEM-5'uPA$^{(loxTlox)}$ plasmid DNA prepared as in section 2.1.1.1, prior to sequencing which identified the constructs

containing 5' uPA in the correct orientation. An *Avr*II-*Sma*I restriction digest product, containing 1636 bp of 3' murine uPA, was then isolated from pDB1519 (figure 4.3b), and cloned into the cognate sites of pGEM-5'uPA$^{(loxTlox)}$, as detailed in figure 4.3c. The resulting pGEM-uPA$^{(loxTlox)}$ vector was fully sequenced and the uPA coding region was found to be identical to the published sequence for murine uPA (GenBank Accession No. X02389), except for the removal of the ATG start codon. In addition, sequencing analysis confirmed that the pGEM-uPA$^{(loxTlox)}$ vector contained the correct sequence for functional uPA expression upon Cre-mediated recombination.

a)

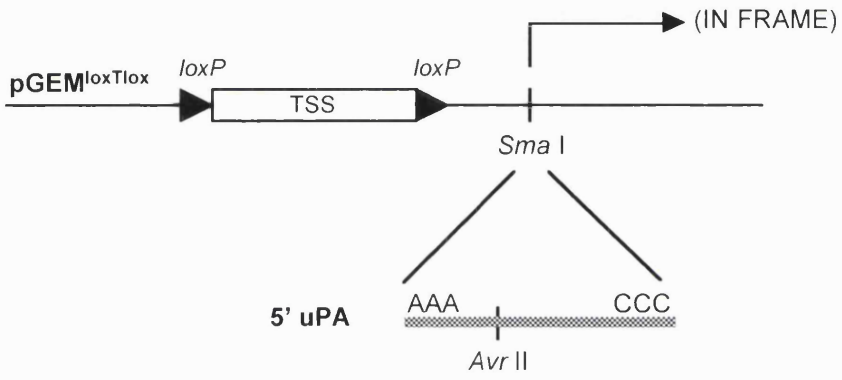

b)

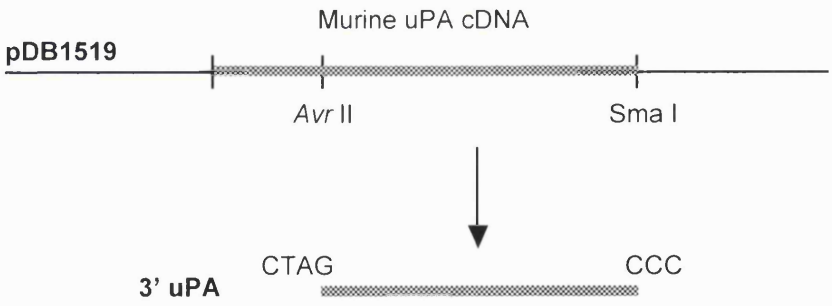

c)

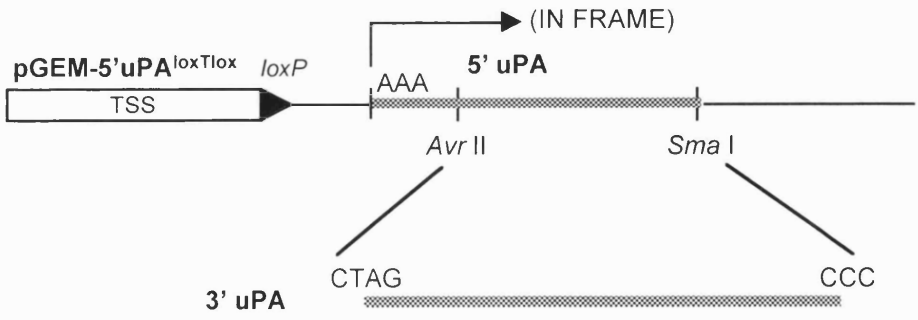

Figure 4.3 Schematic representation of cloning strategy designed to facilitate in-frame expression of uPA. a) PCR product (5' uPA) cloning into pGEM$^{(loxTlox)}$; b) restriction digest facilitating isolation of 3' uPA; c) ligation of 3' uPA with pGEM-5'uPA$^{(loxTlox)}$.

To facilitate *in vitro* and *in vivo* analysis of inducible uPA expression, a 2418 bp uPA$^{(loxTlox)}$ cassette was isolated from pGEM-uPA$^{(loxTlox)}$ by digestion with *Hinc*II and *Sma*I, prior to blunt-end ligation with *Eco*RV digested pcDNA.3 (Invitrogen). Sub-cloning of the uPA$^{(loxTlox)}$ cassette in pcDNA.3 was necessary to ensure availability of cohesive ends required for ligation with the *in vivo* expression vector. The subsequent pcDNA.uPA$^{(loxTlox)}$ vector was then digested with *Bam*HI and *Bgl*II, and an isolated 2132 bp uPA$^{(loxTlox)}$ cassette cloned into the *Bam*HI cloning site of the K14-HGX transgene expression vector (see section 3.2.1), as shown in figure 4.4. Orientation of the cloned sequences was verified after both the blunt-end ligation into pcDNA.3 and ligation of the BamHI-BglII digested uPA$^{(loxTlox)}$ cassette into K14-HGX. As described previously, 15 colonies were selected, plasmid DNA prepared and sequencing performed to identify the constructs containing the correctly orientated sequence.

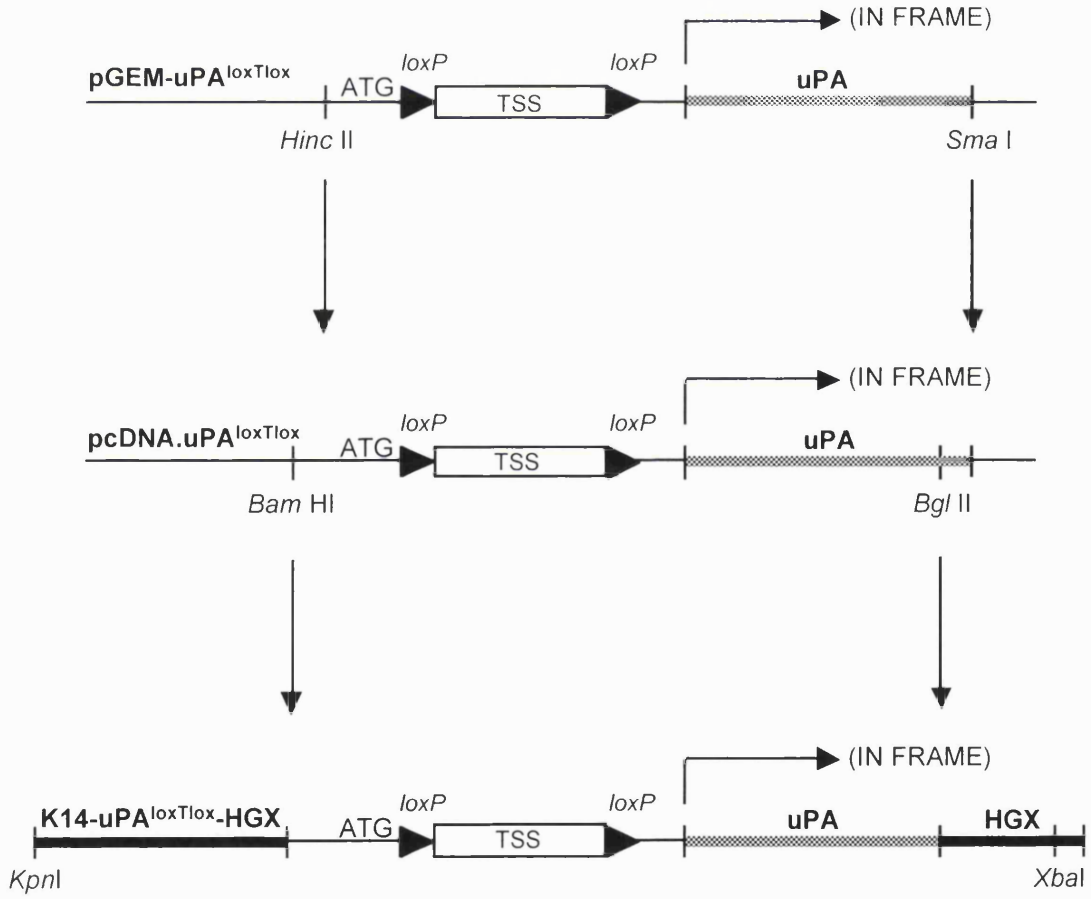

Figure 4.4 Schematic representation of transfer of uPA$^{(loxTlox)}$ cassette from *in vitro* expression vectors to the K14-HGX *in vivo* transgene expression vector.

The K14-uPA$^{(loxTlox)}$-HGX vector was then fully sequenced and the uPA coding region was again found to be identical to the published sequence, except for the removal of the ATG start codon. Representative sequencing data demonstrating the successful removal of the uPA start site is shown in figure 4.5a. Translation of the recombined uPA$^{(loxTlox)}$ cassette would place 17 additional amino acids at the N-terminal end of uPA (figure 4.5b). As these amino acids could affect the functionality of the resulting loxP-uPA fusion protein, *in vitro* analyses were performed to verify uPA bioactivity, as described in section 4.2.3.

a)

b)

Figure 4.5 a) Sequencing data from K14-uPA$^{(loxTlox)}$-HGX vector. LoxP+ve (forward) and uPA-382 (reverse) primers were used in two separate experiments (#2 and #4). The subsequent sequences were aligned with a computer-generated consensus sequence (consensus) and the published uPA sequence (Orig UPA). Note the conversion of original ATG start codon to CCC, and in frame positioning of uPA sequence. b) Sequence of amino acids at N-terminal end of endogenous uPA and the loxP-uPA fusion protein created by recombination of the uPA$^{(loxTlox)}$ cassette. * represents the initiating methionine.

4.2.2 Analysis of *in vitro* Cre-mediated recombination

To facilitate analysis of *in vitro* recombination of the uPA$^{(loxTlox)}$ cassette, the pPGK-CRE expression vector (a kind gift of Prof. Fred Sablitzky, The Institute of Genetics, University of Nottingham) was utilised to provide constitutive Cre recombinase expression. This vector consists of a 507 bp phosphoglycerate kinase-1 promoter (PGK) upstream of a 1052 bp Cre recombinase sequence, derived from wild-type P1 phage, and a 266 bp poly A sequence. Chinese Hamster Ovary (CHO) cells were cultured until 60% confluent and transiently transfected with pcDNA.3 alone, pcDNA.uPA$^{(loxTlox)}$ alone, pPGK-CRE alone, or both pcDNA.uPA$^{(loxTlox)}$ and pPGK-CRE. Following DNA preparation from transfected monolayers, Cre-mediated recombination was detected using a specific *in vitro* PCR strategy, as outlined in figure 4.6a.

As shown in the representative data presented (figure 4.6b), *in vitro*-specific PCR analysis of DNA from CHO cells transfected with pcDNA.uPA$^{(loxTlox)}$ alone, identified a 1068 bp PCR product, corresponding to the wild-type sequence. In contrast, *in vitro*-specific PCR of DNA from CHO cells co-transfected with pcDNA.uPA$^{(loxTlox)}$ and pPGK-CRE, showed low-level amplification of the 1068 bp wild-type PCR product as well as amplification of a smaller 694 bp PCR product, corresponding to the recombined sequence. Analysis of DNA from control transfected CHO cells detected neither wild-type nor recombined sequence, as expected. In addition, a minor PCR product of approximately 900 bp was identified during analysis of DNA from CHO cells transfected with pcDNA.uPA$^{(loxTlox)}$ alone, and with both pcDNA.uPA$^{(loxTlox)}$ and pPGK-CRE. This spurious product was also detected during PCR analysis of pcDNA.uPA$^{(loxTlox)}$ vector DNA (positive control), suggesting it was the result of non-specific PCR amplification.

a)

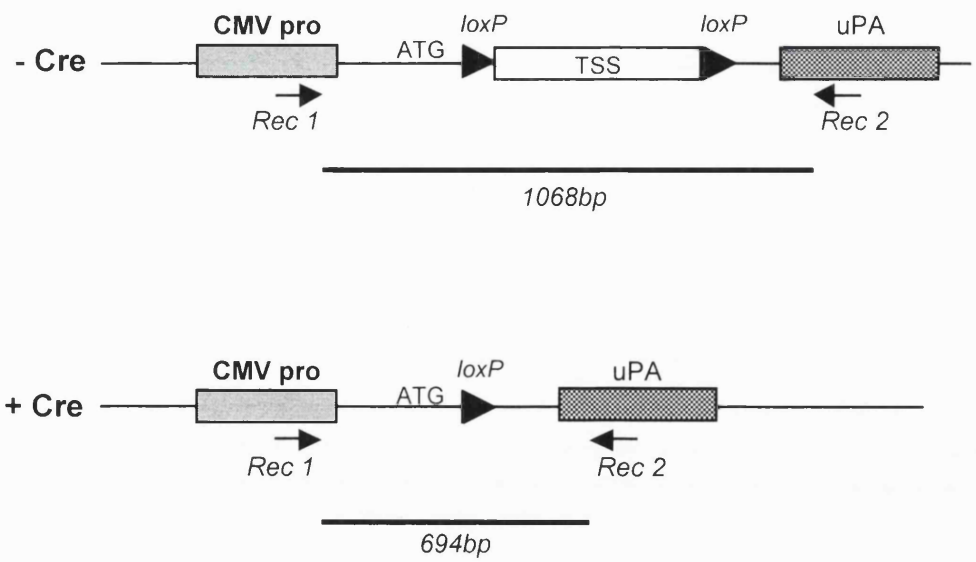

b)

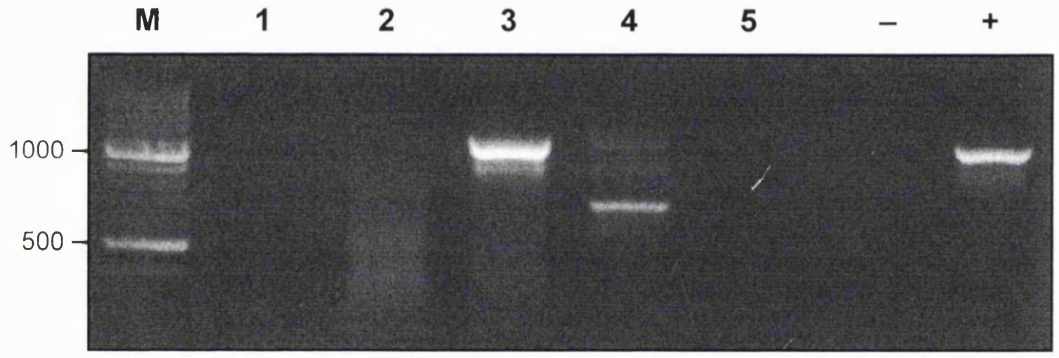

Figure 4.6 a) Schematic representation of PCR strategy to detect *in vitro* Cre recombinase mediated excision of floxed TSS sequence. Rec 1 and Rec 2 refer to specific primers as described in Table 2.2 b) PCR detection of pPGK-CRE mediated recombination in CHO cell transient transfections. Lane 1 = No DNA; Lane 2 = pcDNA.3; Lane 3 = pcDNA.uPA$^{(loxTlox)}$; Lane 4 = pcDNA.uPA$^{(loxTlox)}$ + pPGK-CRE; Lane 5 = pPGK-CRE; – = no template control; + = pcDNA.uPA$^{(loxTlox)}$ (plasmid PCR); M = 100bp DNA ladder (selected marker sizes are indicated in base pairs).

4.2.3 Detection of functional uPA expression by the uPA$^{(loxTlox)}$ cassette

Having detected *in vitro* Cre-mediated recombination of the uPA$^{(loxTlox)}$ cassette, conditioned medium, from CHO cell monolayers transfected as detailed in section 4.2.2, was analysed for uPA activity by both indirect chromogenic peptide assay and plasminogen-linked zymography. Using the indirect chromogenic peptide assay, levels of uPA activity in conditioned medium from CHO cells transfected with any of the selected vectors alone, was shown to be indistinguishable from control samples (figure

4.7). In contrast, analysis of conditioned medium from CHO cells co-transfected with both pcDNA.uPA$^{(loxTlox)}$ and pPGK-CRE, identified an approximate 45 fold increase in uPA activity compared to control samples, and more importantly, compared to samples from CHO cells transfected with pcDNA.uPA$^{(loxTlox)}$ alone. In addition, plasminogen-linked zymography analysis of conditioned medium from CHO cells co-transfected with pcDNA.uPA$^{(loxTlox)}$ and pPGK-CRE, detected a strong band of beta-casein degradation corresponding to murine uPA (45 kDa) (figure 4.8). However, analysis of conditioned medium from cells transfected with pcDNA.uPA$^{(loxTlox)}$ alone, showed no beta-casein degradation. This detection of uPA activity following co-transfection with pcDNA.uPA$^{(loxTlox)}$ and pPGK-Cre, indicated that the Cre recombinase/Lox P system was fully functional *in vitro*. Moreover, the lack of detectable uPA in conditioned medium from cells transfected with pcDNA.uPA$^{(loxTlox)}$ alone, clearly demonstrated that no background expression of uPA had occurred with this construct.

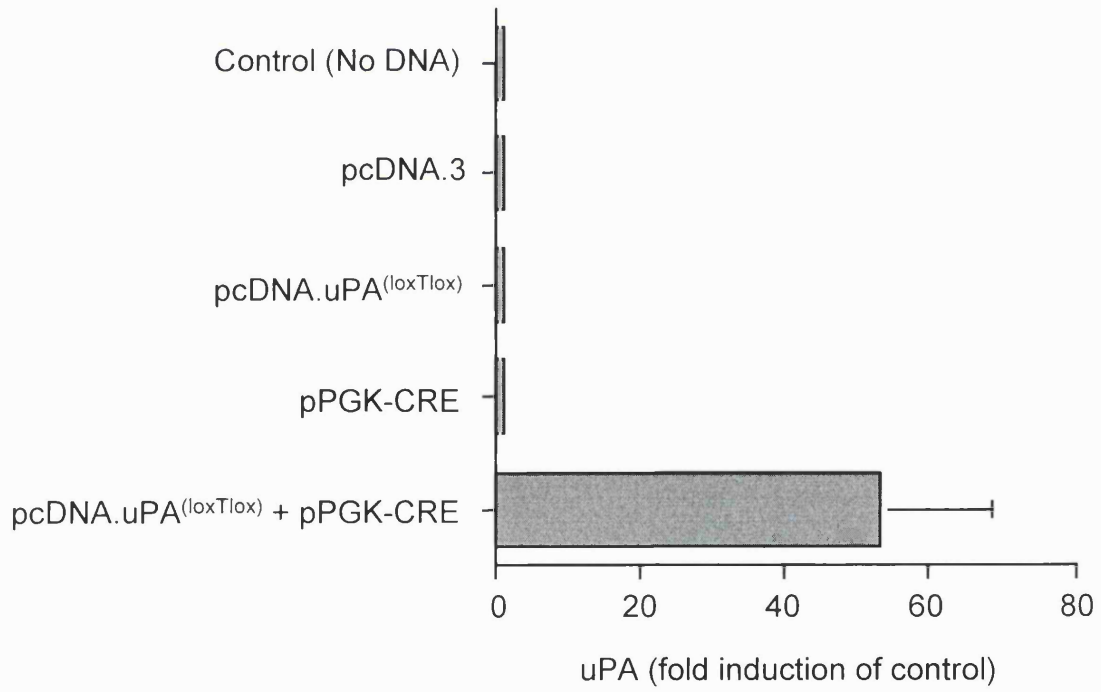

Figure 4.7 Detection of functional uPA expression via Cre recombinase mediated excision of floxed TSS sequence (I). uPA activity in conditioned medium from CHO cell transient transfections as detected by indirect chromogenic peptide assay. Data presented (mean ± SEM) are from triplicate wells in 3 independent experiments.

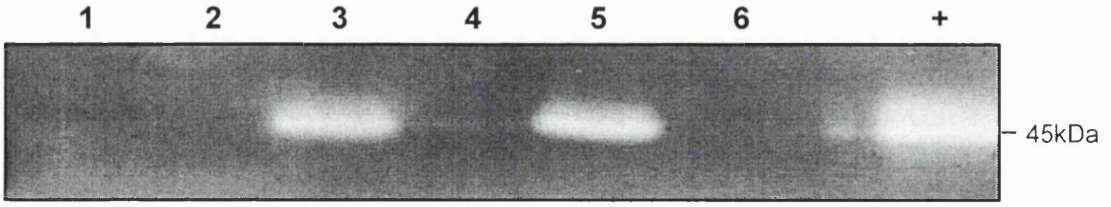

Figure 4.8 Detection of functional uPA expression via Cre recombinase mediated excision of floxed TSS sequence (II). uPA activity in conditioned medium from CHO cell transient transfections as detected by plasminogen-linked zymography. Lane 1 = No DNA; Lane 2 = pcDNA.3; Lane 3 = pcDNA.uPA; Lane 4 = pcDNA.uPA$^{(loxTlox)}$; Lane 5 = pcDNA.uPA$^{(loxTlox)}$ + pPGK-CRE; Lane 6 = pPGK-CRE; + = murine urine. Data presented are representative of 2 independent experiments.

4.2.4 Generation of K14-uPA$^{(loxTlox)}$-HGX transgenic mice

A 6376 bp restriction digest product, containing the human Keratin 14 promoter/enhancer region, the full uPA$^{(loxTlox)}$ cassette and the mutated Human Growth Hormone/Poly A region, was isolated from K14-uPA$^{(loxTlox)}$-HGX by digestion with *Kpn*I and *Xba*I. Following purification (see section 2.1.14), the transgene construct was microinjected into fertilised mouse eggs, prior to transfer to recipient C57BL/6 pseudo-pregnant females. Transgene incorporation in the subsequent progeny was detected by K14 and HGX specific PCR, and representative data, indicating the successful detection of 4 transgenic founder animals (#33, #38, #39 and #51), are presented in figure 4.9.

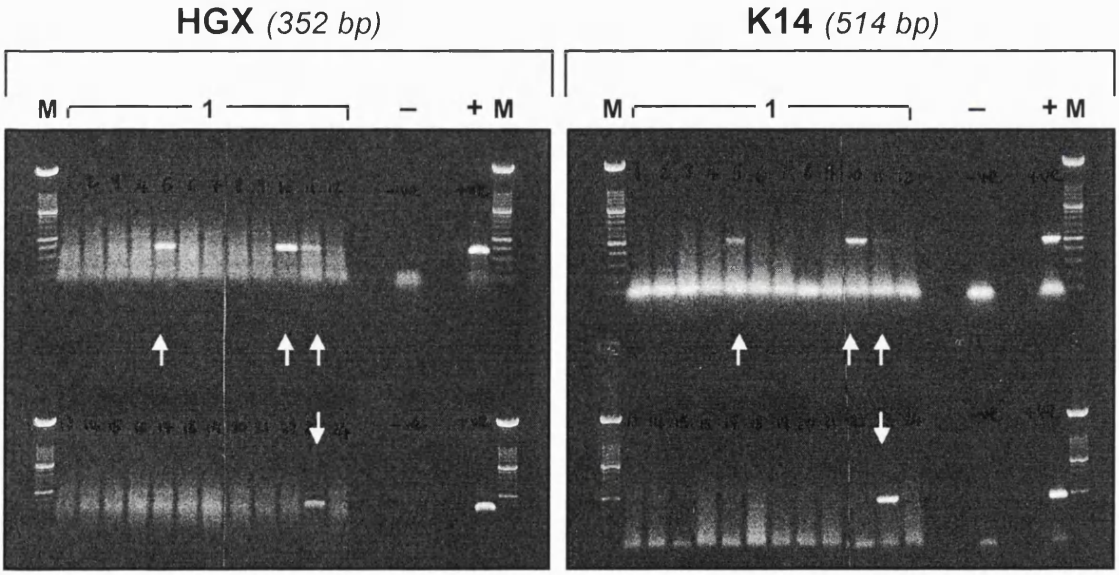

Figure 4.9 PCR detection of founder K14-uPA$^{(loxTlox)}$-HGX mice using K14 and HGX specific primers. Arrows indicate positive lanes. 1 = potential F1 animals (#29-52); - = no template control; + = K14-IL-1α-HGX transgenic positive control. M = 100bp DNA ladder.

Following positive identification, founder animals were mated separately with wild-type C57BL/6 mice and their progeny analysed by K14 and HGX specific PCR. Three of the four founder animals (#33, #38 and #39) mated successfully and subsequently produced heterozygous K14-uPA$^{(loxTlox)}$-HGX positive progeny at a ratio of 1:1 with wild-type offspring.

4.2.5 'Proof of principle' of *in vivo* recombination

To determine the *in vivo* functionality of the uPA$^{(loxTlox)}$ construct, *in vivo* recombination was initiated by intra-dermal injection of pPGK-CRE plasmid DNA. K14-uPA$^{(loxTlox)}$-HGX positive mice from founder lines 33, 38 and 39, received two intra-dermal doses of pPGK-CRE and vehicle, as described in section 2.4.5. Following DNA preparation from injected ears, Cre-mediated recombination was detected using a specific *in vivo* PCR strategy (figure 4.10).

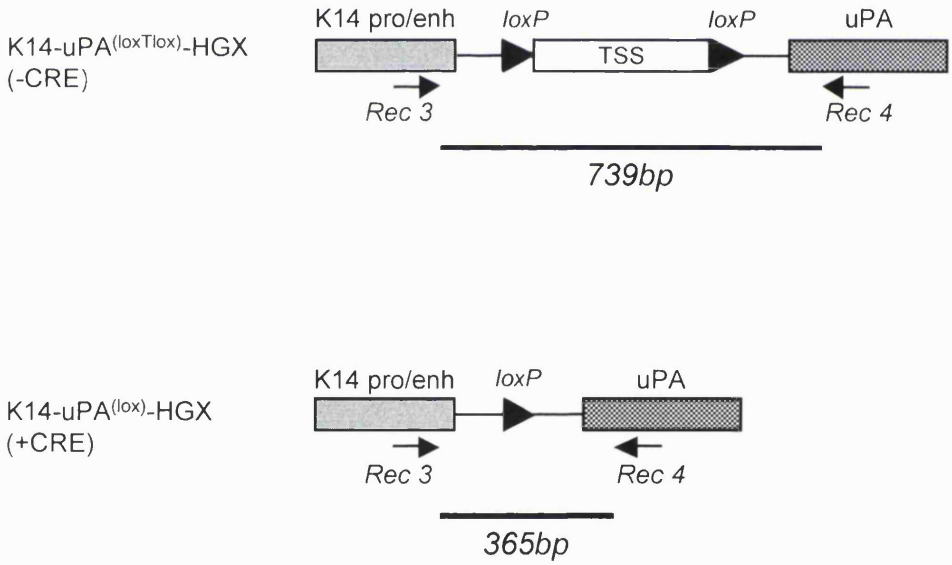

Figure 4.10 Schematic representation of PCR strategy to detect Cre recombinase mediated excision of floxed TSS sequence *in vivo*. Rec 3 and Rec 4 refer to specific primers as described in Table 2.2

As shown in figure 4.11, *in vivo*-specific PCR analysis of DNA from vehicle treated K14-uPA$^{(loxTlox)}$-HGX transgenic mouse ears showed amplification of the 739 bp wild-type sequence, as expected. However, PCR analysis of DNA from pPGK-CRE treated ears, demonstrated amplification of both the 739 bp wild-type sequence, as well as a smaller, 365 bp sequence (K14-uPA$^{(lox)}$-HGX; figure 4.10) indicating that the Cre

recombinase/Lox P system was functional *in vivo*. Moreover, following intra-dermal injection of pPGK-CRE, recombined DNA was detected in all three founder lines. Injected epidermal sheets were also processed for protein, and uPA activity levels assessed using the indirect chromogenic peptide assay. However, uPA activity in both vehicle treated and pPGK-CRE treated ears was below the detectable level for this assay (data not shown).

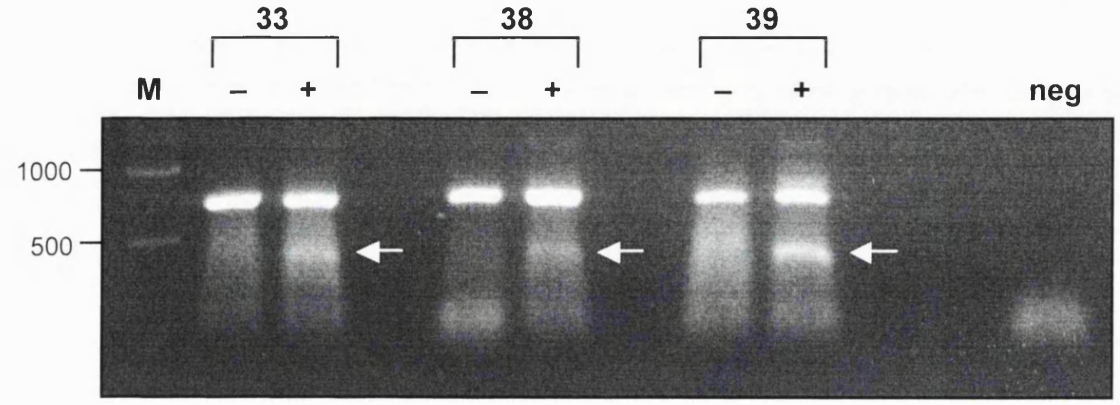

Figure 4.11 PCR detection of *in vivo* Cre-mediated recombination following naked DNA injection using the pPGK-CRE vector. For each founder line, vehicle treated (–) and pPGK-CRE treated (+) samples are shown. Arrows indicate recombined DNA. neg = no template control; M = 100bp DNA ladder (selected marker sizes are indicated in base pairs).

4.2.6 Generation of tamoxifen-inducible uPA transgenic mice

To facilitate *in vivo* manipulation of uPA expression, K14-uPA$^{(loxTlox)}$-HGX positive mice from founder lines 33, 38, and 39 were crossed with K14-Cre-ER^{T2} mice (a kind gift of Dr. Daniel Metzger, Institut de Genetique et de Biologie Moleculaire et Cellulaire, C.U. de Strasbourg, France). K14-Cre-ER^{T2} mice carry a transgene containing the human Keratin 14 promoter/enhancer sequence, the rabbit β-globin intron II, a Cre-ER^{T2} sequence consisting of a 343 bp Cre recombinase gene fused to a 314 bp mutated human oestrogen receptor LBD (ER^{T2}), and the SV40 poly A signal sequence (figure 4.12). Subsequent double transgenic progeny were identified using HGX specific PCR to detect the K14-uPA$^{(loxTlox)}$-HGX transgene, and Cre recombinase specific PCR to detect the K14-Cre-ER^{T2} transgene.

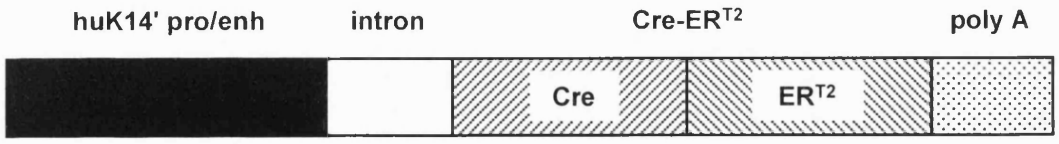

Figure 4.12 Schematic representation of the K14-Cre-ER^{T2} transgene. huK14 pro/enh = human Keratin14 promoter/enhancer sequence; intron = rabbit β-globin intron II; Cre-ER^{T2} = Cre recombinase-ER^{T2} fusion sequence; poly A = poly A site from the SV40 early region.

4.2.7 Analysis of *in vivo* tamoxifen-induced recombination

To demonstrate tamoxifen induction of Cre-ER^{T2} mediated recombination *in vivo*, single transgenic (K14-uPA$^{(loxTlox)}$-HGX) and double transgenic (K14-uPA$^{(loxTlox)}$-HGX/K14-Cre-ER^{T2}) mice from founder lines 33, 38, and 39, were treated with tamoxifen as described in section 2.4.6. Following DNA preparation from dissected tail tissue, Cre-mediated recombination was detected using the specific *in vivo* PCR strategy (figure 4.10), and representative data are shown in figure 4.13. Analysis of single transgenic mouse tail from all founder lines showed amplification of the 739 bp wild-type sequence both before and after tamoxifen treatment, as expected. However, analysis of double transgenic mouse tail showed differential results between founder lines. Whereas PCR of double transgenic tail DNA derived from founder line 38, showed amplification of the 739 bp wild-type sequence prior to tamoxifen treatment, analysis after tamoxifen treatment showed amplification of a band corresponding to the 739 bp wild-type sequence as well as a band corresponding to the 365 bp recombined sequence. In contrast, analysis of double transgenic tail DNA derived from founder lines 33 and 39, showed amplification of the 739 bp wild-type sequence and the 365 bp recombined sequence both before and after tamoxifen treatment. An additional, minor PCR product of approximately 850 bp was indentified during analysis of DNA from double transgenic mice from all three founder lines, both before and after tamoxifen treatment. The significance of this PCR product was not investigated further.

The detection of recombined DNA prior to tamoxifen treatment in lines 33 and 39, suggested that background translocation of the Cre-ER^{T2} fusion protein may be occurring in these mouse lines. However, recombination was exclusively observed post-

tamoxifen in line 38 double transgenic mice, indicating that activity of the Cre-recombinase/Lox P system was entirely tamoxifen-dependent in this mouse line.

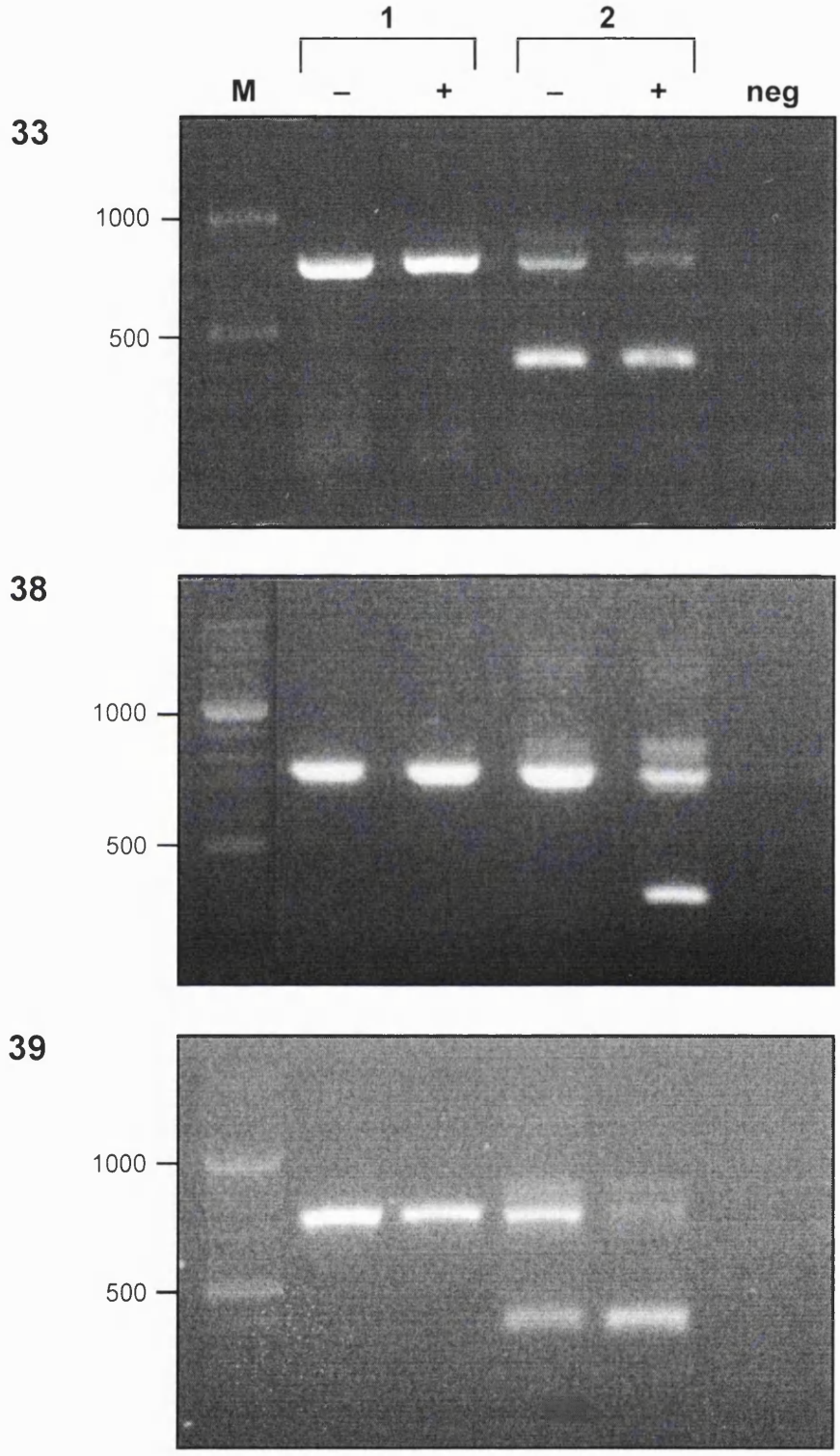

Figure 4.13 Detection of tamoxifen induced Cre-ER^{T2} mediated excision in mice. For each founder line deletion of the floxed TSS sequence in tail tissue was analysed by PCR pre-Tam treatment (–) and 48 hours post-Tam treatment (+). 1 = K14-uPA$^{(loxTlox)}$-HGX single transgenic mice; 2 = K14-uPA$^{(loxTlox)}$-HGX/K14-Cre-ER^{T2} double transgenic mice; neg = no template control. M = 100bp DNA ladder (selected marker sizes are indicated in base pairs).

4.2.8 Analysis of tissue specific *in vivo* recombination

Having demonstrated tamoxifen induction of Cre-ER^{T2} mediated recombination *in vivo*, various organs from tamoxifen treated double transgenic mice (from founder line 38) were analysed to determine the tissue specificity of recombination. Following DNA preparation from dissected tissues, Cre-mediated deletion of the floxed TSS sequence was detected using the specific *in vivo* PCR strategy (figure 4.10). PCR analysis of DNA from tail tissue dissected prior to tamoxifen treatment showed amplification of the 739 bp wild-type sequence (K14-uPA$^{(loxTlox)}$-HGX), as expected (figure 4.14). However, analysis of DNA from tail, ear, skin and tongue tissue, dissected either 48 hours or one week (data not shown since identical) after completion of tamoxifen treatment, showed amplification of both the 739 bp wild-type sequence and the 365 bp recombined sequence (K14-uPA$^{(lox)}$-HGX). In contrast, analysis of DNA from intestine, kidney, and liver tissue, showed amplification of the 739 bp wild-type sequence alone, indicating that activity of the K14-uPA$^{(loxTlox)}$-HGX transgene was effectively restricted to tissues expressing K14.

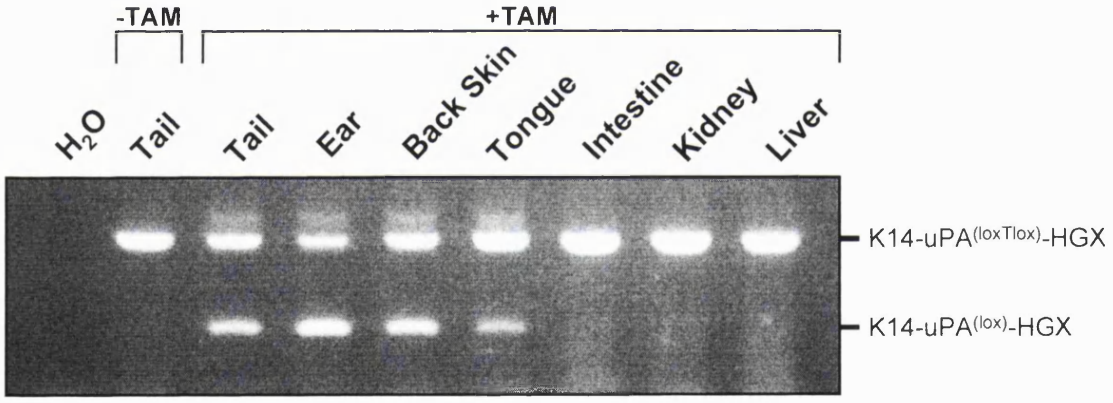

Figure 4.14 Tissue specificity of Cre-ER^{T2} mediated excision in mice. Deletion of the floxed TSS sequence in various organs was analysed by PCR 48 hours post-Tam treatment. PCR was also performed on tail DNA isolated before tamoxifen administration (–TAM). H_2O = no template control.

4.2.9 Preliminary analysis of *in vivo* tamoxifen-induced uPA activity

To demonstrate tamoxifen-induced expression of functional uPA *in vivo*, two single transgenic (K14-uPA$^{(loxTlox)}$-HGX) and two double transgenic (K14-uPA$^{(loxTlox)}$-HGX/K14-Cre-ER^{T2}) mice from founder line 38 were treated with tamoxifen, as described in section 2.4.6. Ear tissue was dissected either 48 hours or one week after completion of tamoxifen treatment, and following protein preparation from pooled ear

tissue, uPA activity was analysed using the indirect chromogenic peptide assay. As expected, uPA activity was only detectable at very low levels in ear tissue homogenates from tamoxifen-treated single transgenic mice at both the 48 hour and one week time points. However, experiments to date have demonstrated that, using the indirect chromogenic peptide assay, uPA activity is also virtually undetectable in tamoxifen treated double transgenic mouse skin, at both the selected time points (figure 4.15).

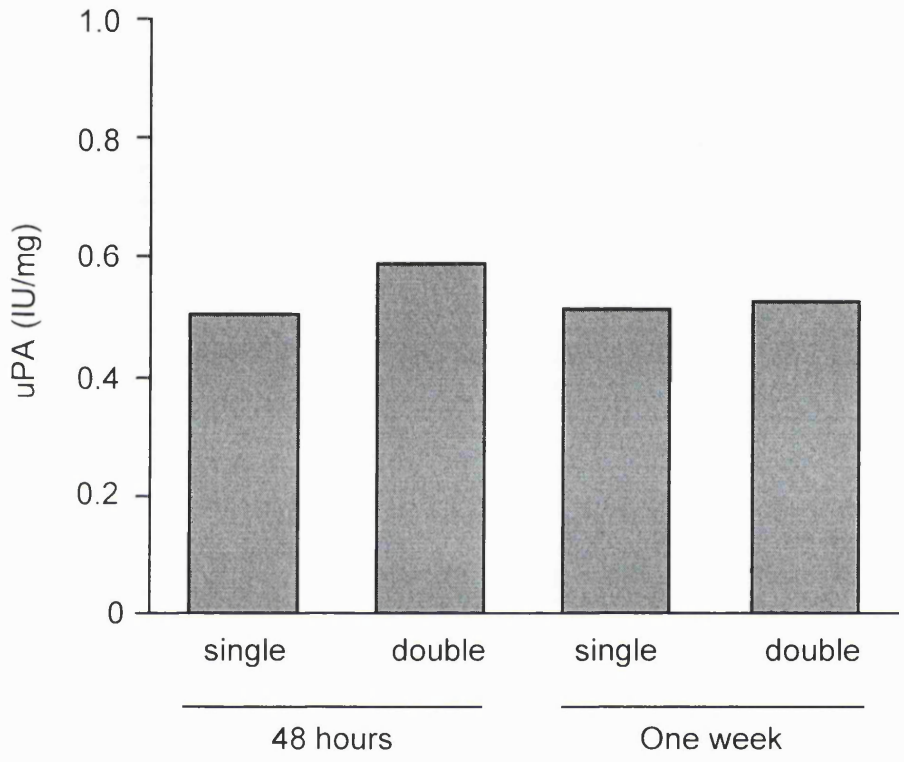

Figure 4.15 Effect of tamoxifen treatment on uPA activity in single and double transgenic mice. Indirect chromogenic peptide assay analysis of functional uPA levels in ear tissue homogenates from single (K14-uPA$^{(loxTlox)}$-HGX) transgenic and double (K14-uPA$^{(loxTlox)}$-HGX/K14-Cre-ER^{T2}) transgenic mice. Tissue samples were harvested at 48 hours and 1 week after tamoxifen treatment.

4.3 DISCUSSION

Precise genetic modification of the mouse genome to facilitate exogenous gene expression constitutes a powerful approach to the analysis of gene function. Moreover, transgene overexpression often results in disease-like phenotypes that can provide essential information regarding the related human condition (e.g. Carroll *et al,* 1995; Larkin *et al,* 1999; Chan *et al,* 2001a). The usefulness of constitutive transgene activation can, however, be limited, as it may result in embryonic or neonatal lethality (Sellheyer *et al,* 1993; Simonet *et al,* 1995), or alternatively stimulate compensatory mechanisms that mask the true function of the gene of interest. As a result of these limitations, systems have been developed that provide a more reliable approach to the study of gene function by allowing control of exogenous transgene expression in both a spatial and temporal manner. Despite the availability of this technology, no skin-specific mechanism of controlled transgene expression had been developed at the onset of this work. In view of this, and considering the primary aim of this project was to examine the effect of elevated uPA on cutaneous wound healing, the present study sought to modify the Cre-ER^T-loxP inducible system to allow synthetic ligand-mediated induction of cutaneous uPA expression *in vivo*. The resulting transgenic mice would therefore demonstrate a novel mechanism of cutaneous gene induction, as well as providing useful information regarding the role of uPA in cutaneous physiology and wound repair.

A critical issue when using any Cre-recombinase/loxP strategy of gene activation is that the gene of interest is cloned in such a way that, following Cre-mediated recombination, transgene expression is in-frame and unaffected by the remaining loxP site (Sauer, 1998). As the pGEM$^{(loxTlox)}$ vector used in this project contains an ATG start codon upstream of the loxP flanked TSS, removal of the existing uPA ATG codon was necessary to facilitate in-frame cloning and, moreover, to reduce background transcriptional read-through, as previously described (Ayrall *et al,* 1998). Following PCR removal of this uPA start site, as outlined in figure 4.2, subsequent restriction digest and ligation strategies resulted in the creation of an inducible construct containing a loxP flanked TSS upstream of an ATG-negative murine uPA sequence (uPA$^{(loxTlox)}$). In keeping with previous reports (Ayrall *et al,* 1998), detection of recombined DNA following co-transfection with pPGK-CRE, confirmed that the uPA$^{(loxTlox)}$ construct contains the correct DNA sequences to facilitate Cre-mediated

recombination. Moreover, successful in-frame cloning and functionality of the ATG-loxP-uPA fusion protein, expressed following Cre-mediated recombination, was conclusively demonstrated as uPA activity was significantly increased in conditioned medium from these co-transfected cells, over single transfected and non-transfected controls. Interestingly, no uPA activity was detected in conditioned medium from cells transfected with the uPA$^{(loxTlox)}$ construct alone, demonstrating tight transcriptional and/or translational control by the TSS.

Following microinjection and subsequent generation of K14-uPA$^{(loxTlox)}$-HGX transgenic mice, the functionality of the uPA$^{(loxTlox)}$ construct was assessed *in vivo*. In keeping with previous reports demonstrating that naked DNA injection results in transient epidermal gene expression *in vivo* (Hengge *et al,* 1995 and 1996), injection of K14-uPA$^{(loxTlox)}$-HGX transgenic mouse ears with pPGK-CRE resulted in Cre-mediated recombination of the uPA$^{(loxTlox)}$ construct. Interestingly, although recombination was detected after naked DNA injection, the level of PCR amplification was extremely low, suggesting that recombination had occurred in only a fraction of epidermal cells and that plasmid uptake in the mouse epidermis was relatively inefficient, a theory supported by previous findings (Hengge *et al,* 1996). This less than efficient uptake of injected plasmid DNA and the subsequent low proportion of cells containing the recombined uPA$^{(loxTlox)}$ construct would also explain our failure to detect uPA activity in pPGK-CRE treated ear tissue. Moreover, the restriction of K14 promoter activity to basal keratinocytes (Vassar *et al,* 1989), would further reduce the proportion of cells likely to be expressing transgene-specific uPA.

Although the detection of recombined DNA following intra-dermal injection of pPGK-CRE demonstrated 'proof of principle', this method of Cre application does not facilitate efficient temporal control of transgene expression. In an attempt to provide a reliable mechanism of transgene control, K14-uPA$^{(loxTlox)}$-HGX transgenic mice from all three founder lines (33, 38, and 39), were crossed with mice expressing the Cre-ER^{T2} fusion protein (Feil *et al,* 1997) under the control of a keratin 14 promoter (Vassar *et al,* 1989). This Cre-ER^{T2} fusion protein has been shown to be highly sensitive to tamoxifen treatment (Feil *et al,* 1997; Indra *et al,* 1999) and has been used to facilitate tamoxifen-induced activation of gene expression both *in vitro* and *in vivo* (Feil *et al,* 1997; Indra *et al,* 1999; Vallier *et al,* 2001). Moreover, tamoxifen treatment of K14-Cre-ER^{T2}/RXRα$^{L2/L2}$ double transgenic mice resulted in the selective ablation of RXRα in

mouse epidermis (Li *et al,* 2000b), demonstrating the efficient localisation of Cre-ER^{T2} expression to basal keratinocytes.

Interestingly, in contrast to K14-Cre-ER^{T2}/RXR$\alpha^{L2/L2}$ mice, recombined DNA was detected in untreated tail tissue from K14-uPA$^{(loxTlox)}$-HGX/K14-Cre-ER^{T2} double transgenic mice derived from two of our founder lines (33 and 39). Moreover, as no recombined DNA was detected in single transgenic mice from either of these founder lines, it is possible that background nuclear translocation of the Cre-ER^{T2} fusion protein occurs, but detection of background Cre-mediated recombination is dependent on the transgene incorporation site. Although recombined DNA was detected in double transgenic mice from lines 33 and 39, it is important to note that the PCR method used is at best semi-quantitative and thus the exact levels of wild-type and recombined DNA, both before and after tamoxifen treatment, remain undefined.

In contrast to double transgenic mice from founder lines 33 and 39, tail tissue from K14-uPA$^{(loxTlox)}$-HGX/K14-Cre-ER^{T2} mice, derived from founder line 38, contained no recombined DNA prior to tamoxifen treatment. However, following tamoxifen application, significant levels of recombined DNA were detected, indicating that the induction of Cre-recombinase activity is entirely tamoxifen-dependent in this mouse line. Furthermore, in line with previous reports (Vassar *et al,* 1989; Cheng *et al,* 1992; Wang *et al,* 1997), the detection of tamoxifen-induced recombination in tail, ear, back skin, and tongue, but not in liver, kidney or intestine, conclusively demonstrated the efficient spatial control of gene expression by the K14 promoter. Interestingly, despite our demonstration of tissue-specific induction of Cre-mediated recombination, preliminary studies showed that uPA activity was virtually undetectable in ear tissue dissected from founder line 38-derived double transgenic mice, either 48 hours or 1 week after tamoxifen treatment.

This inability to detect increased uPA activity could initially suggest that the uPA$^{(loxTlox)}$ construct is non-functional, however, our *in vitro* data convincingly demonstrates that the expressed ATG-loxP-uPA fusion protein is capable of converting plasminogen to plasmin, and thus indicates that there are alternative reasons for this observation. One possible explanation is that the time-points chosen to assess the uPA protein levels were too early. The decision to analyse cutaneous uPA levels at 48 hours and 1 week were based upon the observations of several recent reports demonstrating

detection of epidermal reporter gene expression between 24 hours and 10 days after tamoxifen application (Brocard *et al,* 1997; Indra *et al,* 1999; Vasioukhin *et al,* 1999). Although these studies indicate that transgene activation can occur rapidly following tamoxifen treatment, it is difficult to accurately determine the extent of transgene induction at these time points as X-gal staining methods are capable of detecting even very low-level β-gal activity. Moreover, as no published data exist regarding the temporal pattern of Cre-ER^{T2}-mediated activation of non-reporter genes, it is possible that at our chosen time-points, the level of transgene-specific uPA is too low for our current methods of detection. Other techniques, such as *in situ* hybridisation, immunohistochemistry and perhaps *in situ* zymography may provide more sensitive methods of detecting early expression of transgene-specific uPA.

Although analysis of uPA activity at later time-points may be prudent, an alternative explanation for the lack of detectable uPA could be that the chosen method of tamoxifen application results in a less than efficient level of *in vivo* recombination. Intra-peritoneal injection of tamoxifen has been widely used to facilitate Cre-mediated recombination *in vivo* (Danielian *et al,* 1998; Imai *et al,* 2001; Metzger and Chambon, 2001), and has previously been shown to effectively induce reporter gene expression in epidermal tissues (Brocard *et al,* 1997; Metzger and Chambon, 2001). However, previous studies using Cre-ER^{T} (Feil *et al,* 1996) and a similar fusion protein, CreED4 (Schwenk *et al,* 1998), indicate that the efficiency of *in vivo* recombination can vary depending on the body site and concentration of tamoxifen used. Moreover, our results show amplification of wild-type DNA in tamoxifen treated K14-uPA$^{(loxTlox)}$-HGX/K14-Cre-ER^{T2} mice, derived from founder line 38 (see figures 4.13 and 4.14), therefore suggesting that recombination has only occurred in a proportion of cells containing the uPA$^{(loxTlox)}$ construct. This sub-optimal level of recombination, as well as the restriction of transgene-specific uPA expression to K14 expressing basal keratinocytes, could limit the *in vivo* induction of functional uPA, and thus explain our inability to detect uPA activity in the analysed tissue homogenates. Again more sensitive methods of detection, as well as experimenting with distinct routes of tamoxifen application, such as repeated oral or topical administration, could provide a more accurate assessment of the expression of transgene-specific uPA.

In conclusion, although further analysis of the time-frame of tamoxifen-induced uPA expression is required, and examination of alternative methods of tamoxifen

application may be pertinent, the present studies have convincingly demonstrated the synthetic ligand-derived induction of Cre-ER^{T2}-mediated transgene activation in a skin-specific inducible system. These K14-$uPA^{(loxTlox)}$-HGX/K14-Cre-ER^{T2} transgenic mice therefore constitute an extremely useful template for the design of future skin-specific inducible transgenic animals and may provide essential information on the various roles of uPA in cutaneous physiology and patho-physiology.

CHAPTER 5

CHARACTERISATION OF INDUCIBLE K6-uPA TRANSGENIC MICE AND ANALYSIS OF WOUND HEALING

5.1 INTRODUCTION

Recent advances in genetic manipulation techniques have led to the development of numerous inducible transgene expression systems, as discussed in section 4.1. Since the ultimate aim of these systems is the precise temporal and spatial control of transgene activation, most involve the coupling of an inducible molecular switch with a tissue-specific promoter sequence that targets transgene expression to a particular organ or cell type. In skin, these promoter sequences are predominantly derived from keratin genes, although other epithelial gene sequences can provide efficient skin-specific activation (Carroll *et al,* 1993; DiSepio *et al,* 1995). Keratin promoters are particularly attractive when designing cutaneous inducible systems as their expression is restricted to epithelial tissues, and many are exclusively active within distinct layers of the epidermis, for example K5 and K14 promoters in the basal layer (Vassar *et al,* 1989; Ramirez *et al,* 1994), and the K10 promoter in suprabasal layers (Bailleul *et al,* 1990). Furthermore, in contrast to most other keratin promoters, promoters derived from the K6, K16 and K17 genes have potential for inducible activity. Indeed, K6 promoters have recently been shown to mediate epidermal transgene induction following specific stimulation (e.g Takahashi and Coulombe, 1996; Cui *et al,* 1996; Larcher *et al,* 1998), indicating that these promoter sequences can facilitate temporal, as well as spatial control of transgene expression.

Keratins are a large group of related intermediate filament proteins that contribute significantly to the structure and function of the epithelial cytoskeleton (reviewed in Steinert and Roop, 1988 and Fuchs and Weber, 1994). In skin, keratin proteins are generally co-expressed in defined pairs which serve as markers of terminal differentiation (Fuchs and Green, 1980; Nelson and Sun, 1983). However, some keratins, such as K6, are not associated with a defined program of differentiation and subsequently possess distinct patterns of expression and regulation in normal and activated epidermis (Moll *et al,* 1982). In healthy humans and animals, K6 protein is constitutively expressed in several internal stratified epithelia, such as those of the oral cavity, oesophagus and genital tract (Moll *et al,* 1982; Quinlan *et al,* 1985), as well as in the companion layer of the hair follicle (Stark *et al,* 1987; Heid *et al,* 1988). In contrast, with the exception of palmar-plantar sites, K6 protein is not expressed in interfollicular epidermis (Moll *et al,* 1982; Quinlan *et al,* 1985) except in a variety of cutaneous conditions characterised by hyperproliferation, such as psoriasis, epidermal

malignancies, or wound healing (Weiss *et al,* 1984; Mansbridge and Knapp, 1987; Stoler *et al,* 1988). In addition, epidermal K6 is significantly induced in skin treated with agents that induce hyperproliferation, such as phorbol 12-myristate 13-acetate (PMA) or all-trans retinoic acid (RA) (Schweizer *et al,* 1987; Molloy and Laskin, 1987; Rosenthal *et al,* 1992), as well as following activation of the EGF receptor (Jiang *et al,* 1993). Of interest, K6 induction following cutaneous injury occurs significantly earlier than wound-induced mitotic activity (Paladini *et al,* 1996 and references therein), indicating that alternative non-hyperproliferative mechanisms of K6 activation exist.

The lack of significant K6 expression in normal interfollicular epidermis, coupled with the capacity for induction by cutaneous wounding and hyperproliferative stimulation, forms the basis of several recently developed inducible transgenic expression systems. In the first example of this, Ramirez *et al* generated transgenic mice carrying a *lacZ* gene under the control of a 9 kb bovine K6 regulatory sequence. In these BK6β(-8.8).Z mice, β-gal activity was detected in several internal epithelial tissues, hair follicles and some orthokeratotic regions of tail skin, prior to treatment. More importantly, however, β-gal activity was virtually undetectable in untreated interfollicular epidermis indicating that the K6 promoter was 'off' in normal epidermis. In contrast, following topical application of PMA or RA, and upon cutaneous wounding, β-gal activity was significantly increased in suprabasal keratinocytes within the affected areas. Furthermore, analysis of the kinetics of β-gal stimulation following RA treatment showed direct correlation with the expression of endogenous mouse K6 mRNA, indicating that bovine K6 promoters can effectively mimic the spatial and temporal regulation of endogenous K6 (Ramirez *et al,* 1995). Interestingly, several recent reports have utilised a 2.4 kb sequence of the bovine K6 promoter that is inactive in untreated interfollicular epidermis and mediates inducible transgene activation in an similar manner to the 9 kb sequence (Cui *et al,* 1996; Ramirez *et al,* 1998; Larcher *et al,* 1998), suggesting that crucial regulatory elements reside within this 2.4 kb region (Ramirez *et al,* 1998).

In addition to bovine K6 promoters, regulatory sequences derived from the human K6 promoter have also been used to successfully mediate spatial and temporal control of transgene expression *in vivo*. In [hK6a 5']-LacZ mice (Takahashi and Coulombe, 1996 and 1997), carrying a *lacZ* gene under the control of the human K6a promoter, epidermal β-gal activity was again virtually undetectable in interfollicular

epidermis prior to induction; however, after topical application of PMA or RA, significantly increased β-gal activity was detected throughout the suprabasal layers of affected epidermis. Furthermore, following cutaneous wounding of these mice, β-gal activity was detected in wound-edge keratinocytes after just 3 hours, and remained significantly increased for at least 5 days post-wounding (Takahashi and Coulombe, 1997). Interestingly, whereas cutaneous wounding of either BK6β(-8.8).Z or [hK6a 5']-LacZ mice resulted in β-gal activity in the suprabasal layers of wound-edge epidermis (Ramirez *et al,* 1995; Takahashi and Coulombe, 1997), mouse K6 is detected in both basal and suprabasal layers (Takahashi and Coulombe, 1997), indicating the presence of subtle differences in the regulation of endogenous mouse K6 and bovine or human K6 promoter-driven transgenes.

In view of these data demonstrating effective spatial and temporal control of transgene activation using K6 promoter sequences, the present studies sought to generate transgenic mice carrying murine uPA cDNA under the control of a 2.4 Kb bovine K6 promoter. These K6-uPA transgenic mice would thus constitute an alternative to constitutive and synthetic ligand-based systems of uPA overexpression (see chapters 3 and 4) and, moreover, facilitate detailed analysis of the effect of elevated epidermal uPA expression on cutaneous wound healing. Furthermore, through the characterisation of K6-uPA mice, potentially useful insights into the role of uPA in epidermal responses to hyperproliferative stimuli may be provided.

5.2 RESULTS

5.2.1 Generation and characterisation of K6-uPA transgenic mice

K6-uPA transgenic mice were generated in collaboration with Pfizer Global Research and Development. A 1999 bp sequence, corresponding to positions 38-2036 of the published sequence for murine uPA (GenBank Accession No. X02389), was ligated into *Xba*I-*SmaI* digested pUC19. The pUC19-uPA vector was then digested with *Xba*I and *BglII*, and the resulting 1670 bp fragment, containing the complete murine uPA coding sequence (position: 21–1322), was ligated into *Xba*I-*BamHI* digested pBluescript II (Stratagene). Sub-cloning of the uPA cDNA into pBluescript II was necessary to ensure availability of the cohesive ends required for ligation with the selected transgene expression vector. The pBlue-uPA vector was subsequently digested with *BssHII* and *ApaI*, and the resulting 1750 bp uPA fragment ligated into a *BssHII-ApaI* digested pSE(2.4kb)-polyA vector, containing a previously characterised 2.4 kb bovine keratin 6β promoter (Ramirez *et al*, 1998). A 4.8 kb *BglII/BstEII* fragment containing the 2.4 kb K6β promoter, the 1750 bp uPA sequence, and an SV40 poly A signal sequence (figure 5.1) was isolated and used for microinjection. Two transgenic mice lines were established from founder animals, although only one was found to produce K6-uPA positive progeny at a ratio of 1:1 with wild-type offspring. Characterisation of this line (K6-uPAtg) was performed using various *in vivo* analyses as discussed below.

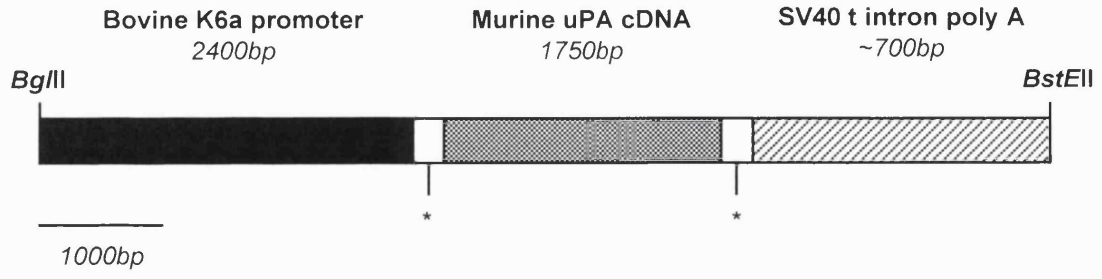

Figure 5.1 Schematic representation of the hyperproliferation inducible uPA construct, K6-uPA. * = short sequences derived from pBluescript II.

5.2.1.1 Transient stimulation of K6-uPA transgene expression

To determine whether K6-uPA transgene expression was induced by hyperproliferative cutaneous stimuli, wild-type and K6-uPAtg mouse ears were tape-stripped, treated with a single topical application of phorbol 12-myristate 13-acetate (PMA) or all-trans retinoic acid (RA), or injected with epidermal growth factor (EGF) as described. After 24 hours, total RNA was prepared from dissected whole ear tissue, and K6-uPA mRNA detected using a transgene-specific RT-PCR strategy, as outline in figure 5.2.

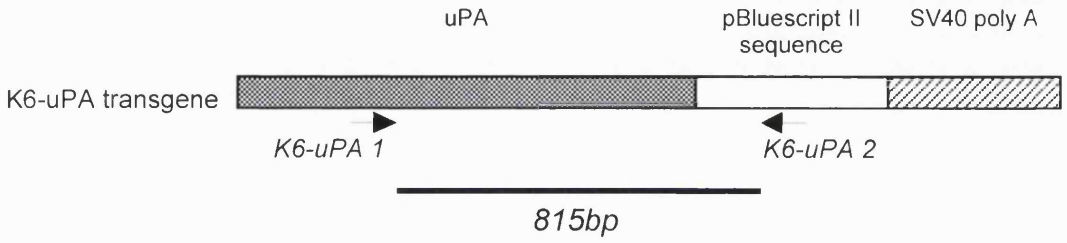

Figure 5.2 Schematic representation of RT-PCR strategy designed to detect K6-uPA specific mRNA.

RT-PCR analysis of RNA prepared from both vehicle treated and PMA treated wild-type mouse ears showed no detectable transgene-specific mRNA, as expected (figure 5.3a). Moreover, vehicle treated K6-uPAtg mouse ears also lacked detectable levels of transgene-specific mRNA. In contrast, RT-PCR analysis of dissected ear tissue from PMA treated K6-uPAtg mice showed strong amplification of an 815 bp band corresponding to K6-uPA-specific mRNA. As shown in figure 5.3b, induction of transgene-specific mRNA was also detected in K6-uPAtg mouse ears treated with RA and EGF, as well as in tape-stripped ears harvested from K6-uPAtg mice. Very low levels of K6-uPA-specific mRNA were occasionally detected in ear tissue from untreated K6-uPAtg mice (figure 5.3b). However, as RNA was prepared from whole ear tissue, this background K6-uPA expression is likely to represent constitutive K6 promoter activity in resident hair follicles, as previously observed (Ramirez *et al,* 1998).

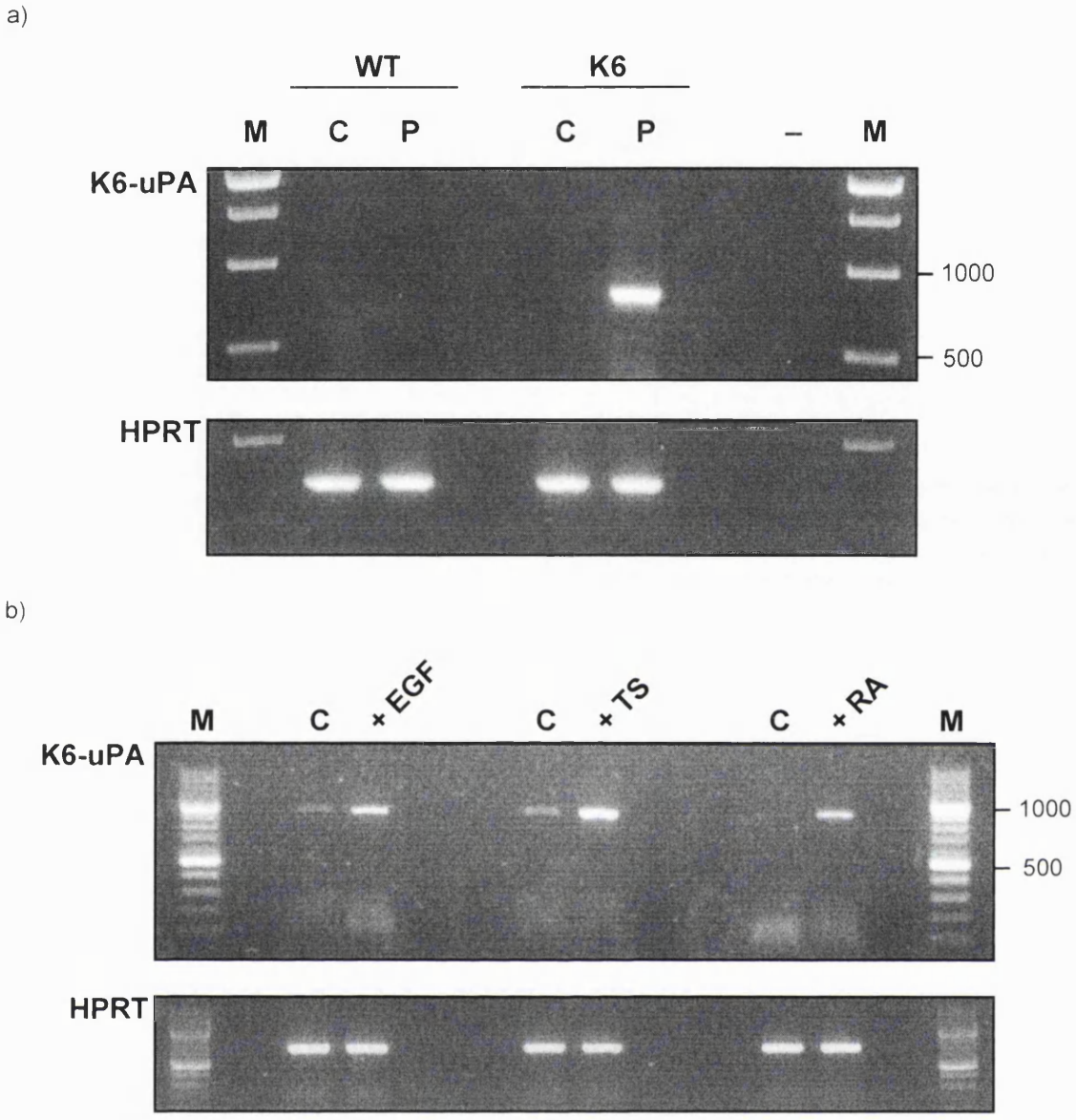

Figure 5.3 Transient induction of K6-uPA transgene by cutaneous stimulation. a) RT-PCR detection of transgene-specific mRNA in wild-type (WT) and K6-uPAtg (K6) mice after administration of a single dose of PMA. C = vehicle treated control; P = PMA treated; – = no template control; M = 500 bp DNA ladder (selected marker sizes are indicated in base pairs). b) RT-PCR detection of transgene-specific mRNA in K6-uPAtg mice following various cutaneous stimuli. C = relevant control; +EGF = EGF treated; +TS = tape-stripped; +RA = RA treated; M = 100 bp DNA ladder (selected marker sizes are indicated in base pairs).

5.2.1.2 Extended stimulation of K6-uPA transgene expression

To assess whether the observed up-regulation of K6-uPA transgene expression led to an increase in functional uPA activity, wild-type and K6-uPAtg mouse ears were repeatedly treated with topical applications of PMA or RA as described. At various times, ear tissue was harvested and protein prepared, prior to analysis of functional uPA levels using both the indirect chromogenic peptide assay and plasminogen-linked zymography. Results are shown in figures 5.4 and 5.5.

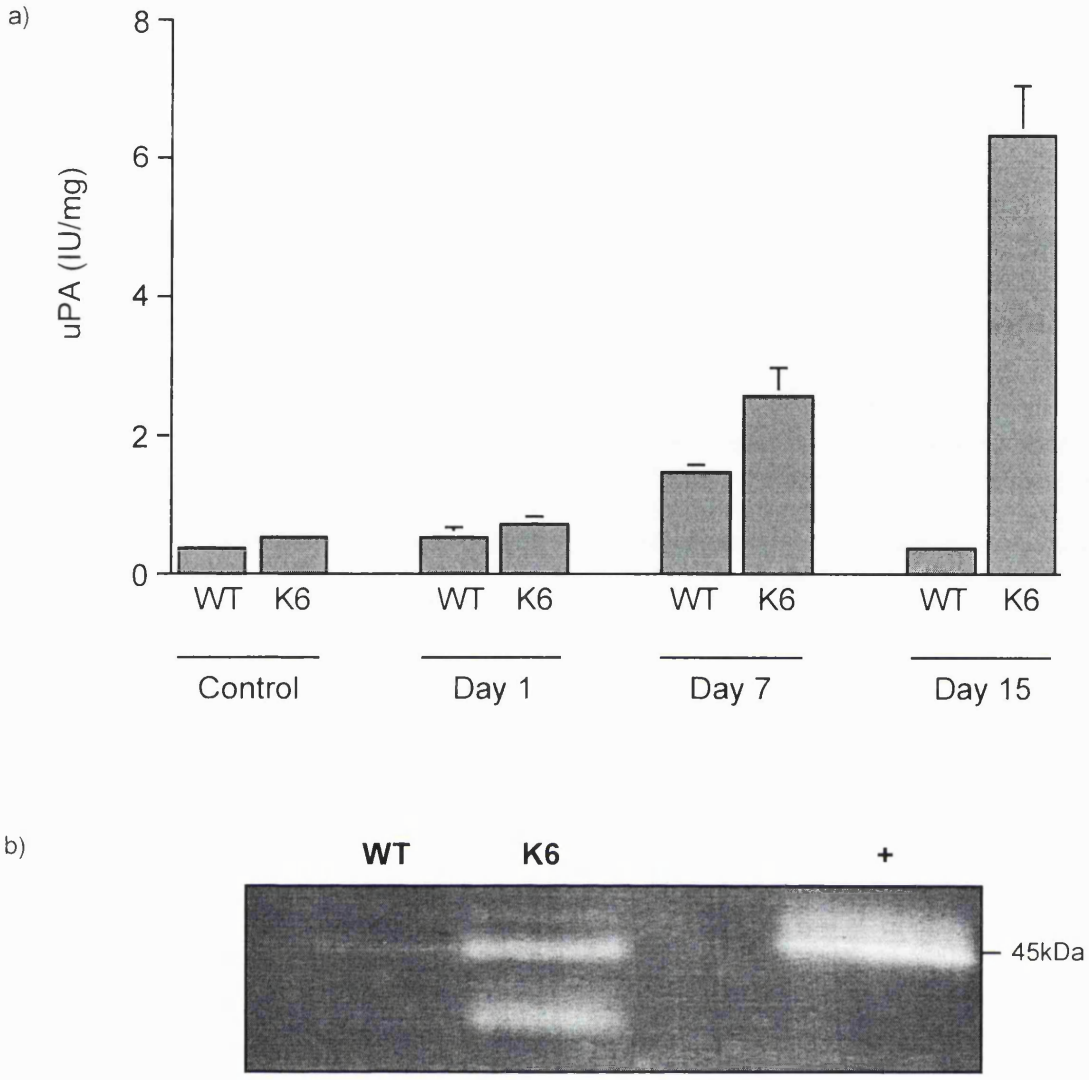

Figure 5.4 Effect of extended PMA treatment on functional uPA levels in K6-uPAtg mice. a) uPA activity in PMA treated wild-type (WT) and K6-uPAtg (K6) mouse ear homogenates, as assessed by indirect chromogenic peptide assay. Data presented (mean ± SEM) are from 3 independent experiments. b) plasminogen-linked zymography of day 15 samples. + = murine urine.

As shown in figure 5.4a, extended PMA treatment of both wild-type and K6-uPAtg mice resulted in significant up-regulation of functional uPA by day 7. Moreover, analysis of wild-type and K6-uPAtg ear tissue homogenates showed that after 7 days of PMA treatment, uPA activity levels were approximately 2-fold higher in transgenic homogenates compared to wild-type homogenates. Surprisingly, after 15 days of PMA treatment, uPA activity levels in wild-type homogenates were reduced 4-fold compared to 7 day wild-type levels. In contrast, uPA activity in 15 day K6-uPAtg homogenates was increased 2.5-fold over 7 day K6-uPA levels, resulting in an approximate 18-fold difference in uPA activity levels between K6-uPAtg and wild-type ear homogenates.

Further confirmation of PMA-mediated induction of functional transgene-derived uPA was provided by plasminogen-linked zymography (figure 5.4b). Analysis of wild-type mouse ear homogenates after 15 days of PMA treatment showed a band of low-level beta-casein degradation corresponding to murine uPA (45 kDa). However, analysis of K6-uPAtg homogenates showed a marked increase in beta-casein degradation associated with increased levels of uPA activity. Interestingly, a second band of beta-casein degradation corresponding to a unknown protein of between 35-40 kDa was detected in 15 day K6-uPAtg ear tissue, but was absent in wild-type ear tissue.

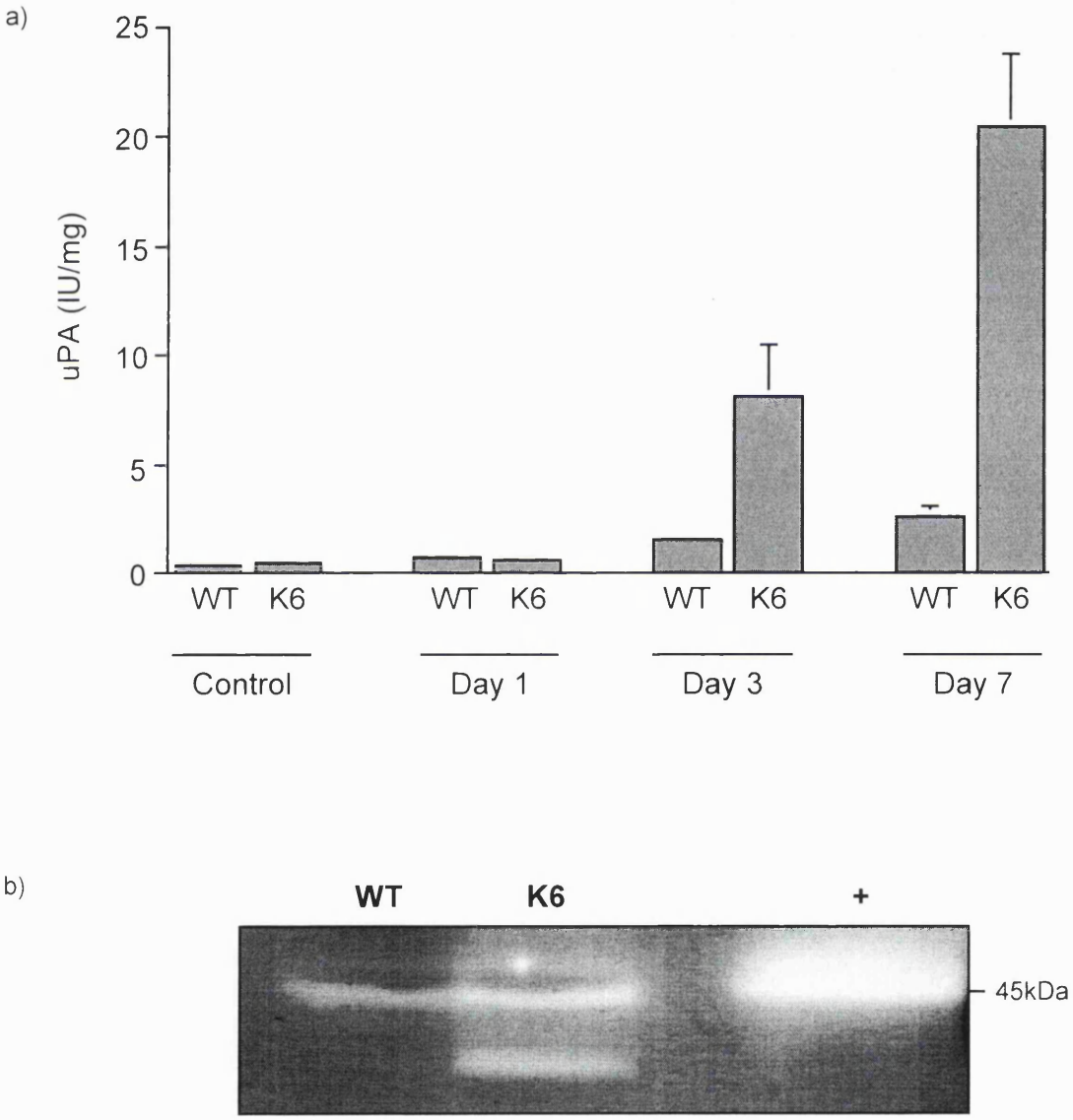

Figure 5.5 Effect of extended RA treatment on functional uPA levels in K6-uPAtg mice. a) uPA activity in RA-treated wild-type (WT) and K6-uPAtg (K6) mouse ear homogenates, as assessed by indirect chromogenic peptide assay. Data presented (mean ± SEM) are from 3 independent experiments. b) plasminogen-linked zymography of day 7 samples. + = murine urine.

Induction of functional transgene-derived uPA in K6-uPAtg mouse ears was also observed with extended RA treatment. Indirect chromogenic peptide assay analysis of mouse ear tissue showed that after 3 days of RA treatment, uPA activity levels were approximately 5-fold higher in transgenic ear homogenates compared to wild-type homogenates (figure 5.5a). Furthermore, after 7 days of RA treatment, uPA activity in K6-uPAtg homogenates was 20.48 ± 3.2 IU/mg compared to a wild-type level of 2.58 ± 0.52 IU/mg, corresponding to an approximate 8-fold difference. As shown above with PMA, plasminogen-linked zymography analysis of ear homogenates from mice treated with RA for 7 days revealed increased uPA-mediated beta-casein degradation in K6-uPAtg samples compared to wild-type samples (figure 5.5b). Moreover, an unknown 35-40 kDa protein capable of beta-casein degradation was again detected, and was only observed in RA-treated K6-uPAtg ear homogenates.

5.2.1.3 Effect of elevated functional uPA on epidermal integrity

Having demonstrated that both PMA and RA were able to significantly upregulate transgene-specific uPA in the skin of K6-uPAtg mice, the effect of this increased functional uPA on epidermal structural integrity was assessed. Ears from four wild-type and four K6-uPAtg mice, treated with PMA for 15 days, were dissected and transferred to formal saline, prior to tissue processing, sectioning and H&E staining. Examination of ear tissue epidermis under light microscopy showed evidence of acanthosis (increased keratinocyte layering) and scale-crust formation (figure 5.6). However, epidermal separation from dermis, a potential consequence of the disruption of the basement membrane due to elevated protease activity, was not observed in either wild-type or K6-uPAtg mouse skin following PMA treatment. Overall, no significant difference in epidermal structure was observed between PMA-treated wild-type and K6-uPAtg mouse skin.

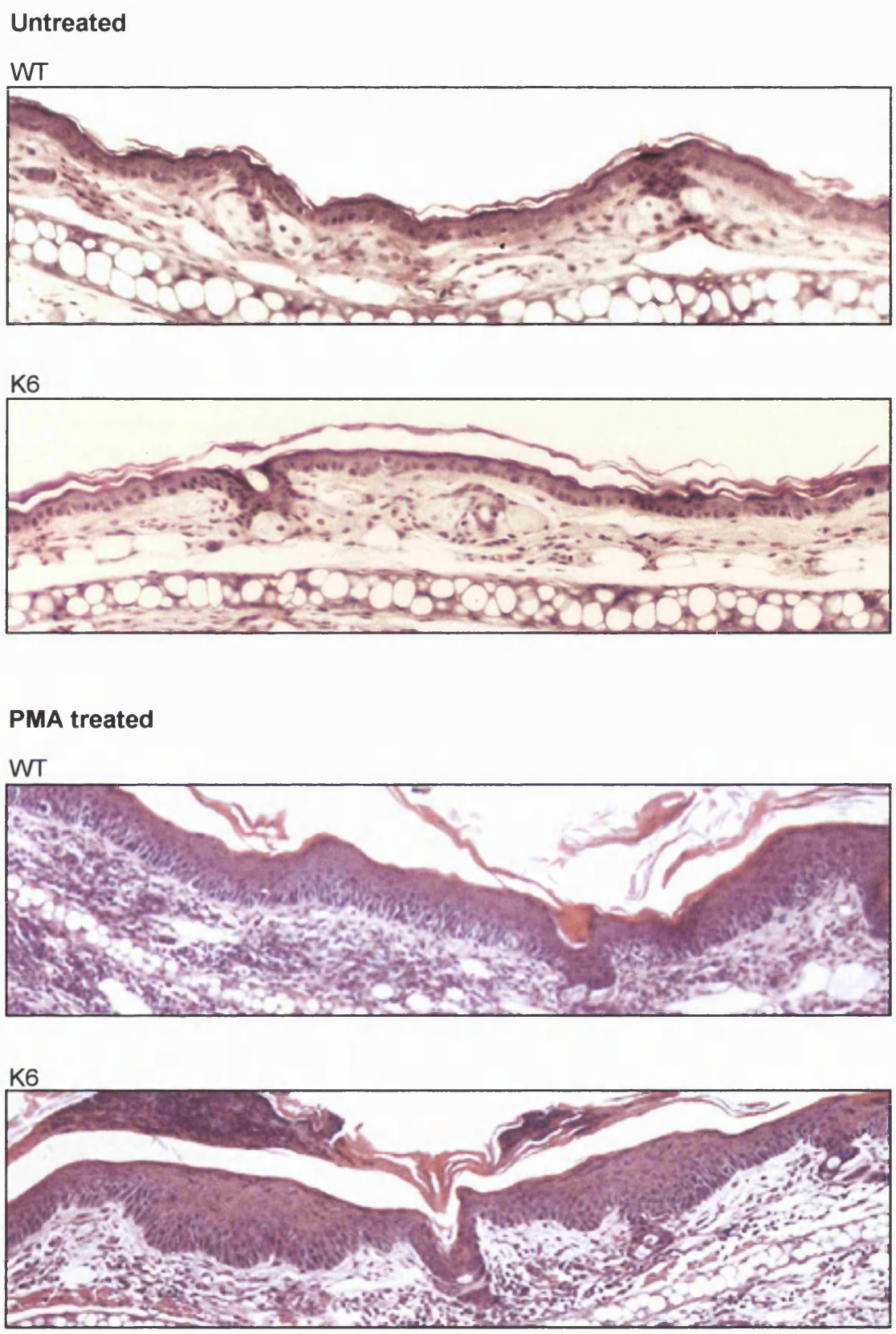

Figure 5.6 Effects of K6-uPA induction on epidermal structural integrity. H&E stained sections of ear tissue from wild-type (WT) and K6-uPAtg mice (K6). Representative sections are shown from untreated ears (untreated) and ears treated with PMA over 15 days (PMA treated).

5.2.1.4 Effect of cutaneous wounding on K6-uPA transgene expression

To confirm that uPA is induced in K6-uPAtg mice upon cutaneous wounding, wild-type and K6-uPAtg mice were wounded as described, and uPA activity in full-thickness excisional wound homogenates assessed after 3, 5, or 7 days. Using plasminogen-linked zymography, a band of beta-casein degradation corresponding to murine uPA (45 kDa) was detected in both wild-type and K6-uPAtg wound homogenates throughout the experiment. However, at all time points, the level of beta-casein degradation was increased in K6-uPAtg wound homogenates compared to wild-type wound homogenates (figure 5.7a), indicating that the K6-uPA transgene was inducible upon cutaneous wounding. Subsequent densitometric analysis of zymography gels revealed an approximate 3.5-fold induction of uPA-derived caseinolytic activity in K6-uPAtg samples over wild-type samples at all time points (Figure 5.7b).

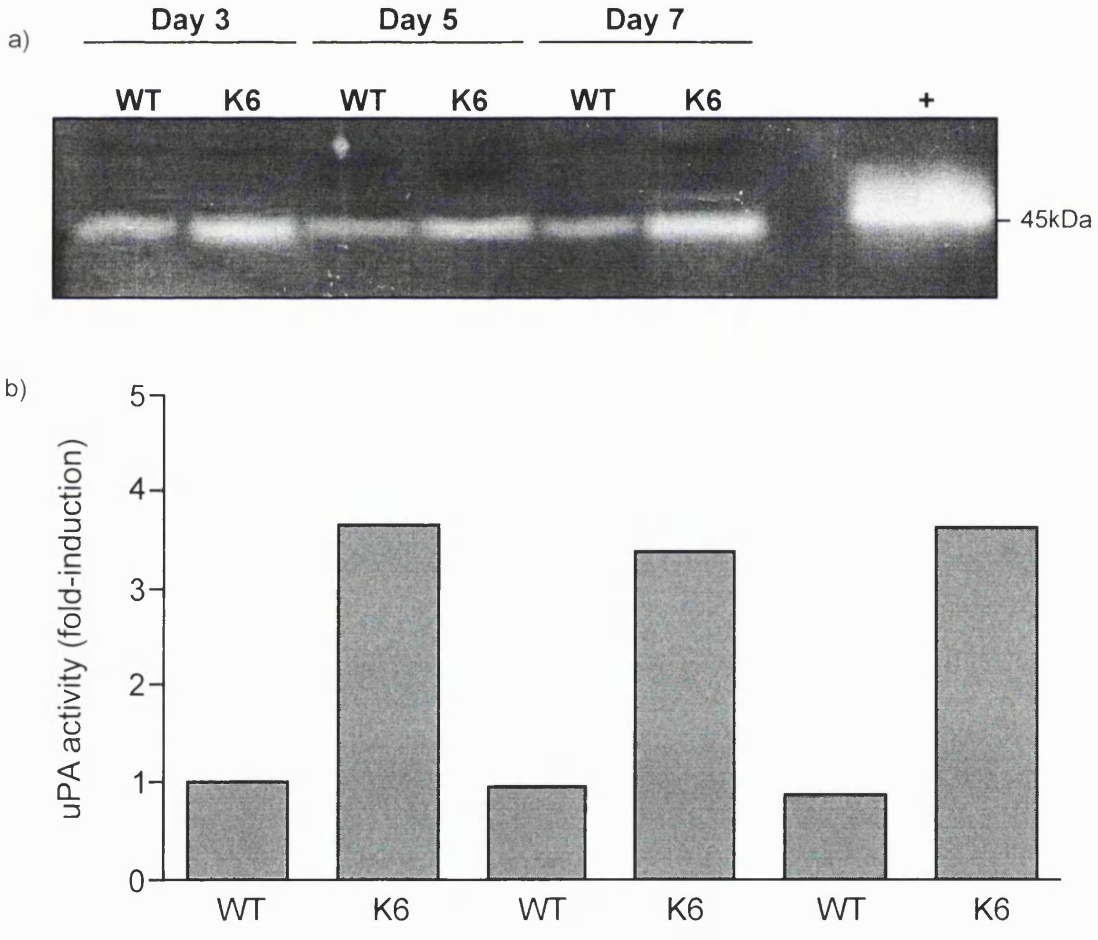

Figure 5.7 Effect of excisional wounding on functional uPA levels in K6-uPAtg mice. a) uPA activity levels in wound homogenates from wild-type (WT) and K6-uPAtg (K6) mice as assessed by plasminogen-linked zymography. + = murine urine. b) Densitometry of zymography gels. Data presented (mean) are from 2 independent experiments.

5.2.2 Analysis of wound healing in K6-uPA transgenic mice

Having demonstrated significant up-regulation of functional transgene-derived uPA in K6-uPAtg mouse wounds, experiments were designed to investigate the effect of elevated uPA levels on cutaneous wound healing. Initially, wound analyses were performed 3, 5 and 7 days post-wounding. However, preliminary observations from the analysis of wound sections indicated that whereas after 3 or 5 days re-epithelialization was not complete, after 7 days a significant proportion of wounds were fully re-epithelialized in both wild-type and K6-uPAtg mice. As a consequence, all subsequent wound analyses were performed 3 or 5 days post-wounding only.

Thus, to assess the potential effects of elevated uPA on cutaneous wound healing, 19 female and 17 male wild-type, and 15 female and 17 male K6-uPAtg mice were wounded as described in section 2.4.11. After 3 or 5 days, wounds were dissected, processed and stained with H&E. Wound sections were subsequently assessed for inclusion using the following criteria: sections should be complete; no folding should be present in the areas to be analysed; no tearing should be present in the areas to be analysed. Using these criteria, sections from 12 wild-type and 12 K6-uPAtg wounds were selected for analysis (see section 2.4.12) at each time point.

As shown in figure 5.8a, the mean diameter of analysed wounds reduced from day 3 post-wounding to day 5 post-wounding, as expected. However, no significant difference in mean wound diameter between wild-type and K6-uPAtg wounds was observed at either 3 or 5 days post-wounding. Similarly, although the mean wound-edge epidermal thickness increased from day 3 post-wounding to day 5 post-wounding, as expected, no significant difference between wild-type and K6-uPAtg wounds was observed at either post-wounding time-point (figure 5.8b). In addition, no significant difference between wild-type and K6-uPAtg wounds was also observed upon analysis of the inflammatory cellular infiltrate 3 days post-wounding (figure 5.8c). However, after analysis of the inflammatory cellular infiltrate 5 days post-wounding the mean cell number in K6-uPAtg wounds was 4919.17 ± 214.8 cell/mm^2, compared to 4400.67 ± 126.5 cells/mm^2 in wild-type wounds, a statistically significant difference ($p < 0.05$). Preliminary visual analysis of the cellular infiltrate suggested that it comprised primarily of fibroblasts and macrophages.

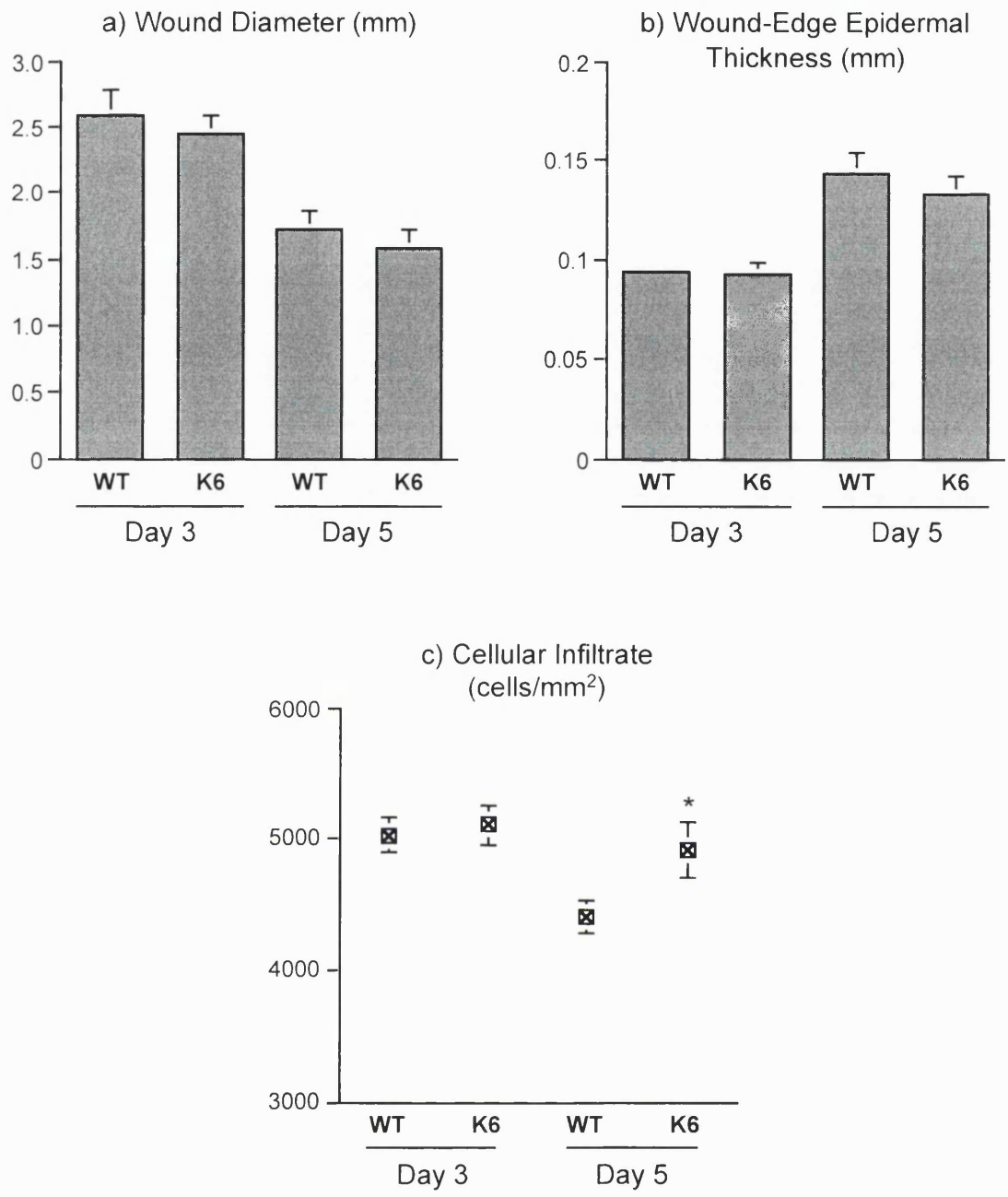

Figure 5.8 Effect of elevated uPA activity on wound healing in K6-uPAtg mice. Wound sections from wild-type (WT) and K6-uPAtg (K6) mice were analysed for wound diameter (a), wound-edge epidermal thickness (b) and inflammatory cellular infiltrate (c). Data presented (mean ± SEM) are from 12 wild-type and 12 K6-uPA mice per time-point. * = $p < 0.05$ (statistically significant from wild-type).

5.3 DISCUSSION

There is now a significant body of data suggesting that uPA-mediated plasminogen activation may play an important role in acute cutaneous wound healing (see section 1.4). Furthermore, the detection of aberrant protease and protease inhibitor expression in many chronic ulcers has suggested a role for elevated uPA activity in the subsequent pathology of these non-healing wounds. This project therefore set out to devise a transgenic system of cutaneous uPA overexpression that would facilitate analysis of the effect of elevated uPA activity on skin development, physiology and repair. In chapters 3 and 4, we have described attempts to develop constitutive and synthetic ligand-based overexpression systems. As an alternate approach, transgenic mice were generated carrying uPA under the control of a bovine K6 promoter. Since K6 promoter activity is negligible in normal interfollicular epidermis, yet is rapidly and significantly induced in wound-edge keratinocytes (Ramirez *et al,* 1995; Takahashi and Coulombe, 1997), it was postulated that these K6-uPAtg mice might provide a powerful tool in the analysis of effects of uPA overexpression on cutaneous wound healing.

The negligible detection of transgene-specific mRNA in vehicle treated K6-uPAtg mouse skin, coupled with the observed significant upregulation of this mRNA following cutaneous stimulation, is consistent with previous reports showing that the 2.4 kb bovine K6β promoter efficiently facilitates transgene induction (Cui *et al,* 1996; Ramirez *et al,* 1998; Larcher *et al,* 1998). In addition, despite RA- and PMA-mediated upregulation of endogenous uPA in wild-type skin, as shown previously (Varani *et al,* 1994; Lund *et al,* 1996; Braungart *et al,* 2001), the detection of significantly higher levels of functional uPA in PMA or RA treated K6-uPAtg skin confirmed both the inducibility and the functionality of the K6-uPA transgene.

An interesting feature of the extended hyperproliferative stimulation of mouse skin was that, whereas PMA treatment of wild-type mice resulted in a significant induction of functional uPA by day 7, by day 15, uPA levels had returned to baseline. As no similar reduction in functional uPA was observed in K6-uPA mice following 15 days of PMA treatment, it is likely that distinct regulatory mechanisms facilitate PMA-mediated induction of the endogenous uPA promoter and the K6 promoter. Another notable feature of the extended RA and PMA treatment was that, in addition to the induction of 45 kDa uPA, a caseinolytic protease of between 35-40 kDa is induced in

K6-uPA mice, but not in wild-type mice. Although the identity of this protease remains undefined, a recent report describing plasmin-mediated formation and rapid internalisation of a 36 kDa GFD-deficient uPA (Poliakov *et al,* 2001), has suggested that in RA or PMA treated K6-uPA mice, high levels of uPA-derived plasmin may result in the initiation of a novel self-regulatory mechanism.

Increased plasmin-mediated proteolysis or MMP activation has previously been implicated in the epidermal disruption associated with several cutaneous disorders, for example pemphigus-related acantholysis (Morioka *et al,* 1987b; Hashimoto *et al,* 1989) and the formation of dermatitis herpetiformis (DH) lesions (Airola *et al,* 1997). In light of this, it was anticipated that the difference in functional uPA activity between PMA treated K6-uPAtg mice and similarly treated wild-type mice might result in altered skin histology in the transgenic animals. Surprisingly, however, after 15 days of intermittent PMA treatment, skin from K6-uPAtg and wild-type mice was indistinguishable. Since PMA treatment of mouse skin activates expression of endogenous uPA (Lund *et al,* 1996), such a result could suggest that this endogenous uPA expression is sufficient to facilitate uPA-mediated histological alterations, thus masking the effects of the transgene-specific uPA. However, this is unlikely as an approximate 18-fold increase in uPA activity was observed in PMA-treated K6-uPAtg skin compared to similarly treated wild-type control skin. As PMA treatment of mouse skin also stimulates endogenous expression of both PAI-1 and PAI-2 (Lund *et al,* 1996), a more likely explanation is that localised compensatory inhibition of uPA restricts the pathological effects of elevated uPA activity and hence the lack of histological differences. Interestingly, recent data has indicated that uPA and uPAR act synergistically to promote epidermal skin defects (Zhou *et al,* 2000), and that the involvement of uPA in pemphigus-related acantholysis is dependent on its interaction with uPAR (Xue *et al,* 1998) suggesting that, in PMA treated K6-uPAtg mice, pathogenic proteolysis may be further limited by the availability of uPAR binding sites.

In addition to chemically-mediated stimulation, several previous reports have shown induction of K6 promoter activity following cutaneous wounding (Ramirez *et al,* 1995; Takahashi and Coulombe, 1996 and 1997). In keeping with these reports, the present studies demonstrated significant upregulation of functional uPA in K6-uPAtg wounds compared to wild-type wounds. Moreover, the consistently increased levels of functional enzyme in K6-uPAtg wounds over the 7 day post-wounding period indicate

that the bovine K6 promoter is activated for a significant period following skin injury, as shown previously with human K6 promoters (Takahashi and Coulombe, 1997). Further analyses of the spatial distribution of transgene-specific uPA in wounded tissues, using immunohistochemical and *in situ* zymography techniques, were unsuccessful (data not shown). These sensitive techniques were primarily hindered by high background detection of uPA, presumably due to significant expression of endogenous uPA upon skin wounding, as previously reported (Grondahl-Hansen *et al,* 1988; Romer *et al,* 1991). However, since previous studies have demonstrated induction of K6 promoter-driven gene expression in wound-edge keratinocytes and suprabasal layers of the wound-proximal epidermis (Ramirez *et al,* 1995; Takahashi and Coulombe, 1996 and 1997), it is highly likely that transgene-specific uPA is similarly expressed in K6-uPAtg mouse wounds.

Despite the induction of transgene-specific uPA throughout the wound healing process, analysis of wound sections revealed no significant difference in the extent of re-epithelialization between K6-uPAtg wounds and wild-type wounds. That cutaneous uPA overexpression had no effect on wound-induced keratinocyte migration is surprising, however, this observation may be explained by regulatory mechanisms functioning in wounded skin. In addition to uPA, cutaneous wound healing is characterised by a marked upregulation of epidermal uPAR, PAI-1 and PAI-2. Although PAI-2 is expressed throughout the wound-proximal epidermis (Bechtel *et al,* 1998), uPAR and PAI-1 are expressed in defined locations (Romer *et al,* 1991 and 1994), strongly suggesting that highly specialised regulatory mechanisms control the function of uPA during epidermal wound repair. In addition, many of the cytokines and growth factors present in a cutaneous wound site (see table 1.1, page 18) stimulate, and are stimulated by, components of the plasminogen activator system *in vitro* (e.g. Lyons *et al,* 1988; George *et al,* 1990; Saksela and Rifkin, 1990; Keski-Oja and Koli, 1992) further suggesting a complex wound-related system of uPA regulation. In view of these regulatory mechanisms, it is conceivable that the upregulation of transgene-specific uPA in K6-uPAtg wounds stimulates compensatory changes in uPAR, PAI-1 or PAI-2, thus counteracting any effect of the exogenous uPA, and maintaining normal wound closure. Alternatively, in a similar manner to hyperproliferative epidermis, this regulation may take the form of a limited number of available uPAR binding sites on leading-edge keratinocytes, which could subsequently limit localised proteolysis and control the rate of re-epithelialization.

Tight regulation of the plasminogen activator system during epidermal wound repair would also explain the lack of effect of uPA overexpression on wound-edge epidermal thickness. uPA has been associated with the promotion of keratinocyte proliferation in several previous reports (Kirchheimer *et al,* 1989; Hibino *et al,* 1999; Jensen and Lavker, 1999). However, as this mitogenic effect of uPA seems to be dependent on the interaction of intact active enzyme with uPAR, at least *in vitro* (Kirchheimer *et al,* 1989), a compensatory increase in PAI-1 or PAI-2, or the saturation of uPAR binding sites in wounded K6-uPAtg mice would suppress any potential proliferative effects of uPA overexpression. Alternatively, as keratinocyte mitotic division is already significantly increased during normal wound re-epithelialization (Garlick and Taichman, 1994, and references therein), it is possible that epidermal proliferation is maximal, and thus, any excess uninhibited uPA in K6-uPAtg wounds would have little or no additional proliferative effect.

The present studies show that cutaneous uPA overexpression increases the number of wound-induced infiltrating cells in 5 day-old wounds. Although further experiments are required to determine the lineage of the affected cells, this finding supports previous data indicating a critical role for uPA in the migration and invasion of several cell types involved in the wound healing process, such as fibroblasts (Knox *et al,* 1987; Anichini *et al,* 1994) and macrophages (Kirchheimer and Remold, 1989; Resnati *et al,* 1996). Moreover, as these wound infiltrating cells use proteolytic enzymes to dissect their way through the provisional wound matrix (reviewed in Mignatti *et al,* 1996 and Parks, 1999), the elevated levels of uPA in K6-uPAtg wounds may well facilitate enhanced matrix degradation, thus enhanced cell migration. Interestingly, no difference in inflammatory cellular infiltrate numbers was observed in 3 day-old wounds, supporting previous data indicating temporal variations in the involvement of the plasminogen activator system in cellular infiltration (Schaefer *et al,* 1994).

In conclusion, the present studies have described the successful generation of K6-uPAtg mice and shown that the bovine K6β promoter is appropriately regulated in these transgenic mice. Moreover, this study has demonstrated that keratinocyte-derived overexpression of uPA in K6-uPAtg mice has no effect on PMA histology or selected indices of wound healing, though an increase in inflammatory cellular infiltrate in 5-day-old wounds was observed. As previous results have indicated a role for uPA in pemphigus- and DH-related epidermal disruption, as well as in wound-related cellular

migration, these findings strongly hint at the existence of complex mechanisms of regulation within the plasminogen activator system. Additional wounding studies, including those designed to analyse uPA-related regulatory pathways, to identify the exact spatial expression of uPA, and to determine the effect of larger wounds, are required before strong conclusions can be drawn. However, in addition to confirming that K6 promoter-driven transgene expression constitutes a powerful approach to the analysis of gene function in skin, the results from this study indicate that K6-uPAtg mice may provide much useful data concerning cutaneous regulation of the plasminogen activator system in various patho-physiological situations.

CHAPTER 6

EFFECT OF HYPOXIA ON KERATINOCYTE REGULATION OF THE PLASMINOGEN ACTIVATOR SYSTEM: uPA-MEDIATED ENHANCEMENT OF CELL MOTILITY

6.1 INTRODUCTION

Cutaneous wounding is characterised by a dramatic sequence of cellular changes that result in the transformation of inert keratinocytes to motile cells, a process essential for re-epithelialization. This wound-induced response is facilitated by various morphological and biochemical modifications that include increased secretion of inflammatory cytokines and growth factors, altered keratin and integrin expression and upregulation of proteolytic enzymes, such as MMPs and plasminogen activators (see section 1.2.3). Wound re-epithelialization, resulting from increased keratinocyte migration and proliferation, is a key feature of normal cutaneous tissue repair and data from *in vivo* wound models indicate that an intact plasminogen activator system is essential for normal re-epithelialization, and subsequently for wound healing overall (Romer *et al,* 1996; Bugge *et al,* 1996a).

Another recognised characteristic of cutaneous wounding is a reduction in tissue oxygen tension or tissue hypoxia (Niinikoski *et al,* 1971; Niinikoski *et al,* 1972a; Chang *et al,* 1983). Although prolonged periods of this wound-induced hypoxia are associated with the pathology of certain chronic ulcers (Stadelmann *et al,* 1998b), conventional wisdom suggests that following normal cutaneous injury, cells functioning within damaged tissue will experience a transient reduction in tissue oxygen tension, which may stimulate beneficial regulatory mechanisms within these cells (Niinikoski *et al,* 1991). Indeed, acute hypoxia has been indicated as an important regulator of enhanced wound re-epithelialization *in vivo* (reviewed in LaVan and Hunt, 1990). Moreover, in keeping with this *in vivo* data, acute hypoxia was recently shown to positively regulate human keratinocyte migration *in vitro*, as cells cultured under hypoxic conditions display enhanced motility compared to normoxic controls (O'Toole *et al,* 1997b). In addition, expression of MMPs, such as MMP-9, and components of the plasminogen activator system, such as uPAR and PAI-1, are also regulated by hypoxia in certain invasive and migratory cell types (O'Toole *et al,* 1997b; Graham *et al,* 1998; Fitzpatrick and Graham, 1998). It is therefore possible that hypoxia modulates cell invasion/migration via the regulation of proteolytic system components.

Throughout the last decade, evidence for the involvement of uPA in both *in vitro* and *in vivo* cellular migration has accumulated. Over-expression of uPA and increased uPA-mediated plasminogen activating activity have been observed in migrating

monocytes (Vassalli *et al,* 1984), endothelial cells (Pepper *et al,* 1987 and 1993) and keratinocytes (Morioka *et al,* 1987a) in culture. Moreover, in a variety of cell types, uPA has been associated with the promotion of *in vitro* migration either by uPA-mediated proteolytic activity (Morimoto *et al,* 1993; Yebra *et al,* 1996; Wijnberg *et al,* 1997), or by a direct chemotactic effect involving the generally non-proteolytic, stimulation of uPAR-derived signalling pathways (Del Rosso *et al,* 1990; Anichini *et al,* 1994; Resnati *et al,* 1996). In addition, *ex-vivo* studies have also demonstrated that uPA-mediated proteolysis is involved in the invasive migration of monocytes (Kirchheimer and Remold, 1989), fibroblasts (Knox *et al,* 1987), and endothelial cells (Koolwijk *et al,* 1996) and *in vivo* analysis of both mouse and human healing wounds has shown increases in uPA mRNA and plasminogen-activating activity (Grondahl-Hansen *et al,* 1988; Romer *et al,* 1991; Schaefer *et al,* 1994). Interestingly, this wound-induced uPA upregulation is often accompanied by a concomitant increase in uPAR, PAI-1 or PAI-2 (Romer *et al,* 1991 and 1994; Schaefer *et al,* 1994; Bechtel *et al,* 1998), suggesting that uPA, as well as other plasminogen activator system components, play an important role in the migration and extracellular matrix invasion required for normal wound healing.

In light of the data indicating that cutaneous tissue damage can result in an acutely hypoxic wound environment, and in consideration of recent evidence suggesting that hypoxia regulates the expression of protease system components in several invasive/migratory cell types, the present studies sought to determine the functional consequence of hypoxia on uPA-mediated plasminogen activation in keratinocytes. Moreover, as hypoxia has also been shown to be a potent stimulus for keratinocyte migration both *in vitro* and *in vivo*, and uPA may have a general function in wound-induced cell migration, these studies also aimed to assess the potential role of any hypoxia regulated protease system components in hypoxia enhanced keratinocyte migration.

6.2 RESULTS

6.2.1 Analysis of oxygen tension in PAM 212 keratinocyte culture medium

To determine the precise level of hypoxia achieved using our culture system, PAM 212 keratinocytes were seeded into 60 mm dishes, grown to approximately 60% confluence and quiesced for 24 hours in serum free medium, prior to culture under normoxic or hypoxic conditions for 24 hours. Oxygen tensions in culture medium were subsequently assessed using an ABL4 analyser (Radiometer, Copenhagen, Denmark). As expected, the percentage oxygen in hypoxic samples was significantly lower than in normoxic samples. Moreover, a mean percentage oxygen of 2.73 ± 0.12% in the hypoxic samples at time 0, indicated that the hypoxic conditions were stable over a 24 hour period (table 6.1). The rate of re-oxygenation in hypoxic tissue culture medium was also assessed. Re-oxygenation of the culture medium was rapid and reached completion only 16 minutes after removal from the hypoxia chamber.

Time (mins)		mm Hg	% O_2
normoxia		152.23 ± 1.02	21.31 ± 0.14
hypoxia	0	19.48 ± 0.88	2.73 ± 0.12
	4	76.63 ± 3.12	10.73 ± 0.44
	8	108.43 ± 2.41	15.18 ± 0.34
	12	124.68 ± 3.15	17.45 ± 0.44
	16	142.43 ± 1.93	19.94 ± 0.27
	20	161.43 ± 5.82	22.60 ± 0.81

Table 6.1 Oxygen tensions in culture medium following 24 hours under normoxic or hypoxic conditions. Time = minutes following opening of hypoxia chamber. Data presented (mean ± SEM) are from 4 independent experiments.

6.2.2 Effect of hypoxia on PAM 212 keratinocyte viability

To determine whether PAM 212 keratinocytes could be maintained in hypoxic conditions without significant loss of viability, cells, seeded into 6 well plates, were grown to 60-70% confluence and quiesced for 24 hours with serum free medium prior to culture under normoxic or hypoxic conditions for 24 hours. Normoxic and hypoxic

keratinocyte cultures were subsequently assessed for LDH release and Trypan blue exclusion. PAM 212 keratinocytes cultured under hypoxic conditions showed no variation in cell morphology at the light microscope level (data not shown). Moreover, Trypan blue exclusion and LDH release analysis showed no significant difference between normoxic and hypoxic samples (table 6.2). In addition, no significant difference was seen in the pH value of conditioned medium from normoxic and hypoxic cultures (table 6.2).

	Normoxia	Hypoxia	*P* (student t-test)
Trypan Blue exclusion*	7.0 ± 1.2	8.1 ± 0.6	0.41
LDH assay*	7.2 ± 1.9	9.6 ± 1.8	0.24
pH	7.3 ± 0.05	7.4 ± 0.06	0.34

Table 6.2 Viability of PAM 212 keratinocytes cultured under normoxic and hypoxic conditions for 24 hours. * = values presented as percentage cell death. Data presented (mean ± SEM) are from triplicate wells in 4 independent experiments.

6.2.3 Analysis of uPA and uPAR mRNA expression in hypoxic PAM 212 keratinocytes

To investigate the effect of hypoxia on keratinocyte expression of uPA and uPAR mRNA, PAM 212 cells, seeded into 60 mm dishes, were grown to approximately 60% confluence and quiesced for 24 hours in serum free medium, prior to culture under normoxic or hypoxic conditions for 24 hours. Following homogenisation of cell monolayers, total RNA was prepared and analysed by Northern blotting as described. As expected, both uPA and uPAR mRNA were detected in normoxic PAM 212 keratinocytes, however, analysis of uPA and uPAR mRNA levels in keratinocytes cultured under hypoxic conditions showed a significant increase over normoxic levels (figure 6.1a). Subsequent densitometric analysis revealed an approximate 2-fold induction of both uPA and uPAR mRNA following 24 hours hypoxia (Figure 6.1b).

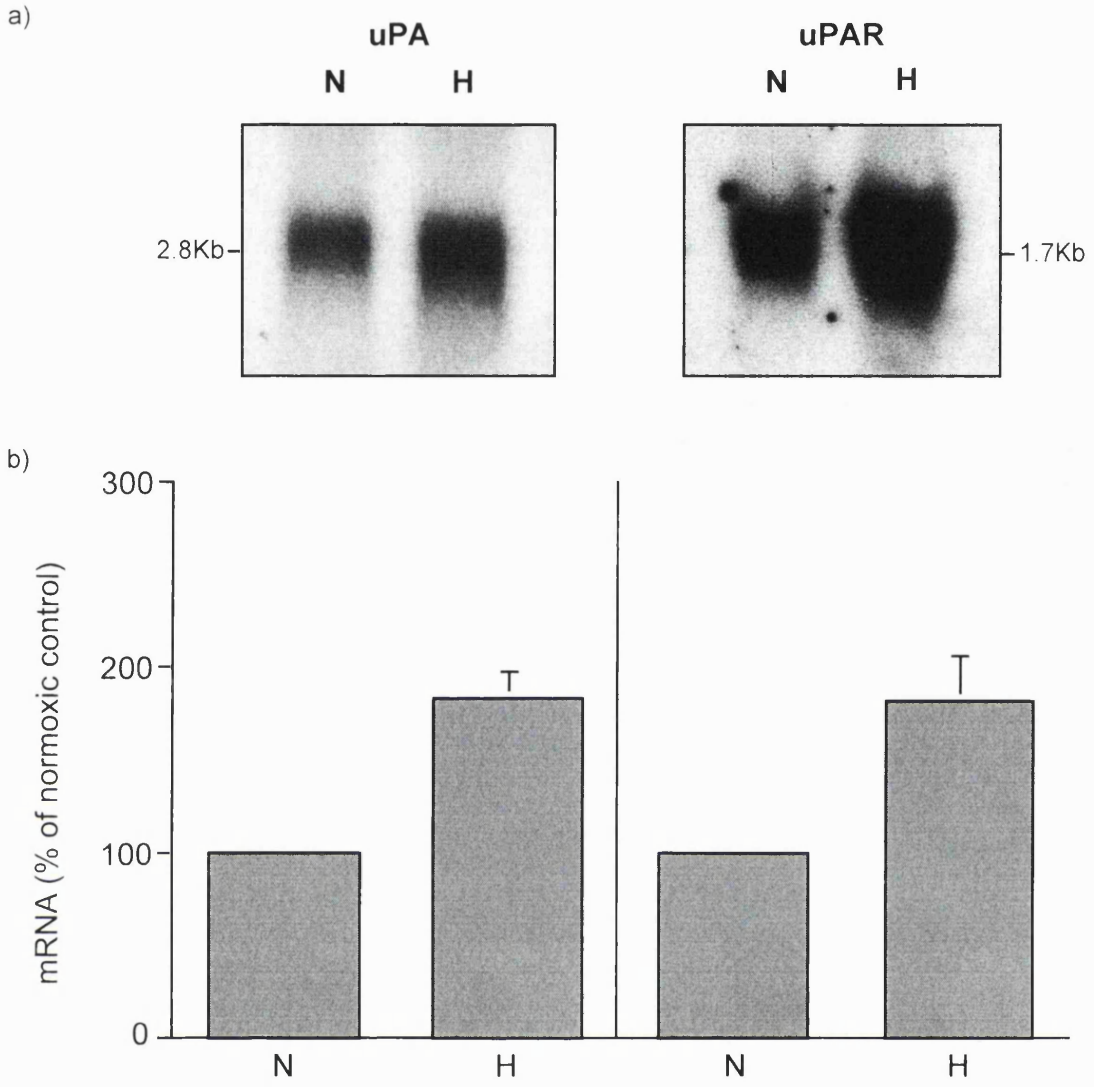

Figure 6.1 Effect of hypoxia on uPA and uPAR mRNA expression in PAM 212 keratinocytes. a) Representative Northern blot analysis of mRNA from keratinocyte cultures maintained in normoxic (N) and hypoxic (H) conditions for 24 hours. b) Densitometry of Northern blots corrected for loading. Data presented (mean ± SEM) are from 3 independent experiments.

6.2.4 Effect of hypoxia on PAM 212 keratinocyte-derived uPA activity

To determine whether hypoxic induction of uPA mRNA facilitated a concomitant increase in uPA activity, conditioned medium from PAM 212 keratinocytes, cultured under normoxic or hypoxic conditions, was assayed for plasminogen activating activity. Using the indirect chromogenic peptide assay, plasminogen activation was detectable in both normoxic and hypoxic samples. Moreover, the detected plasminogen activating activity could be almost entirely inhibited (>96% inhibition) by the addition of a selective uPA inhibitor, amiloride

(0.1mM) (Vassalli and Belin, 1987), indicating that it was uPA-mediated. As shown in figure 6.2a, a 4-fold increase in uPA activity was observed in hypoxic samples compared to normoxic controls. Moreover, plasminogen-linked zymography detected a band of beta-casein degradation corresponding to murine uPA (~45 kDa) that was markedly increased in conditioned medium from hypoxic PAM 212 keratinocytes over normoxic controls (Figure 6.2b).

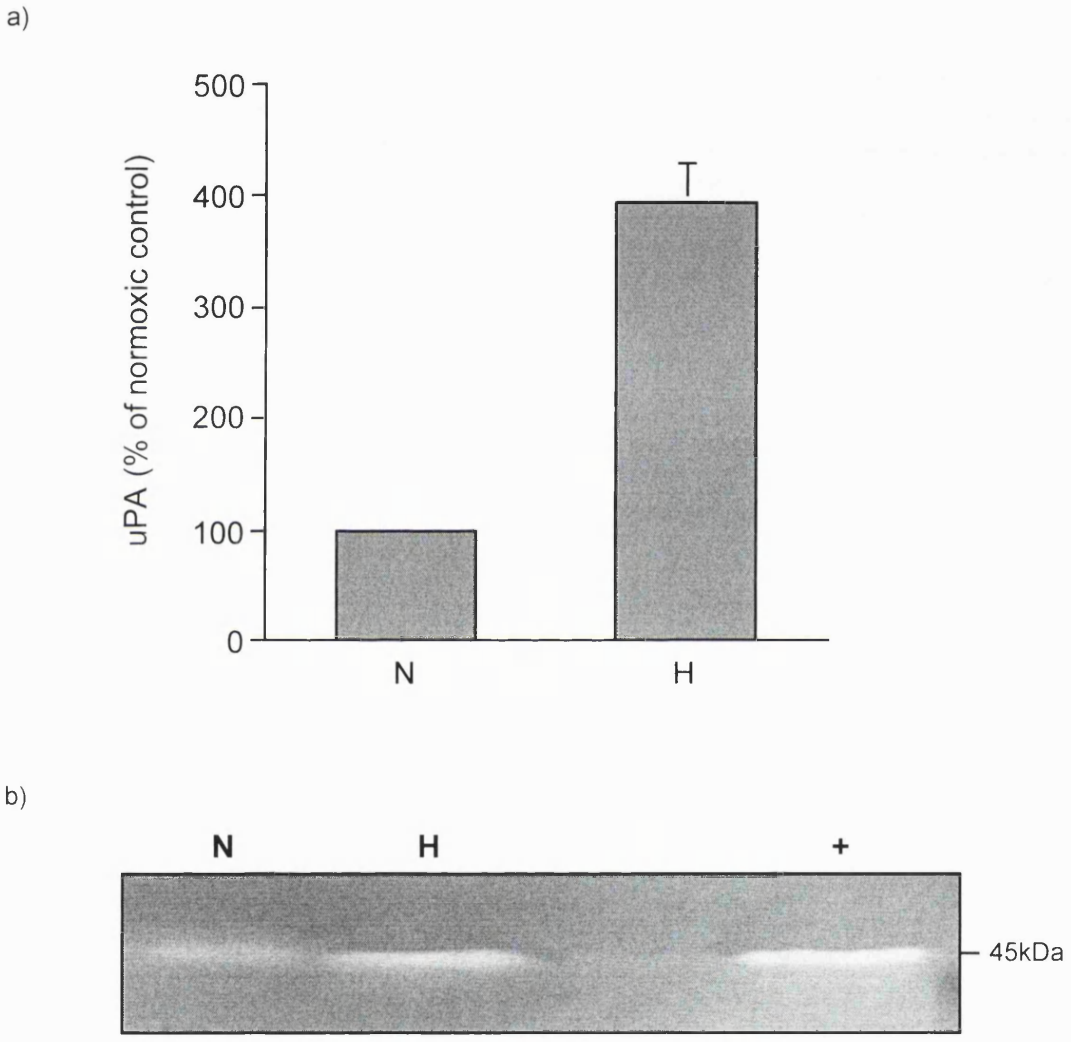

Figure 6.2 PAM 212 keratinocyte-derived uPA activity under hypoxic conditions. uPA levels in conditioned medium from keratinocyte cultures maintained in normoxic (N) or hypoxic (H) conditions as detected by indirect chromogenic peptide assay (a) and plasminogen-linked zymography (b). Data presented are (a) mean ± SEM from triplicate wells in 4 independent experiments and (b) representative of 3 independent experiments. + = murine urine.

6.2.5 Analysis of *in vitro* wound closure in hypoxic PAM 212 keratinocytes

As previous studies had indicated that hypoxia is a potent stimulus for migration of normal human keratinocytes (O'Toole *et al,* 1997b), experiments were designed to assess the effect of hypoxia on *in vitro* wound closure in PAM 212 keratinocytes. Confluent PAM 212 cell monolayers were wounded with a plastic pipette tip and maintained under normoxic or hypoxic conditions for 16 hours, prior to analysis of wound area recovered as described. As shown in figure 6.3a, enhanced wound closure was clearly evident in hypoxic cultures compared to normoxic control cultures. Subsequent image analysis revealed that after 16 hours under normoxic conditions, mean wound closure of $0.169 \pm 0.017 mm^2$ was observed. However, after 16 hours under hypoxic conditions, mean wound closure of $0.27 \pm 0.005 mm^2$ was observed, a $59.8 \pm 2.8\%$ (mean $\pm$ SEM, $p < 0.01$) enhancement (Figure 6.3b).

To determine the mechanism involved in this hypoxic enhancement of *in vitro* wound closure, PAM 212 keratinocyte monolayers were treated with an inhibitor of cell proliferation, mitomycin C, or an inhibitor of cell migration, cytochalasin B, and wounded prior to culture under normoxic or hypoxic conditions. Subsequent analysis of wound area recovered showed that inhibition of keratinocyte proliferation by mitomycin C had no significant effect on normoxic wound closure over a 24 hour period. Moreover, inhibition of proliferation had no significant effect on the enhanced wound closure observed in hypoxic cultures (figure 6.4). In contrast, inhibition of keratinocyte migration by cytochalasin B almost completely prevented wound closure (mean < 9% of control) under both normoxic and hypoxic conditions.

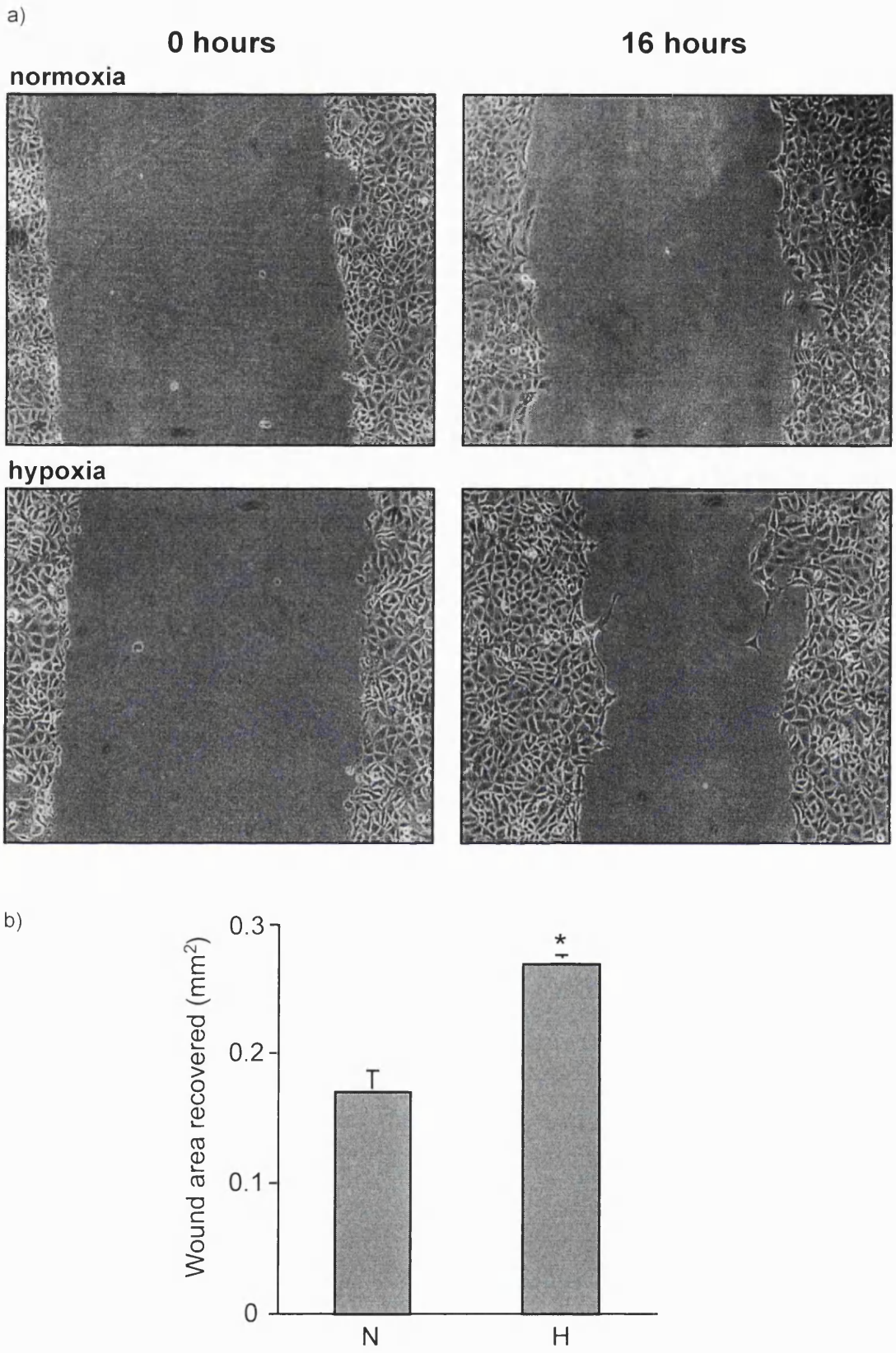

Figure 6.3 Effect of hypoxia on *in vitro* wound closure in PAM 212 keratinocytes. a) Representative photomicrograph of area recovered in wounded normoxic and hypoxic keratinocyte cultures. b) Wound area recovered in keratinocyte cultures maintained in normoxic (N) and hypoxic (H) conditions as determined by image analysis. Data presented (mean ± SEM) are from duplicate wells in 4 independent experiments. * = $p < 0.01$ (significant from normoxic control).

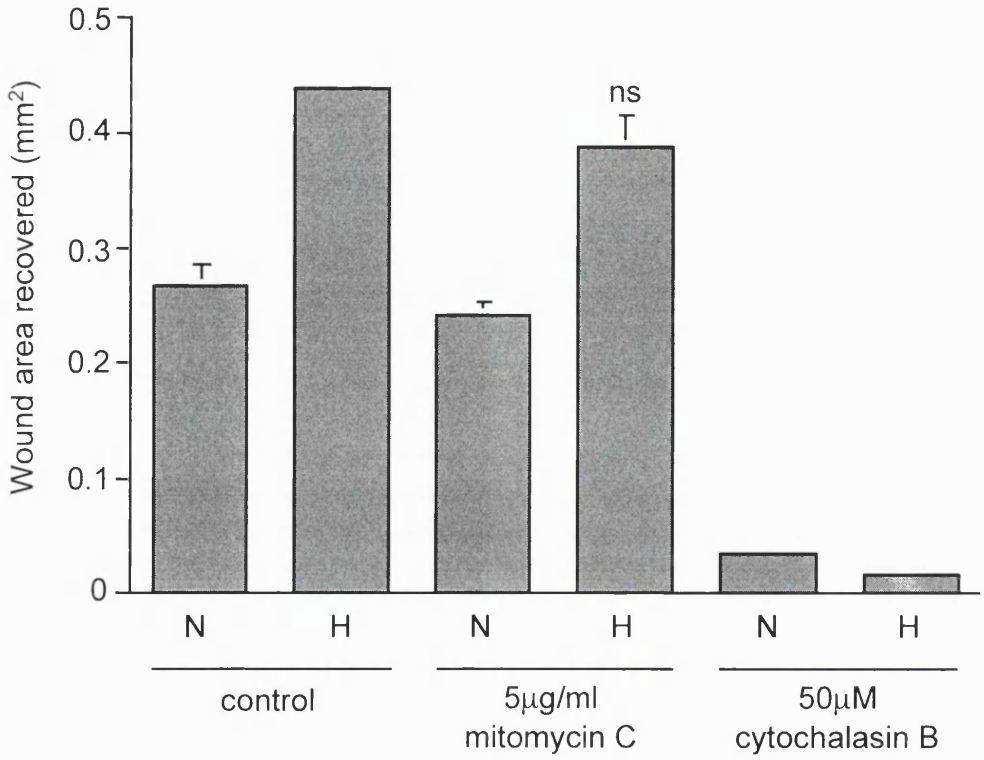

Figure 6.4 Role of keratinocyte proliferation and migration in hypoxic enhancement of *in vitro* wound closure. Image analysis of wound area recovered in normoxic (N) and hypoxic (H) PAM 212 keratinocyte cultures following addition of mitomycin C or cytochalasin B. Data presented (mean ± SEM) are from duplicate wells in 3 independent experiments. ns = $p > 0.1$ (not significant from hypoxic control).

6.2.6 Role of uPA in hypoxia-enhanced *in vitro* wound closure

Having demonstrated both upregulation of functional uPA and increased *in vitro* wound closure in hypoxic PAM 212 keratinocytes, the relationship between these observations was investigated using wounded cell monolayers maintained under normoxic or hypoxic conditions, with or without the addition of uPA inhibitors. To initially determine the optimal concentration of each inhibitor (inhibition vs. toxicity vs. availability*) a range of concentrations were added to wounded monolayers, prior to culture under hypoxic or normoxic conditions for 24 hours. Using the indirect chromogenic peptide assay and the LDH release assay respectively, uPA inhibition and cell viability were assessed and optimal concentrations defined (figure 6.5).

* A specific amount of WX-293 was provided for the uPA inhibition experiments (see section 2.2.6.1), hence the need to assess availability when determining the optimal concentration for this inhibitor.

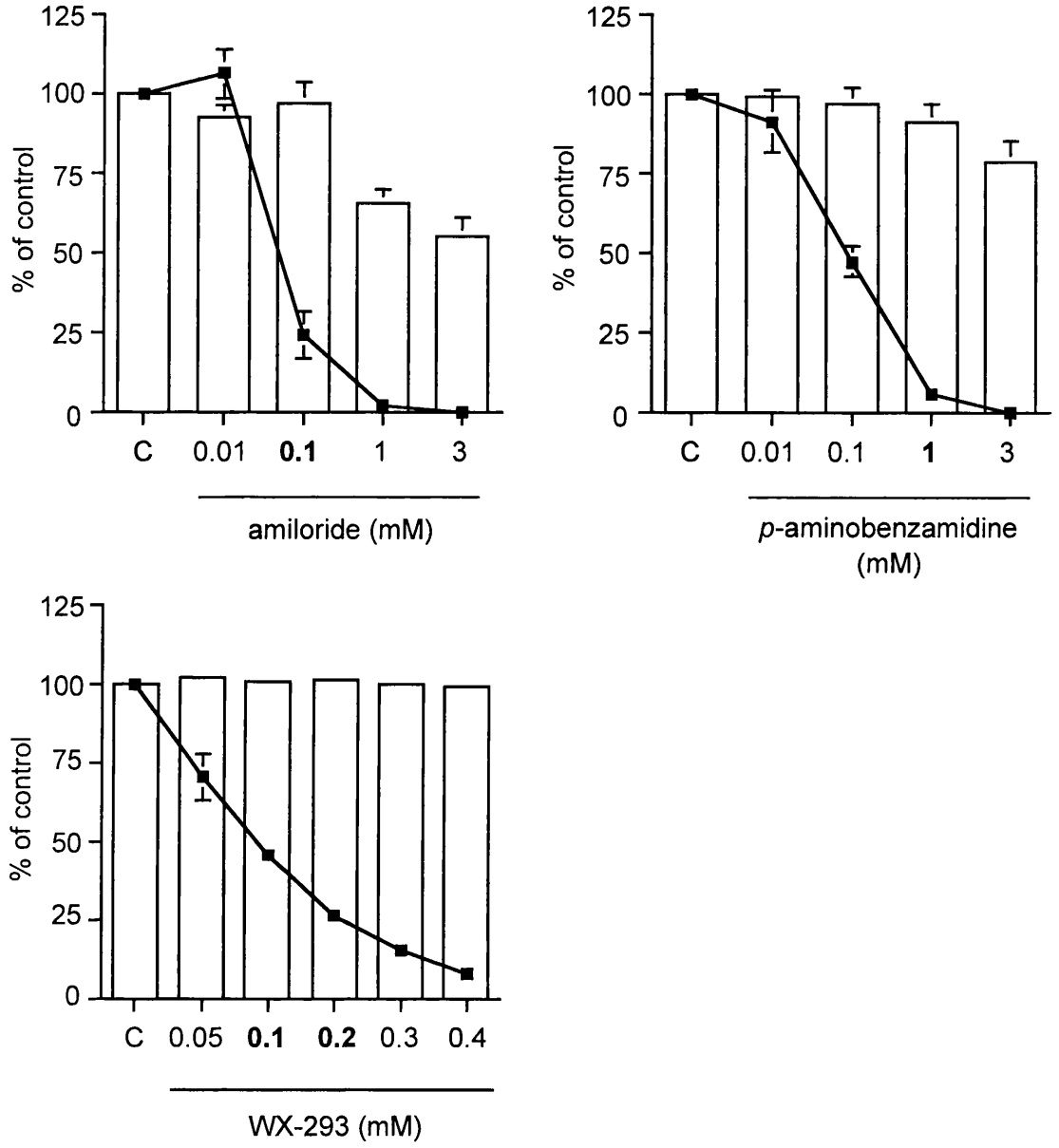

Figure 6.5 Determination of optimal (inhibitory and sub-toxic) concentrations of uPA inhibitors. uPA inhibition (blocked line) and cell viability (open bars) were assessed by indirect chromogenic peptide assay and LDH release assay, respectively. Bold text = optimal concentrations. Data presented (mean ± SEM) are from duplicate wells in 3 independent experiments.

To determine any effect of uPA inhibition on hypoxia enhanced keratinocyte migration, amiloride and p-aminobenzamidine were used at the optimal concentration in repeated *in vitro* wound experiments as described. In control cultures, the area recovered over 16 hours was increased by 67.07 ± 8.7% (mean ± SEM) in hypoxic conditions compared to normoxic conditions. However, following addition of amiloride

the hypoxia-induced enhancement of wound closure was completely abolished and no significant difference in wound area recovered could be observed between normoxic and hypoxic cultures (figure 6.6). In addition, the presence of the broad spectrum protease inhibitor, *p*-aminobenzamidine (Geratz and Cheng, 1975; Geratz *et al,* 1981), significantly reduced wound area recovered in both normoxic and hypoxic cultures.

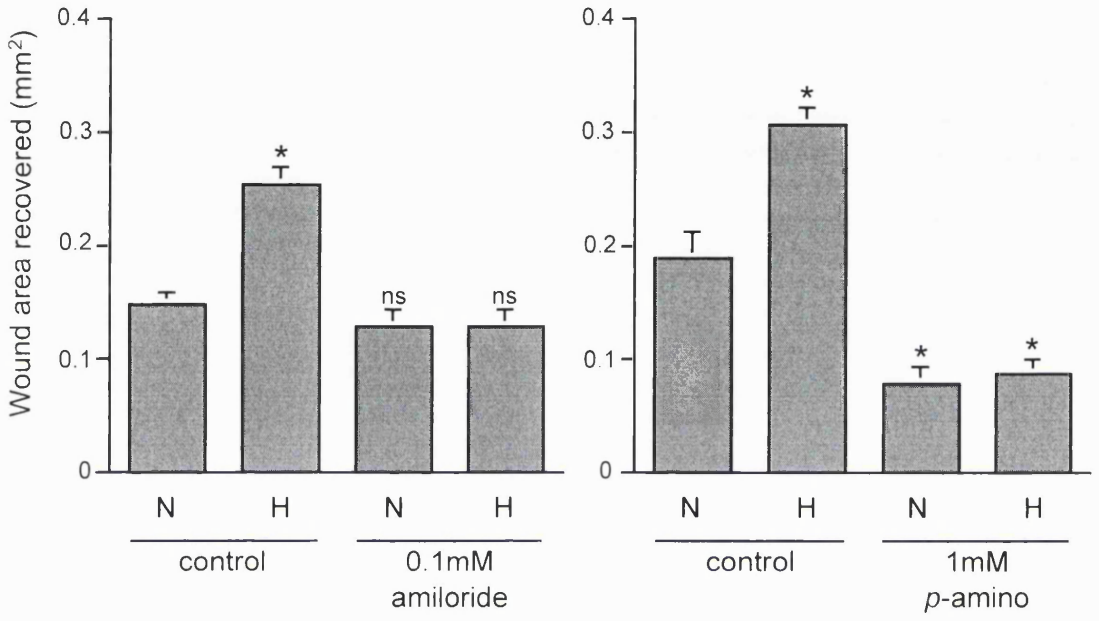

Figure 6.6 Role of uPA in hypoxic enhancement of *in vitro* wound closure. Image analysis of wound area recovered in normoxic (N) and hypoxic (H) PAM 212 keratinocyte cultures following addition of amiloride (amiloride) or *p*-aminobenzamidine (*p*-amino). Data presented (mean ± SEM) are from duplicate wells in 4 independent experiments. * = $p < 0.01$ (significant from normoxic control), ns = $p > 0.1$ (not significant from normoxic control).

Since amiloride and *p*-aminobenzamidine have activity other than uPA inhibition (Costanzo, 1984; Venturini *et al,* 1997), wounded cell monolayers were also maintained under normoxic and hypoxic conditions in the presence of WX-293, a recently described highly selective inhibitor of uPA activity (Sperl *et al,* 2000). At 0.2 mM, a concentration shown to result in ~75% inhibition of uPA activity, WX-293 completely inhibited hypoxic enhancement of wound closure. However, at 0.1 mM, a concentration shown to result in ~50% inhibition of uPA activity, the observed hypoxic enhancement of *in vitro* wound closure was inhibited by 70% (figure 6.7). At both concentrations, WX-293 had no significant effect on the wound area recovered in normoxic cultures.

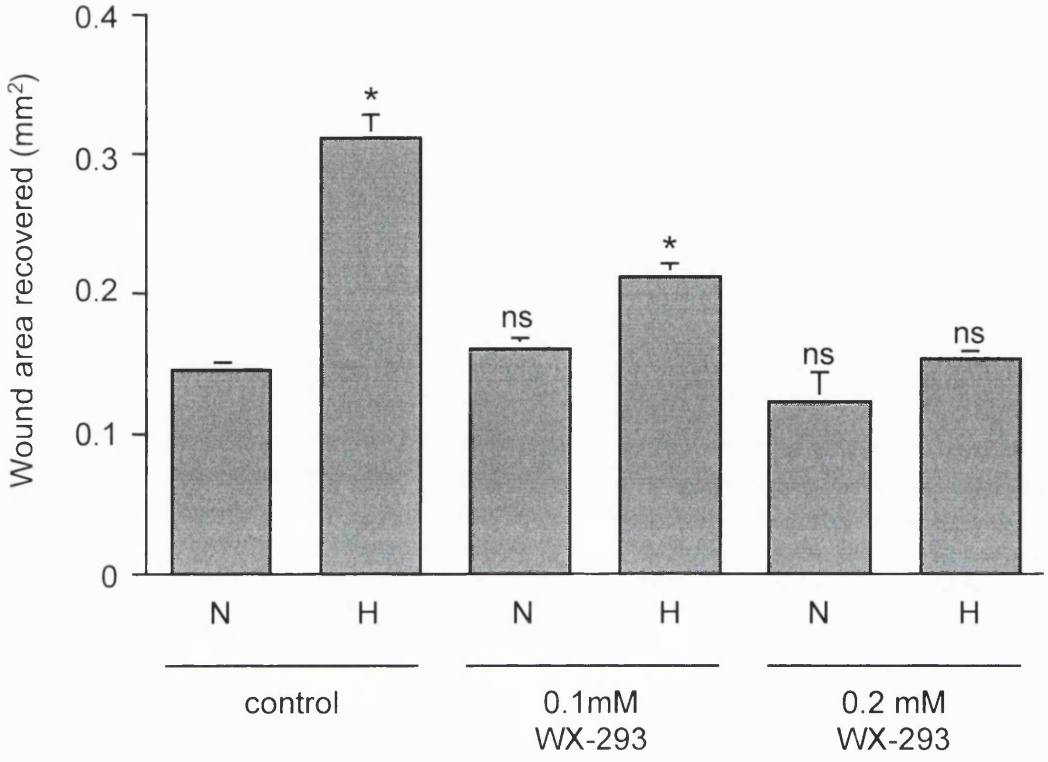

Figure 6.7 Effect of WX-293 on enhanced hypoxic *in vitro* wound closure. Image analysis of wound area recovered in normoxic (N) and hypoxic (H) PAM 212 keratinocyte cultures following addition of WX-293 at the indicated concentration. Data presented (mean ± SEM) are from duplicate wells in 3 independent experiments. * = $p < 0.01$ (significant from normoxic control), ns = $p > 0.1$ (not significant from normoxic control).

6.3 DISCUSSION

Acute cutaneous wounds are characterised by the rapid development of hypoxia secondary to interruption of normal vasculature and the development of a fibrin clot. Cells local to the wound must therefore be able to adapt appropriately to this hypoxic environment such that wound healing progresses as rapidly as possible. In view of this wound-related reduction in tissue oxygen tension, and in consideration of data indicating that uPA and other plasminogen activator system components have a pivotal role in the wound healing process, the present studies examined the functional effect of hypoxia on keratinocyte regulation of uPA-mediated plasminogen activating activity.

In keeping with previous reports demonstrating hypoxic regulation of the plasminogen activator system in several cell types (Fitzpatrick and Graham, 1998; Graham *et al,* 1999; Kroon *et al,* 2000a), this study has demonstrated that hypoxia is a potent regulator of keratinocyte plasminogen activation *in vitro*. Both uPA and uPAR mRNA were induced after 24 hour exposure to hypoxia and there was a marked induction of uPA-mediated proteolytic activity in cell culture conditioned medium following hypoxic stimulation. These findings contrast with the effects of hypoxia in other tissues or cell types, as *in vivo*, hypoxia has been shown to reduce uPA mRNA levels in lung tissue (Pinsky *et al,* 1998), and *in vitro*, hypoxia causes a decrease in uPA-mediated plasminogen activation in trophoblast, carcinoma and endothelial cell conditioned medium. Interestingly however, increased cell-associated plasminogen activation is detected in these cell types, resulting from elevated cell surface expression of uPAR (Graham *et al,* 1998 and 1999; Kroon *et al,* 2000b). These differences between keratinocytes and other cell types likely reflect the differing requirements for regulation of plasminogen activation in different tissues, with diffuse plasminogen activation resulting from soluble uPA being appropriate in the setting of acute cutaneous wounding.

Our observation that PAM 212 keratinocyte wound closure is enhanced under hypoxic conditions, confirms the findings of previous studies using primary human keratinocytes (O'Toole *et al,* 1997b; Xia *et al,* 2001). Moreover, our data extends this observation by indicating that this enhancement is completely blocked following uPA inhibition by amiloride and WX-293, as well as broad range protease inhibition by *p*-aminobenzamidine, providing the first evidence of a role for uPA in hypoxia-mediated

keratinocyte wound closure *in vitro*. Since this hypoxia-mediated wound closure was shown to be dependent on keratinocyte migration, but independent of keratinocyte proliferation, in keeping with previous data (Morioka *et al,* 1987a), our results strongly suggest that the presence of functional uPA is required for increased keratinocyte migration under hypoxic conditions. Interestingly, inhibition of serine protease activity by *p*-aminobenzamidine also reduced the wound area recovered in normoxic cultures. Despite a previous report indicating that keratinocyte migration across a substratum was not dependent on serine protease activity (Ando and Jensen, 1996), our result suggests that broad spectrum protease activation may have a general role in keratinocyte migration under normoxic conditions. As Ando and Jensen used the soya bean trypsin inhibitor as opposed to *p*-aminobenzamidine, it is possible that the variations in our findings are a result of differences in the efficiency or specificity of these inhibitors.

Although the observation that hypoxia mediates an increase in keratinocyte migration via uPA upregulation provides the first evidence for the involvement of the plasminogen activator system in hypoxic keratinocyte migration, the exact molecular mechanisms underlying this remain unclear. In the last decade, much emphasis has been placed on the role of MMPs in epithelial cell motility (Pilcher *et al,* 1997; McCawley *et al,* 1998; Makela *et al,* 1999; Thomas *et al,* 2001) with actively migrating keratinocytes over-expressing type I and type IV collagenases (Salo *et al,* 1994; Inoue *et al,* 1995; Pilcher *et al,* 1997). Moreover, previous studies of human keratinocyte migration under hypoxic conditions demonstrated upregulation of MMP-1 and MMP-9 (O'Toole *et al,* 1997b; Xia *et al,* 2001), though functional evidence of a role for these proteases in hypoxic keratinocyte migration is awaited. Interestingly, several MMPs including MMP-2 and MMP-9, can be activated by uPA-generated plasmin *in vitro* (Mazzieri *et al,* 1997; Baramova *et al,* 1997; Carmeliet *et al,* 1998), and uPA-mediated MMP-9 activation was recently implicated in bronchial epithelial cell migration (Legrand *et al,* 2001), suggesting that hypoxic upregulation of uPA may be a proximal step in the induction of these proteases by hypoxia. The resulting increase in levels of both plasmin and active MMPs following hypoxia could encourage rapid modification of the endogenous extracellular matrix, established by the cultured PAM 212 keratinocytes, thereby facilitating cell motility and enhancing *in vitro* wound closure.

In addition to previous reports indicating a role for uPA-derived proteolytic activity in cellular migration (Wijnberg *et al,* 1997; Strand *et al,* 2000), much data

indicates that uPA-mediated cell migration can occur in the absence of uPA-specific catalytic activity, suggesting alternative roles for this molecule in the regulation of cell migration. One possibility is that uPA has a non proteolytic chemokinetic effect on hypoxic keratinocytes. The chemokinetic/chemotactic properties of uPA on many cell types in culture are well documented, and are generally reliant on uPA:uPAR binding (Anichini *et al,* 1994; Busso *et al,* 1994; Resnati *et al,* 1996; Degryse *et al,* 2001). Moreover, as the chemokinetic/chemotactic effect of this uPA:uPAR interaction is suggested to involve a specialised conformational change in uPAR (Resnati *et al,* 1996; Fazioli *et al,* 1997), it is possible that uPA inhibitor binding interferes with the uPA:uPAR interaction in such a way that chemokinesis/chemotaxis is inhibited. In addition, recent reports have also demonstrated that disruption of uPAR:uPA:PAI-1 complex formation inhibits human muscle cell migration (Planus *et al,* 1997; Chazaud *et al,* 2000), suggesting that uPA interaction with both uPAR and PAI-1 is critical to the non-proteolytic regulation of migration in certain cell types. Since the uPA inhibitors used in the present studies would block uPA:PAI-1 interaction, it is possible that this alternative mechanism of uPA inhibition facilitates the observed abrogation of hypoxia-induced keratinocyte migration.

In conclusion, the present studies demonstrate that inhibition of uPA by three distinct inhibitors completely suppresses the hypoxia-mediated enhancement of keratinocyte migration *in vitro*. Although the exact mechanism by which uPA modulates this hypoxic keratinocyte migration remains to be defined, our findings constitute the first evidence of a role for the plasminogen activator system in keratinocyte migration under hypoxic conditions. Despite long-term hypoxia being an impediment to normal wound healing, migration of keratinocytes is critical for effective wound repair and thus analysis of keratinocyte responses to transient acute hypoxia may provide useful insights into potential methods of accelerating wound closure in therapeutic situations.

CHAPTER 7

EFFECT OF HYPOXIA ON KERATINOCYTE REGULATION OF THE PLASMINOGEN ACTIVATOR SYSTEM: POTENTIAL AUTOCRINE MODULATION OF PAI-1 BY VEGF

7.1 INTRODUCTION

Cell migration and invasion are key features of many physiological and patho-physiological processes, including embryogenesis, inflammation, tumour formation, and, as discussed in section 1.2, cutaneous wound repair. During the past decade much evidence for the involvement of the plasminogen activator system in this cellular migration and invasion has been presented, and various reports now indicate that components of this system have pivotal roles within many of these processes (Littlefield, 1991; Romer *et al,* 1996; Andreasen *et al,* 1997; Ploplis *et al,* 1998). *In vivo*, the movement of cells across and through tissues is primarily facilitated by uPA/plasmin-mediated proteolytic degradation or modification of matrix components. However, this proteolytic activity is tightly regulated by specific, high affinity, inhibitors, of which the most physiologically effective in the cutaneous microenvironment is the type 1 plasminogen activator inhibitor, PAI-1.

PAI-1 is a 52 kDa glycoprotein member of the serpin superfamily (Potempa *et al,* 1994), that is initially secreted as an active inhibitory molecule, but which rapidly converts to a latent inactive form unless stabilised by binding to vitronectin (Salonen *et al,* 1989; Mimuro and Loskutoff, 1989), or association with a fibrin matrix (Wagner *et al,* 1989; Braaten *et al,* 1993). Once stabilised, active PAI-1 is capable of specifically inhibiting both free and uPAR-bound two-chain uPA (Andreasen *et al,* 1986; Ellis *et al,* 1990), via the formation of an irreversible covalent complex. In addition to its inhibitory function, PAI-1 binding of uPA also facilitates the internalisation and degradation of uPA (Cubellis *et al,* 1990), a process involving both uPAR (Olson *et al,* 1992) and the α2-macroglobulin receptor (Nykjaer *et al,* 1992). Since uPAR is not degraded following internalisation, but is recycled to the cell surface (Conese *et al,* 1995; Nykjaer *et al,* 1997), this process constitutes an efficient mechanism whereby uPAR binding sites are made available for active uPA, via the clearance of inactive uPA:PAI-1 complexes.

In recent years an extensive literature has associated PAI-1 with cellular motility and invasion. *In vitro*, PAI-1 upregulation has been detected in migrating monocytes (Vassalli *et al,* 1984), endothelial cells (Pepper *et al,* 1992 and 1993) and keratinocytes (Staiano Coico *et al,* 1996). Moreover, PAI-1 has been shown to directly regulate the motility of various cultured cell types, and this regulation is generally dependent on its capacity to modulate the cellular adhesion/release cycle, via interactions with

vitronectin and integrin receptors, or via the internalisation of uPAR:uPA:PAI-1 complexes (Stefansson and Lawrence, 1996; Waltz *et al,* 1997; Kjoller *et al,* 1997; Stahl and Mueller, 1997). Several studies have also demonstrated an important role for PAI-1 in monocyte migration *ex-vivo* (Kirchheimer *et al,* 1990), and in the migration of smooth muscle cells (Carmeliet *et al,* 1997), endothelial cells, and malignant keratinocytes *in vivo* (Bajou *et al,* 1998). Furthermore, although initial transgenic studies indicated that sufficient biochemical redundancy exists to compensate for the loss of PAI-1 during wound repair (Dougherty *et al,* 1999), the detection of significant PAI-1 upregulation in migrating keratinocytes, fibroblasts, and monocytes in healing animal wounds (Romer *et al,* 1991), indicates a potentially important role for PAI-1 in wound induced cell migration and invasion.

An interesting feature of PAI-1 biology is its capacity for regulation by a variety growth factors, cytokines and hormones. For example, TGF-β (Keski-Oja and Koli, 1992), HGF-SF (Wojta *et al,* 1999), TNF-α (van Hinsbergh *et al,* 1988), VEGF (Pepper *et al,* 1991) and hydrocortisone (Bator *et al,* 1998) have all been shown to stimulate PAI-1 expression and activity in certain cell types *in vitro.* Moreover, intra-peritoneal injection of TNF-α or TGF-β into mice significantly increased PAI-1 mRNA levels in nearly all tissues analysed (Sawdey and Loskutoff, 1991). In addition, hypoxia, has been shown to increase PAI-1 expression in trophoblasts (Fitzpatrick and Graham, 1998), hepatocytes (Kietzmann *et al,* 1999), and macrophages (Pinsky *et al,* 1998) *in vitro*, as well as in lung tissue *in vivo* (Pinsky *et al,* 1998). Interestingly, many of the agents shown to regulate PAI-1 expression also regulate migration and invasion in the same cell types (Mawatari *et al,* 1991; Matsumoto *et al,* 1991; Koolwijk *et al,* 1996; Graham *et al,* 1998; Santibanez *et al,* 1999), further suggesting a primary role for PAI-1 in cellular motility.

In view of the accumulated data associating PAI-1 with the regulation of cellular migration and invasion, and considering the evidence suggesting that cells migrating within a cutaneous wound site will experience acute hypoxia (see section 6.1), the present studies sought to determine the effect of hypoxia on keratinocyte expression of PAI-1.

7.2 RESULTS

7.2.1 Analysis of PAI-1 expression in hypoxic PAM 212 keratinocytes

To determine the effect of hypoxia on PAI-1 mRNA expression in PAM 212 keratinocytes, cells were grown to 60% confluence and quiesced for 24 hours with serum free medium, prior to culture under normoxic and hypoxic conditions for 8 or 24 hours. Following homogenisation of cell monolayers, total RNA was prepared and analysed by Northern blotting as described. As shown in figure 7.1a, PAI-1 mRNA was detected in normoxic PAM 212 keratinocytes throughout the experiment. However, analysis of PAI-1 mRNA levels in keratinocytes cultured under hypoxic conditions showed a marked increase over normoxic levels after both 8 and 24 hours. Subsequent densitometric analysis of Northern blots revealed an approximate 4-fold induction of PAI-1 mRNA following 24 hours hypoxia (Figure 7.1b).

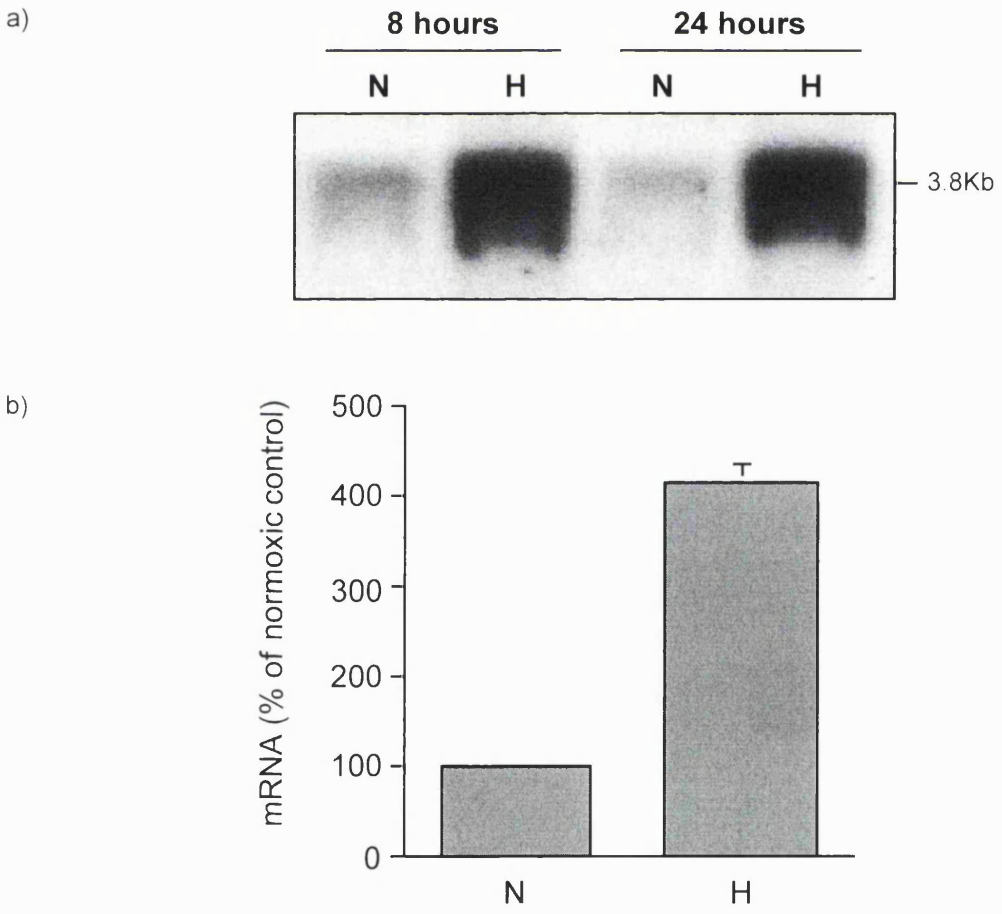

Figure 7.1 Effect of hypoxia on PAI-1 mRNA expression in PAM 212 keratinocytes. a) Northern blot analysis of mRNA from keratinocyte cultures maintained in normoxic (N) and hypoxic (H) conditions for 8 and 24 hours. b) Densitometry of Northern blots from 24 hour time-point corrected for loading. Data presented (mean ± SEM) are from 3 independent experiments.

Detection of a concomitant increase in PAI-1 protein was facilitated by Western blotting analysis of cell lysates and conditioned medium from PAM 212 keratinocyte cultures maintained under normoxic and hypoxic conditions for 24 hours. Prepared samples were separated on denaturing polyacrylamide gels and transferred to nitrocellulose membranes, prior to immunoblotting as described. As shown in figure 7.2, PAI-1 protein was barely detectable in normoxic cell lysates and completely undetectable in conditioned medium from normoxic cultures. In contrast, analysis of PAM 212 keratinocytes cultured under hypoxic conditions showed a strong band corresponding to murine PAI-1 (~52 kDa) in both cell lysates and conditioned medium.

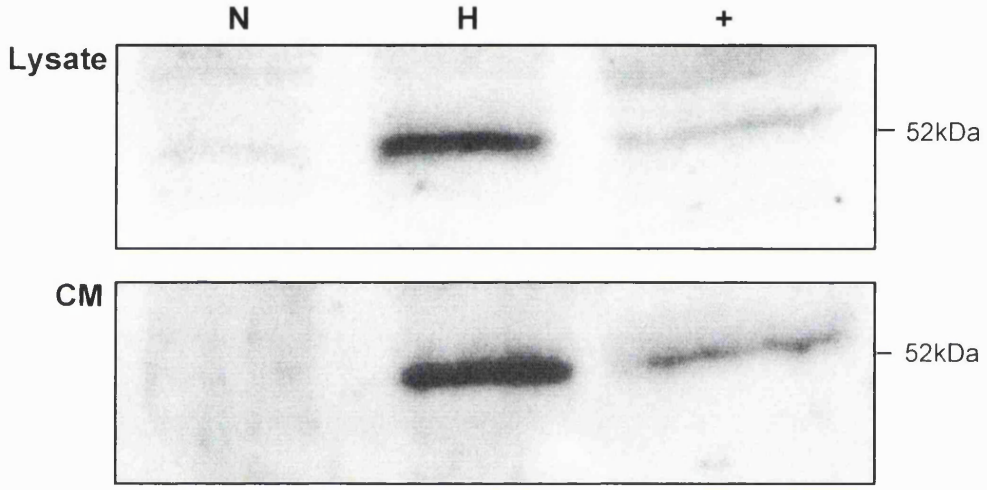

Figure 7.2 Effect of hypoxia on PAI-1 protein levels in PAM 212 keratinocytes. Western blotting analysis of cell lysate (lysate) and conditioned medium (CM) from keratinocyte cultures maintained in normoxic (N) and hypoxic (H) conditions for 24 hours. + = cell lysate from TGF-β treated PAM 212 keratinocytes. Data presented is representative of 4 independent experiments.

7.2.2 Analysis of PAI-1 induction in hypoxic PAM 212 keratinocytes

Previous studies have shown that TGF-β and VEGF are effective inducers of PAI-1 production in specific cultured cells (Pepper *et al,* 1991; Keski-Oja and Koli, 1992; Olofsson *et al,* 1998; Dong-Le Bourhis *et al,* 1998). Moreover, it has also been reported that hypoxia is a potent stimulus for TGF-β and VEGF, again in a variety of cell types (Santilli *et al,* 1991; Tuder *et al,* 1995; Orphanides *et al,* 1997; Detmar *et al,* 1997). As a consequence of these observations, experiments were designed to investigate whether the hypoxic induction of PAI-1 in PAM 212 keratinocytes was mediated via upregulation of TGF-β or VEGF. PAM 212 keratinocytes were grown to 60% confluence, quiesced for 24 hours with serum free medium, and cultured under

normoxic or hypoxic conditions in the presence of TGF-β and/or VEGF neutralising antibodies (see section 2.2.8). Following preparation of cell lysates, PAI-1 protein levels were assessed by Western blotting analysis and representative results are shown in figure 7.3. As expected, murine PAI-1 protein was undetectable in normoxic PBS controls, but was markedly induced in keratinocytes cultured under hypoxic conditions. Cell lysates from hypoxic PAM 212 keratinocytes cultured in the presence of TGF-β neutralising antibody showed PAI-1 protein levels equivalent to hypoxic PBS controls. In contrast, lysates from hypoxic keratinocytes cultured in the presence of VEGF neutralising antibody demonstrated a significant reduction in PAI-1 protein levels. This reduction in detectable PAI-1 was also observed in hypoxic cells cultured in the presence of both neutralising antibodies. Importantly, cell lysates from keratinocytes cultured under hypoxic conditions in the presence of non-specific rabbit IgGs showed levels of PAI-1 protein comparable to hypoxic PBS controls.

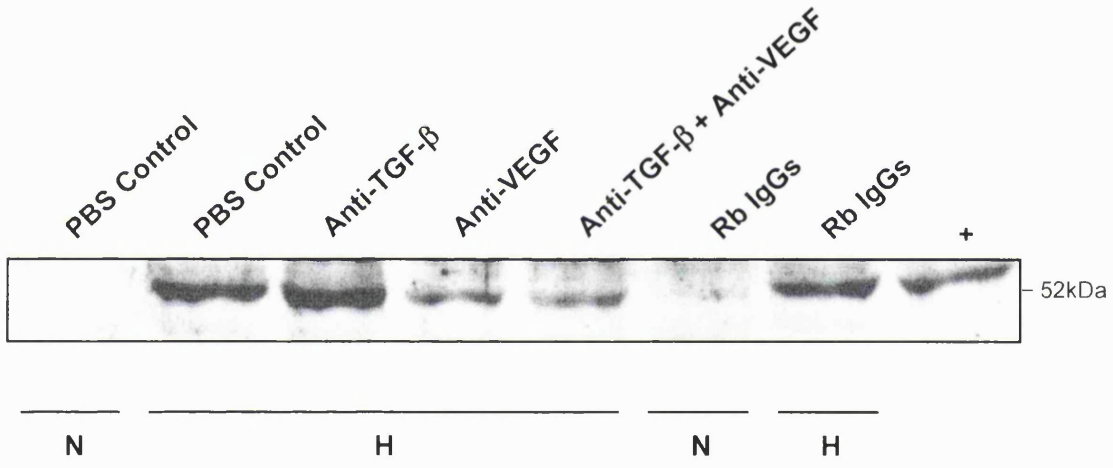

Figure 7.3 Effect of TGF-β and VEGF neutralisation on hypoxic induction of PAI-1 in PAM 212 keratinocytes. Western blot analysis of cell lysates from keratinocyte cultures maintained in normoxic (N) and hypoxic (H) conditions for 24 hours. PBS control = 10% PBS; Anti-TGF-β = 50 µg/ml pan-specific rabbit anti-TGF-β IgG; Anti-VEGF = 50 µg/ml rabbit anti-VEGF IgG; Rb IgGs = 50 µg/ml non-specific rabbit immunoglobulins; + = cell lysate from TGF-β treated PAM 212 keratinocytes. A representative blot from 4 independent experiments is shown.

7.2.3 Analysis of VEGF expression in hypoxic PAM 212 keratinocytes

To investigate whether the hypoxic induction of PAI-1 could be regulated by elevated levels of keratinocyte-derived VEGF, experiments were initially designed to determine the expression of VEGF by PAM 212 keratinocytes cultured under normoxic and hypoxic conditions. PAM 212 cells, seeded in 6 well plates, were grown to 60% confluence and quiesced for 24 hours with serum free medium prior to culture under

normoxic or hypoxic conditions for 4, 8, 16 or 24 hours. Conditioned medium was subsequently retained and VEGF protein levels assessed using a commercially available ELISA. As shown in figure 7.4, no significant difference in VEGF expression was observed between normoxic and hypoxic samples after 4 hours. However, VEGF protein levels were significantly up-regulated by hypoxia at all other time-points, with the greatest induction observed in cells exposed to hypoxia for 24 hours, after which VEGF levels in conditioned medium were 319 pg/ml compared to 61 pg/ml in normoxic samples; equivalent to a > 5-fold increase.

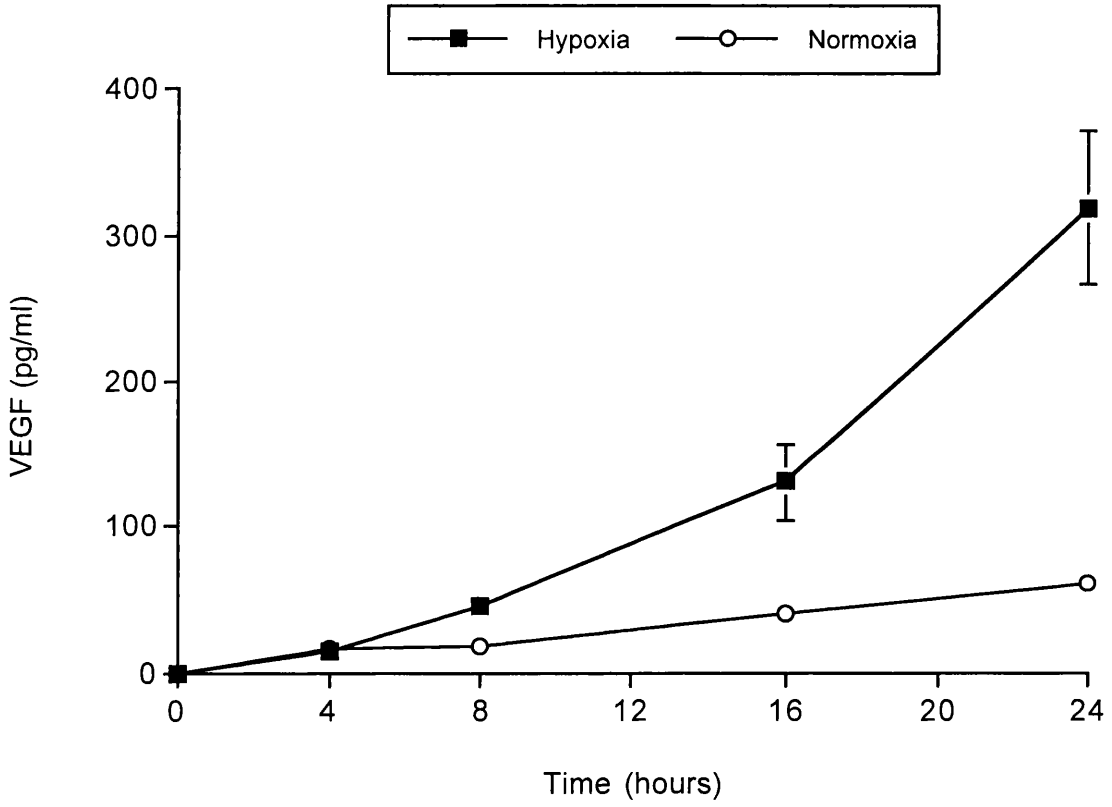

Figure 7.4 Effect of hypoxia on VEGF expression in PAM 212 keratinocytes. ELISA detection of VEGF in conditioned medium from keratinocyte cultures maintained in normoxic (N) and hypoxic (H) conditions for 4, 8, 16 and 24 hours. Data presented (mean ± SEM) are from duplicate wells in 3 independent experiments.

7.2.4 Transfer of normoxic and hypoxic conditioned medium

Since our results indicated that hypoxia increases VEGF production in PAM 212 cultures, it was hypothesised that this keratinocyte-derived VEGF might be responsible for the induction of PAI-1 under hypoxic conditions. To investigate this hypothesis, PAM 212 keratinocytes were exposed to 24 hours normoxia or hypoxia after which

normoxic and hypoxic conditioned medium was transferred to fresh keratinocyte cultures for 24 hours (section 2.2.9). Following preparation of total RNA and protein, PAI-1 levels were analysed by Northern and Western blotting and representative results are shown in figure 7.5. As expected, PAM 212 keratinocytes cultured under normoxic conditions showed little or no detectable PAI-1 expression, whereas keratinocytes cultured under hypoxic conditions showed a marked increase in PAI-1 mRNA and protein. However, PAM 212 keratinocyte cultures maintained in either normoxic or hypoxic conditioned medium for 24 hours showed little or no detectable PAI-1 at both the mRNA or protein level, and no significant difference in PAI-1 expression was observed between the cultures.

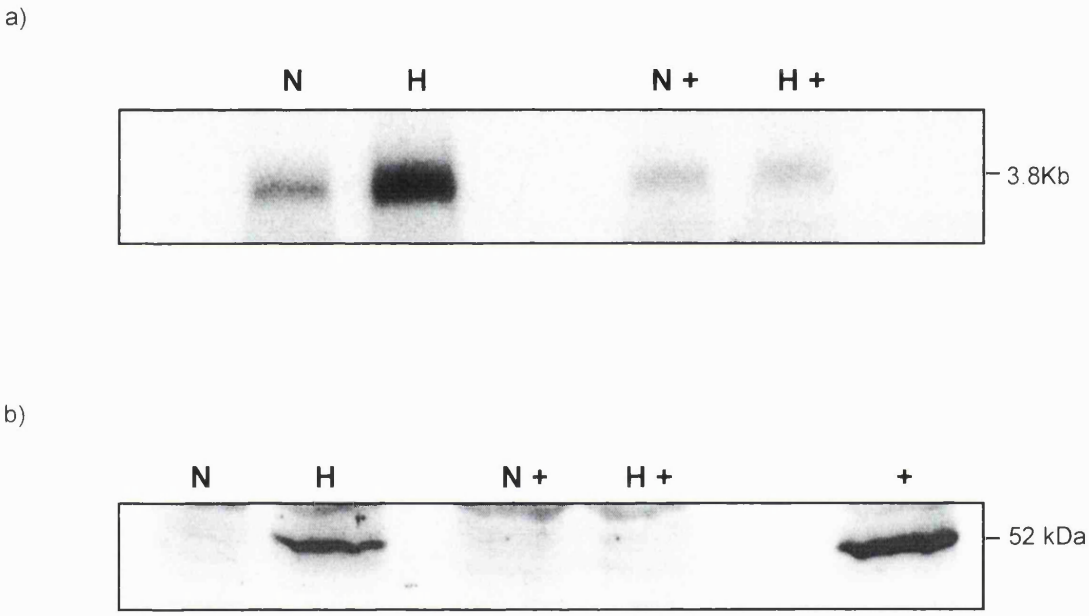

Figure 7.5 Effect of normoxic and hypoxic conditioned medium on PAI-1 expression in PAM 212 keratinocytes. Northern (a) and Western blotting (b) analysis of PAI-1 expression in keratinocyte cultures maintained in normoxic (N) and hypoxic (H) conditions or maintained in normoxic (N+) and hypoxic (H+) conditioned medium. Data presented is representative of 2 independent experiments. + = cell lysate from TGF-β treated PAM 212 keratinocytes.

To confirm that the keratinocyte-derived VEGF was stable throughout the transfer experiment, conditioned medium samples were collected from PAM 212 keratinocytes exposed to normoxia and hypoxia for 24 hours. Following transfer of the remaining conditioned medium to fresh keratinocytes for a further 24 hours, samples were again collected and VEGF protein levels assessed using a commercially available ELISA. The results are shown in figure 7.6. Analysis of VEGF in conditioned medium samples from keratinocytes exposed to 24 hours' normoxia, showed an increase of 81.4 pg/ml over base levels. Moreover, following transfer of this conditioned medium to

fresh keratinocytes for an additional 24 hours, VEGF levels were increased again by 91.0 pg/ml. Similarly, whereas analysis of samples taken from keratinocytes exposed to 24 hours' hypoxia showed VEGF protein levels of 248.2 pg/ml, analysis of the same conditioned medium after transfer to fresh keratinocytes showed levels of 350.8 pg/ml, an increase of 102.6 pg/ml.

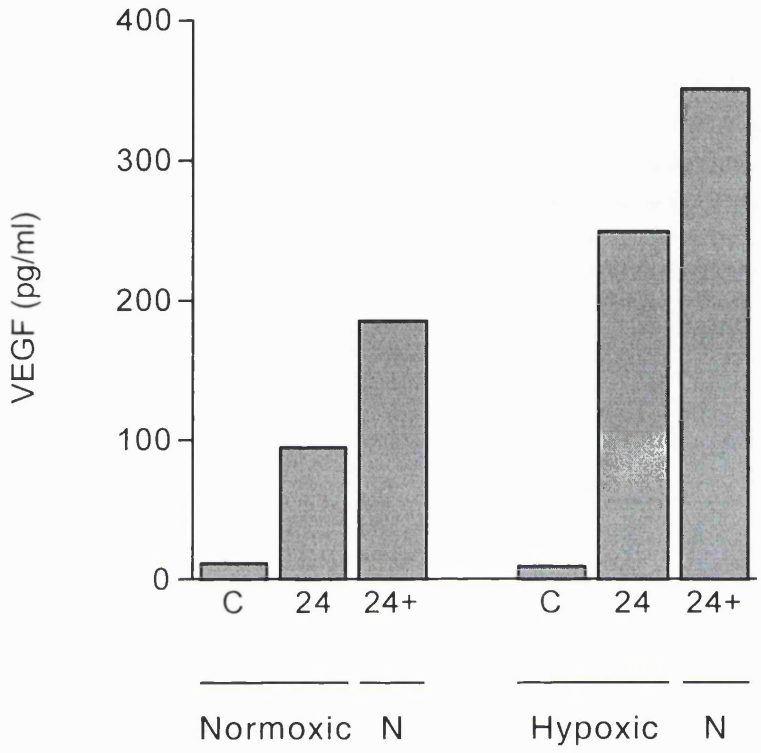

Figure 7.6 Determination of VEGF stability in transfer experiment. ELISA of conditioned medium samples from PAM 212 keratinocytes cultured under normoxic and hypoxic conditions for 24 hours (24) and of samples from the same conditioned medium after transfer to cultures under normoxic conditions (N) for an additional 24 hours (24+). C = Control (RPMI serum free medium). Data presented (mean) are from duplicate wells in 2 independent experiments.

To assess the effect of VEGF on PAI-1 expression in normoxic PAM 212 keratinocytes, cells, seeded into 6 well plates, were grown to 60% confluence and quiesced for 24 hours with serum free medium, prior to addition of recombinant VEGF ($VEGF_{164}$) at various concentrations. Following 24 hours culture under normoxic conditions, cell lysates were prepared and PAI-1 protein levels assessed by Western blotting as described. As shown in figure 7.7, PAI-1 protein was undetectable in PAM 212 keratinocyte cultures treated with VEGF at any of the chosen concentrations.

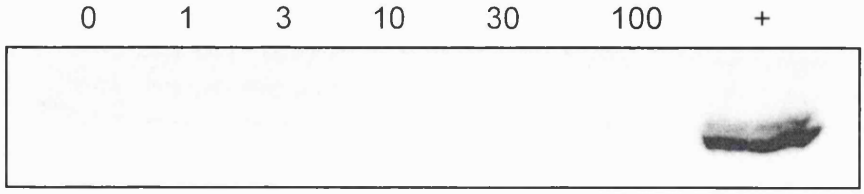

Figure 7.7 Effect of $VEGF_{164}$ on PAI-1 expression in normoxic PAM 212 keratinocytes. Western blotting analysis of cell lysates from keratinocyte cultures treated with various concentrations (ng/ml) of VEGF for 24 hours. + = cell lysate from TGF-β treated PAM 212 keratinocytes.

7.2.5 Analysis of VEGF receptor expression in PAM 212 keratinocytes

Since VEGF functions are primarily mediated through binding to the high affinity tyrosine kinase receptors, Flt-1 and KDR/Flk-1 (human/mouse homologs) (reviewed in Zachary and Gliki, 2001) and neuropilin-1 (NRP-1) has been shown to potentiate VEGF:KDR/Flk-1 signalling interactions (Soker *et al,* 1998), experiments were designed to assess the expression of these VEGF receptors in normoxic and hypoxic PAM 212 keratinocytes using RT-PCR protocols. Initially primers were designed to amplify specific sequences within Flt-1, Flk-1 and neuropilin-1 (NRP-1) cDNA, as detailed in table 7.1. To demonstrate the specificity of this amplification, primer pairs were assessed using murine liver RNA (Flk-1 and Flt-1) or murine heart RNA (NRP-1) as a template for RT-PCR reactions and subsequent PCR products were digested with restriction endonucleases. As shown in figure 7.8, *Eco*RV digestion of the 875 bp Flk-1 RT-PCR product, produced predicted bands of 753 bp and 122 bp. Moreover, *Xba*I digestion of the 462 bp Flt-1 RT-PCR product resulted in the expected production of 298 bp and 164 bp bands. Furthermore, *Bgl*I digestion of the 463 bp NRP-1 RT-PCR product, also produced the predicted bands of 353 bp and 110 bp.

Transcript	Primer Sequences	Size	For	Rev	Genomic
Flk-1	5' GCCTCCACTGTTTATGTCTATGTTC 3' 5' TTGGTGAGGATGACCGTGTAGTT 3'	875	?	?	> 2000
Flt-1	5' TGAAACTGTCCTGTGTGGTCAATAA 3' 5' CCTCATCCTCCTCTGTGACTCTTT 3'	462	13	15	> 2000
NRP-1	5' GTAAGAGGTGTCATCATTCAGGGT 3' 5' TAAAACCGTATGTCGGGAACTCT 3'	463	?	?	> 2000

Table 7.1 Details of primers and associated PCR products used in RT-PCR detection of VEGF receptors. Primer sequences are shown as forward (sense) primer, followed by reverse (antisense) primer. Size = RT-PCR product size (bp); For = exon to which forward primer hybridised; Rev = exon to which reverse primer hybridised; Genomic = size of PCR product (bp) using genomic DNA template; ? = no genomic sequence available.

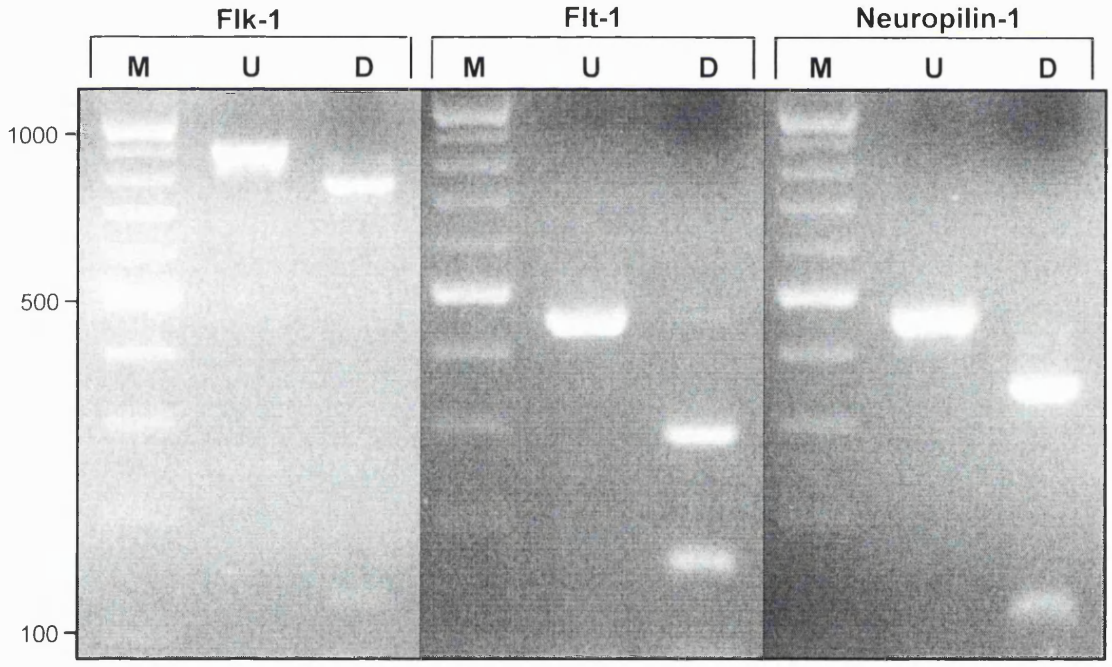

Figure 7.8 Demonstration of primer specificity for VEGF receptor mRNA transcripts. Restriction endonuclease digestion of RT-PCR product from murine liver RNA (Flk-1 and Flt-1) or murine heart RNA (neuropilin-1). For each gene, undigested (U) and digested (D) RT-PCR products are represented. M = 100bp DNA ladder (selected marker sizes are indicated in base pairs).

Having demonstrated the specificity of our primer pairs, expression of VEGF receptors was assessed in PAM 212 keratinocyte cultures maintained under normoxic and hypoxic conditions, using RT-PCR and RT-PCR x PCR protocols (the RT-PCR x PCR protocol involved repeating the RT-PCR amplification stage using 2.5μl of RT-

PCR product as template). Representative data are shown in figure 7.9. Analysis of keratinocyte RNA by RT-PCR (not shown) and RT-PCR x PCR showed no detectable Flk-1 mRNA transcripts in both normoxic and hypoxic cultures. In contrast, RT-PCR analysis of keratinocyte RNA amplified a 462 bp band corresponding to Flt-1 mRNA, and this was detectable in both normoxic and hypoxic PAM 212 keratinocytes. As the band intensity was very low, RT-PCR x PCR was performed, and the resulting Flt-1 specific products are shown in figure 7.9. In addition, RT-PCR analysis of keratinocyte RNA also amplified a 463 bp band corresponding to neuropilin-1, and again this band was detectable in keratinocytes cultured under both normoxic and hypoxic conditions. In all experiments primer pairs were used in genomic PCR (genomic DNA control) to further demonstrate the specificity of amplification.

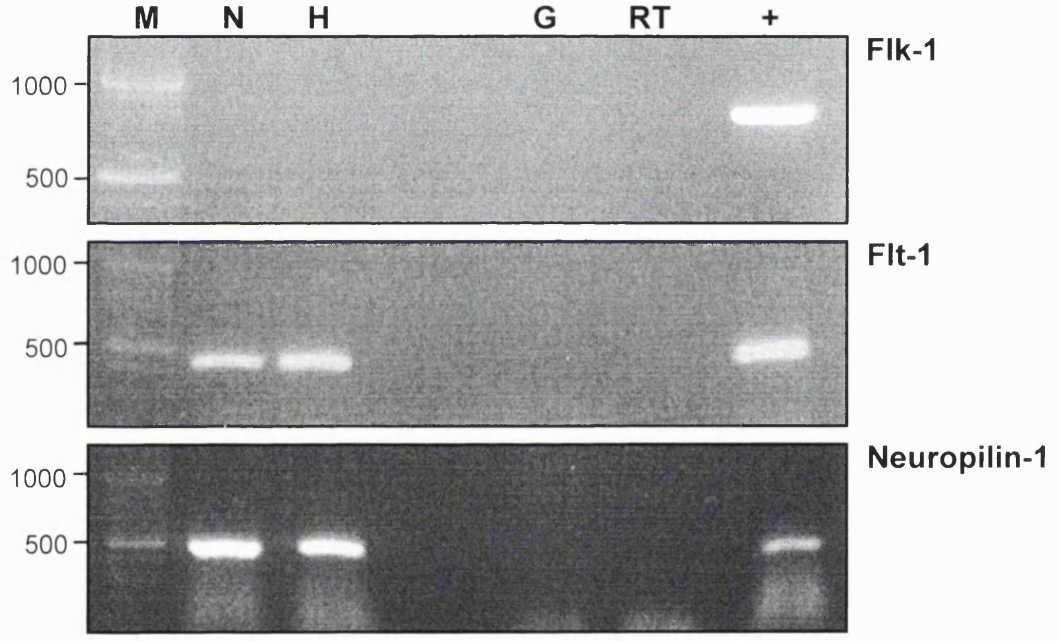

Figure 7.9 Detection of VEGF receptor mRNA in PAM 212 keratinocytes. RT-PCR (neuropilin-1) and RT-PCRxPCR (Flk-1 and Flt-1) of mRNA from PAM 212 keratinocyte cultures maintained in normoxic (N) and hypoxic (H) conditions for 24 hours. G = genomic DNA control; RT = RT-PCR control (i.e. no reverse transcriptase); + = liver mRNA; M = 100bp DNA ladder (selected marker sizes are indicated in base pairs). Data presented are representative of 3 independent experiments.

7.3 DISCUSSION

Despite considerable evidence indicating a role for the plasminogen activator system in wound-related cellular migration and invasion, as well as data suggesting that cutaneous wounds are acutely hypoxic (Niinikoski *et al,* 1991), at the onset of this project, analysis of the effect of acute hypoxia on keratinocyte regulation of this proteolytic system had not been performed. As outlined in chapter 6, our previous studies aimed to assess the effect of hypoxia on the regulation of uPA-mediated plasminogen activation. However, as recent *in vitro* data has suggested additional roles for PAI-1 in cellular migration that are independent of its anti-proteolytic function, the present study was specifically designed to determine the effect of hypoxia on keratinocyte regulation of PAI-1 expression.

In keeping with previous reports using other cell types (Fitzpatrick and Graham, 1998; Pinsky *et al,* 1998; Kietzmann *et al,* 1999; Uchiyama *et al,* 2000), our results have demonstrated that hypoxia is a potent stimulus for PAI-1 expression in cultured keratinocytes. PAI-1 mRNA was induced after just 8 hours exposure to hypoxia and this induction remained apparent for at least 24 hours under hypoxic conditions. Furthermore, PAI-1 protein levels in keratinocyte lysates and conditioned medium were also significantly increased following 24 hours' hypoxia. Interestingly, although TGF-β stimulates PAI-1 expression in keratinocytes *in vitro* (Wikner *et al,* 1990; Keski-Oja and Koli, 1992), and MMP induction in hypoxic keratinocytes is mediated via TGF-β (Xia *et al,* 2001), addition of a TGF-β neutralising antibody had no effect on the hypoxic induction of PAI-1, suggesting that hypoxia can stimulate keratinocyte PAI-1 expression through a TGF-β-independent pathway. In contrast, however, addition of a VEGF-neutralising antibody resulted in reduced PAI-1 protein levels in hypoxic cells, indicating that hypoxic induction of PAI-1 in PAM 212 keratinocytes involves, at least in part, VEGF-mediated stimulation of PAI-1 expression.

Since data from our studies, as well as a previous report (Detmar *et al,* 1997), indicate that VEGF is released by hypoxic keratinocytes, the observed VEGF-mediated modulation of keratinocyte PAI-1 expression under hypoxic conditions initially suggested that the keratinocytes were simply responding in an autocrine fashion to elevated levels of VEGF. However, transfer of VEGF-rich medium from hypoxic cells to normoxic cultures had no effect on PAI-1 expression at either the mRNA or protein

level. Moreover, addition of recombinant $VEGF_{164}$, the most biologically active form of VEGF *in vitro* (Neufeld *et al,* 1999), also had no effect on keratinocyte expression of PAI-1, even at concentrations far in excess of physiological levels. These results strongly suggest that under hypoxic conditions, a "second signal" is required to facilitate stimulation by VEGF.

Cellular responses to VEGF are primarily mediated through binding to either of the two tyrosine kinase receptors, Flt-1 (Barleon *et al,* 1996; Clauss *et al,* 1996; Wang and Keiser, 1998) or Flk-1/KDR (Zachary and Gliki, 2001 and references therein). Moreover, VEGF has also been shown to bind neuropilin-1, though as this receptor has no known signalling functions, it is likely that, by itself, neuropilin-1 is not a functional receptor, but acts as a co-receptor (Soker *et al,* 1998; Zachary and Gliki, 2001). The detection of Flt-1 and neuropilin-1 mRNA in both normoxic and hypoxic PAM 212 keratinocytes, using non-quantitative RT-PCR, indicates that these cells likely have the capacity to both bind and respond to VEGF, and constitutes the first demonstration of VEGF receptor expression by keratinocytes. Although additional experiments are required to determine the effect of hypoxia on the expression and function of these VEGF receptors, previous studies indicate that Flt-1 is up-regulated by hypoxia through a hypoxia response element in its promoter (Gerber *et al,* 1997), suggesting that Flt-1 may be similarly regulated in PAM 212 keratinocytes. Moreover, as neuropilin-1 expression has also been shown to be regulated by hypoxia (Ding *et al,* 2000), and recent reports suggest that interaction of Flt-1 and neuropilin-1 *in vitro* can modulate the binding affinity of one or both of these receptors (Fuh *et al,* 2000; Gluzman-Poltorak *et al,* 2001), it is possible that alterations in Flt-1 and/or neuropilin-1 expression in hypoxic keratinocytes facilitates the observed response to VEGF. Although speculative at present, such a mechanism could explain our observed effect of VEGF on keratinocytes under hypoxic conditions.

Interestingly, data from several recent reports have suggested that the observed induction of keratinocyte-derived PAI-1 may have a specialised function in cutaneous wound repair. Analysis of tumour angiogenesis and choroidal neovascularization in PAI-1 deficient mice revealed severely impaired neo-vessel development (Bajou *et al,* 1998; Lambert *et al,* 2001), strongly indicating that PAI-1 is critical to normal angiogenesis. Moreover, whereas high levels of PAI-1 have been shown to be inhibitory during neovascularization (Soff *et al,* 1995; Stefansson *et al,* 2001), lower, more

physiologically relevant levels actually promote angiogenesis (McMahon *et al,* 2001), presumably by stimulating endothelial cell migration (Isogai *et al,* 2001). The potential regulation of angiogenesis by PAI-1 therefore suggests that the observed VEGF-mediated induction of hypoxic keratinocyte PAI-1 may constitute part of a specialised mechanism whereby keratinocyte-derived VEGF, already identified as a major angiogenic factor in skin (Detmar, 1996), further modulates wound-related angiogenesis.

In conclusion, the present studies have demonstrated that under hypoxic conditions, keratinocytes upregulate PAI-1 expression and this upregulation is mediated, at least in part, by autocrine VEGF stimulation. Furthermore our observation that PAM 212 keratinocytes express mRNA for Flt-1 and neuropilin-1 indicates a potential pathway for this VEGF-mediated induction. Although further analysis of the molecular mechanisms involved in this hypoxia- and VEGF-mediated response is required, the data generated by these studies provide useful information regarding the regulation of PAI-1 in hypoxic cutaneous conditions and, moreover, provides an insight into novel effects of VEGF on hypoxic keratinocytes *in vitro*.

CHAPTER 8

CONCLUDING DISCUSSION AND FUTURE STUDIES

There were two distinct yet related strands to this thesis, the first of which involved the development of a transgenic model of uPA overexpression. Considerable evidence has suggested that the plasminogen activator system is important in cellular migration and tissue remodelling. Moreover, knockout mouse studies have demonstrated a particular requirement for this proteolytic system during wound re-epithelialization (Romer *et al,* 1996; Bugge *et al,* 1996a) and it was therefore hypothesised that transgenic mice with uPA overexpression targeted to the epidermal compartment might provide a useful tool with which to analyse the influence of this protease on skin development, physiology and wound repair. To facilitate the generation of these uPA transgenic mice, both constitutive and inducible systems of transgene expression were developed. Our initial results suggested that constitutive targeting of uPA to basal keratinocytes results in embryonic lethality, therefore two inducible systems of transgene expression were studied in parallel. Transgenic mice were generated using a tamoxifen-inducible Cre/loxP-derived uPA expression system and have shown great potential as a powerful tool for the general analysis of cutaneous uPA function. In addition, transgenic mice expressing uPA under the control of a hyperproliferation- and wound-inducible K6 promoter were generated, characterised and subsequently used in wound healing studies. Although a 3.5-fold induction of uPA was detected in K6-uPAtg wounds compared to wild-type wounds, no gross histological differences were observed between these wound groups, suggesting that other components of the plasminogen activator system may be modulating the activity of uPA, and indicating that this proteolytic system is tightly regulated during cutaneous wound repair.

The second strand of this thesis was concerned with the effect of hypoxia on the plasminogen activator system in cultured keratinocytes. Hypoxia is an inevitable physiological consequence of wound-related vascular disruption and tissue damage. Moreover, it has been shown to enhance keratinocyte migration and to regulate the plasminogen activator system in a variety of other cell types *in vitro*. The effect of hypoxia on keratinocyte expression of plasminogen activator system components was assessed by Northern blotting and enzymatic analyses and uPA and uPAR mRNA, as well as secreted functional uPA, were shown to be significantly increased under hypoxic conditions. Additional experiments to determine the potential role of the induced uPA and uPAR in hypoxia-induced keratinocyte migration demonstrated that the hypoxia-mediated promotion of *in vitro* wound closure was blocked by uPA and

serine protease inhibitors, strongly suggesting that hypoxic enhancement of keratinocyte motility is facilitated by hypoxic upregulation of uPA, and possibly uPAR.

In order to further characterise the effects of hypoxia on keratinocyte expression of plasminogen activator system components, the expression of PAI-1 was assessed by Northern and Western blotting and, as observed with uPA and uPAR, PAI-1 was significantly upregulated in hypoxic PAM 212 keratinocytes. Moreover, additional analyses revealed that the induction of PAI-1 under hypoxic conditions was mediated both directly by hypoxia and indirectly via an autocrine stimulation pathway involving hypoxia-induced VEGF. Importantly, VEGF had no effect on PAI-1 expression in normoxic keratinocytes. In addition, RT-PCR of normoxic and hypoxic keratinocyte RNA detected the expression of both Flt-1 and neuropilin-1 mRNA, thus indicating a potential signalling pathway for VEGF-mediated stimulation of PAI-1 under hypoxic conditions.

KEY POINTS:

- **Constitutive K14 promoter-driven expression of uPA results in embryonic lethality**

- **Cre/loxP-mediated inducible uPA expression shows potential as a tool for analysis of cutaneous role *in vivo***

- **Elevated functional uPA in the cutaneous microenvironment has no apparent effect on gross wound histology**

- **Hypoxic enhancement of keratinocyte motility is mediated by induction of uPA**

- **Induction of keratinocyte PAI-1 expression under hypoxic conditions involves VEGF-mediated autocrine stimulation**

Although our results provide important insights into the regulation of the plasminogen activator system following cutaneous wounding and its associated environmental alterations, a number of fundamental questions concerning the data arising from this work remain unanswered and will be worth pursuing in future experiments.

1. Is the observed null effect of uPA overexpression on cutaneous wound repair due to compensatory regulation by uPAR, PAI-1 and/or PAI-2?

The lack of gross histological differences between K6-uPAtg and wild-type mouse wounds led us to speculate that other components of the plasminogen activator system regulate the activity of the excess transgene-specific uPA. Since this hypothesis is supported by very recent data demonstrating that increased fibrinolysis is associated with enhanced wound closure in PAI-1 deficient mice (Chan *et al,* 2001b), it would be pertinent to investigate the regulation of other plasminogen activator system components in K6-uPA transgenic wounds. The relative levels of uPAR, PAI-1 and PAI-2 could be directly assessed in K6-uPAtg and wild-type wound tissue, however, endogenous upregulation of these molecules is a characteristic of normal wound repair (Romer *et al,* 1991 and 1994; Bechtel *et al,* 1998), and thus, as is suggested by our results, analysis of potentially modest compensatory changes may be problematic. Moreover, normal wound-induced expression of these molecules may already be sufficient to regulate the activity of transgene-specific uPA in K6-uPAtg wounds. One approach to assessing the potential role of uPAR, PAI-1 and PAI-2 in the regulation of transgene uPA in K6-uPAtg wounds would be to cross K6-uPAtg mice with mouse lines deficient in, or overexpressing, components of the plasminogen activator system. Thus, wound analysis of progeny from K6-uPAtg mice crossed with either PAI-1 (Carmeliet *et al,* 1993) or PAI-2 (Dougherty *et al,* 1999) knockout mice would potentially indicate if either of these inhibitors were involved in the regulation of excess transgene-specific uPA. Moreover, crossing the K6-uPAtg mice with uPA knockout mice (Bugge *et al*, 1996a) would allow analysis of the function and regulation of transgene-specific uPA in the absence of high background endogenous uPA. In addition, as it has also been suggested that the activity of uPA may be limited by the availability of uPAR binding sites (see section 5.3), crossing K6-uPA mice with K5-uPAR mice (Zhou *et al,* 2000) would enable this hypothesis to be tested.

2. How does hypoxia-induced uPA promote keratinocyte migration under hypoxic conditions?

Whilst uPA may mediate the hypoxia-enhanced motility of cultured keratinocytes directly via its proteolytic properties or via conformation-specific interactions with uPAR and/or PAI-1, recent data has indicated that TGF-β stimulation of MMPs 1 and 9 may have a crucial role in this process (Xia *et al,* 2001). Although the culture systems used by Xia *et al* differed from our own, most notably in that keratinocyte migration was observed on a type I collagen substrate, previous studies have indicated that MMP activity is also involved in keratinocyte migration on uncoated surfaces (Makela *et al,* 1999). Moreover, since TGF-β has been shown to upregulate uPA activity in cultured keratinocytes (Keski-Oja and Koli, 1992), and uPA/plasmin can activate several MMPs, including MMP-1 and MMP-9 (He *et al,* 1989; Baramova *et al,* 1997), it could be speculated that our observations and those of Xia *et al* are linked. Experiments designed to investigate the effect of TGF-β neutralisation on uPA expression under hypoxic conditions, as well as the effects of both uPA inhibitors on MMP activation and MMP inhibitors on hypoxic keratinocyte migration would potentially determine whether a hypothetical TGF-β–dependent pathway involving interaction of the plasminogen activator and MMP systems exists

3. How does VEGF mediate the induction of PAM 212 keratinocyte-derived PAI-1 under hypoxic conditions?

Our results indicating a role for VEGF in the induction of keratinocyte PAI-1 under hypoxic conditions provides the first evidence of VEGF responsiveness in keratinocytes. Moreover, the detection of Flt-1 and neuropilin-1 mRNA in PAM 212 cells also indicates a potential signalling pathway for this VEGF-mediated effect. However, further experiments must be performed before the precise mechanisms involved are elucidated. Thus, additional semi-quantitative RT-PCR, TaqMan® PCR, and/or Western blotting analysis of the effect of hypoxia on the expression of these VEGF receptors is essential. Moreover, although technically difficult when working with cells under hypoxic conditions, analysis of signal transduction pathways and activated transcription factors may provide more information on the identity of the VEGF receptors involved. In addition, although again technically demanding, the development of a stable VEGF-deficient keratinocyte line, similar to previously reported PAI-1-deficient keratinocytes (Li *et al,* 2000a), would allow VEGF-I^{125} binding

studies, as well as analysis of the effects of exogenous VEGF on PAI-1 expression under hypoxic conditions.

It is now exactly 5 years since the importance of the plasminogen activator system in cutaneous wound healing was conclusively demonstrated using various knockout mice (Romer *et al,* 1996; Bugge *et al,* 1996a) and in that time, major advances have been made regarding the proteolytic and non-proteolytic roles of different components of this system in wound-related migration and invasion *in vitro*, and tissue repair *in vivo*. The present studies have suggested that during wound healing in the skin, the plasminogen activator system is tightly regulated and is capable of compensating for increased expression of the predominant cutaneous plasminogen activator, uPA. Moreover, our experiments examining the effect of hypoxia on expression of plasminogen activator system components have provided an intriguing insight into the manner in which keratinocytes may respond to wound-induced hypoxic environments. Although some of the data requires additional experimental confirmation, given the accessibility of the skin for wound analysis, the continuing advances in the understanding of the complexities of the plasminogen activator system and refinements in *in vitro* and *in vivo* techniques, the next 5 years are likely to yield a much more thorough comprehension of the role of this proteolytic system in cutaneous wound healing.

REFERENCES

Adair TH, Gay WJ and Montani JP: Growth regulation of the vascular system: evidence for a metabolic hypothesis. *Am J Physiol* 259:R393-R404, 1990

Airola K, Reunala T, Salo S and Saarialho-Kere UK: Urokinase plasminogen activator is expressed by basal keratinocytes before interstitial collagenase, stromelysin-1, and laminin-5 in experimentally induced dermatitis herpetiformis lesions . *J Invest Dermatol* 108(1):7-11, 1997

Alvarez OM, Mertz PM and Eaglstein WH: The effect of occlusive dressings on collagen synthesis and re-epithelialization in superficial wounds. *J Surg Res* 35:142-148, 1983

Ando Y and Jensen PJ: Epidermal growth factor and insulin-like growth factor 1 enhance keratinocyte migration. *J Invest Dermatol* 100:633-639, 1993

Ando Y and Jensen PJ: Protein kinase C mediates up-regulation of urokinase and its receptor in the migrating keratinocytes of wounded cultures, but urokinase is not required for movement across a substratum *in vitro*. *J Cell Physiol* 167:500-511, 1996

Andra K, Lassmann H, Bittner R, Shorny S, Fassler R, Propst F and Wiche G: Targeted inactivation of plectin reveals essential function in maintaining the integrity of skin, muscle, and heart cytoarchitecture. *Genes and Development* 11:3143-3156, 1997

Andreasen PA, Nielsen LS, Kristensen P, Grondahl-Hansen J, Skriver L and Dano K: Plasminogen activator inhibitor from human fibrosarcoma cells binds urokinase-type plasminogen activator, but not its proenzyme. *J Biol Chem* 261:7644-7651, 1986

Andreasen PA, Kjoller L, Christensen L and Duffy MJ: The urokinase-type plasminogen activator system in cancer metastasis: A review. *Int J Cancer* 72:1-22, 1997

Anichini E, Fibbi G, Pucci M, Caldini R, Chevanne M and Del Rosso M: Production of second messengers following chemotactic and mitogenic urokinase-receptor interactions in human fibroblasts and mouse fibroblasts transfected with human urokinase receptor. *Exp Cell Res* 213:438-448, 1994

Antalis TM, LaLinn M, Donnan K, Mateo L, Gardner J, Dickinson JL, Buttibeg K and Suhrbier A: The serine proteinase inhibitor (serpin) plasminogen activator inhibitor type 2 protects against viral cytopathic effects by constitutive interferon α/β priming. *J Exp Med* 187:1799-1811, 1998

Appella E, Robinson EA, Ullrich SJ, Stoppelli MP, Corti A, Cassani G and Blasi F: The receptor-binding sequence of urokinase. A biological function for the growth factor module of proteases. *J Biol Chem* 262:4437-4440, 1987

Arumugam S, Young-Chul J, Chen-Jensen C, Gibran NS and Isik FF: Temporal activity of plasminogen activators and matrix metalloproteinases during cutaneous wound repair. *Surgery* 125:587-593, 1999

Astrup, T. *Fibrinolysis: An overview.* In Progress in Chemical: Fibrinolysis and Thrombolysis. J.F. Davidson, R.M. Rowan, M.M. Samama, and P.D. Desnoyers, editors. Raven Press, New York. 1-57. 1978

Ayrall A-M, Kolossov E, Serwe M and Sablitzky F: Reporter gene activation in transgenic mice mediated through induced cre/loxP recombination. *Transgenics* 2:225-231, 1998

Baggiolini M, Dewald B and Moser B: Interleukin-8 and related chemotactic cytokines-CXC and CC chemokines. *Adv Immunol* 55:97-179, 1994

Bailleul B, Surani MA, White S, Barton SC, Brown K, Blessing M, Jorcano JL and Balmain A: Skin hyperkeratosis and papilloma formation in transgenic mice expressing a ras oncogene from a suprabasal keratin promoter. *Cell* 62:697-708, 1990

Bajou K, Noel A, Gerard RD, Masson V, Brunner N, Holst-Hansen C, Skobe M, Fusenig NE, Carmeliet P, Collen D and Foidart JM: Absence of host plasminogen activator inhibitor 1 prevents cancer invasion and vascularization. *Nat Med* 4(8):923-928, 1998

Baramova EN, Bajou K, Remacle A, L'Hoir C, Krell HW, Weidle UH, Noel A and Foidart JM: Involvement of PA/plasmin system in the processing of pro-MMP-9 and in the second step of pro-MMP-2 activation. *FEBS Lett* 405:157-162, 1997

Barleon B, Sozzani S, Zhou D, Weich HA, Mantovani A and Marme D: Migration of human monocytes in response to vascular endothelial growth factor (VEGF) is mediated via the VEGF receptor flt-1. *Blood* 87:3336-3343, 1996

Barrandon Y and Green H: Cell migration is essential for sustained growth of keratinocyte colonies: the roles of transforming growth factor-α and epidermal growth factor. *Cell* 50:1131-1137, 1987

Bator JM, Cohen RL and Chambers DA: Hydrocortisone regulates the dynamics of plasminogen activator and plasminogen activator inhibitor expression in cultured murine keratinocytes. *Exp Cell Res* 242:110-119, 1998

Bechtel MJ, Reinartz J, Rox JM, Inndorf S, Schaefer BM and Kramer MD: Upregulation of cell-surface-associated plasminogen activation in cultured keratinocytes by interleukin-1β and tumor necrosis factor-α. *Exp Cell Res* 223:395-404, 1996

Bechtel MJ, Wysocki NS, Heidtmann A, Stark HJ, Fusenig NE, Kramer MD and Schaefer BM: Plasminogen activator inhibitor type 2 is expressed in keratinocytes during re-epithelialisation of epidermal defects. *Br J Dermatol* 138:22-28, 1998

Beer H-D, Florence C, Dammeier J, McGuire L, Werner S and Duan DR: Mouse fibroblast growth factor 10: cDNA cloning, protein characterization, and regulation of mRNA expression. *Oncogene* 15:2211-2218, 1997

Behrendt N, Ploug M, Patthy L, Houen G, Blasi F and Dano K: The ligand-binding domain of the cell surface receptor for urokinase-type plasminogen activator. *J Biol Chem* 266:7842-7847, 1991

Behrendt N, Ronne E and Dano K: Domain interplay in the urokinase receptor. Requirement for the third domain in high affinity ligand binding and demonstration of ligand contact sites in distinct receptor domains. *J Biol Chem* 271:22885-22894, 1996

Belin D, Vassalli J-D, Combepine C, Godeau F, Nagamine Y, Reich E, Kocher HP and Duvoisin RM: Cloning, nucleotide sequencing and expression of cDNAs encoding mouse urokinase-type plasminogen activator. *Eur J Biochem* 148:225-232, 1985

Belin D, Wohlwend A, Schleuning W-D, Kruithof EK and Vassalli J-D: Facultative polypeptide translocation allows a single mRNA to encode the secreted and cytosolic forms of plasminogen activators inhibitor 2. *EMBO J* 8(11):3287-3294, 1989

Bell WR: The fibrinolytic system in neoplasia. *Seminars in Thrombosis and Hemostasis* 22(6):459-478, 1996

Bloch W, Forsberg E, Lentini S, Brakebusch C, Martin K, Krell HW, Weidle UH, Addicks K and Fassler R: β1 integrin is essential for teratoma growth and angiogenesis. *J Cell Biol* 139:265-276, 1997

Borradori L and Sonnenberg A: Structure and function of hemidesmosomes: more than simple adhesion complexes. *J Invest Dermatol* 112(4):411-418, 1999

Braaten JV, Handt S, Jerome WG, Kirkpatrick J, Lewis JC and Hantgan RR: Regulation of fibrinolysis by platelet-released plasminogen activator inhibitor 1: light scattering and ultrastructural examination of lysis of a model platelet-fibrin thrombus. *Blood* 81:1290-1299, 1993

Bradham DM, Igarashi A, Potter RL and Grotendorst GR: Connective tissue growth factor: a cysteine-rich mitogen secreted by human vascular endothelial cells is related to the SRC-induced immediate early gene product CEF-10. *J Cell Biol* 114:1285-1294, 1991

Braungart E, Magdolen V and Degitz K: Retinoic acid upregulates the plasminogen activator system in human epidermal keratinocytes. *J Invest Dermatol* 116(5):778-784, 2001

Breuss JM, Gallo J, DeLisser HM, Klimanskaya IV, Folkesson HG, Pittet JF, Nishimura SL, Aldape K, Landers DV, Carpenter W, Gillet N, Sheppard D, Matthay MA, Albelda SM, Kramer RH and Pytela R: Expression of the β6 integrin subunit in development, neoplasia and tissue repair suggests a role in epithelial remodeling. *J Cell Sci* 108:2241-2251, 1995

Brinster RL, Chen HY, Warren R, Sarthy A and Palmiter RD: Regulation of metallothionein-thymidine kinase fusion plasmids injected into mouse eggs. *Nature* 296:39-42, 1982

Brizel DM, Scully SP, Harrelson JM, Layfield LJ, Bean JM, Prosnitz LR and Dewhirst MW: Tumor oxygenation predicts for the likelihood of distant metastases in human soft tissue sarcoma. *Cancer Res* 56:941-943, 1996

Broadley KN, Aquino AM, Woodward SC, Buckley-Sturrock A, Sato Y, Rifkin DB and Davidson JM: Monospecific antibodies implicate basic fibroblast growth factor in normal wound repair. *Lab Invest* 61:571-575, 1989

Brocard J, Warot X, Wendling O, Messaddeq N, Vonesch J-L, Chambon P and Metzger D: Spatio-temporally controlled site-specific somatic mutagenesis in the mouse. *Proc Natl Acad Sci USA* 94:14559-14563, 1997

Brocard J, Feil R, Chambon P and Metzger D: A chimeric cre recombinase inducible by synthetic, but not by natural ligands of the glucocorticoid receptor. *Nucleic Acids Res* 26(17):4086-4090, 1998

Brooks PC, Clark RA and Cheresh DA: Requirement of vascular integrin αvβ3 for angiogenesis. *Science* 264:569-571, 1994

Brown GL, Curtsinger L, Brightwell JR, Ackerman DM, Tobin GR, Polk HC, George-Nascimento C, Valenzuela P and Schultz GS: Enhancement of epidermal regeneration by biosynthetic epidermal growth factor. *J Exp Med* 163:1319-1324, 1986

Brown GL, Nanney LB, Griffen J, Cramer AB, Yancey JM, Curtsinger LJ, Holtzin L, Schultz GS, Jurkiewicz MJ and Lynch JB: Enhancement of wound healing by topical treatment with epidermal growth factor [see comments]. *N Engl J Med* 321:76-79, 1989

Brown LF, Yeo K-T, Berse B, Yeo T-K, Senger DR, Dvorak HF and Van de Water L: Expression of vascular permeability factor (vascular endothelial growth factor) by epidermal keratinocytes during wound healing. *J Exp Med* 176:1375-1379, 1992

Brunner G, Vettel U, Jobstmann S, Kramer MD and Schirrmacher V: A T-cell-related proteinase expressed by T-lymphoma cells activates their endogenous pro-urokinase. *Blood* 79:2099-2106, 1992

Bugge TH, Flick MJ, Danton MJ, Daugherty CC, Romer J, Dano K, Carmeliet P, Collen D and Degen JL: Urokinase-type plasminogen activator is effective in fibrin clearance in the absence of its receptor or tissue-type plasminogen activator. *Proc Natl Acad Sci USA* 93:5899-5904, 1996a

Bugge TH, Kombrinck KW, Flick MJ, Daugherty CC, Danton MJ and Degen JL: Loss of fibrinogen rescues mice from the pleiotropic effects of plasminogen deficiency. *Cell* 87:709-719, 1996b

Bullen EC, Longaker MT, Updike DL, Benton R, Ladin D, Hou Z and Howard EW: Tissue inhibitor of metalloproteinases-1 is decreased and activated gelatinases are increased in chronic wounds. *J Invest Dermatol* 104:236-240, 1995

Busso N, Masur SK, Lazega D, Waxman S and Ossowski L: Induction of cell migration by pro-urokinase binding to its receptor: possible mechanism for signal transduction in human epithelial cells. *J Cell Biol* 126(1):259-270, 1994

Byrne C, Tainsky M and Fuchs E: Programming gene expression in developing epidermis. *Development* 120:2369-2383, 1994

Carmeliet P, Kieckens L, Schoonjans L, Ream B, Van Nuffelen A, Prendergast G, Cole M, Bronson R, Collen D and Mulligan RC: Plasminogen activator inhibitor-1 gene-deficient mice. I. Generation by homologous recombination and characterisation. *J Clin Invest* 92:2746-2755, 1993

Carmeliet P, Moons L, Lijnen R, Janssens S, Lupu F, Collen D and Gerard RD: Inhibitory role of plasminogen activator inhibitor-1 in arterial wound healing and neointima formation: a gene targeting and gene transfer study in mice. *Circulation* 96:3180-3191, 1997

Carmeliet P, Moons L, Dewerchin M, Rosenberg S, Herbert JM, Lupu F and Collen D: Receptor-independent role of urokinase-type plasminogen activator in pericellular plasmin and matrix metalloproteinase proteolysis during vascular wound healing in mice. *J Cell Biol* 140(1):233-245, 1998

Carmeliet P and Jain RK: Angiogenesis in cancer and other diseases. *Nature* 407:249-257, 2000

Carroll JM, Albers KM, Garlick JA, Harrington R and Taichman LB: Tissue- and stratum-specific expression of the human involucrin promoter in transgenic mice. *Proc Natl Acad Sci USA* 90:10270-10274, 1993

Carroll JM, Romero MR and Watt FM: Suprabasal integrin expression in the epidermis of transgenic mice results in developmental defects and a phenotype resembling psoriasis. *Cell* 83:957-968, 1995

Cavani A, Zambruno G, Marconi A, Manca V, Marchetti M and Gianetti A: Distinctive integrin expression in the newly forming epidermis during wound healing in humans. *J Invest Dermatol* 101:600-604, 1993

Chan LS, Robinson N and Xu L: Expression of interleukin-4 in the epidermis of transgenic mice results in a pruritic inflammatory skin disease: An experimental animal model to study atopic dermatitis. *J Invest Dermatol* 117:977-983, 2001a

Chan JCY, Duszczyszyn DA, Castellino FJ and Ploplis VA: Accelerated skin wound healing in plasminogen activator inhibitor-1-deficient mice. *Am J Pathol* 159:1681-1688, 2001b

Chang N, Goodson WH, Gottrup F and Hunt TK: Direct measurement of wound and tissue oxygen tension in postoperative patients. *Ann Surg* 197(4):470-478, 1983

Chapman HA: Plasminogen activators, integrins, and the coordinated regulation of cell adhesion and migration. *Curr Opin Cell Biol* 9:714-724, 1997

Chazaud B, Bonavaud S, Plonquet A, Pouchelet M, Gherardi RK and Barlovatz-Meimon G: Involvement of the [uPAR:uPA:PAI-1:LRP] complex in human myogenic cell motility. *Exp Cell Res* 258:237-244, 2000

Chen JD, Kim JP, Sarret Y, Wynn KC, Kramer RH and Woodley DT: Epidermal growth factor (EGF) promotes human keratinocyte locomotion on collagen by increasing the α2 subunit. *Exp Cell Res* 209:216-223, 1993

Chen WY, Rogers AA and Lydon MJ: Characterization of biologic properties of wound fluid collected during early stages of wound healing. *J Invest Dermatol* 99:559-564, 1992

Cheng J, Turksen K, Yu Q-C, Schreiber H, Teng M and Fuchs E: Cachexia and graft-vs.-host-disease-type skin changes in keratin promoter-driven TNFα transgenic mice. *Genes and Development* 6:1444-1456, 1992

Christofidou-Solomidou M, Bridges M, Murphy GF, Albelda SM and DeLisser HM: Expression and function of endothelial cell αv integrin receptors in wound-induced human angiogenesis in human skin/SCID mice chimeras. *Am J Pathol* 151:975-983, 1997

Clark RAF, DellaPelle P, Manseau E, Lanigan JM, Dvorak HF and Colvin RB: Blood vessel fibronectin increases in conjunction with endothelial cell proliferation and capillary ingrowth during wound healing. *J Invest Dermatol* 79:269-276, 1982a

Clark RAF, Quinn JH, Winn HJ, Lanigan JM, DellaPelle P and Colvin RB: Fibronectin is produced by blood vessels in response to injury. *J Exp Med* 156:646-651, 1982b

Clark RAF, Lanigan JM, DellaPelle P, Manseau E, Dvorak HF and Colvin RB: Fibronectin and fibrin provide a provisional matrix for epidermal cell migration during wound reepithelialization. *J Invest Dermatol* 70:264-269, 1982c

Clark, RAF. *Wound Repair: overview and general considerations.* In The molecular and cellular biology of wound repair. R.A.F. Clark, editor. Plenum Press, New York. 3-50. 1996a

Clark RAF, Ashcroft GS, Spencer M-J, Larjava H and Ferguson MWJ: Re-epithelialization of normal human excisional wounds is associated with a switch from αvβ5 to αvβ6 integrins. *Br J Dermatol* 135:46-51, 1996b

Clark, RAF. The Molecular and Cellular Biology of Wound Repair. Plenum Press, New York. 1996c

Clark RAF, Tonnesen MG, Gailit J and Cheresh DA: Transient functional expression of αvβ3 on vascular cells during wound repair. *Am J Pathol* 148:1407-1421, 1996d

Clauss M, Weich H, Breier G, Knies U, Roeckl W, Waltenberger J and Risau W: The vascular endothelial growth factor receptor Flt-1 mediates biological activities. Implications for a functional role of placenta growth factor in monocyte activation and chemotaxis. *J Biol Chem* 271:17629-17634, 1996

Collen D and Lijnen RH: Basic and clinical aspects of fibrinolysis and thrombolysis. *Blood* 78(12):3114-3124, 1991

Collin C, Moll R, Kubicka S, Ouhayoun JP and Franke WW: Characterization of human cytokeratin 2, an epidermal cytoskeletal protein synthesised late during differentiation. *Exp Cell Res* 202:132-141, 1992

Conese M, Nykjaer A, Petersen CM, Cremona O, Pardi R, Andreasen PA, Gliemann J, Christensen EI and Blasi F: α-2 macroglobulin receptor/Ldl receptor-related protein(Lrp)-dependent internalization of the urokinase receptor. *J Cell Biol* 131:1609-1622, 1995

Connolly DT, Heuvelman DM, Nelson R, Olander JV, Eppley BL, Delfino JJ, Siegel NR, Leimgruber RM and Feder J: Tumor vascular permeability factor stimulates endothelial cell growth and angiogenesis. *J Clin Invest* 84:1470-1478, 1989

Conway EM, Collen D and Carmeliet P: Molecular mechanisms of blood vessel growth. *Cardiovasc Res* 49:507-521, 2001

Costanzo LS: Comparison of calcium and sodium transport in early and late rat distal tubules: effect of amiloride. *Am J Physiol* 246:F937-F945, 1984

Coulombe PA, Hutton EM, Letai A, Hebert A, Paller AS and Fuchs E: Point mutations in human keratin 14 genes of epidermolysis bullosa simplex patients: genetic and functional analyses. *Cell* 66:1301-1311, 1991

Crowe MJ, Doetschman T and Greenhalgh DG: Delayed wound healing in immunodeficient TGF-β1 knockout mice. *J Invest Dermatol* 115(1):3-11, 2000

Cubellis MV, Wun T and Blasi F: Receptor-mediated internalization and degradation of urokinase is caused by its specific inhibitor PAI-1. *EMBO J* 9(4):1079-1085, 1990

Cui W, Fowlis DJ, Cousins FM, Duffie E, Bryson S, Balmain A and Akhurst RJ: Concerted action of TGF-β1 and its type II receptor in control of epidermal homeostasis in transgenic mice. *Genes and Development* 9:945-955, 1995

Cui W, Fowlis DJ, Bryson S, Duffie E, Ireland H, Balmain A and Akhurst RJ: TGFβ1 inhibits the formation of benign skin tumors, but enhances progression to invasive spindle carcinomas in transgenic mice. *Cell* 86:531-542, 1996

Damsky CH and Werb Z: Signal transduction by integrin receptors for extracellular matrix: cooperative processing of extracellular information. *Curr Opin Cell Biol* 4:772-781, 1992

Danielian PS, Muccino D, Rowitch DH, Michael SK and McMahon AP: Modification of gene activity in mouse embryos in utero by a tamoxifen-inducible form of cre recombinase. *Current Biology* 8:1323-1326, 1998

Dano K, Andreasen PA, Grondahl-Hansen J, Kristensen P, Nielsen LS and Skriver L: Plasminogen activators, tissue degradation, and cancer. *Adv Cancer Res* 44:139-266, 1985

Davis GE and Camarillo CW: Regulation of endothelial cell morphogenesis by integrins, mechanical forces, and matrix guidance pathways. *Exp Cell Res* 216:113-123, 1995

De Luca M, Tamura RN, Kajiji S, Bondanza S, Rossino P, Cancedda R, Marchisio PC and Quaranta V: Polarized integrin mediates human keratinocyte adhesion to basal lamina. *Proc Natl Acad Sci USA* 87:6888-6892, 1990

De Petro G, Copeta A and Barlati S: Urokinase-type and tissue-type plasminogen activators as growth factors of human fibroblasts. *Exp Cell Res* 213:286-294, 1994

Declerck PJ, De Mol M, Vaughan DE and Collen D: Identification of a conformationally distinct form of plasminogen activator inhibitor-1, acting as a non-inhibitory substrate for tissue-type plasminogen activator. *J Biol Chem* 267:11693-11696, 1992

Degryse B, Orlando S, Resnati M, Rabbani SA and Blasi F: Urokinase/urokinase receptor and vitronectin/ $\alpha v\beta 3$ integrin induce chemotaxis and cytoskeleton reorganization through different pathways. *Oncogene* 20:2032-2043, 2001

Del Rosso M, Fibbi G, Dini G, Grappone C, Pucci M, Caldini R, Magnelli L, Fimiani M, Lotti T and Panconesi E: Role of specific membrane receptors in urokinase-dependant migration of human keratinocytes. *J Invest Dermatol* 94(3):310-316, 1990

Del Rosso M, Anichini E, Pedersen N, Blasi F, Fibbi G, Pucci M and Ruggiero M: Urokinase-urokinase receptor interaction: non-mitogenic signal transduction in human epidermal cells. *Biochem Biophys Res Commun* 190:347-352, 1993

Deng G, Curriden SA, Wang S, Rosenberg S and Loskutoff DJ: Is plasminogen activator inhibitor-1 the molecular switch that governs urokinase receptor-mediated cell adhesion and release. *J Cell Biol* 134:1563-1571, 1996

Desmouliere, A. and G. Gabbiani. *The role of the myofibroblast in wound healing and fibrocontractive diseases.* In The Molecular and Cellular Biology of Wound Healing. R.A.F. Clark, editor. Plenum Press, New York. 391-423. 1996

Detmar M, Yeo K-T, Nagy JA, Van de Water L, Brown LF, Berse B, Elicker BM, Ledbetter S and Dvorak HF: Keratinocyte-derived vascular permeability factor (vascular endothelial growth factor) is a potent mitogen for dermal microvascular endothelial cells. *J Invest Dermatol* 105(1):44-50, 1995

Detmar M: Molecular regulation of angiogenesis in the skin. *J Invest Dermatol* 106:207-208, 1996

Detmar M, Brown LF, Berse B, Jackman RW, Elicker BM, Dvorak HF and Claffey KP: Hypoxia regulates the expression of vascular permeability factor/vascular endothelial growth factor (VPF/VEGF) and its receptors in human skin. *J Invest Dermatol* 108:263-268, 1997

Devalaraja MN and Richmond A: Multiple chemotactic factors: fine control or redundancy? *Trends Pharmacol Sci* 236:151-156, 1999

Devalaraja RM, Nanney LB, Qian Q, Du J, Yu Y, Devalaraja MN and Richmond A: Delayed wound healing in CXCR2 knockout mice. *J Invest Dermatol* 115(2):234-244, 2000

Dickinson JL, Bates EJ, Ferrante A and Antalis TM: Plasminogen activator inhibitor type 2 inhibits tumor necrosis factor α-induced apoptosis. Evidence for an alternate biological function. *J Biol Chem* 270(46):27894-27904, 1995

Ding H, Wu X, Roncari L, Lau N, Shannon P, Nagy A and Guha A: Expression and regulation of neuropilin-1 in human astrocytomas. *Int J Cancer* 88:584-592, 2000

DiSepio D, Jones A, Longley MA, Bundman D, Rothnagel JA and Roop DR: The proximal promoter of the mouse loricrin gene contains a functional AP-1 element and directs keratinocyte-specific but not differentiation specific expression. *J Biol Chem* 270:10792-10799, 1995

Dong-Le Bourhis X, Lambrecht V and Boilly B: Transforming growth factor β1 and sodium butyrate differentially modulate urokinase plasminogen activator and plasminogen activator inhibitor-1 in human breast normal and cancer cells. *Br J Cancer* 77:396-403, 1998

Dougherty KM, Pearson JM, Yang AY, Westrick RJ, Baker MS and Ginsburg D: The plasminogen activator inhibitor-2 gene is not required for normal murine development or survival. *Proc Natl Acad Sci USA* 96:686-691, 1999

Dumin JA, Kent Dickeson,S., Stricker TP, Bhattacharyya-Pakrasi M, Roby JD, Santoro SA and Parks WC: Pro-collagenase-1 (matrix metalloproteinase-1) binds the α2β1 integrin upon release from keratinocytes migrating on type I collagen. *J Biol Chem* 276:29368-29374, 2001

Duncan MR, Frazier K, Abramson S, Williams S, Klapper H, Huang X and Grotendorst GR: Connective tissue growth factor mediates transforming growth factor β-induced collagen synthesis: down-regulation by cAMP. *FASEB J* 13:1774-1786, 1999

Eckes, B., M. Aumailley, and T. Krieg. *Collagens and the reestablishment of dermal integrity*. In The Molecular and Cellular Biology of Wound Repair. R.A.F. Clark, editor. Plenum Press, New York. 493-507. 1996

Ellis V, Scully MF and Kakkar VV: Plasminogen activation by single-chain urokinase in functional isolation. a kinetic study. *J Biol Chem* 262:14998-15003, 1987

Ellis V, Wun TC, Behrendt N, Ronne E and Dano K: Inhibition of receptor-bound urokinase by plasminogen-activator inhibitors. *J Biol Chem* 265:9904-9908, 1990

Ellis V, Behrendt N and Dano K: Plasminogen activation by receptor-bound urokinase. A kinetic study with both cell-associated and isolated receptor. *J Biol Chem* 266:12752-12758, 1991

Enenstein J, Waleh NS and Kramer RH: Basic FGF and TGF-β differentially modulate integrin expression of human microvascular endothelial cells. *Exp Cell Res* 203:499-503, 1992

Engelhardt E, Toksoy A, Goebeler M, Debus S, Brocker E-B and Gillitzer R: Chemokines IL-8, GROα, MCP-1, IP-10 and Mig are sequentially and differentially expressed during phase-specific infiltration of leukocyte subsets in human wound healing. *Am J Pathol* 153(6):1849-1860, 1998

Estreicher A, Muhlhauser J, Carpentier JL, Orci L and Vassalli J-D: The receptor for urokinase type plasminogen activator polarizes expression of the protease to the leading edge of migrating monocytes and promotes degradation of enzyme inhibitor complexes. *J Cell Biol* 111:783-792, 1990

Evans CP, Elfman F, Parangi S, Conn M, Cunha G and Shuman MA: Inhibition of prostate cancer neovascularization and growth by urokinase-plasminogen activator receptor blockade. *Cancer Res* 57:3594-3599, 1997

Fadok VA, Bratton DL, Konowal A, Freed PW, Westcott JY and Henson PM: Macrophages that have ingested apoptotic cells *in vitro* inhibit proinflammatory cytokine production through autocrine/paracrine mechanisms involving TGF-β, PGE2 and PAF. *J Clin Invest* 101:890, 1998

Falabella, A. F. and V. Falanga. *Wound healing.* In The Biology of the Skin. R.K. Freinkel and D.T. Woodley, editors. Parthenon Publishing, New York. 281-297. 2001

Falanga V, Qian SW, Danielpour D, Katz MH, Roberts AB and Sporn MB: Hypoxia upregulates the synthesis of TGF-β1 by human dermal fibroblasts. *J Invest Dermatol* 97:634-637, 1991

Falanga V and Kirsner RS: Low oxygen stimulates proliferation of fibroblasts seeded as single cells. *J Cell Physiol* 154:506-510, 1993

Falanga V, Martin TA, Takagi H, Kirsner RS, Helfman T, Pardes J and Ochoa MF: Low oxygen tension increases mRNA levels of α-1 (I) procollagen in human dermal fibroblasts. *J Cell Physiol* 157:408-412, 1993

Fazioli F, Resnati M, Sidenius N, Higashimoto Y, Appella E and Blasi F: A urokinase-sensitive region of the human urokinase receptor is responsible for its chemotactic activity. *EMBO J* 16(24):7279-7286, 1997

Feiken E, Romer J, Eriksen J and Lund LR: Neutrophils express tumor necrosis factor-α during mouse skin wound healing. *J Invest Dermatol* 105(1):120-123, 1995

Feil R, Brocard J, Mascrez B, LeMeur M, Metzger D and Chambon P: Ligand-activated site-specific recombination in mice. *Proc Natl Acad Sci USA* 93:10887-10890, 1996

Feil R, Wagner J, Metzger D and Chambon P: Regulation of cre recombinase activity by mutated estrogen receptor ligand-binding domains. *Biochem Biophys Res Commun* 237:752-757, 1997

Feng X, Clark RAF, Galanakis D and Tonnesen MG: Fibrin and collagen differentially regulate human dermal microvascular endothelial cell integrins: stabilization of αvβ3 mRNA by fibrin. *J Invest Dermatol* 113:913-919, 1999

Fibbi G, Magnelli L, Pucci M and Del Rosso M: Interaction of urokinase A chain with the receptor of human keratinocytes stimulates release of urokinase-like plasminogen activator. *Exp Cell Res* 187:33-38, 1990

Fitzpatrick TE and Graham CH: Stimulation of plasminogen activator inhibitor-1 expression in immortalized human trophoblast cells cultured under low levels of oxygen. *Exp Cell Res* 245:155-162, 1998

Folkman J and Klagsbrun M: Angiogenic factors. *Science* 235:442-448, 1987

Frank S, Hubner G, Breier G, Longaker MT, Greenhalgh DG and Werner S: Regulation of the vascular endothelial growth factor expression in cultured keratinocytes. *J Biol Chem* 270:12607-12613, 1995

Frank S, Stallmeyer B, Kampfer H, Kolb N and Pfeilschifter J: Leptin enhances wound re-epithelialization and constitutes a direct function of leptin in skin repair. *J Clin Invest* 106(4):501-509, 2000

Franklin B and Poyton RO: Oxygen sensing and molecular adaptation to hypoxia. *Physiol Rev* 76:839-885, 1996

Frazier K, Williams S, Kothapalli D, Klapper H and Grotendorst GR: Stimulation of fibroblast cell growth, matrix production and granulation tissue formation by connective tissue growth factor. *J Invest Dermatol* 107:404-411, 1996

Fuchs E and Green H: Changes in keratin gene expression during terminal differentiation of the keratinocyte. *Cell* 19:1033-1042, 1980

Fuchs E and Weber K: Intermediate filaments: structure, dynamics, function, and disease. *Annu Rev Biochem* 63:345-382, 1994

Fuh G, Garcia KC and de Vos AM: The interaction of neuropilin-1 with vascular endothelial growth factor and its receptor Flt-1. *J Biol Chem* 275:26690-26695, 2000

Furth PA, St Onge L, Boger H, Gruss P, Gossen M, Kistner A, Bujard H and Hennighausen L: Temporal control of gene expression in transgenic mice by a tetracycline-responsive promoter. *Proc Natl Acad Sci USA* 91:9302-9306, 1994

Gailit J, Welch MP and Clark RA: TGF-β1 stimulates expression of keratinocyte integrins during re-epithelialization of cutaneous wounds. *J Invest Dermatol* 103:221-227, 1994

Galindo M, Santiago B, Alcami J, Rivero M, Martin-Serrano J and Pablos JL: Hypoxia induces expression of the chemokines monocyte chemoattractant protein-1 (MCP-1) and IL-8 in human dermal fibroblasts. *Clin Exp Immunol* 123:36-41, 2001

Gan H, Newman GW and Remold HG: Plasminogen activator inhibitor type 2 prevents programmed cell death of human macrophages infected with Mycobacterium avium, serovar 4. *J Immunol* 155:1304-1315, 1995

Gardsvoll H, Dano K and Ploug M: Mapping part of the functional epitope for ligand binding on the receptor for urokinase-type plasminogen activator by site-directed mutagenesis. *J Biol Chem* 274(53):37995-38003, 1999

Garlick JA and Taichman LB: Fate of human keratinocytes during reepithelialization in an organotypic culture model. *Lab Invest* 70(6):916-924, 1994

Genton C, Kruithof EK and Schleuning W-D: Phorbol ester induces the biosynthesis of glycosylated and nonglycosylated plasminogen activator inhibitor 2 in high excess over urokinase-type plasminogen activator in human U-937 lymphoma cells. *J Cell Biol* 104:705-712, 1987

George F, Pourreau-Schneider N, Arnoux D, Boutiere B, Dussault N, Roux-Dosseto M, Alessi MC, Martin PM and Sampol J: Modulation of tPA, PAI-1 and PAI-2 antigen and mRNA levels by EGF in the A431 cell line. *Blood Coagul Fibrinolysis* 1:689-693, 1990

Georges-Labouesse E, Messaddeq N, Yehia G, Cadalbert L, Dierich A and Le Meur M: Absence of integrin α6 leads to epidermolysis bullosa and neonatal death in mice. *Nat Genet* 13:370-373, 1996

Geratz JD and Cheng MCF: The inhibition of urokinase by aromatic diamidines. *Thromb Diath Haemorrh* 33:230-243, 1975

Geratz JD, Shaver SR and Tidwell RR: Inhibitory effect of amidino-substituted heterocyclic compounds on the amidase activity of plasmin and of high and low molecular weight urokinase and on urokinase-induced plasminogen activation. *Thromb Res* 24:73-83, 1981

Gerber H-P, Condorelli F, Park J and Ferrara N: Differential transcriptional regulation of the two vascular endothelial growth factor receptor genes. *J Biol Chem* 272(38):23659-23667, 1997

Ginsburg D, Zeheb R, Yang AY, Rafferty UM, Andreasen PA, Nielsen LS, Dano K, Lebo RV and Gelehrter TD: cDNA cloning of human plasminogen activator-inhibitor from endothelial cells. *J Clin Invest* 78:1673-1680, 1986

Gluzman-Poltorak Z, Cohen T, Shibuya M and Neufeld G: Vascular endothelial growth factor receptor-1 and neuropilin-2 form complexes. *J Biol Chem* 276(22):18688-18694, 2001

Goretzki L, Schmitt M, Mann K, Calvete J, Chucholowski N, Kramer M, Gunzler WA, Janicke F and Graeff H: Effective activation of the proenzyme form of the urokinase-type plasminogen activator (pro-uPA) by the cysteine protease cathepsin L. *FEBS Lett* 297:112-118, 1992

Gossen M and Bujard H: Tight control of gene expression in mammalian cells by tetracycline-responsive promoters. *Proc Natl Acad Sci USA* 89:5547-5551, 1992

Gossen M, Freundlieb S, Bender G, Muller G, Hillen W and Bujard H: Transcriptional activation by tetracyclines in mammalian cells. *Science* 268:1766-1769, 1995

Gottschling C, Huber J and Oberbaumer I: Expression of the laminin-A chain is down-regulated by a noncanonical polyadenylation signal. *Eur J Biochem* 216:293-299, 1993

Graham CH, Fitzpatrick TE and McCrae KR: Hypoxia stimulates urokinase receptor expression through a heme protein-dependent pathway. *Blood* 91:3300-3307, 1998

Graham CH, Forsdike J, Fitzgerald CJ and Macdonald Goodfellow S: Hypoxia-mediated stimulation of carcinoma cell invasiveness via upregulation of urokinase receptor expression. *Int J Cancer* 80:617-623, 1999

Granelli Piperno A, Vassalli J-D and Reich E: Secretion of plasminogen activator by human polymorphonuclear leukocytes. Modulation by glucocorticoids and other effectors. *J Exp Med* 146:1693-1706, 1977

Gray AJ, Bishop JE, Reeves JT and Laurent GJ: Aα and Bβ chains of fibrinogen stimulate proliferation of human fibroblasts. *J Cell Sci* 104:409-413, 1993

Greiling D and Clark RAF: Fibronectin provides a conduit for fibroblast transmigration from collagenous stroma into fibrin clot provisional matrix. *J Cell Sci* 110:861-870, 1997

Grinnell F and Zhu M: Fibronectin degradation in chronic wounds depends on the relative levels of elastase, α1-proteinase inhibitor, and α2-macroglobulin. *J Invest Dermatol* 106:335-341, 1996

Grondahl-Hansen J, Lund LR, Ralfkiaer E, Ottevanger V and Dano K: Urokinase and tissue-type plasminogen activators in keratinocytes during wound reepithelialization *in vivo*. *J Invest Dermatol* 90:790-795, 1988

Groves RW, Mizutani H, Kieffer JD and Kupper TS: Inflammatory skin disease in transgenic mice that express high levels of interleukin 1α in basal epidermis. *Proc Natl Acad Sci USA* 92:11874-11878, 1995

Gudewicz PW and Bilboa N: Human urokinase-type plasminogen activator stimulates chemotaxis of human neutrophils. *Biochem Biophys Res Commun* 147:1176-1181, 1987

Gunzler WA, Steffens GJ, Otting F, Kim S-MA, Frankus E and Flohe L: The primary structure of high molecular mass urokinase from human urine. *Hoppe-Seyler's Z Physiol Chem* 363:1155-1165, 1982

Guo L, Degenstein L and Fuchs E: Keratinocyte growth factor is required for hair development but not for wound healing. *Genes and Development* 10:165-175, 1996

Guo M, Kim LT, Akiyama SK, Gralnick HR, Yamada KM and Grinnell F: Altered processing of integrin receptors during keratinocyte activation. *Exp Cell Res* 195(2):315-322, 1991

Gyetko MR, Todd RF, Wilkinson CC and Sitrin RG: The urokinase receptor is required for human monocyte chemotaxis *in vitro*. *J Clin Invest* 93:1380-1387, 1994

Haake, A., G. A. Scott, and K. A. Holbrook. *Structure and function of the skin: overview of the epidermis and dermis.* In The Biology of the Skin. R.K. Freinkel and D.T. Woodley, editors. Parthenon Publishing, New York. 19-45. 2001

Haapasalmi K, Zhang K, Tonnesen M, Olerud J, Sheppard D, Salo T, Kramer R, Clark RAF, Uitto V-J and Larjava H: Keratinocytes in human wounds express αvβ6 integrin. *J Invest Dermatol* 106(1):42-48, 1996

Han Y-P, Tuan T-L, Hughes M, Wu H and Garner WL: Transforming growth factor-β- and tumor necrosis factor-α-mediated induction and proteolytic activation of MMP-9 in human skin. *J Biol Chem* 276(25):22341-22350, 2001

Haroon ZA, Raleigh JA, Greenberg CS and Dewhirst MW: Early wound healing exhibits cytokine surge without evidence of hypoxia. *Ann Surg* 231(1):137-147, 2000

Hashimoto K, Wun T-C, Baird J, Lazarus GS and Jensen PJ: Characterization of keratinocyte plasminogen activator inhibitors and demonstration of the prevention of pemphigus IgG-induced acantholysis by a purified plasminogen activator inhibitor. *J Invest Dermatol* 92:310-315, 1989

Hashimoto K, Higashiyama S, Asada H, Hashimura E, Kobayashi T, Sudo K, Nakagawa T, Damm D, Yoshikawa K and Taniguchi N: Heparin-binding epidermal growth factor-like growth factor is an autocrine growth factor for human keratinocytes. *J Biol Chem* 269:20060-20066, 1994

He CS, Wilhelm SM, Pentland AP, Marmer BL, Grant GA, Eisen AZ and Goldberg GI: Tissue cooperation in a proteolytic cascade activating human interstitial collagenase. *Proc Natl Acad Sci USA* 86:2632-2636, 1989

Heckel JL, Sandgren EP, Degen JL, Palmiter RD and Brinster RL: Neonatal bleeding in transgenic mice expressing urokinase-type plasminogen activator. *Cell* 62:447-456, 1990

Heid HW, Moll I and Franke WW: Patterns of expression of trichocytic and epithelial cytokeratins in mammalian tissue I. Human and bovine hair follicles. *Differentiation* 37:137-157, 1988

Heipel JM and Ossowski L: Human neutrophil plasminogen activator is localised in specific granules and is translocated to the cell surface by exocytosis. *J Exp Med* 164:826-840, 1986

Heldin, C-H. and B. Westermark. *Role of platelet-derived growth factor* in vivo. In The Molecular and Cellular Biology of Wound Repair. R.A.F. Clark, editor. Plenum Press, New York. 249-273. 1996

Hengge UR, Chan EF, Foster RA, Walker PS and Vogel JC: Cytokine gene expression in epidermis with biological effects following injection of naked DNA. *Nat Genet* 10:161-166, 1995

Hengge UR, Walker PS and Vogel JC: Expression of naked DNA in human, pig, and mouse skin. *J Clin Invest* 97:2911-2916, 1996

Herrick SE, Ireland GW, Simon D, McCollum CN and Ferguson MWJ: Venous ulcer fibroblasts compared with normal fibroblasts show differences in collagen but not fibronectin production under both normal and hypoxic conditions. *J Invest Dermatol* 106:187-193, 1996

Hertle MD, Kubler MD, Leigh IM and Watt FM: Aberrant integrin expression during epidermal wound healing and in psoriatic epidermis. *J Clin Invest* 89:1892-1901, 1992

Heymans S, Luttun A, Nuyens D, Theilmeier G, Creemers E, Moons L, Dyspersin GD, Cleutjens JP, Shipley M, Angellilo A, Levi M, Nube O, Baker A, Keshet E, Lupu F, Herbert JM, Smits JF, Shapiro SD, Baes M, Borgers M, Collen D, Daemen MJ and Carmeliet P: Inhibition of plasminogen activators or matrix metalloproteinases prevents cardiac rupture but impairs therapeutic angiogenesis and causes cardiac failure. *Nat Med* 5:1135-1142, 1999

Heyneker H, Holmes W, Rey M, Pennica D, Shepard HM, Seeburg P, Hayflick J, Ward C and Vehar G: Functional expression of the human urokinase gene in E. coli. *Proceedings of the Fourth International Symposium on Genetics of Industrial Microorganisms*, 214-221, 1983

Hibino T, Matsuda Y, Takahashi T and Goetinck PF: Suppression of keratinocyte proliferation by plasminogen activator inhibitor-2. *J Invest Dermatol* 112(1):85-90, 1999

Hockel M, Schlenger K, Knoop C and Vaupel P: Oxygenation of carcinomas of the uterine cervix: evaluation by computerized O_2 tension measurements. *Cancer Res* 51:6098-6102, 1991

Hoess RH, Ziese M and Sternberg N: P1 site-specific recombination: nucleotide sequence of the recombining sites. *Proc Natl Acad Sci USA* 79:3398-3402, 1982

Holmes WE, Pennica D and Blaber M: Cloning and expression of the gene for pro-urokinase in Escherichia coli. *Bio/Technology* 3:923-929, 1985

Howe JR, Skryabin BV, Belcher SM, Zerillo CA and Schmauss C: The responsiveness of a tetracycline-sensitive expression system differs in different cell lines. *J Biol Chem* 23:14168-14174, 1995

Hoyer-Hansen G, Ronne E, Solberg H, Behrendt N, Ploug M, Lund LR, Ellis V and Dano K: Urokinase plasminogen activator cleaves its cell surface receptor releasing the ligand binding domain. *J Biol Chem* 267:18224-18229, 1992

Hoylaerts M, Rijken DC, Lijnen HR and Collen D: Kinetics of the activation of plasminogen by human tissue plasminogen activator. Role of fibrin. *J Biol Chem* 257:2912-2919, 1982

Huang X, Wu J, Spong S and Sheppard D: The integrin αvβ6 is critical for keratinocyte migration on both its known ligand, fibronectin, and on vitronectin. *J Cell Sci* 111:2189-2195, 1998

Huang X, Griffiths M, Wu J, Farese Jnr RV and Sheppard D: Normal development, wound healing, and adenovirus susceptibility in β5-deficient mice. *Mol Cell Biol* 20:755-759, 2000

Hubner G, Brauchle M, Smola H, Madlener M, Fassler R and Werner S: Differential regulation of pro-inflammatory cytokines during wound healing in normal and glucocorticoid-treated mice. *Cytokine* 8(7):548-556, 1996

Hynes RO: Integrins: versatility, modulation, and signaling in cell adhesion. *Cell* 69:11-25, 1992

Ichinose A, Fujikawa K and Suyama T: The activation of pro-urokinase by plasma kallikrein and its inactivation by thrombin. *J Biol Chem* 261:3486-3489, 1986

Igarashi A, Okochi H, Bradham DM and Grotendorst GR: Regulation of connective tissue growth factor gene expression in human skin fibroblasts and during woung healing. *Mol Biol Cell* 4:637-645, 1993

Igarashi M, Finch PW and Aaronson SA: Characterization of recombinant human fibroblast growth factor (FGF)-10 reveals functional similarities with keratinocyte growth factor (FGF-7). *J Biol Chem* 21:13230-13235, 1998

Ignotz RA and Massague J: Transforming growth factor-β stimulates the expression of fibronectin and collagen and their incorporation into the extracellular matrix. *J Biol Chem* 261:4337-4345, 1986

Imai T, Jiang M, Chambon P and Metzger D: Impaired adipogenesis and lipolysis in the mouse upon selective ablation of the retinoid X receptor-α mediated by a tamoxifen-inducible chimeric cre recombinase (Cre-ERt2) in adipocytes. *Proc Natl Acad Sci USA* 98(1):224-228, 2001

Indra AK, Warot X, Brocard J, Bornert J-M, Xiao J-H, Chambon P and Metzger D: Temporally-controlled site-specific mutagenesis in the basal layer of the epidermis: comparison of the recombinase activity of the tamoxifen-inducible Cre-ER^T and Cre-ER^{T2} recombinases. *Nucleic Acids Res* 27(22):4324-4327, 1999

Inoue M, Kratz G, Haegerstrand A and Stahle-Backdahl M: Collagenase expression is rapidly induced in wound-edge keratinocytes after acute injury in human skin, persists during healing, and stops at re-epithelialization. *J Invest Dermatol* 104:479-483, 1995

Ishida-Yamamoto A, McGrath JA, Judge MR, Leight IM, Lane EB and Eady RAJ: Selective involvement of keratins K1 and K10 in the cytoskeletal abnormality of epidermolytic hyperkeratosis (bullous congenital ichthyosiform erythroderma). *J Invest Dermatol* 99:19-26, 1992

Isogai C, Laug WE, Shimada H, Declerck PJ, Stins MF, Durden DL, Erdreich-Epstein A and DeClerck YA: Plasminogen activator inhibitor-1 promotes angiogenesis by stimulating endothelial cell migration towards fibronectin. *Cancer Res* 61:5587-5594, 2001

Jaenisch R: Transgenic animals. *Science* 240:1468-1474, 1988

Jensen PJ and Rodeck U: Autocrine/paracrine regulation of keratinocyte urokinase plasminogen activator through the TGF-α/EGF receptor. *J Cell Physiol* 155:333-339, 1993

Jensen PJ, Wu QY, Janowitz P, Ando Y and Schechter NM: Plasminogen activator inhibitor type 2: an intracellular keratinocyte differentiation product that is incorporated into the cornified envelope. *Exp Cell Res* 217:65-71, 1995

Jensen PJ and Lavker RM: Urokinase is a positive regulator of epidermal proliferation *in vivo*. *J Invest Dermatol* 112(2):240-244, 1999

Jiang C-K, Magnaldo T, Ohtsuki M, Freedberg IM, Bernerd F and Blumenberg M: Epidermal growth factor and transforming growth factor-α specifically induce the activation- and hyperproliferation-associated keratins 6 and 16. *Proc Natl Acad Sci USA* 90:6786-6790, 1993

Jimenez PA, Teliska M, Liu B and Antonaccio MJ: Urokinase-type plasminogen activator stimulates wound healing in the diabetic mouse. *Inflamm Res* 46 Suppl 2:S169-S170, 1997

Jimenez PA and Rampy MA: Keratinocyte growth factor-2 accelerates wound healing in incisional wounds. *J Surg Res* 81:238-242, 1999

Jornvall H, Pohl G, Bergsdorf N and Wallen P: Differential proteolysis and evidence for a residue exchange in tissue plasminogen activator suggest possible association between two types of protein microheterogeneity. *FEBS Lett* 156:47-50, 1983

Juhasz I, Murphy GF, Yan HC, Herlyn M and Albelda SM: Regulation of extracellular matrix proteins and integrin cell substratum adhesion receptors on epithelium during cutaneous human wound healing *in vivo*. *Am J Pathol* 143(5):1458-1469, 1993

Kanse SM, Kost C, Wilhelm OG, Andreasen PA and Preissner KT: The urokinase receptor is a major vitronectin-binding protein on endothelial cells. *Exp Cell Res* 224:344-353, 1996

Karakurum M, Shreeniwas R, Chen J, Pinsky D, Yan SD, Anderson M, Sunouchi K, Major J, Hamilton T and Kuwabara K: Hypoxic induction of interleukin-8 gene expression in human endothelial cells. *J Clin Invest* 93(4):1564-1570, 1994

Kawano T, Morimoto K and Uemura Y: Urokinase inhibitor in human placenta. *Nature* 217:253-254, 1968

Kellendonk C, Tronche F, Monaghan AP, Angrand PO, Stewart F and Schutz G: Regulation of Cre recombinase activity by the synthetic steroid RU 486. *Nucleic Acids Res* 24:1404-1411, 1996

Keski-Oja J and Koli K: Enhanced production of plasminogen activator activity in human and murine keratinocytes by transforming growth factor-β1. *J Invest Dermatol* 99(2):193-200, 1992

Kibe Y, Takenaka H and Kishimoto S: Spatial and temporal expression of basic fibroblast growth factor protein during wound healing of rat skin. *Br J Dermatol* 143:720-727, 2000

Kietzmann T, Roth U and Jungermann K: Induction of the plasminogen activator inhibitor-1 gene expression by mild hypoxia via a hypoxia response element binding the hypoxia-inducible factor-1 in rat hepatocytes. *Blood* 94(12):4177-4185, 1999

Kim JP, Zhang K, Chen JD, Wynn KC, Kramer RH and Woodley DT: Mechanism of human keratinocyte migration on fibronectin: unique roles of RGD site and integrins. *J Cell Physiol* 151:443-450, 1992

Kim JP, Zhang K, Chen JD, Kramer RH and Woodley DT: Vitronectin-driven human keratinocyte locomotion is mediated by the αvβ5 integrin receptor. *J Biol Chem* 269(43):26926-26932, 1994

Kirchheimer JC, Christ G and Binder BR: Growth stimulation of human epidermal cells by urokinase is restricted to the intact active enzyme. *Eur J Biochem* 181:103-107, 1989

Kirchheimer JC and Remold HG: Endogenous receptor-bound urokinase mediates tissue invasion of human monocytes. *J Immunol* 143:2634-2639, 1989

Kirchheimer JC, Binder BR and Remold HG: Matrix-bound plasminogen activator inhibitor type 1 inhibits the invasion of human monocytes into interstitial tissue. *J Immunol* 145:1518-1522, 1990

Kiso U, Kaudewitz H, Henschen A, Astedt B, Kruithof EK and Bachmann F: Determination of intermediates, products and cleavage site in the reaction between plasminogen activator inhibitor type 2 and urokinases. *FEBS Lett* 230:51-56, 1988

Kistner A, Gossen M, Zimmermann F, Jerecic J, Ullmer C, Lubbert H and Bujard H: Doxycycline-mediated quantitative and tissue-specific control of gene expression in transgenic mice. *Proc Natl Acad Sci USA* 93:10933-10938, 1996

Kjoller L, Kanse SM, Kirkegaard T, Rodenburg KW, Ronne E, Goodman SL, Preissner KT, Ossowski L and Andreasen PA: Plasminogen activator inhibitor-1 represses integrin- and vitronectin-mediated cell migration independently of its function as an inhibitor of plasminogen activation. *Exp Cell Res* 232:420-429, 1997

Knighton DR, Silver IA and Hunt TK: Regulation of wound-healing angiogenesis - effect of oxygen gradients and inspired oxygen concentration. *Surgery* 90:262-270, 1981

Knighton DR, Hunt TK, Scheuenstuhl H, Halliday BJ, Werb Z and Banda MJ: Oxygen tension regulates the expression of angiogenesis factor by macrophages. *Science* 221:1283-1285, 1983

Knox P, Crooks S, Scaife MC and Patel S: Role of plasminogen, plasmin and plasminogen activators in the migration of fibroblasts into plasma clots. *J Cell Physiol* 132:501-508, 1987

Knudsen BS, Harpel PC and Nachman RL: Plasminogen activator inhibitor is associated with the extracellular matrix of cultured bovine smooth muscle cells. *J Clin Invest* 80:1082-1089, 1987

Kobayashi H, Schmitt M, Goretzki L, Chucholowski N, Calvete J, Kramer MD, Gunzler WA, Janicke F and Graeff H: Cathepsin B efficiently activates the soluble and the tumor cell receptor-bound form of the proenzyme urokinase-type plasminogen activator (pro-uPA). *J Biol Chem* 266:5147-5152, 1991

Koolwijk P, Van Erck MGM, De Vree WJA, Vermeer MA, Weich HA, Hanemaaijer R and van Hinsbergh VWM: Cooperative effect of TNFα, bFGF, and VEGF on the formation of tubular structures of human microvascular endothelial cells in a fibrin matrix. Role of urokinase activity. *J Cell Biol* 132:1177-1188, 1996

Koolwijk P, Sidenius N, Peters E, Sier CFM, Hanemaaijer R, Blasi F and van Hinsbergh VWM: Proteolysis of the urokinase-type plasminogen activator receptor by metalloproteinase-12: implication for angiogenesis in fibrin matrices. *Blood* 97(10):3123-3131, 2001

Kroon ME, Koolwijk P, van Goor H, Weidle U, Collen A, van der Pluijm G and van Hinsbergh VWM: Role and localization of urokinase receptor in the formation of new microvascular structures in fibrin matrices. *Am J Pathol* 154:1731-1742, 1999

Kroon ME, Koolwijk P, van der Vecht B and van Hinsbergh VWM: Urokinase receptor expression on human microvacular endothelial cells is increased by hypoxia: implications for capillary-like tube formation in a fibrin matrix. *Blood* 96(8):2775-2783, 2000a

Kroon ME, Koolwijk P, van der Vecht B and van Hinsbergh VWM: Hypoxia in combination with FGF-2 induces tube formation by human microvascular endothelial cells in a fibrin matrix: involvement of at least two signal transduction pathways. *J Cell Sci* 114(4):825-833, 2000b

Kruithof EK, Baker MS and Bunn CL: Biological and clinical aspects of plasminogen activator inhibitor type 2. *Blood* 86:4007-4024, 1995

Kuhn R, Schwenk F, Aguet M and Rajewsky K: Inducible gene targeting in mice. *Science* 269:1427-1429, 1995

Kumar S and Baglioni C: Protection from tumor necrosis factor-mediated cytolysis by overexpression of plasminogen activator inhibitor type-2. *J Biol Chem* 266:20960-20964, 1991

Kuwabara K, Ogawa S, Matsumoto M, Koga S, Clauss M, Pinsky DJ, Lyn P, Leavy J, Witte L, Joseph-Silverstein J, Furie MB, Torcia G, Cozzolino F, Kamada T and Stern DM: Hypoxia-mediated induction of acidic/basic fibroblast growth factor and platelet-derived growth factor in mononuclear phagocytes stimulates growth of hypoxic endothelial cells. *Proc Natl Acad Sci USA* 92:4606-4610, 1995

Lakso M, Sauer B, Mosinger B, Lee EJ, Manning RW, Yu SH, Mulder KL and Westphal H: Targeted oncogene activation by site-specific recombination in transgenic mice. *Proc Natl Acad Sci USA* 89:6232-6236, 1992

Lambert V, Munaut C, Noel A, Frankenne F, Bajou K, Gerard R, Carmeliet P, Defresne MP, Foidart JM and Rakic JM: Influence of plasminogen activator inhibitor type-1 on choroidal neovascularization. *FASEB J* 15:1021-1027, 2001

Larcher F, Murillas R, Bolontrade M, Conti CJ and Jorcano JL: VEGF/VPF overexpression in skin of transgenic mice induces angiogenesis, vascular hyperpermeability and accelerated tumor development. *Oncogene* 17:303-311, 1998

Larjava H, Peltonen J, Akiyama SK, Yamada SS, Gralnick HR, Uitto J and Yamada KM: Novel function for β1 integrins in keratinocyte cell-cell interactions. *J Cell Biol* 110:803-815, 1990

Larkin J, Clayton M, Sun B, Perchonock CE, Morgan JL, Siracusa LD, Michaels FH and Feitelson MA: Hepatitis B virus transgenic mouse model of chronic liver disease. *Nat Med* 5:907-912, 1999

Lauer G, Solberg S, Cole M, Flamme I, Sturzebecher J, Mann K, Krieg T and Eming SA: Expression and proteolysis of vascular endothelial growth factor is increased in chronic wounds. *J Invest Dermatol* 115(1):12-18, 2000

LaVan F and Hunt TK: Oxygen and wound healing. *Clin Plastic Surg* 17:463-472, 1990

Legrand C, Polette M, Tournier J-M, De Bentzmann S, Huet E, Monteau M and Birembaut P: uPA/plasmin system-mediated MMP-9 activation is implicated in bronchial epithelial cell migration. *Exp Cell Res* 264:326-336, 2001

Levenson SM, Geever EF, Crowley LV, Oates III JF, Berard CW and Rosen H: The healing of rat skin wounds. *Ann Surg* 161:293-308, 1965

Levin EG and Santell L: Association of a plasminogen activator inhibitor (PAI-1) with the growth substratum and membrane of human endothelial cells. *J Cell Biol* 105:2543-2549, 1987

Li F, Goncalves J, Faughnan K, Steiner MG, Pagan-Charry I, Esposito D, Chin B, Providence KM, Higgins PJ and Staiano Coico L: Targeted inhibition of wound-induced PAI-1 expression alters migration and differentiation in human epidermal keratinocytes. *Exp Cell Res* 258:245-253, 2000a

Li N, Indra AK, Warot X, Brocard J, Messaddeq N, Kato S, Metzger D and Chambon P: Skin abnormalities generated by temporally controlled RXRalpha mutations in mouse epidermis. *Nature* 407:633-636, 2000b

Lijnen HR, Van Hoef B, Nelles L and Collen D: Plasminogen activation with single-chain urokinase-type plasminogen activator (scu-PA). *J Biol Chem* 265:5232-5236, 1990

Lijnen HR, Arza B, Van Hoef B, Collen D and Declerck PJ: Inactivation of plasminogen activator inhibitor-1 by specific proteolysis with stromelysin-1 (MMP-3). *J Biol Chem* 275:37645-37650, 2000

Liotta LA, Goldfarb RH, Brundage R, Siegal GP, Terranova V and Garbisa S: Effect of plasminogen activator (urokinase), plasmin, and thrombin on glycoprotein and collagenous components of basement membrane. *Cancer Res* 41:4629-4636, 1981a

Liotta LA, Goldfarb RH and Terranova VP: Cleavage of laminin by thrombin and plasmin: α-thrombin selectively cleaves the β chain of laminin. *Thromb Res* 21:663-673, 1981b

List K, Jensen ON, Bugge TH, Lund LR, Ploug M, Dano K and Behrendt N: Plasminogen-independent initiation of the pro-urokinase activation cascade *in vivo*. activation of pro-urokinase by glandular kallikrein (mGK-6) in plasminogen-deficient mice. *Biochemistry* 39:508-515, 2000

Littlefield BA: Plasminogen activators in endometrial physiology and embryo implantation: a review. *Ann N Y Acad Sci* 622:167-175, 1991

Liu X, Alexander V, Vijayachandra K, Bhogte E, Diamond I and Glick A: Conditional epidermal expression of TGFβ1 blocks neonatal lethality but causes a reversible hyperplasia and alopecia. *Proc Natl Acad Sci USA* 98:9139-9144, 2001

Lloyd C, Yu QC, Cheng J, Turksen K, Degenstein L, Hutton EM and Fuchs E: The basal keratin network of stratified squamous epithelia: defining K15 function in the absence of K14. *J Cell Biol* 129:1329-1344, 1995

Longstaff C, Merton RE, Fabregas P and Felez J: Characterization of cell-associated plasminogen activation catalyzed by urokinase-type plasminogen activator, but independent of urokinase receptor (uPAR, CD87). *Blood* 93(11):3839-3846, 1999

Loskutoff DJ and Edgington TS: Synthesis of a fibrinolytic activator and inhibitor by endothelial cells. *Proc Natl Acad Sci USA* 74:3903-3907, 1977

Loskutoff, D. J., M. S. Sawdey, and J. Mimuro. *Type I plasminogen activator inhibitor*. In Progress in Hemostasis and Thrombosis. B. Coller, editor. Bermedica Production, Columbia. 87-115. 1989

Lotti T and Benci M: Plasminogen activators, venous leg ulcers and reepithelialization. *Int J Dermatol* 34:696-699, 1995

Lu H, Mabilat C, Yeh P, Guitton J-D, Li H, Pouchelet M, Shoevaert D, Legrand Y, Soria J and Soria C: Blockage of urokinase receptors reduces *in vitro* the motility and deformability of endothelial cells. *FEBS Lett* 380:21-24, 1996

Lund LR, Eriksen J, Ralfkiaer E and Romer J: Differential expression of urokinase-type plasminogen activator, its receptor, and inhibitors in mouse skin after exposure to a tumor-promoting phorbol ester. *J Invest Dermatol* 106:622-630, 1996

Lund LR, Romer J, Bugge TH, Nielsen BS, Frandsen TL, Degen JL, Stephens RW and Dano K: Functional overlap between two classes of matrix-degrading proteases in wound healing. *EMBO J* 18(17):4645-4656, 1999

Lynley AM and Dale BA: The characterization of human epidermal filaggrin: a histidine rich keratin filament aggregating protein. *Biochem Biophys Acta* 744:28-35, 1983

Lyons RM, Keski-Oja J and Moses HL: Proteolytic activation of latent transforming growth factor-β from fibroblast conditioned medium. *J Cell Biol* 106:1659-1665, 1988

Madlener M, Mauch C, Conca W, Brauchle M, Parks WC and Werner S: Growth factor regulation of stromelysin-2 expression by keratinocytes: implications for normal and impaired wound healing. *Biochem J* 320:659-664, 1996

Magnaldo T, Bernerd F, Asselineau D and Darmon M: Expression of loricrin is negatively controlled by retinoic acid in human epidermis reconstructed *in vitro*. *Differentiation* 49:39-46, 1992

Makela M, Larjava H, Pirila E, Maisi P, Salo T, Sorsa T and Uitto V-J: Matrix metalloproteinase 2 (gelatinase A) is related to migration of keratinocytes. *Exp Cell Res* 251(1):67-78, 1999

Mansbridge JN and Knapp AM: Changes in keratinocyte maturation during wound healing. *J Invest Dermatol* 89:253-263, 1987

Marchese C, Chedid M, Dirsch OR, Csaky KG, Santanelli F, Latini C, LaRochelle WJ, Torrisi MR and Aaronson SA: Modulation of keratinocyte growth factor and its receptor in reepithelializing human skin. *J Exp Med* 182:1369-1376, 1995

Marchese C, Felici A, Visco V, Lucania G, Igarashi M, Picardo M, Frati L and Rosaria Torrisi M: Fibroblast growth factor 10 induces proliferation and differentiation of human cultured keratinocytes. *J Invest Dermatol* 116:623-628, 2001

Marchisio PC, Bondanza S, Cremona O, Cancedda R and De Luca M: Polarized expression of integrin receptors (α6β4, α2β1, α3β1, and αvβ5) and their relationship with the cytoskeleton and basement membrane matrix in cultured human keratinocytes. *J Cell Biol* 112:761-773, 1991

Marshall JS and Bienenstock J: The role of mast cells in inflammatory reactions of the airways, skin and intestine. *Curr Opin Immunol* 6:853-859, 1994

Marti HH and Risau W: Systemic hypoxia changes the organ-specific distribution of vascular endothelial growth factor and its receptors. *Proc Natl Acad Sci USA* 95:15809-15814, 1998

Martin P: Wound healing - aiming for perfect skin regeneration. *Science* 276:75-81, 1997

Matsumoto K, Hashimoto K, Yoshikawa K and Nakamura T: Marked stimulation of growth and motility of human keratinocytes by hepatocyte growth factor. *Exp Cell Res* 196:114-120, 1991

Mawatari M, Okamura K, Matsuda T, Hamanaka R, Mizoguchi H, Higashio K, Kohno K and Kuwano M: Tumor necrosis factor and epidermal growth factor modulate migration of human microvascular endothelial cells and production of tissue-type plasminogen activator and its inhibitor. *Exp Cell Res* 192:574-580, 1991

Mazzieri R, Masiero L, Zanetta L, Monea S, Onisto M, Garbisa S and Mignatti P: Control of type IV collagenase activity by components of the urokinase-plasmin system: a regulatory mechanism with cell-bound reactants. *EMBO J* 16(9):2319-2332, 1997

McCawley LJ, O'Brien P and Hudson LG: Epidermal growth factor (EGF)- and scatter factor/hepatocyte growth factor (SF/HGF)-mediated keratinocyte migration is coincident with induction of matrix metalloproteinase (MMP)-9. *J Cell Physiol* 176:255-265, 1998

McClain SA, Jones SM, Nandi A, Gailit J, Tonnesen MG, Newman D and Clark RA: Mesenchymal cell activation is the rate-limiting step of granulation tissue induction. *Am J Pathol* 149:1257-1270, 1996

McMahon GA, Petitclerc E, Stefansson S, Smith E, Wong MKK, Westrick RJ, Ginsburg D, Brooks PC and Lawrence DA: Plasminogen activator inhibitor-1 regulates tumour growth and angiogenesis. *J Biol Chem* 276:33964-33968, 2001

McNeill H and Jensen PJ: A high-affinity receptor for urokinase plasminogen activator on human keratinocytes: characterisation and potential modulation during migration. *Cell Regulation* 1:843-852, 1990

Meszaros AJ, Reichner JS and Albina JE: Macrophage-induced neutrophil apoptosis. *J Immunol* 165:435-441, 2000

Metzger D and Chambon P: Site- and time-specific gene targeting in the mouse. *Methods* 24:71-80, 2001

Mignatti P, Mazzieri R and Rifkin DB: Expression of the urokinase receptor in vascular endothelial cells is stimulated by basic fibroblast growth factor. *J Cell Biol* 113:1193-1201, 1991

Mignatti, P., D. B. Rifkin, H. G. Welgus, and W. C. Parks. *Proteinases and tissue remodeling.* In The Molecular and Cellular Biology of Wound Repair. R.A.F. Clark, editor. Plenum Press, New York. 427-461. 1996

Mikus P and Ny T: Intracellular polymerization of the serpin plasminogen activator inhibitor type 2. *J Biol Chem* 271:10048-10053, 1996

Miles LA and Plow EF: Plasminogen receptors: ubiquitous sites for cellular regulation of fibrinolysis. *Fibrinolysis* 2:61-71, 1989

Mimuro J and Loskutoff DJ: Purification of a protein from bovine plasma that binds to type 1 plasminogen activator inhibitor and prevents its interaction with extracellular matrix. Evidence that the protein is vitronectin. *J Biol Chem* 264:936-939, 1989

Moll R, Franke WW, Schiller DL, Geiger B and Krepler R: The catalog of human cytokeratins: patterns of expression in normal epithelia, tumors and cultured cells. *Cell* 31:11-24, 1982

Molloy CJ and Laskin JD: Specific alterations in keratin biosynthesis in mouse epidermis *in vivo* and in explant culture following a single exposure to the tumor promoter 12-O-tetradecanoylphorbol-13-acetate. *Cancer Res* 47:4674-4680, 1987

Morimoto K, Mishima H, Nishida T and Otori T: Role of urokinase type plasminogen activator (u-PA) in corneal epithelial migration. *Thromb Haemost* 69:387-391, 1993

Morioka S, Lazarus GS, Baird JL and Jensen PJ: Migrating keratinocytes express urokinase-type plasminogen activator. *J Invest Dermatol* 88(4):418-423, 1987a

Morioka S, Lazarus GS and Jensen PJ: Involvement of urokinase-type plasminogen activator in acantholysis induced by pemphigus IgG. *J Invest Dermatol* 89:474-477, 1987b

Mosher DF, Sottile J, Wu C and McDonald JA: Assembly of extracellular matrix. *Curr Opin Cell Biol* 4:810-818, 1992

Mukhina SA, Stepanova VV, Traktouev DO, Poliakov AA, Beabealashvilly R, Gursky YG, Minashkin MM, Shevelev A and Tkachuk VA: The chemotactic action of urokinase on smooth muscle cells is dependent on its kringle domain. *J Biol Chem* 275(22):16450-16458, 2000

Muller-Rover S, Rossiter H, Paus R, Handjiski B, Peters EMJ, Murphy J-E, Mecklenburg L and Kupper TS: Overexpression of Bcl-2 protects from ultraviolet B-induced apoptosis but promotes hair follicle regression and chemotherapy-induced alopecia. *Am J Pathol* 156:1395-1405, 2000

Murphy G and Gavrilovic J: Proteolysis and cell migration: creating a path? *Curr Opin Cell Biol* 11:614-621, 1999

Mustjoki S, Sidenius N and Vaheri A: Enhanced release of soluble urokinase receptor by endothelial cells in contact with peripheral blood cells. *FEBS Lett* 486:237-242, 2000

Mustoe TA, Pierce GF, Thomason A, Gramates P, Sporn MB and Deuel TF: Accelerated healing of incisional wounds in rats induced by transforming growth factor-β. *Science* 237:1333-1336, 1987

Nagamine Y, Pearson D, Altus MS and Reich E: cDNA and gene nucleotide sequence of porcine plasminogen activator. *Nucleic Acids Res* 12:9525-9541, 1984

Nagaoka T, Kaburagi Y, Hamaguchi Y, Hasegawa M, Takehara K, Steeber DA, Tedder TF and Sato S: Delayed wound healing in the absence of intracellular adhesion molecule-1 or L-selectin expression. *Am J Pathol* 157(1):237-247, 2000

Naldini L, Tamagnone L, Vigna E, Sachs M, Hartmann G, Birchmeier W, Daikuhara Y, Tsubouchi H, Blasi F and Comoglio PM: Extracellular proteolytic cleavage by urokinase is required for activation of hepatocyte growth factor/scatter factor. *EMBO J* 11:4825-4833, 1992

Namiki A, Brogi E, Kearney M, Kim EA, Wu T, Couffinhal T, Varticovski L and Isner JM: Hypoxia induces vascular endothelial growth factor in cultured human endothelial cells. *J Biol Chem* 270(52):31189-31195, 1995

Nanney, L. B. and L. E. King Jr. *Epidermal growth factor and transforming growth factor-alpha.* In The Molecular and Cellular Biology of Wound Repair. R.A.F. Clark, editor. Plenum Press, New York. 171-188. 1996

Nelson WG and Sun TT: The 50- and 58-kd keratin classes as molecular markers for stratified squamous epithelia: cell culture studies. *J Cell Biol* 97:244-251, 1983

Neufeld G, Cohen T, Gengrinovitch S and Poltorak Z: Vascular endothelial growth factor (VEGF) and its receptors. *FASEB J* 13:9-22, 1999

Niinikoski J, Heughan C and Hunt TK: Oxygen and carbon dioxide tensions in experimental wounds. *Surg Gynecol Obstet* 133(6):1003-1007, 1971

Niinikoski J, Heughan C and Hunt TK: Oxygen tensions in human wounds. *J Surg Res* 12(2):77-82, 1972a

Niinikoski J, Hunt TK and Dunphy JE: Oxygen supply in healing tissue. *Am J Surg* 123:247-252, 1972b

Niinikoski, J., F. Gottrup, and T. K. Hunt. *The role of oxygen in wound repair.* In Wound Healing. D. Janssen, R. Rooman, and J. Robertson, editors. Wrightson Biomedical Publishing, London. 165-174. 1991

Nissen NN, Polverini PJ, Koch AE, Volin MV, Gamelli RL and DiPietro LA: Vascular endothelial growth factor mediates angiogenic activity during the proliferative phase of wound healing. *Am J Pathol* 152:1445-1452, 1998

No D, Yao TP and Evans RM: Ecdysone-inducible gene expression in mammalian cells and transgenic mice. *Proc Natl Acad Sci USA* 93:3346-3351, 1996

Ny T, Sawdey MS, Lawrence D, Millan JL and Loskutoff DJ: Cloning and sequence of a cDNA coding for the human β-migrating endothelial-cell-type plasminogen activator inhibitor. *Proc Natl Acad Sci USA* 83:6776-6780, 1986

Nykjaer A, Petersen CM, Moller B, Jensen PH, Moestrup SK, Holtet TL, Etzerodt M, Thogersen HC, Munch M and Andreasen PA: Purified α2-macroglobulin receptor/LDL receptor-related protein binds urokinase.plasminogen activator inhibitor type-1 complex. Evidence that the α2-macroglobulin receptor mediates cellular degradation of urokinase receptor-bound complexes. *J Biol Chem* 267:14543-14546, 1992

Nykjaer A, Conese M, Christensen EI, Olson D, Cremona O, Gliemann J and Blasi F: Recycling of the urokinase receptor upon internalization of the uPA:serpin complexes. *EMBO J* 16(10):2610-2620, 1997

O'Toole EA, Marinkovich MP, Hoeffler H, Furthmayr H and Woodley DT: Laminin-5 inhibits keratinocyte motility. *Exp Cell Res* 233:330-339, 1997a

O'Toole EA, Marinkovich MP, Peavey CL, Amieva MR, Furthmayr H, Mustoe TA and Woodley DT: Hypoxia increases human keratinocyte motility on connective tissue. *J Clin Invest* 100(11):2881-2891, 1997b

Okada A, Tomasetto C, Lutz Y, Bellocq J-P, Rio M-C and Bassett P: Expression of matrix metalloproteinases during rat skin wound healing: evidence that membrane type-1 matrix metalloproteinase is a stromal activator of pro-gelatinase A. *J Cell Biol* 137:67-78, 1997

Okada SS, Tomaszewski JE and Barnathan ES: Migrating vascular smooth muscle cells polarize cell surface urokinase receptors after injury *in vitro*. *Exp Cell Res* 217:180-187, 1995

Okumura Y, Sato H, Seiki M and Kido H: Proteolytic activation of the precursor of membrane type I matrix metalloproteinase by human plasmin: a possible cell surface activator. *FEBS Lett* 402:181-184, 1997

Olofsson B, Korpelainen E, Pepper MS, Mandriota SJ, Aase K, Kumar V, Gunji Y, Jeltsch MM, Shibuya M, Alitalo K and Eriksson U: Vascular endothelial growth factor B (VEGF-B) binds to VEGF receptor-1 and regulates plasminogen activator activity in endothelial cells. *Proc Natl Acad Sci USA* 95:11709-11714, 1998

Olson D, Pollanen J, Hoyer-Hansen G, Ronne E, Sakaguchi K, Wun T, Appella E, Dano K and Blasi F: Internalization of the urokinase-plasminogen activator inhibitor type-1 complex is mediated by the urokinase receptor. *J Biol Chem* 267(13):9129-9133, 1992

Orban PC, Chui D and Marth JD: Tissue- and site-specific DNA recombination in transgenic mice. *Proc Natl Acad Sci USA* 89:6861-6865, 1992

Orphanides C, Fine LG and Norman JT: Hypoxia stimulates proximal tubular cell matrix production via a TGF-β1-independent mechanism. *Kidney Int* 52:637-647, 1997

Ossowski L and Aguirre-Ghiso JA: Urokinase receptor and integrin partnership: coordination of signalling for cell adhesion, migration and growth. *Curr Opin Cell Biol* 12:613-620, 2000

Paladini RD, Takahashi K, Bravo NS and Coulombe PA: Onset of reepithelialization after skin injury correlates with a reorganization of keratin filaments in wound edge keratinocytes: defining a potential role for keratin 16. *J Cell Biol* 132:381-397, 1996

Palmiter RD, Chen HY and Brinster RL: Differential regulation of metallothionein-thymidine kinase fusion genes in transgenic mice and their offspring. *Cell* 29:701-710, 1982

Palolahti M, Lauharanta J, Stephens RW, Kuusela P and Vaheri A: Proteolytic activity in leg ulcer exudate. *Exp Dermatol* 2:29-37, 1993

Parks WC: Matrix metalloproteinases in repair. *Wound Rep Reg* 7:423-432, 1999

Patthy L: Evolution of the proteases of blood coagulation and fibrinolysis by assembly from modules. *Cell* 41:657-663, 1985

Pedersen N, Schmitt M, Ronne E, Nicoletti MI, Hoyer-Hansen G, Conese M, Giavazzi R, Dano K, Kuhn W and Janicke F: A ligand-free, soluble urokinase receptor is present in the ascitic fluid from patients with ovarian cancer. *J Clin Invest* 92:2160-2167, 1993

Peltonen J, Larjava H, Jaakkola S, Gralnick HR, Akiyama SK, Yamada SS, Yamada KM and Uitto J: Localization of integrin receptors for fibronectin, collagen, and laminin in human skin. *J Clin Invest* 84:1916-1923, 1989

Pennica D, Holmes WE, Kohr WJ, Harkins RN, Vehar GA, Ward CA, Bennet WF, Yelverton E, Seeburg PH, Heyneker HL, Goeddel DV and Collen D: Cloning and expression of human tissue-type plasminogen activator cDNA in E.coli. *Nature* 301:214-221, 1983

Pepper MS, Vassalli J-D, Montesano R and Orci L: Urokinase-type plasminogen activator is induced in migrating capillary endothelial cells. *J Cell Biol* 105:2535-2541, 1987

Pepper MS, Ferrara N, Orci L and Montesano R: Vascular endothelial growth factor (VEGF) induces plasminogen activators and plasminogen activator inhibitor-1 in microvascular endothelial cells. *Biochem Biophys Res Commun* 181:902-906, 1991

Pepper MS, Sappino AP, Montesano R, Orci L and Vassalli J-D: Plasminogen activator inhibitor-1 is induced in migrating endothelial cells. *J Cell Physiol* 153:129-139, 1992

Pepper MS, Sappino AP, Stocklin R, Montesano R, Orci L and Vassalli J-D: Upregulation of urokinase receptor expression on migrating endothelial cells. *J Cell Biol* 122:673-684, 1993

Petersen LC, Johannessen M, Foster D, Kumar A and Mulvihill E: The effect of polymerised fibrin on the catalytic activities of one-chain tissue-type plasminogen activator as revealed by an analogue resistant to plasmin cleavage. *Biochem Biophys Acta* 952:245-254, 1988a

Petersen LC, Lund LR, Nielsen LS, Dano K and Skriver L: One chain urokinase-type plaminogen activator from human sarcoma cells is a proenzyme with little or no intrinsic activity. *J Biol Chem* 263:11189-11195, 1988b

Pfarr DS, Rieser LA, Woychik RP, Rottman FM, Rosenberg M and Reff ME: Differential effects of polyadenylation regions on gene expression in mammalian cells. *DNA* 5:115-122, 1986

Picone R, Kajtaniak EL, Nielsen LS, Behrendt N, Mastronicola MR, Cubellis MV, Stoppelli MP, Pedersen S, Dano K and Blasi F: Regulation of urokinase receptors in monocyte-like U937 cells by the phorbol ester phorbol myristate acetate. *J Cell Biol* 108:693-702, 1989

Pilcher BK, Dumin JA, Sudbeck BD, Krane SM, Welgus HG and Parks WC: The activity of collagenase-1 is required for human keratinocyte migration on a type I collagen matrix. *J Cell Biol* 137:1445-1457, 1997

Pilcher BK, Dumin JA, Schwartz MJ, Mast BA, Schultz GS, Parks WC and Welgus HG: Keratinocyte collagenase-1 expression requires an epidermal growth factor receptor autocrine mechanism. *J Biol Chem* 274(15):10372-10381, 1999

Pinsky DJ, Liao H, Lawson CA, Yan SD, Chen X, Carmeliet P, Loskutoff DJ and Stern DM: Coordinated induction of plasminogen activator inhibitor-1 (PAI-1) and inhibition of plasminogen activator gene expression by hypoxia promotes pulmonary vascular fibrin deposition. *J Clin Invest* 102(5):919-928, 1998

Planus E, Barlovatz-Meimon G, Rogers RA, Bonavaud S, Ingber DE and Wang N: Binding of urokinase to plasminogen activator inhibitor type-1 mediates cell adhesion and spreading. *J Cell Sci* 110:1091-1098, 1997

Ploplis VA, French EL, Carmeliet P, Collen D and Plow EF: Plasminogen deficiency differentially affects recruitment of inflammatory cell populations in mice. *Blood* 91:2005-2009, 1998

Ploug M, Ronne E, Behrendt N, Jensen AL, Blasi F and Dano K: Cellular receptor for urokinase plasminogen activator: carboxyl terminal processing and membrane anchoring. *J Biol Chem* 266:1926-1933, 1991

Ploug M: Identification of specific sites involved in ligand binding by photoaffinity labeling of the receptor for the urokinase-type plasminogen activator. Residues located at equivalent positions in uPAR domains I and III participate in the assembly of a composite ligand-binding site. *Biochemistry* 37:16494-16505, 1998

Podor TJ, Peterson CB, Lawrence DA, Stefansson S, Shaughnessy SG, Foulon DM, Butcher M and Weitz JI: Type 1 plasminogen activator inhibitor binds to fibrin via vitronectin. *J Biol Chem* 275:19788-19794, 2000

Poliakov AA, Tkachuk V, Ovchinnikova T, Potapenko N, Bagryantsev S and Stepanova V: Plasmin-dependent elimination of the growth-factor-like domain in urokinase causes its rapid cellular uptake and degradation. *Biochem J* 355:639-645, 2001

Potempa J, Korzus E and Travis J: The serpin superfamily of proteinase inhibitors: structure, function, and regulation. *J Biol Chem* 269:15957-15960, 1994

Quan T, He T, Kang S, Voorhees JJ and Fisher GJ: Connective tissue growth factor: expression in human skin *in vivo* and inhibition by ultraviolet irradiation. *J Invest Dermatol* 118:402-408, 2002

Quax PHA, van Leeuwen RTJ, Verspaget HW and Verheijen JH: Protein and messenger RNA levels of plasminogen activators and inhibitors analysed in 22 human tumor cell lines. *Cancer Res* 50:1488-1494, 1990

Quinlan RA, Schiller DL, Hatzfeld M, Achtstatter T, Moll R, Jorcano JL, Magin TM and Franke WW: Patterns of expression and organisation of cytokeratin intermediate filaments. *Ann N Y Acad Sci* 455:282-306, 1985

Raghow R, Postlethwaite AE, Keski-Oja J, Moses HL and Kang AH: Transforming growth factor β increases steady state levels of type 1 procollagen and fibronectin mRNAs posttranslationally in cultured fibroblasts. *J Clin Invest* 79:1285-1288, 1987

Rajewsky K, Gu H, Kuhn R, Betz UAK, Muller W, Roes J and Schwenk F: Conditional gene targeting. *J Clin Invest* 98(3):600-603, 1996

Rajput B, Degen SF, Reich E, Waller EK, Axelrod J, Eddy RL and Shows TB: Chromosomal locations of human tissue plasminogen activator and urokinase genes. *Science* 230:672-674, 1985

Ramirez A, Bravo A, Jorcano JL and Vidal M: Sequences 5' upstream of the bovine keratin 5 gene direct tissue- and cell-type-specific expression of a lacZ gene in the adult and during development. *Differentiation* 58:53-64, 1994

Ramirez A, Vidal M, Bravo A, Larcher F and Jorcano JL: A 5'-upstream region of a bovine keratin 6 gene confers tissue-specific expression and hyperproliferation-related induction in transgenic mice. *Proc Natl Acad Sci USA* 92:4783-4787, 1995

Ramirez A, Vidal M, Bravo A and Jorcano JL: Analysis of sequences controlling tissue-specific and hyperproliferation-related keratin 6 gene expression in transgenic mice . *DNA Cell Biol* 17:177-185, 1998

Ramos-DeSimone N, Hahn-Dantona E, Sipley J, Nagase H, French DL and Quigley JP: Activation of matrix metalloproteinase-9 (MMP-9) via a converging plasmin/stromelysin-1 cascade enhances tumor cell invasion. *J Biol Chem* 274(19):13066-13076, 1999

Resnati M, Guttinger M, Valcamonica S, Sidenius N, Blasi F and Fazioli F: Proteolytic cleavage of the urokinase receptor substitutes for the agonist-induced chemotactic effect . *EMBO J* 15:1572-1582, 1996

Riccio A, Grimaldi G, Verde P, Sebastio G, Boast S and Blasi F: The human urokinase-plasminogen activator gene and its promoter. *Nucleic Acids Res* 13(8):2759-2771, 1985

Rice RH and Green H: Presence in human epidermal cells of a soluble protein precursor of the cross-linked envelope: activation of the crosslinking by calcium ions. *Cell* 18:681-694, 1979

Ritchie H and Booth NA: Secretion of plasminogen activator inhibitor 2 by human peripheral blood monocytes occurs via an endoplasmic reticulum-golgi-independent pathway. *Exp Cell Res* 242:439-450, 1998

Ritchie H, Robbie LA, Kinghorn S, Exley R and Booth NA: Monocyte plasminogen activator inhibitor 2 (PAI -2) inhibits u-PA-mediated fibrin clot lysis and is cross-linked to fibrin. *Thromb Haemost* 81:96-103, 1999

Roberts AB, Sporn MB, Assoian RK, Smith JM, Roche NS, Wakefield LM, Heine UI, Liotta L, Falanga V, Kehrl JR and Fauci AS: Transforming growth factor type β: rapid induction of fibrosis and angiogenesis *in vivo* and stimulation of collagen formation *in vitro*. *Proc Natl Acad Sci USA* 83:4167-4171, 1986

Roberts, A. B. and M. B. Sporn. *Transforming growth factor-beta*. In The Molecular and Cellular Biology of Wound Repair. R.A.F. Clark, editor. Plenum Press, New York. 275-298. 1996

Roldan AL, Cubellis MV, Masucci MT, Behrendt N, Lund LR, Dano K, Appella E and Blasi F: Cloning and expression of the receptor for human urokinase plasminogen activator, a central molecule in cell surface, plasmin dependent proteolysis [published erratum appears in EMBO J ;9(5):1674, 1990]. *EMBO J* 9(2):467-474, 1990

Romer J, Lund LR, Eriksen J, Ralfkiaer E, Zeheb R, Gelehrter TD, Dano K and Kristensen P: Differential expression of urokinase-type plasminogen activator and its type-1 inhibitor during healing of mouse skin wounds. *J Invest Dermatol* 97(5):803-811, 1991

Romer J, Lund LR, Eriksen J, Pyke C, Kristensen P and Dano K: The receptor for urokinase-type plasminogen activator is expressed by keratinocytes at the leading edge during re-epithelialization of mouse skin wounds. *J Invest Dermatol* 102(4):519-522, 1994

Romer J, Bugge TH, Pyke C, Lund LR, Flick MJ, Degen JL and Dano K: Impaired wound healing in mice with a disrupted plasminogen gene. *Nat Med* 2(3):287-292, 1996

Ronfard V and Barrandon Y: Migration of keratinocytes through tunnels of digested fibrin. *Proc Natl Acad Sci USA* 98:4504-4509, 2001

Ronne E, Pappot H, Grondahl-Hansen J, Hoyer-Hansen G, Plesner T, Hansen NE and Dano K: The receptor for urokinase plasminogen activator is present in plasma from healthy donors and elevated in patients with paroxysmal nocturnal haemoglobinuria. *Br J Haematol* 89:576-581, 1995

Rosenthal DS, Griffiths CE, Yuspa SH, Roop DR and Voorhees JJ: Acute or chronic topical retinoic acid treatment of human skin *in vivo* alters the expression of epidermal transglutaminase, loricrin, involucrin, filaggrin and keratins 6 and 13 but not keratins 1, 10, and 14. *J Invest Dermatol* 98:343-350, 1992

Rox JM, Reinartz J and Kramer MD: Interleukin-1β upregulates tissue-type plasminogen activator in a keratinocyte cell line (HaCaT). *Arch Dermatol Res* 288:554-558, 1996

Saarialho-Kere UK, Kovacs SO, Pentland AP, Olerud JE, Welgus HG and Parks WC: Cell-matrix interactions modulate interstitial collagenase expression by human keratinocytes actively involved in wound healing. *J Clin Invest* 92:2858-2866, 1993

Saarialho-Kere UK, Kovacs SO, Pentland AP, Parks WC and Welgus HG: Distinct populations of keratinocytes express stromelysin-1 and -2 in chronic wounds. *J Clin Invest* 94:79-88, 1994

Saksela O, Moscatelli D and Rifkin DB: The opposing effects of basic fibroblast growth factor and transforming growth factor β on the regulation of plasminogen activator activity in capillary endothelial cells. *J Cell Biol* 105:957-963, 1987

Saksela O and Rifkin DB: Cell-associated plasminogen activation: regulation and physiological functions. *Annu Rev Cell Biol* 4:93-126, 1988

Saksela O and Rifkin DB: Release of basic fibroblast growth factor-heparan sulfate complexes from endothelial cells by plasminogen activator-mediated proteolytic activity. *J Cell Biol* 110:767-775, 1990

Salo T, Makela M, Kylmaniemi M, Autio H-H and Larjava H: Expression of matrix metalloproteinase-2 and -9 during early human wound healing. *Lab Invest* 70:176-182, 1994

Salonen EM, Vaheri A, Pollanen J, Stephens R, Andreasen P, Mayer M, Dano K, Gailit J and Ruoslahti E: Interaction of plasminogen activator inhibitor (PAI-1) with vitronectin. *J Biol Chem* 264:6339-6343, 1989

Santibanez JF, Frontelo P, Iglesias M, Martinez J and Quintanilla M: Urokinase expression and binding activity associated with the transforming growth factor β1-induced migratory and invasive phenotype of mouse epidermal keratinocytes. *J Cell Biochem* 74:61-73, 1999

Santilli SM, Fiegel VD, Aldridge DE and Knighton DR: Rabbit aorta endothelial cell hypoxia induces secretion of transforming growth factor β and augments macrophage adhesion *in vitro*. *Ann Vasc Surg* 5:429-438, 1991

Sauer B and Henderson N: Site-specific DNA recombination in mammalian cells by the Cre recombinase of bacteriophage P1. *Proc Natl Acad Sci USA* 85:5166-5170, 1988

Sauer B and Henderson N: Cre-stimulated recombination at loxP-containing DNA sequences placed into the mammalian genome. *Nucleic Acids Res* 17:147-161, 1989

Sauer B: Inducible gene targeting in mice using the cre/lox system. *Methods* 14:381-392, 1998

Sawdey MS and Loskutoff DJ: Regulation of murine type 1 plasminogen activator inhibitor gene expression *in vivo*. *J Clin Invest* 88:1346-1353, 1991

Schaefer BM, Maier K, Eickhoff U, Todd RF and Kramer MD: Plasminogen activation in healing human wounds. *Am J Pathol* 144(6):1269-1280, 1994

Schultz GS, White M, Mitchell R, Brown G, Lynch J, Twardzik DR and Todaro GJ: Epithelial wound healing enhanced by transforming growth factor-α and vaccinia growth factor. *Science* 235:350-352, 1987

Schultze N, Burki Y, Lang Y, Certa U and Bluethmann H: Efficient control of gene expression by single step integration of the tetracycline system in transgenic mice. *Nat Biotech* 14:499-503, 1996

Schwartz BS: Differential inhibition of soluble and cell surface receptor-bound single-chain urokinase by plasminogen activator inhibitor type 2. a potential regulatory mechanism. *J Biol Chem* 269:8319-8323, 1994

Schweizer J, Furstenberger G and Winter H: Selective suppression of two postnatally acquired 70 kD and 65 kD keratin proteins during continuous treatment of adult mouse tail epidermis with vitamin A. *J Invest Dermatol* 89:125-131, 1987

Schwenk F, Kuhn R, Angrand P-O, Rajewsky K and Francis Stewart A: Temporally and spatially regulated somatic mutagenesis in mice. *Nucleic Acids Res* 26(6):1427-1432, 1998

Sellheyer K, Bickenbach JR, Rothnagel JA, Bundman D, Longley MA, Krieg T, Roche NS, Roberts AB and Roop DR: Inhibition of skin development by overexpression of transforming growth factor β1 in the epidermis of transgenic mice. *Proc Natl Acad Sci USA* 90:5237-5241, 1993

Senger DR, Galli SJ, Dvorak AM, Perruzzi CA, Harvey VS and Dvorak HF: Tumor cells secrete a vascular permeability factor that promotes accumulation of ascites fluid. *Science* 219:983-985, 1983

Senger DR, Ledbetter SR, Claffey KP, Papadopoulos-Sergiou A, Perruzzi CA and Detmar M: Stimulation of endothelial cell migration by vascular permeability factor/vascular endothelial growth factor through cooperative mechanisms involving the αvβ3 integrin, osteopontin, and thrombin. *Am J Pathol* 149:293-305, 1996

Senger DR, Claffey KP, Benes JE, Perruzzi CA, Sergiou AP and Detmar M: Angiogenesis promoted by vascular endothelial growth factor: regulation through α1β1, and α2β1 integrins. *Proc Natl Acad Sci USA* 94:13612-13617, 1997

Shockett P, Difilippantonio M, Hellman N and Schatz DG: A modified tetracycline-regulated system provides autoregulatory, inducible gene expression in cultured cells and transgenic mice. *Proc Natl Acad Sci USA* 92:6522-6526, 1995

Shreeniwas R, Koga S, Karakurum M, Pinsky D, Kaiser E, Brett J, Wolitzky BA, Norton C, Plocinski J and Benjamin W: Hypoxia-mediated induction of endothelial cell interleukin-1α. An autocrine mechanism promoting expression of leukocyte adhesion molecules on the vessel surface. *J Clin Invest* 90(6):2333-2339, 1992

Shull MM, Ormsby I, Kier AB, Pawlowski S, Diebold RJ, Yin M, Allen R, Sidman C, Proetzel G and Calvin D: Targeted disruption of the mouse transforming growth factor-β1 gene results in multifocal inflammatory disease. *Nature* 359:693-699, 1992

Sidenius N, Sier CFM and Blasi F: Shedding and cleavage of the urokinase receptor (uPAR): identification and characterisation of uPAR fragments *in vitro* and *in vivo*. *FEBS Lett* 475:52-56, 2000

Simonet WS, DeRose ML, Bucay N, Nguyen HQ, Wert SE, Zhou L, Ulich TR, Thomason A, Danilenko DM and Whitsett JA: Pulmonary malformation in transgenic mice expressing human keratinocyte growth factor in the lungs. *Proc Natl Acad Sci USA* 92:12461-12465, 1995

Singer AJ and Clark RAF: Cutaneous wound healing. *N Engl J Med* 341(10):738-746, 1999

Soff GA, Sanderowitz J, Gately S, Verrusio E, Weiss I, Brem S and Kwaan HC: Expression of plasminogen activator inhibitor type 1 by human prostate carcinoma cells inhibits primary tumor growth, tumor-associated angiogenesis, and metastasis to lung and liver in an athymic mouse model. *J Clin Invest* 96:2593-2600, 1995

Soker S, Takashima S, Miao HQ, Neufeld G and Klagsbrun M: Neuropilin-1 is expressed by endothelial and tumor cells as an isoform-specific receptor for vascular endothelial growth factor. *Cell* 92:735-745, 1998

Sperl S, Jacob U, Arroyo de Prada N, Sturzebecher J, Wilhelm OG, Bode W, Magdolen V, Huber R and Moroder L: (4-Aminomethyl)phenylguanidine derivatives as nonpeptidic highly selective inhibitors of human urokinase. *Proc Natl Acad Sci USA* 97(10):5113-5118, 2000

Springer TA: Traffic signals for lymphocyte recirculation and leukocyte emigration: the multistep paradigm. *Cell* 76:301-314, 1994

St Onge L, Furth PA and Gruss P: Temporal control of the Cre recombinase in transgenic mice by a tetracycline responsive promoter. *Nucleic Acids Res* 24:3875-3877, 1996

Stacey MC, Burnand KG, Mahmoud Alexandroni M, Gaffney PJ and Bhogal BS: Tissue and urokinase plasminogen activators in the environs of venous and ischaemic leg ulcers. *Br J Surg* 80:596-599, 1993

Stack MS and Johnson DA: Human mast cell tryptase activates single-chain urinary-type plasminogen activator (pro-urokinase). *J Biol Chem* 269:9416-9419, 1994

Stadelmann WK, Digenis AG and Tobin GR: Physiology and healing dynamics of chronic cutaneous wounds. *Am J Surg* 176:26S-38S, 1998a

Stadelmann WK, Digenis AG and Tobin GR: Impediments to wound healing. *Am J Surg* 176:39S-47S, 1998b

Stahl A and Mueller BM: Melanoma cell migration on vitronectin: regulation by components of the plasminogen activation system. *Int J Cancer* 71:116-122, 1997

Staiano Coico L, Carano K, Allan VM, Steiner MG, Pagan Charry I, Bailey BB, Babaar P, Rigas B and Higgins PJ: PAI-1 gene expression is growth state-regulated in cultured human epidermal keratinocytes during progression to confluence and postwounding. *Exp Cell Res* 227:123-134, 1996

Stallmeyer B, Kampfer H, Podda M, Kaufmann R, Pfeilschifter J and Frank S: A novel keratinocyte mitogen: regulation of leptin and its functional receptor in skin repair. *J Invest Dermatol* 117(1):98-105, 2001

Stark HJ, Breitkreutz D, Limat A, Bowden P and Fusenig NE: Keratins of the human hair follicle: "hyperproliferative" keratins consistently expressed in outer root sheath cells *in vivo* and *in vitro*. *Differentiation* 35:236-249, 1987

Stefansson S and Lawrence DA: The serpin PAI-1 inhibits cell migration by blocking integrin $\alpha v\beta 3$ binding to vitronectin. *Nature* 383:441-443, 1996

Stefansson S, Petitclerc E, Wong MKK, McMahon GA, Brooks PC and Lawrence DA: Inhibition of angiogenesis *in vivo* by plasminogen activator inhibitor-1. *J Biol Chem* 276:8135-8141, 2001

Steinbrech DS, Longaker MT, Mehrara BJ, Saadeh PB, Chin GS, Gerrets RP, Chau DC, Rowe NM and Gittes GK: Fibroblast responses to hypoxia: the relationship between angiogenesis and matrix regulation. *J Surg Res* 84:127-133, 1999

Steinert PM and Roop DR: Molecular and cellular biology of intermediate filaments. *Annu Rev Biochem* 57:593-625, 1988

Sternberg N and Hamilton DL: Bacteriophage P1 site-specific recombination. I. Recombination between loxP sites. *J Mol Biol* 150:467-486, 1981

Steven AC, Bisher ME, Roop DR and Steinert PM: Biosynthetic pathways of filaggrin and loricrin - two major proteins expressed by terminally differentiated epidermal keratinocytes. *J Struct Biol* 104:150-162, 1990

Stoler A, Kopan R, Duvic M and Fuchs E: Use of monospecific antisera and cRNA probes to localize the major changes in keratin expression during normal and abnormal epidermal differentiation. *J Cell Biol* 107:427-446, 1988

Stoppelli MP, Corti A, Soffientini G, Cassani F, Blasi F and Assoian RK: Differentiation-enhanced binding of the amino-terminal fragment of human urokinase plasminogen activator to a specific receptor on U937 monocytes. *Proc Natl Acad Sci USA* 82:4939-4943, 1985

Strand K, Murray J, Aziz S, Ishida A, Rahman S, Patel Y, Cardona C, Hammond WP, Savidge G and Wijelath ES: Induction of the urokinase plasminogen activator system by oncostatin M promotes endothelial migration. *J Cell Biochem* 79:239-248, 2000

Stump DC, Lijnen HR and Collen D: Purification and characterization of a novel low molecular weight form of single-chain urokinase-type plasminogen activator. *J Biol Chem* 261:17120-17126, 1986

Subramaniam M, Saffaripour S, Van de Water L, Frenette PS, Mayadas TN, Hynes RO and Wagner DD: Role of endothelial selectins in wound repair. *Am J Pathol* 150(5):1701-1709, 1997

Suzuma K, Takagi H, Otani A and Honda Y: Hypoxia and vascular endothelial growth factor stimulate angiogenic integrin expression in bovine retinal microvascular endothelial cells. *Invest Opthalmol Vis Sci* 39:1028-1035, 1998

Swerlick RA, Brown EJ, Xu Y, Lee KH, Manos S and Lawley TJ: Expression and modulation of the vitronectin receptor on human dermal microvascular endothelial cells. *J Invest Dermatol* 99:715-722, 1993

Takahashi K and Coulombe PA: A transgenic mouse model with an inducible skin blistering disease phenotype. *Proc Natl Acad Sci USA* 93:14776-14781, 1996

Takahashi K and Coulombe PA: Defining a region of the human keratin 6a gene that confers inducible expression in stratified epithelia of transgenic mice. *J Biol Chem* 272(18):11979-11985, 1997

Thomas GJ, Poomsawat S, Lewis MP, Hart IR, Speight PM and Marshall JF: $\alpha v\beta 6$ integrin upregulates matrix metalloproteinase 9 and promotes migration of normal oral keratinocytes. *J Invest Dermatol* 116(6):898-904, 2001

Timpl R: Structure and biological activity of basement membrane proteins. *Eur J Biochem* 180:487-502, 1989

Timpl R: Macromolecular organization of basement membranes. *Curr Opin Cell Biol* 8:618-624, 1996

Timpl R and Brown JC: Supramolecular assembly of basement membranes. *Bioessays* 18:123-132, 1996

Tonnesen MG, Feng X and Clark RAF: Angiogenesis in wound healing. *J Invest Dermatol* 5(1):40-46, 2000

Tsuboi R, Sato C, Kurita Y, Ron D, Rubin JS and Ogawa H: Keratinocyte growth factor (FGF-7) stimulates migration and plasminogen activator activity of normal human keratinocytes. *J Invest Dermatol* 101:49-53, 1993

Tuder RM, Flook BE and Voelkel NF: Increased gene expression for VEGF and the VEGF receptors KDR/Flk and Flt in lungs exposed to acute or to chronic hypoxia. Modulation of gene expression by nitric oxide. *J Clin Invest* 95:1798-1807, 1995

Uchiyama T, Kurabayashi M, Ohyama Y, Utsugi T, Akuzawa N, Sato M, Tomono S, Kawazu S and Nagai R: Hypoxia induces transcription of the plasminogen activator inhibitor-1 gene through genistein-sensitive tyrosine kinase pathways in vascular endothelial cells. *Arterioscler Thromb Vasc Biol* 20:1155-1161, 2000

Ugwu F, Van Hoef B, Bini A, Collen D and Lijnen HR: Proteolytic cleavage of urokinase-type plasminogen activator by stromelysin-1 (MMP-3). *Biochemistry* 37:7231-7236, 1998

Unkeless JC, Gordon S and Reich E: Secretion of plasminogen activator by stimulated macrophages. *J Exp Med* 139:834-850, 1974

Vaalamo M, Mattila L, Johansson N, Kariniemi AL, Karjalainen-Lindsberg ML and Saarialho-Kere UK: Patterns of matrix metalloproteinase and TIMP-1 expression in chronic and normally healing cutaneous wounds. *Br J Dermatol* 135:52-59, 1996

Vallier L, Mancip J, Markossian S, Lukaszewicz A, Dehay C, Metzger D, Chambon P, Samarut J and Savatier P: An efficient system for conditional gene expression in embryonic stem cells and their *in vitro* and *in vivo* differentiated derivatives. *Proc Natl Acad Sci USA* 98:2467-2472, 2001

van der Neut R, Krimpenfort P, Calafat J, Niessen CM and Sonnenberg A: Epithelial detachment due to absence of hemidesmosomes in integrin β4 null mice. *Nat Genet* 13:366-369, 1996

van Hinsbergh VWM, Kooistra T, van der Berg EA, Princen HMG, Fiers W and Emeis JJ: Tumor necrosis factor increases the production of plasminogen activator inhibitor in human endothelial cells *in vitro* and in rats *in vivo*. *Blood* 72:1467-1473, 1988

van Zonneveld AJ, Veerman H and Pannekoek H: On the interaction of the finger and kringle domain of tissue-type plasminogen activator with fibrin. *J Biol Chem* 261:14214-14218, 1986

Varani J, Burmeister B, Sitrin RG, Shollenberger SB, Inman DR, Fligiel SE, Gibbs DF and Johnson K: Expression of serine proteinases and metalloproteinases in organ-cultured human skin. Altered levels in the presence of retinoic acid and possible relationship to retinoid-induced loss of epidermal cohesion. *Am J Pathol* 145:561-573, 1994

Varghese MC, Balin AK, Carter DM and Caldwell D: Local environment of chronic wounds under synthetic dressings. *Arch Dermatol* 122:52-57, 1986

Vasioukhin V, Degenstein L, Wise B and Fuchs E: The magical touch: genome targeting in epidermal stem cells induced by tamoxifen application to mouse skin. *Proc Natl Acad Sci USA* 96:8551-8556, 1999

Vassalli J-D, Dayer JM, Wohlwend A and Belin D: Concomitant secretion of prourokinase and of a plasminogen activator-specific inhibitor by cultured human monocytes-macrophages. *J Exp Med* 159:1653-1668, 1984

Vassalli J-D and Belin D: Amiloride selectively inhibits the urokinase-type plasminogen activator. *FEBS Lett* 214(1):187-191, 1987

Vassar R, Rosenberg M, Ross S, Tyner A and Fuchs E: Tissue-specific and differentiation-specific expression of a human K14 keratin gene in transgenic mice. *Proc Natl Acad Sci USA* 86:1563-1567, 1989

Vassar R and Fuchs E: Transgenic mice provide new insights into the role of TGF-α during epidermal development and differentiation. *Genes and Development* 5:714-727, 1991

Venturini G, Menegatti E and Ascenzi P: Competitive inhibition of nitric oxide synthase by p-aminobenzamidine, a serine proteinase inhibitor. *Biochem Biophys Res Commun* 232:88-90, 1997

von Heijne G, Liljestrom P, Mikus P, Andersson H and Ny T: The efficiency of the uncleaved secretion signal in the plasminogen activator inhibitor type 2 protein can be enhanced by point mutations that increase its hydrophobicity. *J Biol Chem* 266:15240-15243, 1991

Wagner OF, de Vries C, Hohmann C, Veerman H and Pannekoek H: Interaction between plasminogen activator inhibitor type 1 (PAI-1) bound to fibrin and either tissue-type plasminogen activator (t-PA) or urokinase-type plasminogen activator (u-PA). Binding of t-PA/PAI-1 complexes to fibrin mediated by both the finger and the kringle-2 domain of t-PA. *J Clin Invest* 84:647-655, 1989

Wahlberg K, Hoyer-Hansen G and Casslen B: Soluble receptor for urokinase plasminogen activator in both full-length and a cleaved form is present in high concentration in cystic fluid from ovarian cancer. *Cancer Res* 58:3294-3298, 1998

Waltz DA and Chapman HA: Reversible cellular adhesion to vitronectin linked to urokinase receptor occupancy. *J Biol Chem* 269:14746-14750, 1994

Waltz DA, Natkin LR, Fujita RM, Wei Y and Chapman HA: Plasmin and plasminogen activator inhibitor type 1 promote cellular motility by regulating the interaction between the urokinase receptor and vitronectin. *J Clin Invest* 100:58-67, 1997

Wang H and Keiser JA: Vascular endothelial growth factor upregulates the expression of matrix metalloproteinases in vascular smooth muscle cells. Role of Flt1. *Circ Res* 83:832-840, 1998

Wang X, Zinkel S, Polonsky K and Fuchs E: Transgenic studies with a keratin promoter-driven growth hormone transgene: prospects for gene therapy. *Proc Natl Acad Sci USA* 94:219-226, 1997

Wawersik M and Coulombe PA: Forced expression of keratin 16 alters adhesion, differentiation, and migration of mouse skin keratinocytes. *Mol Biol Cell* 11:3315-3327, 2000

Weckroth M, Vaheri A, Lauharanta J, Sorsa T and Konttinen YT: Matrix metalloproteinases, gelatinase and collagenase, in chronic leg ulcers. *J Invest Dermatol* 106:1119-1124, 1996

Wei Y, Waltz DA, Rao N, Drummond RJ, Rosenberg S and Chapman HA: Identification of the urokinase receptor as an adhesion receptor for vitronectin. *J Biol Chem* 269(51):32380-32388, 1994

Weiss RA, Eichner R and Sun TT: Monoclonal antibody analysis of keratin expression in epidermal diseases: a 48- and 56-kdalton keratin as molecular markers for hyperproliferative keratinocytes. *J Cell Biol* 98:1397-1406, 1984

Werner S, Peters KG, Longaker MT, Fuller-Pace F, Banda M and Williams LT: Large induction of keratinocyte growth factor expression in the dermis during wound healing. *Proc Natl Acad Sci USA* 89:6896-6900, 1992

Werner S, Smola H, Liao X, Longaker MT, Krieg T, Hofschneider PH and Williams LT: The function of KGF in morphogenesis of epithelium and reepithelialization of wounds. *Science* 266:819-822, 1994

Werner S: Keratinocyte growth factor: a unique player in epithelial repair processes. *Cytokine Growth Factor Rev* 9:153-165, 1998

Werner S and Munz B: Suppression of keratin 15 expression by transforming growth factor β *in vitro* and by cutaneous injury *in vivo*. *Exp Cell Res* 254:80-90, 2000

Werner S and Smola H: Paracrine regulation of keratinocyte proliferation and differentiation. *Trends Cell Biol* 11(4):143-146, 2001

Wijnberg MJ, Quax PH, Nieuwenbroek NM and Verheijen JH: The migration of human smooth muscle cells *in vitro* is mediated by plasminogen activation and can be inhibited by α-2-macroglobulin receptor associated protein. *Thromb Haemost* 78:880-886, 1997

Wikner NE, Elder JT, Persichitte KA, Mink P and Clark RAF: Transforming growth factor-β modulates plasminogen activator activity and plasminogen activator inhibitor type-1 expression in human keratinocytes *in vitro*. *J Invest Dermatol* 95(5):607-613, 1990

Wilkie TM, Brinster RL and Palmiter RD: Germline and somatic mosaicism in transgenic mice. *Dev Biol* 118:9-18, 1986

Williams IR, Rawson EA, Manning L, Karaoli T, Rich BE and Kupper TS: IL-7 overexpression in transgenic mouse keratinocytes causes a lymphoproliferative skin disease dominated by intermediate TCR cells - evidence for heirarchy in IL-7 responsiveness among cutaneous T cells. *J Immunol* 159:3044-3056, 1997

Winter GD: Formation of the scab and the rate of epithelialization of superficial wounds in the skin of the young domestic pig. *Nature* 193:293-294, 1962

Wohlwend A, Belin D and Vassalli J-D: Plasminogen activator-specific inhibitors produced by human monocytes/macrophages. *J Exp Med* 165:320-339, 1987

Wojta J, Kaun C, Breuss JM, Koshelnick Y, Beckmann R, Hattey E, Mildner M, Weninger W, Nakamura T, Tschachler E and Binder BR: Hepatocyte growth factor increases expression of vascular endothelial growth factor and plasminogen activator inhibitor-1 in human keratinocytes and the vascular endothelial growth factor receptor flk-1 in human endothelial cells. *Lab Invest* 79(4):427-438, 1999

Woodley DT, Bachmann PM and O'Keefe EJ: Laminin inhibits human keratinocyte migration. *J Cell Physiol* 136:140-146, 1988

Woodley DT and Kim YH: A double-blind comparison of adhesive bandages with the use of uniform suction blister wounds. *Arch Dermatol* 128:1354-1357, 1992

Wysocki AB, Staiano Coico L and Grinnell F: Wound fluid from chronic leg ulcers contains elevated levels of metalloproteinases MMP-2 and MMP-9. *J Invest Dermatol* 101:64-68, 1993

Xia Y-P, Zhao Y, Tyrone JW, Chen A and Mustoe TA: Differential activation of migration by hypoxia in keratinocytes isolated from donors of increasing age: implications for chronic wounds in the elderly. *J Invest Dermatol* 116(1):50-56, 2001

Xia YP, Zhao Y, Marcus J, Jimenez PA, Ruben SM, Moore PA, Khan F and Mustoe TA: Effects of keratinocyte growth factor-2 (KGF-2) on wound healing in an ischaemia-impaired rabbit ear model and on scar formation. *J Pathol* 188:431-438, 1999

Xiong M, Elson G, Legarda D and Leibovich SJ: Production of vascular endothelial growth factor by murine macrophages: regulation by hypoxia, lactate, and the inducible nitric oxide synthetase pathway. *Am J Pathol* 153:587-598, 1998

Xu J and Clark RAF: Extracellular matrix alters PDGF regulation of fibroblast integrins. *J Cell Biol* 132:239-249, 1996

Xue W, Hashimoto K and Toi Y: Functional involvement of urokinase-type plasminogen activator receptor in pemphigus acantholysis. *J Cutan Pathol* 25:469-474, 1998

Yager DR, Zhang LY, Liang HX, Diegelmann RF and Cohen IK: Wound fluids from human pressure ulcers contain elevated matrix metalloproteinase levels and activity compared to surgical wound fluids. *J Invest Dermatol* 107:743-748, 1996

Yamanaka M and Ishikawa O: Hypoxic conditions decrease the mRNA expression of pro-α–1(i) and (III) collagens and increase matrix metalloproteinase-1 of dermal fibroblasts in three-dimensional cultures. *J Dermatol Sci* 24:99-104, 2000

Yarranton GT: Inducible vectors for expression in mammalian cells. *Curr Opin Biotech* 3:506-511, 1992

Ye RD, Wun TC and Sadler JE: Mammalian protein secretion without signal peptide removal. biosynthesis of plasminogen activator inhibitor-2 in U-937 cells . *J Biol Chem* 263:4869-4875, 1988

Yebra M, Parry GCN, Stromblad S, Mackman N, Rosenberg S, Mueller BM and Cheresh DA: Requirement of receptor-bound urokinase-type plasminogen activator for integrin αvβ5-directed cell migration. *J Biol Chem* 271:29393-29399, 1996

Yebra M, Goretzki L, Pfeifer M and Mueller BM: Urokinase-type plasminogen activator binding to its receptor stimulates tumor cell migration by enhancing integrin-mediated signal transduction. *Exp Cell Res* 250:231-240, 1999

Yurchenco PD and O'Rear JJ: Basal lamina assembly. *Curr Opin Cell Biol* 6:674-681, 1994

Zachary I and Gliki G: Signaling transduction mechanisms mediating biological actions of the vascular endothelial growth factor family. *Cardiovasc Res* 49:568-581, 2001

Zhang Y, Riesterer C, Ayrall A-M, Sablitzky F, Littlewood TD and Reth M: Inducible site-directed recombination in mouse embryonic stem cells. *Nucleic Acids Res* 24:543-548, 1996

Zhou H-M, Nichols A, Wohlwend A, Bolon I and Vassalli J-D: Extracellular proteolysis alters tooth development in transgenic mice expressing urokinase-type plasminogen activator in the enamel organ. *Development* 126:903-912, 1999

Zhou H-M, Nichols A, Meda P and Vassalli J-D: Urokinase-type plasminogen activator and its receptor synergize to promote pathogenic proteolysis. *EMBO J* 19(17):4817-4826, 2000